INSIGHTS INTO THE MECHANISM OF ASPARAGINE-LINKED GLYCOSYLATION: KINETIC STUDIES WITH SUBSTRATES AND INHIBITORS

Thesis by

Tamara Lynn Hendrickson

In Partial Fulfillment of the Requirements

for the Degree of

Doctor of Philosophy

California Institute of Technology

Pasadena, California

1996

(May 17, 1996)

In Loving Memory of My Grandparents

George and Dorothy Sanstead

and

George and Florence Hendrickson

Acknowledgements

I would like to begin by thanking my advisor, Professor Barbara Imperiali. One of the main reasons that I came to Caltech was because of Barbara's enthusiasm for science and the creativity of her ideas. She has been a constant source of support and encouragement and her ideas and insights into the field of mechanistic enzymology have been invaluable. Without her help and guidance, this dissertation would not have been possible.

I would also like to thank the members of my thesis committee, Professors Andy Myers, Carl Parker and Harry Gray. They have been a great source of advice and encouragement.

Over the years, I have been fortunate to work with a great group of people. In particular, I will always treasure the friendships of Drs. Jeff Spencer and Keith Rickert who were great collaborators and sources of information. Mihoko Kato has been an invaluable coworker and I wish her luck in graduate school next year! Mary Struthers, Ranabir Sinha Roy, Richard Cheng, Grant Walkup, Karen Shih, Dr. Karen Shannon, Dr. Stew Fisher, Dr. Alicia Torrado and Dr. Bill Shrader all deserve special thanks as well. As friends and as scientists, these people have been constant sources of encouragement, insight and information and they have contributed to a great lab environment. Thanks also to Sarah O'Connor, Lance Martin, Chris Davis and Grant Walkup for reading various drafts of this dissertation.

In addition, I would like to thank the many friends that I have made outside of the Imperiali group, especially Colby Stanton, Tracey Burr, Nat Finney, Michelle Parks, Eva Birnbaum, Rhonda Larson, Tim Johann, Dave Liberles, Martha Oakley, Bob Terbrueggen and Dian Buchness. (And a special thanks to Steve Fryer for keeping me amused during aerobics!) Thanks also

to Professors Nancy Kolodny and David Haines at Wellesley College for continuing to watch over and encourage me.

Mary Struthers and Ranabir Sinha Roy have been the best, as friends, coworkers and classmates! Over the years, they have supported and encouraged me when I needed it most and I can't imagine what graduate school would have been like without them. I will always treasure their friendships. Congratulations on your impending marriage!!!!!!!! I can't wait until we are reunited in Boston. Also, a special thanks to John Wright who has given me a new perspective on life at Caltech. He has brought me so much joy and has been a phenomenal source of unwavering strength and support.

Finally, I would like to thank my parents and my sister Marissa. These three people have been incredible pillars of support throughout the years. Thanks for believing in me!!!!!!

The work presented in this dissertation was funded by the National Institutes of Health. I was also the recipient of an NIH pre-doctoral training grant.

Abstract

Investigations into the mechanism of action of oligosaccharyl transferase (OT), the enzyme that catalyzes the first committed step in the biosynthesis of all asparagine-linked glycoproteins, were conducted. Research focused on kinetic studies with small reactive molecules and tripeptide substrates and inhibitors; these experiments were designed to specifically probe the OT active site. Commercially available chemical modification agents were used to identify a reactive cysteine residue in or near the oligosaccharide binding site. Based on this observation, a novel biotinylated sufhydryl modification reagent, methyl *N*-biotinoyl(aminoethane)-thiolsulfonate (BMTS), was developed. BMTS selectively modified the Wbp1p subunit of OT, thereby identifying this subunit as the site of the reactive cysteine and all or part of the oligosaccharide binding site.

The role of the required divalent metal cofactor was examined through a series of parallel kinetic experiments on two substrates for OT: the asparagine-containing tripeptide Bz-Asn-Leu-Thr-NHMe and the corresponding thioasparagine tripeptide Bz-Asn(γS)-Leu-Thr-NHMe. These substrates were evaluated with OT which had been treated to remove metal and independently reconstituted with four different metal cations. The sizes and thiophilicities of the metal cations had a different, but direct impact on the kinetic behavior of each of the two peptides. These results place the metal cofactor in proximity to the peptide substrate during catalysis and suggest that it may play a direct mechanistic role. In addition, a detailed analysis of the glycopeptide product of the thioasparagine tripeptide suggests that OT plays a specific role in directing the regiochemistry of asparagine glycosylation.

Through an iterative process, a new class of competitive inhibitors for OT was designed which exhibit nanomolar binding constants and are the first

reported potent inhibitors for OT. The slow, tight binding inhibition observed with these peptides suggests that they may mimic the transition state of the glycosylation reaction. Nine irreversible peptidyl inactivators for OT were also evaluated; these affinity labels were designed to probe the peptide binding site of the enzyme. Based on the results with these inactivators, a proposal for the design of more potent affinity labels for OT is presented.

Table of Contents

List of Figures

Chapter 1

Chapter 2

Chapter 3

Chapter 4

Chapter 5

Appendix B

Appendix C

List of Tables

Chapter 1

Chapter 2

Chapter 3

Chapter 4

Abbreviations Used

Standard one and three letter codes are used for the naturally occurring amino acids.

Aa	Amino acid
Ac	Acetyl
AcAnh	Acetic anhydride
Aib	α-Aminoisobutyric acid
AEBSF	4-(2-Aminoethyl)-benzenesulfonylfluoride
AIBN	Azoisobutyronitrile
Amb	γ-Aminobutyrine
Asn(γS)	Thioasparagine
BMTS	*N*-Biotinoyl(aminoethane)thiolsulfonate
Boc	*tert*-Butoxycarbonyl
Bz	Benzoyl
BzAnh	Benzoic anhydride
Cbz	*N*-Benzyloxycarbonyl
CD	Circular dichroism
DCC	*N,N'*-Dicyclohexylcarbodiimide
DCM	Dichloromethane
DCU	*N,N'*-Dicyclohexylurea
DEPC	Diethylpyrocarbonate
DIPCDI	Diisopropylcarbodiimide
DMF	Dimethylformamide
DMSO	Dimethylsulfoxide
Dns	Dansyl

Dol	Dolichol
Dol-P	Dolichol phosphate
Dol-P-P	Dolichol pyrophosphate
Dpm	Disintegrations per minute
DTNB	5,5'-Dithiobis-(2-nitrobenzoic acid)
DTT	Dithiothreitol
EDTA	Ethylenediaminetetraacetic acid
ER	Endoplasmic reticulum
FAB	Fast atom bombardment
FET	Fluorescence energy transfer
Fmoc	9-Fluorenylmethoxycarbonyl
GalNAc	*N*-Acetylgalactosamine
Glc	Glucose
GlcNAc	*N*-Acetylglucosamine
GPI	Glycosyl phosphatidyl inositol
HEPES	*N*-[2-Hydroxyethyl]-piperazine-*N'*-2-ethanesulfonic acid
HF	Hydrofluoric acid
HOBT	5-Hydroxybenzotriazole
HPLC	High performance liquid chromatography
Hse	L-Homoserine
IAA	Iodoacetic acid
IAM	Iodoacetamide
isoAsn	Isoasparagine
Leu	Leucine
MALDI	Matrix assisted laser desorbtion ionization
Man	Mannose
m-CPBA	*m*-Chloroperbenzoic acid

α-MeMan	α-Methylmannopyranoside
MES	2-[*N*-Morpholino]ethane sulfonic acid
MMTS	Methyl methanethiolsulfonate
MS	Mass spectroscopy
NEM	*N*-Ethylmaleimide
NMR	Nuclear magnetic resonance
NOE	Nuclear Overhauser enhancements
OBn	Benzyl ether
Orn	Ornithine
OT	Oligosaccharyl transferase
PAGE	Polyacrylamide gel electrophoresis
PCMBS	*p*-Chloromercuribenzenesulfonic acid
PC	Phosphatidylcholine
PMSF	Phenylmethylsulfonyl fluoride
OpNP	*p*-Nitrophenyl ester
SDS	Sodium dodecyl sulfate
SuccAnh	Succininc anhydride
TBDMS	*tert*-butyldimethylsilyl
TFA	Trifluoroacetic acid
THF	Tetrahydrofuran
TLC	Thin layer chromatography
Tris	Tris(hydroxymethyl)aminomethane
TUP	Theoretical upper phase
UDP	Uridine diphosphate
UDP-GalNAc	Uridine diphosphate-*N*-acetylgalactosamine

Chapter 1. Asparagine-Linked Glycosylation

1.1 Introduction

Glycosylation is potentially the most complex category of protein modification reactions within eukaryotic systems.[1] An incredible degree of diversity is introduced into glycoproteins by the wide array of monosaccharides available as well as by the potential for different chemical linkages between each pair of carbohydrates.[2] The size of each oligosaccharide chain in glycoproteins can vary greatly, ranging from a single monosaccharide to complex, branched structures comprising of as many as 15 to 40 sugars. In addition, many proteins are glycosylated at multiple sites with different carbohydrate groups; more than twenty terminal oligosaccharide sequences are available and can be used in combination to generate further diversity.[3] In many cases, this structural diversity defines the biological role of each of the modified proteins. Glycoproteins have been implicated in such varied processes as the immune response,[4] proper intracellular targeting,[5] intercellular recognition,[6] and protein folding, stability and solubility.[7-10] These functions are often modulated by the structure of both the oligosaccharide and the protein. An understanding of the biosynthesis of glycoproteins is of intense interest because of the diversity displayed by these critical biomolecules.

The most common forms of protein-carbohydrate modifications fall into three general categories: *N*-linked modification of asparagine, *O*-linked modification of serine or threonine, and glycosylphosphatidyl inositol derivatization of the C-terminus carboxyl group (Figure 1-1).[11] Each of these transformations is catalyzed by one or more enzymes which demonstrate different peptide sequence requirements and reaction specificities. *N*-linked glycosylation is catalyzed by a single enzyme, oligosaccharyl transferase (OT), and involves the co-translational transfer of a lipid-linked tetradecasaccharide ($GlcNAc_2$-Man_9-Glc_3) to an asparagine side chain within a nascent polypeptide.

The subsequent diversification of these conjugates arises from enzyme catalyzed processing steps that occur in the endoplasmic reticulum (ER) and Golgi apparatus *after* the addition of the first triantennary oligosaccharide complex.

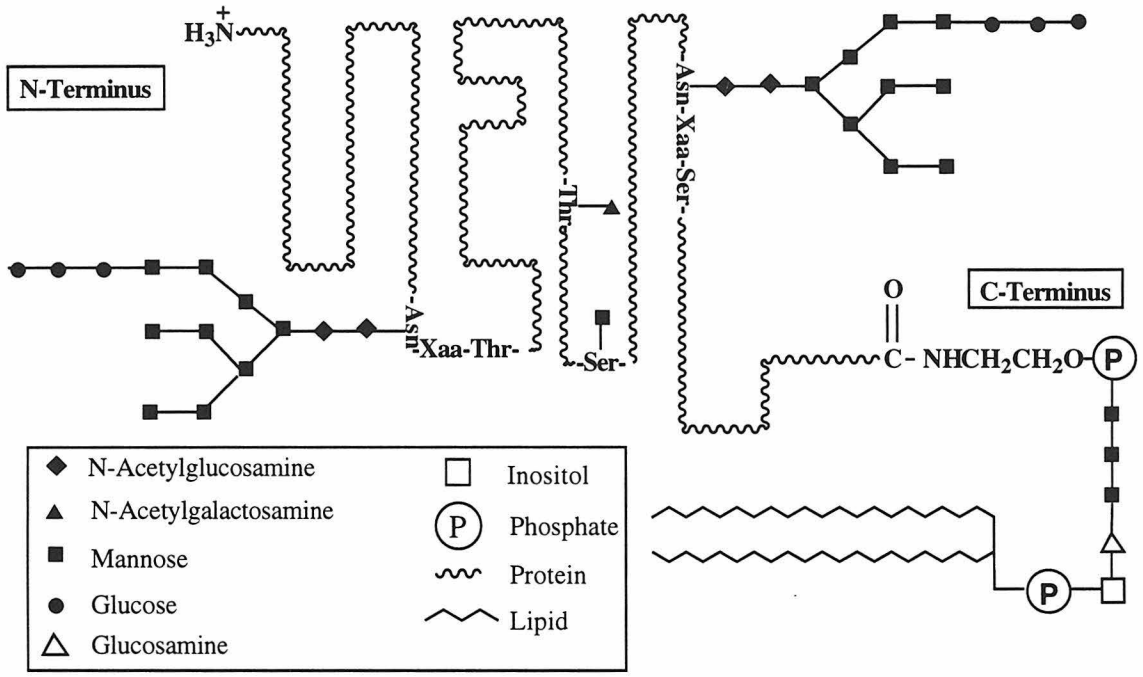

Figure 1-1. A Schematic Representation of the Major Types of Carbohydrate-Protein Linkages. The core oligosaccharide structures (shown here) can be further modified through the addition of new monosaccharides or the cleavage of terminal saccharides.

In contrast, *O*-linked glycosylation proceeds through the direct, post-translational transfer of single monosaccharides to threonine and/or serine residues within folded polypeptides. In general, the peptide sequence specificities of the *O*-linked glycosylation enzymes are not well understood[12] and activity is attributed to several different enzymes. For example, the principal mode of *O*-linked glycosylation in yeast involves the transfer of a single mannose from the lipid-linked donor dolichol phosphate mannose (Dol-P-Man) to a

hydroxy amino acid,[13] while one example of *O*-linked glycosylation in mammalian systems involves the transfer of an *N*-acetylgalactosamine residue from uridine diphosphate-*N*-acetylgalactosamine (UDP-GalNAc) to threonine.[14,15] *O*-linked glycoprotein modifications with xylose and fucose residues have also been observed in mammalian systems (not shown in Figure 1-1).[16,17]

Proteins can also be modified with a complex glycosylphosphatidyl inositol (GPI) construct at the polypeptide carboxyl terminus; this derivatization confers new properties by anchoring the protein to membrane bilayers.[18] Substrates for GPI modification must terminate with one of six amino acids: Cys, Asp, Asn, Gly, Ala, or Ser.[19] The α-carboxylic acid of these polypeptides is modified by an ethanolamine phosphate which is attached to a glycan with the sequence Man-α1,2-Man-α1,6-Man-α1,4-$GlcNH_2$. The terminal glucosamine of this tetrasaccharide is attached to the C-6 of a *myo*-inositol ring which is linked to a diglyceride through a phosphate. The core structure, ethanolamine phosphate-Man-α1,2-Man-α1,6-Man-α1,4-$GlcNH_2$-*myo*-inositol phosphate-diglyceride is conserved, however the length of the glyceride chains is variable. Further alterations of this sequence follow the initial modification and can include the addition of a second ethanolamine phosphate, additional monosaccharides, or the palmitoylation of the *myo*-inositol.[19]

Following protein glycosylation, the core oligosaccharide structures are subject to a sophisticated array of glycosyl transferase and hydrolase enzymes. For example, in the case of *N*-linked glycosylation, following transfer to an asparagine residue within the protein, the core tetradecasaccharide $GlcNAc_2$-Man_9-Glc_3 is immediately processed in a series of reactions which cleave the three terminal glucose and four mannose residues. This processed glycoprotein is subsequently translocated to the Golgi where glycosyl transferases catalyze the

elaboration of the glycoprotein through the transfer of additional monosaccharides such as fucose, galactose and sialic acid from the corresponding nucleotide diphosphates. These reactions act in concert to produce the diverse *N*-linked glycoconjugate structures characteristic of mature proteins.[20] The final oligosaccharide sequence often determines the cellular destination of the assembled glycoprotein. It is estimated that 100-200 glycosyl transferases are required to generate the diversity observed within glycoproteins.[5,21,22] Several of the enzymes involved in the assembly and cleavage of extended oligosaccharides have been isolated and characterized and significant progress has been made in developing a mechanistic understanding of these processes.[23,24] In contrast to carbohydrate trimming and elongation, details pertaining to the mechanism of the transfer of carbohydrate groups to the side chains of amino acids within proteins is less well understood. In particular, how do the enzymes involved in these processes mediate transfer to the target amino acid side chain in the presence of much more reactive moieties within the protein? Also, what factors govern the specificities of these transfers, as not all seemingly acceptable sequences undergo glycosylation? The mechanism of transfer to asparagine side chains is one of the most intriguing glycosylation reactions in this regard because of the seemingly inherent lack of reactivity of the carboxamide side chain.

This introductory chapter presents a summary of the current literature on oligosaccharyl transferase, the enzyme that catalyzes asparagine-linked glycosylation. Specifically, recent advances in the purification and characterization of the enzymatic complex, mechanistic and conformational elucidation of the reaction process and the conformational consequences of asparagine glycosylation will be discussed. Finally, a summary of the thesis research presented in this dissertation and how it contributes to the current understanding of this complex enzymatic system will be outlined.

1.2 Asparagine-Linked Glycosylation

Oligosaccharyl transferase is a membrane associated, multimeric enzyme localized in the lumen of the endoplasmic reticulum. In the reaction catalyzed by OT, illustrated in Figure 1-2, a complex oligosaccharide is transferred from a lipid-linked pyrophosphate donor (**1**) to a nascent polypeptide chain as the peptide is translocated into the lumen of the endoplasmic reticulum. The peptide primary sequence requirements for glycosylation are minimal; the asparagine must reside within the consensus sequence Asn-Xaa-Thr/Ser (NXT/S) where Xaa can be any of the 20 natural amino acids except proline.[25-27] *In vivo*, threonine-containing sequences are almost 3 times more likely to be glycosylated than the corresponding serine-containing analogs.[28] However, the efficiency of NXT glycosylation *in vitro* exceeds that of NXS sequences by as much as 40 fold.[29] This first step in the *N*-linked glycosylation process appears to be conserved throughout eukaryotic evolution.[30]

1.3 Biochemical Characterization of Oligosaccharyl Transferase

Future research on the mechanism of action of OT will be greatly facilitated by the availability of a significant quantity of pure enzyme; however, purification efforts towards this end have been hindered by the inherent lability of enzyme activity during solubilization. Recently, significant advances have been made in achieving stable enzyme extracts, through the addition of phosphatidylcholine (PC),[31] sucrose or glycerol. In the presence of these additives, several research groups have succeeded in purifying OT to homogeneity; sequencing and analysis of several of the subunits have also been accomplished. OT has been purified from three mammalian sources (canine pancreas,[32] porcine liver microsomes[33] and human liver microsomes[34]), one avian source (hen oviduct microsomes),[35] and the yeast *S. cerevisiae*.[30,36,37]

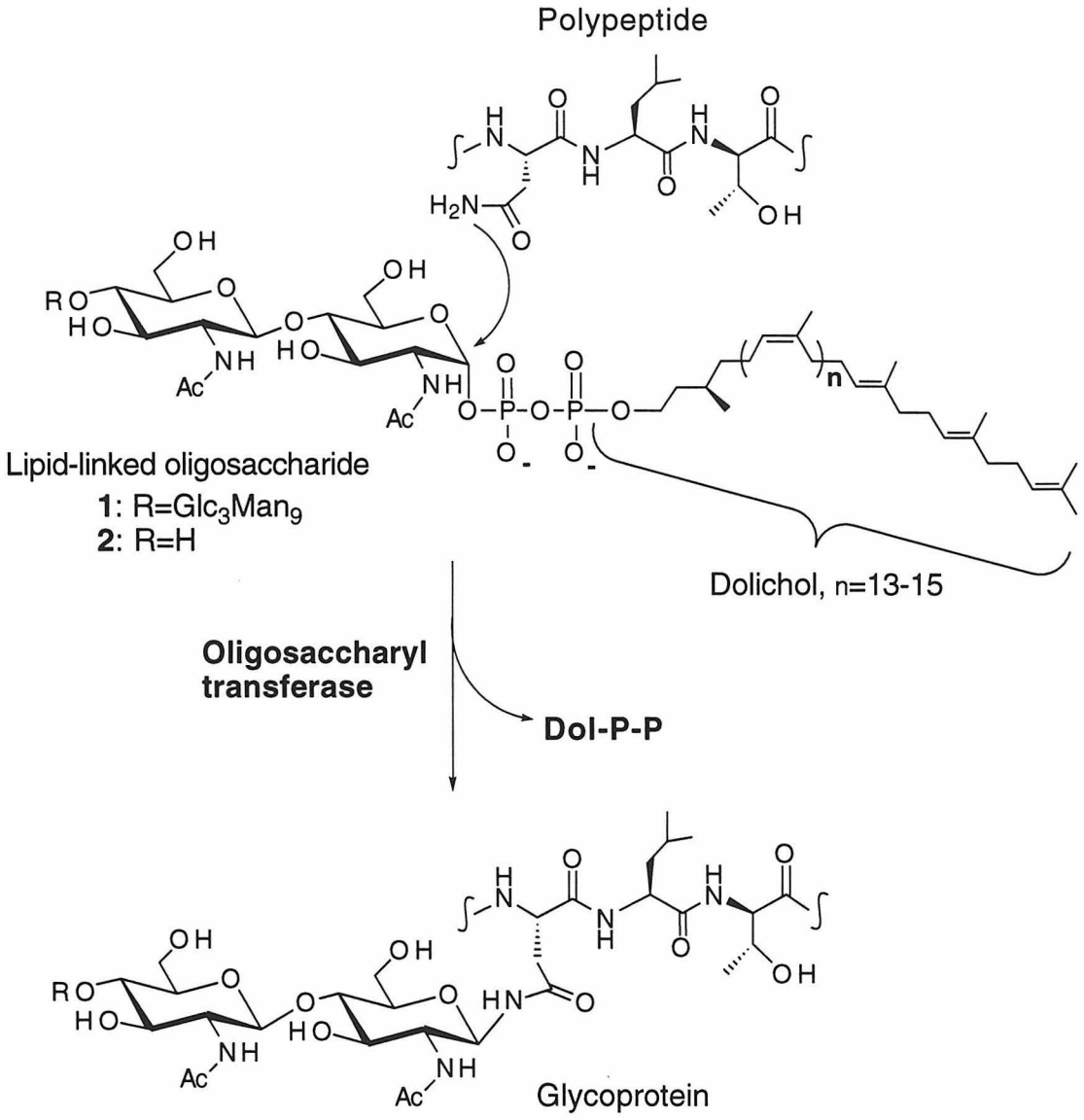

Figure 1-2. The Glycosylation Reaction Catalyzed by Oligosaccharyl Transferase.

Comparison of the protein subunits from each of these purifications evidences a high degree of conservation throughout evolution (see Table 1-1). In fact, a subunit of OT, from the insect *Drosophila melananogaster*, has recently been identified and sequenced using a PCR-mediated cloning strategy guided by the conserved regions of the canine and yeast enzymes.[38]

Table 1-1 - Comparison of Genetically Characterized Subunits of OT Isolated from Different Sources.

Mammalian (Canine[32,39]/Porcine[33]/ Human[34])	Avian Oviduct[35]	Yeast (*S. cerevisiae*)[40,41]
Ribophorin I (66/66/65 kDa)	Ribophorin I (65 kDa)	Nlt1p/Ost1p (64 kDa)
Ribophorin II (63/63/65 kDa)	Ribophorin II (65 kDa)	Swp1p (30 kDa)
OST48 (48/48/50 kDa)	OST48 (50 kDa)	Wbp1p (45 kDa)

The first purification reported was that of the canine pancreas enzyme which was isolated as a trimeric complex of polypeptides with molecular weights of 66, 63 and 48 kDa.[32] The 48 kDa polypeptide has been designated as OST48 and is not homologous with any known proteins. Sequence comparisons and protein immunoblotting of the 66 and 63 kDa subunits demonstrated that they are identical to Ribophorin I and Ribophorin II respectively (two previously identified integral membrane proteins found only in the rough endoplasmic reticulum). The porcine liver OT has been purified as a tetrameric complex of polypeptides and is similar to the canine pancreatic enzyme.[33] Ribophorin I, Ribophorin II and OST48 have all been identified, as well as an additional 40 kDa polypeptide not observed in the canine enzyme complex. Further purification to a dimeric complex of OST48 and Ribophorin I yielded an unstable enzyme with

partial activity. Treatment of this dimer with trypsin demonstrated that Ribophorin I was more susceptible to proteolysis than OST48; partial activity was retained during proteolysis suggesting that OST48 is the catalytically competent subunit. However, this experiment does not rule out the participation of a proteolytic fragment of Ribophorin I. The remaining two subunits, Ribophorin II and the 40 kDa polypeptide, are suggested to be involved in stabilizing the enzymatic complex.[33]

Similar to the canine enzyme, the avian OT enzyme was purified as a trimeric complex of polypeptides with molecular weights of 65, 65 and 50 kDa.[35] The 50 kDa polypeptide was completely sequenced by overlaying peptide fragments obtained from cleavage by various different enzymatic and chemical methods. This sequence was found to be 92% identical to OST48. The two 65 kDa fragments were resistant to *N*-terminal sequencing, but cyanogen bromide cleavage followed by separation and sequencing of several fragments suggests that these two polypeptides correspond to Ribophorin I and Ribophorin II. The human OT enzyme was purified from liver microsomes and found to contain three subunits, identified as Ribophorin I (66kDa), Ribophorin II (63 kDa) and a third subunit with a molecular weight of 50 kDa which was found to be 98% identical to the canine OST48.[34]

The multimeric enzyme complex in yeast has been isolated as both a tetrameric and a hexameric complex of polypeptides.[30,36,37] Two of the subunits have been identified as Wbp1p and Swp1p, with molecular weights of 45 and 30 kDa, respectively. The remaining polypeptides have molecular weights of 64 and 34 kDa in the tetrameric complex[30,36] and 64, 34, 16, and 9 kDa in the hexameric complex.[37] Independent depletion studies have indicated that both Wbp1p and Swp1p are absolutely required for *in vivo* and *in vitro* OT activity.[42,43] Additionally, these two subunits can be chemically crosslinked suggesting that

the polypeptides are members of the same multisubunit complex.[43] The 34 kDa subunit, Ost3p, is not essential for glycosylation; however, deletion of this subunit produces an impaired oligosaccharyl transferase complex which selectively underglycosylates membrane bound proteins.[44] Ost2p, the 16 kDa subunit, is essential for yeast viability and mutations in this subunit have been shown to produce an enzyme complex with decreased *in vitro* activity.[45] Comparison of the yeast and mammalian enzyme complexes reveals a remarkable degree of similarity: Wbp1p exhibits 25% sequence homology to OST48;[39] the 64 kDa polypeptide, designated Nlt1p or Ost1p, is homologous to Ribophorin I;[30,36,40] Swp1p is similar to the carboxyl-terminal half of Ribophorin II;[37] a peptide which would be analogous to the amino-terminal half of Ribophorin II has not yet been identified in yeast.

Five of the subunits of the yeast enzyme complex, Wbp1p,[46] Swp1p,[43] Ost1p[40]/Nlt1p[36] Ost2p,[45] and Ost3p[44] have been sequenced and characterized. The results of these studies are summarized in Figure 1-3. Each of the subunits contains at least one C-terminal hydrophobic domain. Additionally, four of the polypeptides include an amino terminus signal sequence (17-20 amino acids) which is cleaved prior to complete maturation of the protein; Ost2p does not contain a signal sequence, suggesting that the *N*-terminus of this subunit is located in the cytosol.[45] Wbp1p and Nlt1p are both multiply glycosylated with *N*-linked high mannose oligosaccharides, indicating that mature OT is a self-processing enzyme.[37] In fact, concanavalin A (a high mannose binding lectin) was successfully used to partially purify OT in two of the procedures described above.[36,37] Ost3p contains one potential *N*-linked glycosylation site, but this site does not appear to be glycosylated.[44]

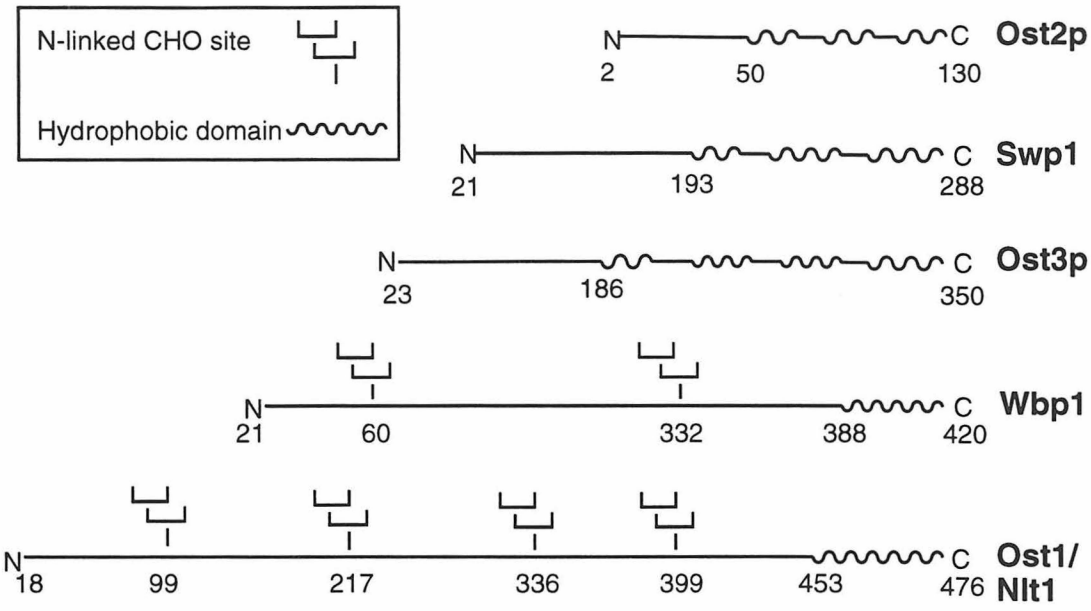

Ost2p
130aa,
Terminal Met removed
Three short *C*-terminal
hydrophobic domains

Swp1
288aa,
20aa signal peptide removed
Three short *C*-terminal
hydrophobic domains

Ost3p
350aa,
22aa signal peptide removed
Four *C*-terminal
hydrophobic domains
Not essential for viability

Wbp1
420aa
20aa signal peptide removed
One *C*-terminal hydrophobic domain
KKTN ER retention sequence

Ost1/Nlt1
476aa
17aa signal peptide removed
One *C*-terminal hydrophobic
domain

Figure 1-3. A Schematic Representation of the Oligosaccharyl Transferase Subunits Characterized to Date.[40-45]

1.4 Substrates for *N*-linked Glycosylation

1.4.1 Lipid-Linked Oligosaccharide Donor

The normal physiological glycosylation process results in the transfer of a triantennary branched oligosaccharide made up from two *N*-acetyl glucosamine, nine mannose and three glucose residues (**1**, Dol-P-P-$GlcNAc_2$-Man_9-Glc_3, Figure 1-2).[47,48] This tetradecasaccharide derivative is biosynthesized through a series of stepwise transfers to dolichol phosphate before being transferred *en bloc* to the peptide acceptor.[49,50] The first step in the biosynthesis of the lipid-linked donor involves transfer of a single *N*-acetyl glucosamine from UDP-GlcNAc to dolichol phosphate and the formation of a pyrophosphate bond with concomitant release of UMP. The second GlcNAc is subsequently transferred to the newly formed Dolichol-P-P-GlcNAc in a reaction that results in the formation of a β-1,4-glycosidic linkage. The remaining 12 sugars are subsequently added to this lipid-linked disaccharide. The first five mannose residues are directly transferred from GDP-Man, while the last four mannose residues, as well as the terminal glucose residues (from UDP-Glc) are added *via* the intermediacy of a dolichol phosphate derivative before being added to the assembling glycolipid. The oligosaccharide of the final glycolipid is located on the lumenal side of the ER.[51,52]

Although the substrate recognized by OT *in vivo* is a complex tetradecasaccharide, the enzyme catalyzed reaction *in vitro* proceeds with similar efficiencies utilizing simpler truncated substrates such as the di-*N*-acetylglucosamine derivative **2**, (Dol-P-P-$GlcNAc_2$, Figure 1-2) and Dol-P-P-$GlcNAc_2$-Man_1. However, the lipid-linked monosaccharide Dol-P-P-GlcNAc is not a substrate for the solubilized enzyme.[50] The ability of OT to readily utilize a simple lipid-linked disaccharide as the carbohydrate donor in the glycosylation of asparagine residues has greatly facilitated the study of this enzyme. These

truncated substrates are accessible through synthetic and enzymatic methods and radiolabeled monosaccharides can be incorporated into the desired compounds for enzymatic assays. The chitobiosyl analog **2** has been chemically synthesized by two different methods.[53,54] These synthetic methods are hindered by availability of reactants and difficulty in purification. Compound **2** has also been prepared enzymatically by incubating liver microsomes with radiolabeled UDP-GlcNAc in the presence of divalent magnesium. The reactions catalyzed by the microsomal enzymes are as follows:

$$\text{Dol-P} + \text{UDP-GlcNAc} \xrightarrow{\text{Enzyme I}} \text{Dol-P-P-GlcNAc} + \text{UMP}$$

$$\text{Dol-P-P-GlcNAc} + \text{UDP-GlcNAc} \xrightarrow{\text{Enzyme II}} \text{Dol-P-P-(GlcNAc)}_2 + \text{UDP}$$

(2)

The biosynthesis of **2** from dolichol phosphate and UDP-GlcNAc appears to be limited due to low conversions to the desired lipid-linked mono- and disaccharides. This technical problem has recently been overcome by applying a combination of chemical and enzymatic methods. Efficient preparations of lipid-linked substrates for assaying *N*-linked glycosylation are generated by treating synthetic Dol-P-P-GlcNAc with UDP-GlcNAc, in the presence of divalent magnesium and liver microsomes.[55] This process results in conversions in excess of 60% and allows for the selective incorporation of radiolabeled GlcNAc (^{3}H at C-6) at the terminal saccharide position; the specific activity of the substrate can therefore be varied as needed.

1.4.2 Peptide Acceptor

The second substrate for *N*-linked glycosylation is a nascent polypeptide chain containing an asparagine residue within an NXT/S consensus sequence. As previously stated, OT does not accept peptides which contain proline as the middle residue in the NXT/S triad. The exclusion of NPT/S sequences suggests that local secondary structure plays an important role in determining the outcome of glycosylation. This theory is further underscored by the fact that 10-30% of all NXT/S sequences remain unglycosylated in mature proteins, even though they meet the primary sequence requirements.[28,56] Proteins that are destined for glycosylation are synthesized by membrane-associated ribosomes with an initial signal peptide (approximately 16 residues) which guides the newly synthesized protein through the intracellular membrane bilayer into the lumen of the endoplasmic reticulum (ER). The signal peptide is subsequently cleaved by a signal peptidase. The NXT/S sequence must clear the lumenal side of the membrane bilayer by 12-14 residues before glycosylation can occur; however, the nascent polypeptide remains bound to the membrane of the ER and is likely to be only locally folded during OT mediated catalysis.[57] In fact, a direct correlation between *lack* of tertiary structure and glycosylation acceptor ability has been observed by subjecting unglycosylated NXT/S sequences in native proteins to varying levels of reducing and denaturing conditions and then reexamining these unfolded proteins for substrate behavior with OT. In many cases, the proteins did not exhibit any glycosyl acceptor properties prior to unfolding; however, three out of seven of the proteins examined were efficiently glycosylated following sulfitolysis.[58]

In the cellular process, OT recognizes an extended peptide sequence as it crosses the membrane bilayer; however, the tripeptide recognition sequence is sufficient for *in vitro* glycosylation, provided the two termini are capped by

protecting groups which mimic the amide backbone of an extended peptide. With synthetic tripeptides, OT will glycosylate peptides capped with benzoyl (Bz), octanoyl, butanoyl, acetyl (Ac), carbobenzyloxy (Cbz) and *tert*-butoxycarbonyl (Boc) groups at the amino terminus, although the carbamate modifications of the Cbz and Boc groups yield very poor substrates.[59-62] The carboxy terminus is most effectively protected as a primary or secondary amide, although methyl esters are tolerated. The tripeptide Bz-Asn-Leu-Thr-NHMe (**3**, Bz-NLT-NHMe), where the amino terminus has been protected with a benzoyl group and the carboxy terminus as a methyl amide, is an effective synthetic tripeptide for *in vitro* investigations.[62]

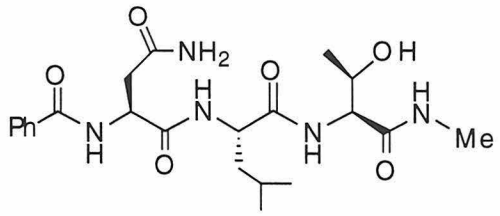

3

The tripeptide consensus sequence has been thoroughly investigated by selective replacement of each amino acid with key natural and synthetic amino acids and reexamination of the substrate behavior of the new tripeptide analog. These studies have revealed that the first position in the sequence almost invariably requires an asparagine residue. Tripeptides containing glutamine or N^{δ}–methylasparagine are not tolerated by the enzyme nor do they inhibit the glycosylation of natural sequences.[62] Tripeptides containing β-fluoroasparagine are very poorly glycosylated, at a rate of less than 2% that of Bz-Asn-Leu-Thr-NHMe (**3**).[63] However, the enzyme has been shown to tolerate a tripeptide which contains a thioasparagine [Asn(γ*S*)] residue in the first position. This compound exhibits a similar K_{Mapp}, but has a greatly reduced V_{max} when

compared to Bz-Asn-Leu-Thr-NHMe.[64] The second position in the consensus tripeptide may include most of the 20 natural amino acids except proline; in addition, incorporation of aspartic acid as the center residue depresses glycosyl acceptor efficiency. The unnatural amino acids α-aminoisobutryic acid and D-alanine in the central position are not recognized.[59] The third position, a hydroxy amino acid in the natural substrate sequences, is also invariant. Tripeptides containing Val,[29] Thr(β-OMe),[29,65] β-hydroxynorvaline[66] and *allo*-Thr[67] in the C-terminal position are not recognized by OT. Peptides which incorporate cysteine in this position show a low, but measurable, level of glycosyl acceptor activity.

1.5 Conformational Requirements for *N*-Linked Glycosylation

Oligosaccharyl transferase exhibits a simple requirement for peptidyl substrates containing the NXT/S consensus sequence, yet it catalyzes an unusual and specific reaction wherein the nucleophilicity of the asparagine side chain is greatly enhanced. In addition to the asparagine residue, the absolute requirement for an unmodified hydroxyl amino acid implies a direct role for the hydroxyl group in catalysis. Beyond these straightforward tripeptide requirements, additional features are important since many seemingly acceptable NXT/S sequences still remain unglycosylated following translation and translocation into the lumen of the ER.[28,56] Understanding the potential role of substrate conformation in contributing to the specificity of the reaction is a prerequisite for developing a satisfactory mechanistic model. At the time of glycosylation, the peptide substrate is relatively free of tertiary structure, although local secondary structural motifs are still available as recognition elements. Since tripeptides are accepted as substrates, the length of the consensus triad limits the types of available hydrogen-bonded motifs to simple

turns, since other structural features such as α-helices or β-sheets tend to require longer peptides for complete formation. Tripeptide substrates are most readily compatible with two types of turns: The β-turn and the Asx-turn. These two turns are illustrated in Figure 1-4 for the peptide Ac-Asn-Xaa-Thr-NHMe.

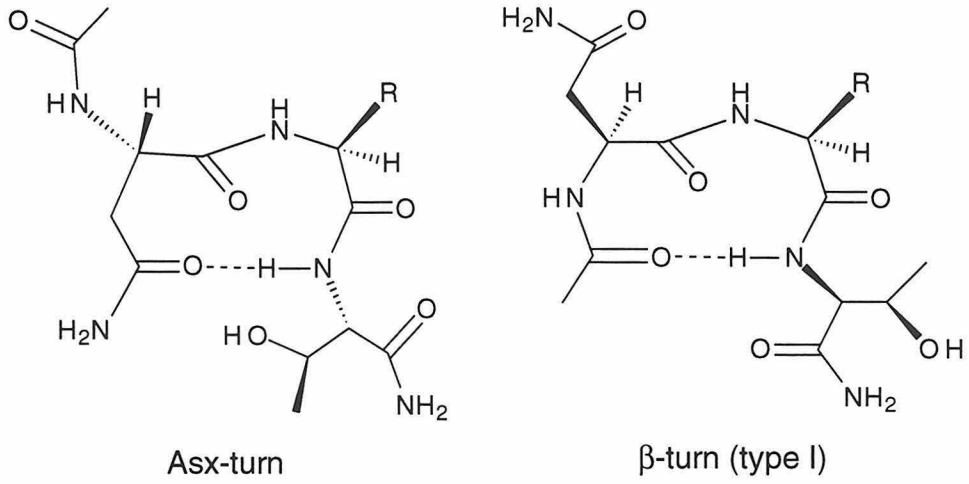

Figure 1-4. A Comparison Between an Asx-Turn and a β-Turn for the Tripeptide Ac-Asn-Xaa-Thr-NH_2.

The β-turn results in a complete chain reversal, and is characterized by a hydrogen bond between the threonine amide and the carbonyl of the residue immediately preceeding the asparagine. In the case of Ac-Asn-Xaa-Thr-NHMe (Figure 1-4), the hydrogen-bonding carbonyl is provided by the acetyl group. The Asx-turn involves a hydrogen-bonding array similar to that of a β-turn; however, in this case, the hydrogen bond acceptor is the carbonyl oxygen of the asparagine side chain. The polypeptide backbone has a more extended conformation and does not experience a complete chain reversal. Approximately 18% of all asparagine and aspartic acid side chains appear to be involved in Asx-turns in proteins.[68] In fact, a statistical survey of globular proteins by Baker *et*

al.[69] indicates that 55% of all hydrogen bonds to the carbonyl side chain of asparagine residues are provided by the backbone NH of the (*i*+2) residue. It is noteworthy that the homologous residue glutamine is never glycosylated and this apparent contradiction in reactivity may be explained by the distinct conformational preferences of this residue. Specifically, the carboxamide side chain of glutamine is seldom involved in short range hydrogen-bonding interactions. The possibility that the Asx-turn or the β-turn is the unique secondary motif preferentially recognized by OT has been considered as an explanation for both the specificity of the enzyme and the enhanced nucleophilicity of the peptidyl substrate, particularly in model mechanisms which rely on secondary structure to position the hydroxyl moiety within direct proximity to the asparagine side chain.[25,26,64]

The ability of OT to recognize and glycosylate short peptidyl substrates has enabled researchers to investigate the structural requirements for glycosylation by designing molecules which contain all of the recognition elements of the consensus sequence, but which are constrained or restricted to specific conformations. Kinetic analyses of these compounds have provided a detailed understanding of the role of conformation in asparagine-linked glycosylation.

Initial studies correlating substrate acceptor properties and solution state conformation suggested that the Asx-turn might be the key recognition motif.[59] To rigorously distinguish between the Asx-turn and the β-turn, a study was carried out which placed the reactive tripeptide sequence with asparagine in either the (*i*) or (*i* + *1*) position of a constrained type I β-turn that had been built into the architecture of a cyclic hexapeptide (**4a** and **4b**).[60] The type I β-turn was fixed by the incorporation of a prolyl-D-amino acid dipeptide at the non-reactive end of the cyclic compound. This dipeptide sequence imposes a constrained type

II β-turn in the cyclic peptide and therefore limits the conformations accessible to the stucture.[70]

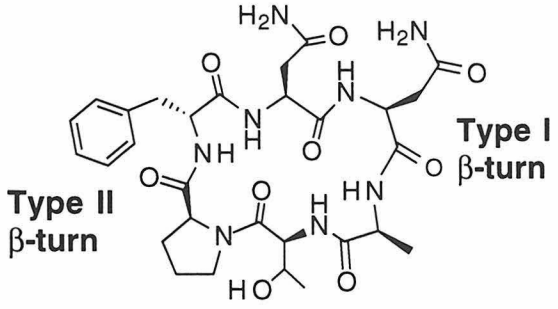

4a

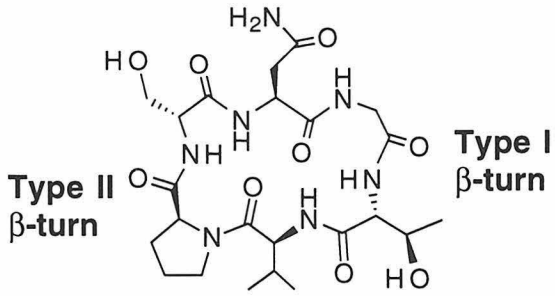

4b

One and two dimensional NMR studies were utilized to verify the turn conformations of compounds **4a** and **4b**. These two compounds were assayed for substrate activity with OT and compared to the activities of two standard peptides, Ac-Asn-Leu-Thr-OMe and Ac-Asn-Leu-Thr-NHMe. The results of these studies are summarized in Table 1-2. With the reactive asparagine conformationally constrained into a β-turn (as in compounds **4a** and **4b**), the resultant peptides did not exhibit any detectable substrate behavior with OT.

Table 1-2 - Kinetic Analysis of Conformationally Constrained Peptides with Porcine Liver OT[60]

Peptide	Apparent K_M(mM)	Relative V (%)[a]
Ac-Asn-Leu-Thr-OMe	6.7	100
Ac-Asn-Leu-Thr-NHMe	0.3	150
c(Pro-D-Ser-Asn-Gly-Thr-Val) (**6a**)	>20	
c(Pro-D-Phe-Asn-Asn-Ala-Thr) (**6b**)	>20	

[a]Ac-Asn-Leu-Thr-OMe as standard

In complementary studies, a constrained Asx-turn was incorporated into a cyclic NXT sequence, c[Asn-Add]-Thr-NHMe (**5**), through a side chain to main chain lactam cyclization. An unnatural amino acid, (*S*)-2-aminodecanedioic acid (Add), was utilized in the central position to provide functionality for cyclization with the amino terminus.[71] This cyclization was selected because modeling studies indicated that it would constrain the critical Asn ψ and Xaa ϕ dihedral angles to generate an Asx-turn. The presence of an Asx-turn was confirmed through NMR experiments on an aqueous solution of the peptide (43% methanol). The peptide was analyzed for substrate activity with OT and compared to the linear analog, N^{α}-Butanoyl-Asn-Leu-Thr-NHMe (**6**). Introduction of a cyclic constraint improved the K_M tenfold, from 800 μM for **6** to 78 μM for **5**, indicating that the preorganization provided by the Asx-turn enhanced enzyme/substrate affinity. The relative maximal velocities of the two compounds remained similar. The enhancement of enzyme affinity for the constrained peptide, **5**, with a well-defined Asx-turn conformation firmly demonstrates the importance of the Asx-turn over the β-turn, as the recognition motif for OT.

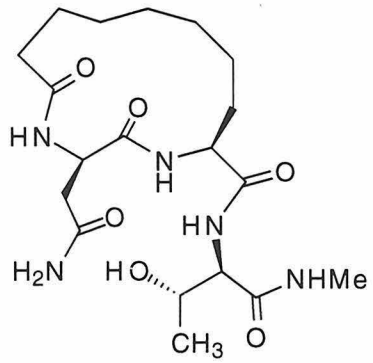

5

6: N^{α}-Butanoyl-Asn-Leu-Thr-NHMe
7: N^{α}-Butanoyl-Gln-Leu-Thr-NHMe

In addition, circular dichroism (CD) studies were carried out on **5**, **6** and N^{α}-Butanoyl-Gln-Leu-Thr-NHMe (**7**). The spectrum obtained for **7**, which is not a substrate for OT, resembled that of a random coil (Figure 1-5) with a strong negative ellipticity at 198 nM. However, the CD spectrum for **5** was quite distinct, with a greatly diminished negative ellipticity at 198 nm and a strong signal at 218 nm, providing complementary spectroscopic evidence of the ordered secondary structure promoted by the cyclic constraint. These results were independent of the solution composition which was varied from 2%-43% methanol in water. While the CD spectrum for **6** was primarily random coil, a small signal was present at 218 nm indicating the presence of some secondary structure.[71]

Previous studies by Bause[72] had examined the effects of disulfide constraints on glycosylation acceptor properties. In all cases where the presence of the disulfide enhanced a β-turn structure, glycosyl acceptor properties diminished. In light of the proposal that an Asx-turn is the recognition motif for *N*-linked glycosylation, reexamination of the Bause results support the hypothesis that acceptor ability of an NXT sequence is related to peptides which can access an Asx-turn motif. With a complete understanding of the necessary secondary structural features required for *N*-linked glycosylation, mechanistic investigations can be designed to consider the roles of the hydroxy amino acid and the amide backbone in enhancing the nucleophilicity of the asparagine side chain.

1.6 Mechanistic Considerations

To complete *N*-linked glycosylation, cooperation between OT and the hydrogen-bonding array provided by the peptidyl substrate results in the activation of a normally non-nucleophilic amino acid. Currently, the generation

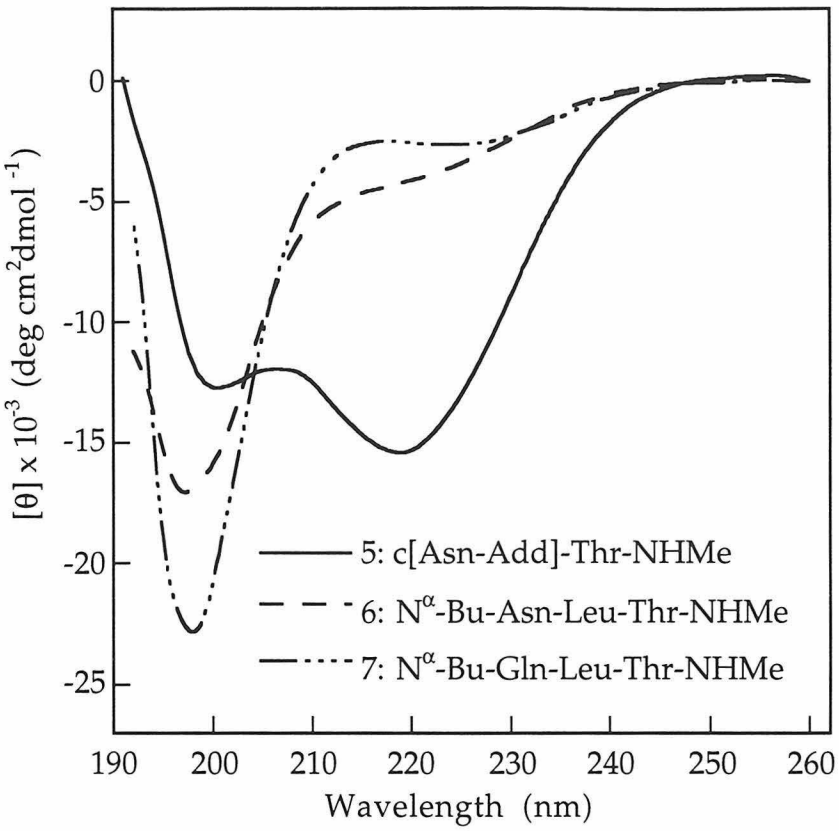

Figure 1-5. CD Spectra of Constrained and Linear Tripeptide Substrates for Oligosaccharyl Transferase.[71] Samples were prepared by dissolving each tripeptide in a 40% methanol/water solution at pH 4.5. In each case, the final peptide concentration was 500 μM.

of this unusual reactivity is the main focus of mechanistic investigations. Evidence in support of or against different mechanistic proposals is most readily obtained by examining the kinetic properties of substrate analogs. By selectively altering different features of a natural substrate to generate a nonnatural substrate or an inhibitor, information about specific features of the active site, or of the reaction intermediates, can be surmised.

Initially, Marshall[25] proposed that the acidity of one of the asparagine amide protons is increased by the presence of a hydrogen bond between the hydroxyl moiety of the threonine or serine and the carbonyl of the carboxamide side chain (Figure 1-6A). This interaction would increase the acidity of the carboxamide protons and thereby facilitate ionization to affording a nucleophilic anionic nitrogen species that could subsequently engage in the glycosylation event. Bause[29] proposed a different hydrogen-bonding array wherein one of the carboxamide protons of the asparagine side chain serves as a proton donor to the hydroxyl group of the threonine or serine, thus increasing the nucleophilicity of the carboxamide nitrogen (Figure 1-6B). Both of these mechanisms rely on the ability of the tripeptide substrate to position the hydroxyl moiety within hydrogen-bonding distance of the asparagine side chain.

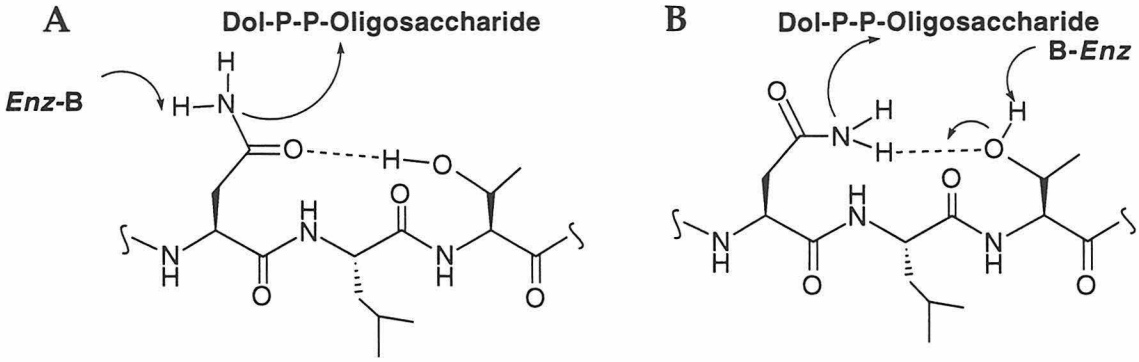

Figure 1-6. Schematic Representations of Two Different Peptide Activation Mechanisms for Oligosaccharyl Transferase. Figure 1-6A, proposed by Marshall.[25] Figure 1-6B proposed by Bause.[29]

Two different peptides have been examined which incorporate an aspartic acid in place of the required asparagine residue within the consensus triad. If, during the reaction course of glycosylation, a negative charge is developed on the asparagine nitrogen, then the aspartate replacement would potentially mimic the charge distribution of this intermediate and therefore afford a competitive inhibitor. The peptides Tyr-Asp-Leu-Thr-Ser-Val[29] and Bz-Asp-Leu-Thr-NHMe[64] (**8**, Table 1-3) do not inhibit OT, even at high concentrations (>5mM), although each would be expected to maintain the hydrogen-bonding array of an Asx-turn; this result suggests that a negative charge is not developed at this center during the reaction process.[64]

An additional mechanism for asparagine linked glycosylation has been proposed which incorporates aspects of the favored mechanism for some of the glutamine amidotransferase family of enzymes.[73] This proposal[61] involves the release of an active site bound "NH_3" from the asparagine side chain in conjunction with the formation of a cyclic isoasparagine intermediate. The activated ammonia reacts with the lipid-linked oligosaccharide donor to form

chitobiosyl amine which reopens the isoasparagine to complete the glycosylation event. This mechanism is unlikely as the constrained peptide **5** is an optimized substrate for OT in spite of its inability to cyclize to isoasparagine (isoAsn). In addition, synthetic preparations of Bz-isoAsn-Leu-Thr-NH_2 revealed that this tripeptide is neither a substrate for nor an inhibitor of OT. Finally, this mechanistic proposal does not consider the absolute requirement for a hydroxyl amino acid.

The conformational studies identifying the Asx-turn as the likely recognition motif for asparagine linked glycosylation have prompted the development of a new mechanistic proposal for OT-mediated catalysis. In this proposal, the unique hydrogen-bonding array provided by the Asx-turn is suggested to facilitate protonation of the carbonyl of the asparagine side chain. Enzyme-mediated deprotonation at the nitrogen subsequently induces the tautomerization of the carboxamide to the imidol. This tautomerization would yield the neutral nucleophilic species which could then react with the electrophilic lipid-linked oligosaccharide (Figure 1-7).

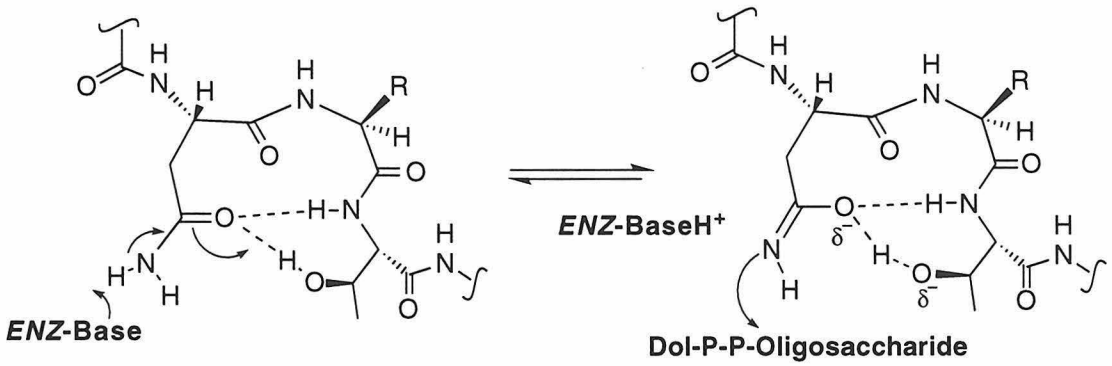

Figure 1-7. Mechanism of Activation for Oligosaccharyl Transferase as Proposed by Imperiali.[64]

The mechanistic proposal shown in Figure 1-7 incorporates both the issues of specificity and reactivity as well as the absolute requirement for a hydroxyl amino acid by integrating substrate structural requirements with participation of enzyme active site residues. Thus, the likelihood of an NXT/S sequence to undergo glycosylation would be governed by the ability of each potential substrate to adopt an Asx-turn conformation within the active site of the enzyme.

Four tripeptide analogs of **3** were designed to probe different aspects of the OT peptide binding site during catalysis; a summary of the kinetic analyses of these compounds is listed in Table 1-3.[64] Bz-Asp-Leu-Thr-NHMe (**8**), as discussed previously, exhibited no binding to OT. Replacement of the asparagine carboxamide with a methyl ester, in Bz-Asp(Oγ Me)-Leu-Thr-NHMe (**9**), removes the ionizable group from the side chain and affords a tripeptide which is not recognized by OT. Incorporation of γ-aminobutyrine (Amb) in place of asparagine yields Bz-Amb-Leu-Thr-NHMe (**10**), a peptide with a significantly lower pK_a at the Amb side chain. Tripeptide **10** is a competitive inhibitor of OT with a K_i that is similar to the K_M of **3**; the increased acidity of the side chain in **10** apparently facilitates binding to the enzyme and compensates for the peptide not having the appropriate functionality to adopt an Asx-turn. Finally, the tripeptide Bz-Asn(γS)-Leu-Thr-NHMe (**11**) is a substrate for OT. This heteroatom replacement ($CSNH_2$) increases the acidity of the hydrogen-bond donor site and decreases the basicity at the hydrogen-bond acceptor site relative to the corresponding oxoamide ($CONH_2$).[74,75] Additionally, the sulfur substitution in **11** introduces steric perturbations into the system by increasing the double bond length (C=S > C=O) and atomic radius (S > O) by approximately 25% relative to the corresponding carboxamide.[74] The binding of **11** to OT is scarcely affected by the thiocarbonyl replacement which is consistent with the ability of this compound to adopt an Asx-turn-like conformation. However, the relative

maximal velocity of **11** in a standard OT assay is reduced to 8.4% of that observed for **3**.

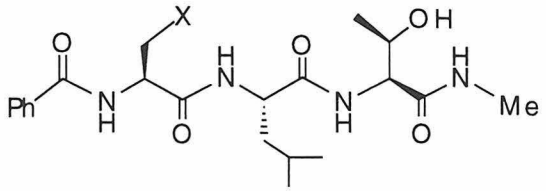

8: X=CO_2H
9: X=CO_2Me
10: X=$CH_2NH_3^+$
11: X=$CSNH_2$

Table 1-3 - Kinetic Analysis of Tripeptides with Porcine Liver OT.[64]

Peptide	Apparent K_M (mM)	Relative V (%)[a]	K_i (mM)
Bz-Asn-Leu-Thr-NHMe (**3**)	0.24	100	
Bz-Asp-Leu-Thr-NHMe (**8**)			>10[b]
Bz-Asp(OγMe)-Leu-Thr-NHMe (**9**)			>10[b]
Bz-Amb-Leu-Thr-NHMe (**10**)			1.0
Bz-Asn(γS)-Leu-Thr-NHMe (**11**)	0.26	8.4	

[a]Peptide **3** as standard; [b]no inhibition observed at concentrations below 5 mM.

Together, the results obtained from this substrate analog study suggest that in order for recognition by OT to occur, there is a prerequisite for side chain functionality with ionization properties similar to those of the native substrate. Tripeptide **10** is readily deprotonated and is a competive inhibitor, while **11** is a substrate for the enzyme. For **10**, the lower pK_a of the nitrogen appears to have allowed recognition by OT, despite the loss of the Asx-turn motif. For peptide

11, the K_M remains similar to that of the native substrate; however, the change in electronic properties have resulted in a lower glycosylation rate. These results support mechanistic proposals which do not involve the generation of a nitrogen anion and are consistent with the mechanism proposed by Imperiali and coworkers[64] which suggests that an intricate interplay between protonation and deprotonation is critical for the enhanced reactivity of the asparagine side chain. The microenvironment afforded by the hydrogen-bonding array of the Asx-turn provides the ideal arrangement to facilitate tautomerization. The presence of an active site base is a central element of this proposal as deprotonation of the imidol tautomer would result in the formation of a competent nucleophilic species. This active site base remains unidentified.

1.7 Conformational Consequences of Protein Glycosylation

As demonstrated above, a great deal of recent research has focused on the conformation of the peptidyl acceptor prior to glycosylation. However, since glycosylation is a co-translational event, the impact of the modification on the final folded protein structure and stability are also of current interest. Comparisons between glycosylated and non-glycosylated peptides and proteins can offer information on the consequences of the modification on the conformation of the peptide and the oligosaccharide. In many cases, the effects of *N*-linked glycosylation on the microenvironment of the asparagine residue has been directly observed. Several different techniques are available for analysis of glycopeptide structure including NMR[76-79] and CD spectroscopies,[80-82] molecular modeling predictions[82,83] and fluorescence energy transfer (FET) experiments.[7] These types of analyses have been performed on proteins and smaller peptide fragments.

Nuclear Overhauser effects (NOE), amide temperature coefficient and deuterium isotope exchange kinetics experiments have all been used to investigate the structural implications of protein glycosylation. The structure of a glycosylated 22 residue peptide fragment, isolated from human serum immunoglobulin M and containing one NVS glycosylation site, was investigated using selected NOE and amide temperature coefficient studies.[76] The isolated polypeptide contained three different glycoforms at the asparagine sidechain which varied in mannose content from 6 to 9 residues. Comparisons of the NOE data from the isolated glycopeptide and the analogous, synthetic, non-glycosylated peptide revealed that the presence of the oligosaccharide decreased the conformational mobility of both the backbone and the side chains of the amino acids immediately surrounding the glycosylation site. In addition, the amides in this same region were significantly more solvent shielded in the glycopeptide. Analysis of the coupling constant between GlcNAc1-C1H and Asn9-NδH revealed that the protein-glycan linkage is rigid and planar. The presence of the three different glycoforms did not effect the resolution of the peptide peaks, suggesting that protein conformation is not directly affected by the terminal saccharide residues.[76] Additionally, hydrogen isotope exchange experiments were used to compare the structures of RNase A and its glycosylated counterpart RNase B.[77] Although the presence of the oligosaccharide did not dramatically affect the global protein conformation, glycosylation did enhance the stability of the molecule. This result was evidenced by the decreased deuterium/proton exchange rates observed for several of the amides, even those buried within the protein and away from the oligosaccharide in RNAse B.[77]

Disulfide bond equilibria and two-dimensional NMR experiments were used to investigate the effects of glycosylation on a 17 residue peptide derived

from the nicotinic acetylcholine receptor.[79] This peptide is constrained by a disulfide bond, with one of the two cysteines in the central position of the sole glycosylation site (-NCT-). An analysis of the thermodynamics of disulfide bond formation demonstrated that the glycopeptide was more readily oxidized to the disulfide than the non-glycosylated peptide. In addition, NMR analysis of the non-glycosylated peptide revealed that approximately 50% of the proline residue exists as the *cis* isomer; glycosylation reduced this isomerism to 20% *cis*. The results from this study suggest that asparagine-linked glycosylation can have indirect effects on both proline isomerism and disulfide bond formation, two processes which are important for protein folding.[79]

Circular dichroism (CD) spectroscopy provides less direct structural information than NMR experiments; however, it requires significantly less sample and can still be used to observe dramatic conformational differences.[80,81] Analysis of eight pairs of model peptides and glycopeptides by CD has revealed that in hydrophobic solvent systems like trifluoroethanol or acetonitrile, glycosylation results in a decrease in type I β-turn character and a concomitant increase in type II β-turn character.[82] This trend is reversed when the CD spectra are acquired in aqueous environments. One possible explanation for this observation is that in the more hydrophobic environments, the oligosaccharide interacts with the peptide backbone and side chains through a hydrogen-bonding array; when the sample is in an aqueous environment, the medium provides competition for these hydrogen bonds.

Fluorescence energy transfer experiments (FET) can also be used to investigate the conformational consequences of glycosylation. FET is only suitable for peptides which can be modified to incorporate a fluorescent donor and acceptor. Generally, the indole side chain of the naturally occurring amino acid tryptophan is employed as the donor fluorophore. Similar to CD, FET

requires minute quantities of sample (nmoles) and is useful for observing gross structural changes in peptide conformations. However, unlike CD, FET can be used to determine the distances between acceptor and donor moieties. Additionally, FET measurements can be made on the same time scale as that for conformational fluctuations within the molecule, so the data are not subject to the problems of conformational averaging observed with slower NMR experiments. FET has been used to investigate the direct consequences of glycosylation by comparing interfluorophore distances in peptides and the corresponding glycopeptides.[7] For example, FET studies on the glycosylated and non-glycosylated sequence Ac-Orn(δDns)-Ala-Val-Pro-Asn-Gly-Thr-Trp-Val-NH_2 (**12**, based on residues A19-26 of hemagglutinin[12,84]) revealed the presence of two ensembles of populations with distinct interfluorophore distances (Figure 1-8). For this peptide, a distribution of conformers, centered around an interfluorophore distance of 15Å, was observed. Upon glycosylation with a chitobiosyl disaccharide, this average interfluorophore distance was reduced to 9.5Å. Glycosylation appeared to induce the formation of a more compact structure which approximates the conformation of the glycopeptide within the native protein. This result implies that the glycosylation event has a direct impact on local peptide conformation and as it is a co-translational process, may play a distinct role in the process of protein folding.[7]

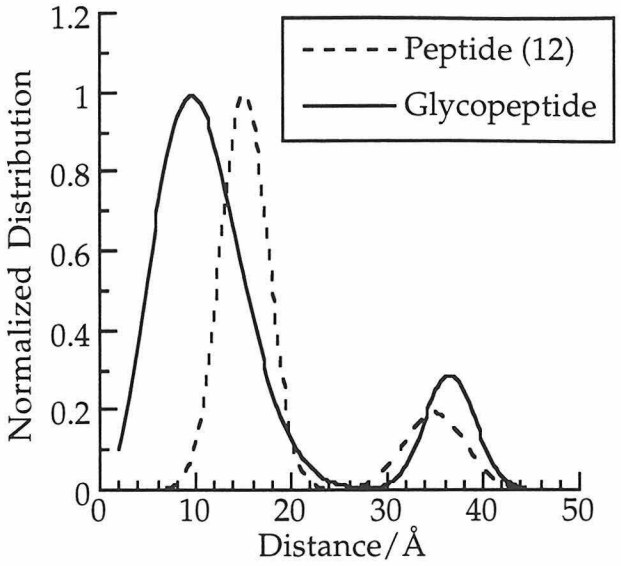

Figure 1-8. Dynamic Distribution Plots of **12** and Corresponding Glycopeptide in Aqueous Solution.[7]

1.8. Dissertation Research

An examination of the current literature readily reveals the recent and intense interest in asparagine-linked glycosylation. Advances have been made in understanding both the specificity of the modification and of its consequences on protein structure and function. However, many questions still remain on how nature catalyzes this modification. The research presented in this dissertation was designed and executed in an effort to answer some of these questions by further characterizing the enzyme oligosaccharyl transferase and examining its role in catalysis.

Chapter two describes a series of chemical modification experiments designed to probe the active site of oligosaccharyl transferase for reactive amino acid side chains. These experiments identified a specific cysteine in the

oligosaccharide binding site. Further investigations, including the development of a novel modification reagent, localized this cysteine on the Wbp1p subunit of OT.

The role of the required divalent metal cofactor is investigated in chapter three. Experiments with a synthetic tripeptide substrate and OT which had been reconstituted with several different divalent metals confirmed that, during catalysis, the metal binding site is in direct proximity to the peptide substrate. This is the first evidence that the metal may play a catalytic role in *N*-linked glycosylation. These studies have also provided insight on how OT directs glycosylation to the nitrogen of the asparagine side chain rather than the oxygen; this regiochemical control is crucial for the generation of stable glycoproteins *in vivo*.

Chapter four discusses the synthesis and kinetic characterization of a new class of slow, tight binding inhibitors for OT. The nanomolar binding constants of these inhibitors make them more than three orders of magnitude more effective than any other previously reported inhibitor of OT. In addition, the slow binding nature of the inhibition has implications on the catalytic mechanism of OT.

Finally, chapter five will provide some perspective on how the synthesis of the cyclic inhibitors described in chapter four can be applied to the preparation of several potential mechanistic inactivators of OT. Originally, a series of linear peptide affinity labels were prepared by introducing electrophilic moieties into tripeptides in place of the target asparagine residue. However, the electrophilic side chains spontaneously cyclized with the peptide amide backbone to generate analogs that were no longer useful as mechanistic probes. The cyclic nature of the inhibitors in chapter four is readily introduced into peptides via solid phase synthesis methods and can be easily adapted to introduce electrophilic groups

onto amino acid side chains. The cyclic constraint will prohibit cyclization by hindering access to the amide backbone, thereby making this class of mechanistic inactivators synthetically accessible.

1.9 Acknowledgements

A significant portion of this introductory chapter has appeared in the following review article: Imperiali, B.; Hendrickson, T. L. (1995). Asparagine-Linked Glycosylation: Specificity and Function of Oligosaccharyl Transferase. *Bioorganic and Medicinal Chemistry* **3**, 1565-1578.

1.10 References

1. Baenziger, J. U. "Protein-Specific Glycosyltransferases: How and Why They Do It!" *FASEB J.* **1994**, *8*, 1019-1025.

2. Varki, A. "Biological Roles of Oligosaccharides: All of the Theories are Correct," *Glycobiology* **1993**, *3*, 97-130.

3. Paulson, J. C. "Glycoproteins: What Are the Sugar Chains For?" *Trends in Biol. Sci.* **1989**, *14*, 272-276.

4. Opdenakker, G.; Rudd, P. R.; Ponting, C. P.; Dwek, R. A. "Concepts and Principles of Glycobiology," *FASEB J.* **1993**, *7*, 1330-1337.

5. Gleeson, P. A.; Teasdale, R. D.; Burke, J. "Targeting of Proteins to the Golgi Apparatus," *Glycoconjugate J.* **1994**, *11*, 381-394.

6. Wagner, G.; Wyss, D. F. "Cell Surface Adhesion Receptors," *Curr. Opin. Struct. Biol.* **1994**, *4*, 841-851.

7. Imperiali, B.; Rickert, K. W. "Conformational Implications of Asparagine-Linked Glycosylation," *Proc. Natl. Acad. Sci. U.S.A.* **1995**, *92*, 97-101.

8. Riederer, M. A.; Hinnen, A. "Removal of N-Glycosylation Sites of the Yeast Acid Phosphatase Severely Affects Protein Folding," *J. Bacteriol.* **1991**, *173*, 3539-3546.

9. Allen, S.; Naim, H. Y.; Bulleid, N. J. "Intracellular Folding of Tissue-type Plasminogen Activator: Effects of Disulfide Bond Formation on N-Linked Glycosylation and Secretion," *J. Biol. Chem.* **1995**, *270*, 4797-4804.

10. Duranti, M.; Gius, C.; Sessa, F.; Vecchio, G. "The Saccharide Chain of Lupin Seed Conglutin g is not Responsible for the Protection of the Native Protein from Degradation by Trypsin, but Facilitates the Refolding of the Acid-Treated Protein to the Resistant Conformation," *Eur. J. Biochem.* **1995**, *230*, 886-891.

11. Rudd, P. M.; Dwek, R. A. "Glycobiology: a Coming of Age," *Chem. Ind.* **1991**, *18*, 660-663.

12. Wilson, I. B. H.; Gavel, Y.; von Heijne, G. "Amino Acid Distributions Around O-Linked Glycosylation Sites," *Biochem. J.* **1991**, *275*, 529-534.

13. Strahl-Bolsinger, S.; Immervoll, T.; Deutzmann, R.; Tanner, W. "PMT1, The Gene for a Key Enzyme of Protein O-Glycosylation in *Saccharomyces-Cerevisiae*," *Proc. Natl. Acad. Sci. U.S.A.* **1993**, *90*, 8164-8168.

14. Carraway, K. L.; Hull, S. R. "O-Glycosylation Pathway for Mucin-Type Glycoproteins," *BioEssays* **1989**, *10*, 117-121.

15. Elhammer, A. P.; Poorman, R. A.; Brown, E.; Maggiora, L. L.; Hoogerheide, J. G.; Kezdy, F. J. "The Specificity of UDP-GalNAc-Polypeptide *N*-Acetylgalactosyaminyltransferase as Inferred From a Database of *In Vivo* Substrates and From the *In Vitro* Glycosylation of Proteins and Peptides," *J. Biol. Chem.* **1993**, *268*, 10029-10038.

16. Nishimura, H.; Yamashita, S.; Zeng, Z.; Walz, D. A.; Iwanaga, S. "Evidence for the Existence of *O*-Linked Sugar Chains Consisting of Glucose and Xylose in Bovine Thrombospondin," *J. Biochem.* **1992**, *111*, 460-464.

17. Harris, R. J.; Vanhalbeek, H.; Glushka, J.; Basa, L. J.; Ling, V. T.; Smith, K. J.; Spellman, M. W. "Identification and Structural Analysis of the Tetrasaccharide NeuAcα(2-6)Galβ(1-4)GlcNAcβ(1-3)Fucα1-O-Linked to Serine 61 of Human Factor IX," *Biochemistry* **1993**, *32*, 6539-6547.

18. Englund, P. T. "The Structure and Biosynthesis of Glycosyl Phosphatidylinositol Protein Anchors," *Ann. Rev. Biochem.* **1993**, *62*, 121-138.

19. Dwek, R. A. "Glycobiology:"Towards Understanding the Function of Sugars"," *Biochem. Soc. Trans.* **1994**, *23*, 1-25.

20. Presper, K. A.; Heath, E. C. In *The Enzymology of Post-translational Modification of Proteins*; Academic Press: London, 1985; Vol. 2; pp 54-93.

21. Roseman, S. "The Synthesis of Complex Carbohydrates by Multiglycosyltransferase Systems and Their Potential Function in Intercellular Adhesion," *Chem. Phys. Lipids* **1970**, *5*, 270-297.

22. Paulson, J. C.; Colley, K. J. "Glycosyltransferases: Structure, Localization, and Control of Cell Type-Specific Glycosylation," *J. Biol. Chem.* **1989**, *264*, 17615-17618.

23. Sinnot, M. L. "Catalytic Mechanisms of Enzymatic Glycosyl Transferases," *Chem. Rev.* **1990**, *90*, 1171-1202.

24. Shaper, J. H.; Shaper, N. L. "Enzymes Associated With Glycosylation," *Curr. Opin. Struct. Biol.* **1992**, *2*, 701-709.

25. Marshall, R. D. "The Nature and Metabolism of the Carbohydrate-Peptide Linkages of Glycoproteins," *Biochem. Soc. Symp.* **1974**, *40*, 17-26.

26. Bause, E. "Active-Site-Directed Inhibition of Asparagine *N*-Glycosyltransferases with Epoxy-Peptide Derivatives," *Biochem. J.* **1983**, *209*, 323-330.

27. Roitsch, T.; Lehle, L. "Structural Requirements for Protein *N*-Glycosylation: Influence of Acceptor Peptides on Cotranslational Glycosylation of Yeast

Invertase and Site-Directed Mutagenesis Around a Sequon Sequence," *Eur. J. Biochem.* **1989**, *181*, 525-529.

28. Gavel, Y.; von Heijne, G. "Sequence Differences Between Glycosylated and Non-glycosylated Asn-X-Thr/Ser Acceptor Sites: Implications for Protein Engineering," *Protein Eng.* **1990**, *3*, 433-442.

29. Bause, E. "Model Studies on *N*-Glycosylation of Proteins," *Biochem. Soc. Trans.* **1984**, *12*, 514-517.

30. Knauer, R.; Lehle, L. "The *N*-oligosaccharyltransferase Complex From Yeast," *FEBS Lett.* **1994**, *344*, 83-86.

31. Chalifour, R. J.; Spiro, R. G. "Effects of Phospholipids on Thyroid Oligosaccharyltransferase activity and Orientation - Evaluation of Structural Determinants for Stimulation of *N*-Glycosylation," *J. Biol. Chem.* **1988**, *263*, 15673-15680.

32. Kelleher, D. J.; Kreibich, G.; Gilmore, R. "Oligosaccharyltransferase Activity Is Associated with a Protein Complex Composed of Ribophorins I and II and a 48 kD Protein," *Cell* **1992**, *69*, 55-65.

33. Breuer, W.; Bause, E. "Oligosaccharyl Transferase is a Constitutive Component of an Oligomeric Protein Complex From Pig Liver Endoplasmic Reticulum," *Eur. J. Biochem.* **1995**, *228*, 689-696.

34. Kumar, V.; Korza, G.; Heinemann, F. S.; Ozols, J. "Human Oligosaccharyltransferase: Isolation, Characterization, and the Complete Amino Acid Sequence of 50-kDa Subunit," *Arch. Biochem. Biophys.* **1995**, *320*, 217-223.

35. Kumar, V.; Heinemann, F. S.; Ozols, J. "Purification and Characterization of Avian Oligosaccharyltransferase: Complete Amino Acid Sequence of the 50 kDa Subunit," *J. Biol. Chem.* **1994**, *269*, 13451-13457.

36. Pathak, R.; Hendrickson, T. L.; Imperiali, B. "Sulfhydryl Modification of the Yeast Wbp1p Inhibits Oligosaccharyl Transferase Activity," *Biochemistry* **1995**, *34*, 4179-4185.

37. Kelleher, D. J.; Gilmore, R. "The *Saccharomyces cerevisiae* Oligosaccharyltransferase Is a Protein Complex Composed of Wbp1p, Swp1p, and Four Additional Polypeptides," *J. Biol. Chem.* **1994**, *269*, 12908-12917.

38. Stagljar, I.; Aebi, M.; Te Heesen, S. "PCR-Mediated Cloning and Sequencing of the *Dm*OST50 gene, a WBP1/*Av*OST50/OST48 Homologue, from *Drosophila melanogaster*," *Gene* **1995**, *158*, 209-212.

39. Silberstein, S.; Kelleher, D. J.; Gilmore, R. "The 48-kDa Subunit of the Mammalian Oligosaccharyltransferase Complex is Homologous to the Essential Yeast Protein WBP1," *J. Biol. Chem.* **1992**, *267*, 23658-23663.

40. Silberstein, S.; Collins, P. G.; Kelleher, D. J.; Rapiejko, P. J.; Gilmore, R. "The α Subunit of the *Saccharomyces cerevisiae* Oligosaccharyltransferase Complex Is Essential for Vegetative Growth of Yeast and Is Homologous to Mammalian Ribophorin I," *J. Cell Biol.* **1995**, *128*, 525-536.

41. Pathak, R.; Parker, C. S.; Imperiali, B. "The Essential Yeast NLT1 Gene Encodes the 64kDa Glycoprotein Subunit of the Oligosaccharyl Transferase," *FEBS Lett.* **1995**, *362*, 229-234.

42. te Heesen, S.; Janetzky, B.; Lehle, L.; Aebi, M. "The Yeast WBP1 is Essential for Oligosaccharyl Transferase Activity *in vivo* and *in vitro*," *EMBO* **1992**, *11*, 2071-2075.

43. te Heesen, S.; Knauer, R.; Lehle, L.; Aebi, M. "Yeast Wbp1p and Swp1p Form a Protein Complex Esssential For Oligosaccharyl Transferase Activity," *EMBO* **1993**, *12*, 279-284.

44. Karaoglu, D.; Kelleher, D. J.; Gilmore, R. "Functional Characterization of Ost3p. Loss of the 34-kD Subunit of the *Saccharomyces cerevisiae*

Oligosaccharyltransferase Results in Biased Underglycosylation of Acceptor Substrates," *J. Cell Biol.* **1995**, *130*, 567-577.

45. Silberstein, S.; Collins, P. G.; Kelleher, D. J.; Gilmore, R. "The Essential *OST2* Gene Encodes the 16-kD Subunit of the Yeast Oligosaccharyltransferase, a Highly Conserved Protein Expressed in Diverse Eukaryotic Organisms," *J. Cell Sci.* **1995**, *131*, 371-383.

46. te Heesen, S.; Rauhut, R.; Aeversold, R.; Abelson, J.; Aebi, M.; Clark, M. W. "An Essential 45 kDa Yeast Transmembrane Protein Reacts With Anti-Nuclear Pore Antibodies: Purification of the Protein Immunolocalization and Cloning of the Gene," *Eur. J. Cell. Biol.* **1991**, *56*, 8-18.

47. Behrens, N. H.; Tabora, E. "Dolichol Intermediates in the Glycosylation of Proteins," *Meth. Enzym.* **1977**, *50*, 402.

48. Hubbard, S. C.; Ivatt, R. J. "Synthesis and Processing of Asparagine-Linked Oligosaccharides," *Ann. Rev. Biochem.* **1981**, *50*, 555-583.

49. Lennarz, W. J. "Protein Glycosylation in the Endoplasmic Reticulum: Current Topological Issues," *Biochemistry* **1987**, *26*, 7205-7210.

50. Sharma, C. B.; Lehle, L.; Tanner, W. "N-Glycosylation of Yeast Proteins: Characterization of the Solubilized Oligosaccharyl Transferase," *Eur. J. Biochem.* **1981**, *116*, 101-108.

51. Abeijon, C.; Hirschberg, C. B. "Topography of Glycosylation Reactions in the Endoplasmic Reticulum," *Trends in Biol. Sci.* **1992**, *17*, 32-36.

52. Hirschberg, C. B.; Snider, M. D. "Topography of Glycosylation on the Rough Endoplasmic Reticulum and Golgi Apparatus," *Ann. Rev. Biochem.* **1987**, *56*, 63-87.

53. Warren, C. D.; Jeanloz, R. W. "Chemical Synthesis of Dolichyl Phosphate and Glycosyl Phosphates and Pyrophosphates or "Dolichol Intermediates"," *Meth. Enzym.* **1978**, *50*, 122-137.

54. Lee, J.; Coward, J. K. "Enzyme-Catalyzed Glycosylation of Peptides Using a Synthetic Lipid Disaccharide Substrate," *J. Org. Chem.* **1992**, *57*, 4126-4135.

55. Imperiali, B.; Zimmerman, J. W. "Synthesis of Dolichylpyrophosphate-Linked Oligosaccharides," *Tetrahedron Lett.* **1990**, *31*, 6485-6488.

56. Mononen, I.; Karjalainen, E. "Structural Comparison of Protein Sequences Around Potential *N*-Glycosylation Sites," *Biochim. Biophys. Acta* **1984**, *788*, 364-367.

57. Nilsson, I.; von Heijne, G. "Determination of the Distance Between the Oligosaccharyltransferase Active Site and the Endoplasmic Reticulum Membrane," *J. Biol. Chem.* **1993**, *268*, 5798-5801.

58. Pless, D. D.; Lennarz, W. J. "Enzymatic Conversion of Proteins to Glycoproteins," *Proc. Natl. Acad. Sci. U.S.A.* **1977**, *74*, 134-138.

59. Imperiali, B.; Shannon, K. L. "Differences Between Asn-Xaa-Thr Containing Peptides: A Comparison of Solution Conformation and Substrate Behavior with Oligosaccharyltransferase," *Biochemistry* **1991**, *30*, 4374-4380.

60. Imperiali, B.; Shannon, K. L.; Rickert, K. W. "Role of Peptide Conformation in Asparagine-Linked Glycosylation," *J. Am. Chem. Soc.* **1992**, *114*, 7942-7944.

61. Clark, R. S.; Banerjee, S.; Coward, J. K. "Yeast Oligosaccharyltransferase: Glycosylation of Peptide Substrates and Chemical Characterization of the Glycopeptide Product," *J. Org. Chem.* **1990**, *55*, 6275-6285.

62. Welply, J. K.; Shenbagamurthi, P.; Lennarz, W. J.; Naider, F. "Substrate Recognition by Oligosaccharyltransferase: Studies on Glycosylation of Modified Asn-X-Thr/Ser Tripeptides," *J. Biol. Chem.* **1983**, *258*, 11856-11863.

63. Rathod, P. K.; Tashjian Jr., A. H.; Abeles, R. H. "Incorporation of β-Fluoroasparagine into Peptides Prevents *N*-Linked Glycosylation," *J. Biol. Chem.* **1986**, *261*, 6461-6469.

64. Imperiali, B.; Shannon, K. L.; Unno, M.; Rickert, K. W. "A Mechanistic Proposal for Asparagine-Linked Glycosylation," *J. Am. Chem. Soc.* **1992**, *114*, 7944-7945.

65. Bause, E.; Legler, G. "The Role of the Hydroxy Amino Acid in the Triplet Sequence Asn-Xaa-Thr(Ser) for the *N*-Glycosylation Step During Glycoprotein Biosynthesis," *Biochem. J.* **1981**, *195*, 639-644.

66. Hortin, G.; Boime, I. "Inhibition of Asparagine-Linked Glycosylation by Incorporation of a Threonine Analog into Nascent Peptide Chains," *J. Biol. Chem.* **1980**, *255*, 8007-8010.

67. Shannon, K. L. Ph.D. Thesis, California Institute of Technology, 1992.

68. Abbadi, A.; Mcharfi, M.; Aubry, A.; Premilat, S.; Marraud, M. "Involvement of Side Functions in Peptide Structures: The Asx Turn. Occurrence and Conformational Aspects," *J. Am. Chem. Soc.* **1991**, *113*, 2729-2735.

69. Baker, E. N.; Hubbard, R. E. "Hydrogen Bonding of Globular Proteins," *Prog. Biophys. Mol. Biol.* **1984**, *44*, 97-179.

70. Imperiali, B.; Fisher, S. L.; Moats, R. A.; Prins, T. J. "A Conformational Study of Peptides with the General Structure Ac-L-Xaa-Pro-D-Xaa-L-Xaa-NH_2: Spectroscopic Evidence for a Peptide with Significant β-Turn Character in Water and in Dimethyl Sulfoxide," *J. Am. Chem. Soc.* **1992**, *114*, 3182-3188.

71. Imperiali, B.; Spencer, J. R.; Struthers, M. D. "Structural and Functional Characterization of a Constrained Asx-Turn Motif," *J. Am. Chem. Soc.* **1994**, *116*, 8424-8425.

72. Bause, E.; Hettkamp, H.; Legler, G. "Conformational Aspects of N-Glycosylation of Proteins," *Biochem. J.* **1982**, *203*, 761-768.

73. Zalkin, H. In *Advances in Enzymology and Related Areas of Molecular Biology*; A. Meister, Ed.; Interscience Publishers: New York, 1993; Vol. 66; pp 203-309.

74. Challis, B. C.; Challis, J. In *The Chemistry of Amides*; J. Zabicky, Ed.; Wiley Interscience: London, 1970; pp 731-858.

75. Bordwell, F. G. "Equilibrium Acidities in Dimethyl Sulfoxide Solution," *Acc. Chem. Res.* **1988**, *21*, 456-463.

76. Wormald, M. R.; Wooten, E. W.; Bazzo, R.; Edge, C. J.; Feinstein, A.; Rademacher, T. W.; Dwek, R. A. "The Conformational Effects of *N*-Glycosylation on the Tailpiece for serum IgM," *Eur. J. Biochem.* **1991**, *198*, 131-139.

77. Joao, H. C.; Scragg, I. G.; Dwek, R. A. "Effects of Glycosylation on Protein Conformation and Amide Proton Exchange Rates in RNase B," *FEBS Lett.* **1992**, *307*, 343-346.

78. Davis, J. T.; Hirani, S.; Bartlett, C.; Reid, B. R. "^{1}H NMR Studies on an Asn-Linked Glycopeptide: GlcNAc-1 C2-N2 Bond is Rigid in H_2O," *J. Biol. Chem.* **1994**, *269*, 3331-3338.

79. Rickert, K. W.; Imperiali, B. "Analysis of the Conserved Glycosylation Site in the Nicotinic Acetylcholine Receptor: Potential Roles in Complex Assembly," *Chem. Biol.* **1995**, *2*, 751-759.

80. Aubert, J. P.; Helbecque, N.; Loucheux-Lefebvre, M. H. "Circular Dichroism Studies of Synthetic Asn-X-Ser/Thr-Containing Peptides: Structure-Glycosylation Relationship," *Arch. Biochem. Biophys.* **1981**, *208*, 20-29.

81. Otvos Jr., L.; Thurin, J.; Kollat, E.; Urge, L.; Mantsch, J. J.; Hollosi, M. "Glycosylation of Synthetic Peptides Breaks Helices," *Int. J. Pept. Protein Res.* **1991**, *38*, 476-482.

82. Perczel, A.; Kollat, E.; Hollasi, M.; Fasman, G. "Synthesis and Conformational Analysis of N-Glycopeptides. II. CD, Molecular Dynamics, and NMR Spectoscopic Studies on Linear N-Glycopeptides," *Biopolymers* **1993**, *33*, 665-685.

83. Gabriel, J. L.; Mitchell, W. M. "Proposed Atomic Structure of a Truncated Human Immunodeficiency Virus Glycoprotein Gp120 Derived by Molecular

Modeling: Target CD4 Recognition and Docking Mechanism," *Proc. Natl. Acad. Sci. U.S.A.* **1993**, *90*, 4186-4190.

84. Wilson, I. A.; Skehel, J. J.; Wiley, D. C. "Structure of the Haemagglutinin Membrane Glycoprotein of Influenza Virus at 3 Å Resolution," *Nature* **1981**, *289*, 366-373.

Chapter 2. Chemical Modification Studies of Oligosaccharyl Transferase

2.1 Introduction

Studies on enzyme mechanisms have often relied on kinetic assays to investigate reaction pathways. Historically, one of the most successful methods of characterizing enzyme active sites has been to observe changes in activity in the presence and absence of small reactive molecules. When combined with the proper controls, the predictable reactivity of these chemical modifiers can be used to suggest the identity of specific amino acids within the enzyme active site and may provide clues to the reaction mechanism utilized by the enzyme.[1-3] Commercially available reagants can be used to target nearly all of the reactive amino acid side chains including cysteine, lysine, histidine, serine, aspartic acid and glutamic acid.[2] Successful examples of this approach include the use of diethylpyrocarbonate (DEPC) to identify catalytic histidines in thermolysin[4] and lactate dehydrogenase,[5] and the modification of the active site cysteine of papain with 5,5'-dithiobis-(2-nitrobenzoic acid) (DTNB).[6]

Chemical modification experiments are most effectively used to identify residues positioned within the active site of an enzyme by monitoring the rate of inactivation in the presence and absence of the substrate(s) recognized by the enzyme. If the substrate protects the enzyme from inactivation, then the target amino acid probably resides in or near the active site. However, this observation does not automatically point to a residue that is directly involved in catalysis as inactivation by chemical modification invariably leads to the covalent attachment of a non-native chemical group to the enzyme. This variation in the enzyme structure could produce a decrease in activity through steric crowding of the active site or through the alteration of a crucial catalytic residue and both of these possibilities must be considered. For example, a cysteine in creatine kinase

was identified following inactivation with several different sulfhydryl modifiers including iodoacetamide (IAM), iodoacetic acid (IAA) and *p*-chloromercuribenzoic acid. However, when creatine kinase was treated with methyl methanethiolsulfonate (MMTS), a cysteine modifier which introduces only an additional -S-CH_3 group to the enzyme, the enzyme remained fully active, suggesting that the previously observed inactivation was due to steric occlusion and not mechanistic inactivation.[7]

Once an active-site residue has been identified through chemical modification studies, additional experiments can be used to further characterize the overall environment of the enzyme. Most commonly, these experiments include modification of the enzyme with compounds which covalently introduce a detectable marker such as a UV chromophore, spin label[8] or fluorescent group.[3,9] Experiments designed to examine these markers can then be performed on the inactivated enzyme to provide information about the site of modification and sometimes the local environment of the active site. For example, the chromophore of DTNB has a known extinction coefficient and can be used to quantitate the number of free thiols and, when combined with dithiothreitol or β-mercaptoethanol treatment, the total number of disulfides in the enzyme. In addition, cross-linking agents often take advantage of modifiable residues to covalently link catalytic residues or protein subunits.[10]

The mechanism of action for asparagine-linked glycosylation, as catalyzed by the enzyme oligosaccharyl transferase (OT), is a prime target for characterization by chemical modification studies. OT has only recently been purified from several sources and, although several subunits have been characterized, the enzyme is not yet available in large quantities.[11-17] The fact that OT is a multi subunit, membrane bound enzyme has hindered the

overexpression of native activity, and even with an increase in availability, membrane bound enzymes have been notoriously difficult to crystallize.[18] For now, structural and mechanistic information is most readily obtained through the use of biochemical and kinetic experiments, including chemical modification studies, which require only small amounts of enzyme.

The reaction catalyzed by OT involves the transfer of an extended oligosaccharide from dolichol pyrophosphate to the nitrogen of an asparagine residue, an unusual reaction due to the low reactivity of this carboxamide side chain. Imperiali and coworkers[19] have proposed a mechanism in which the asparagine side chain carboxamide tautomerizes to an imidate with concomitant deprotonation by an active site basic residue; it is this deprotonated imidate which is sufficiently nucleophilic to complete the glycosylation event (Figure 2-1). The identity of the proposed active site base, shown in Figure 2-1, is unknown. Because this mechanism relies on a base which is sufficiently reactive to promote catalysis, the identification of this residue is a prime target for chemical modification studies.

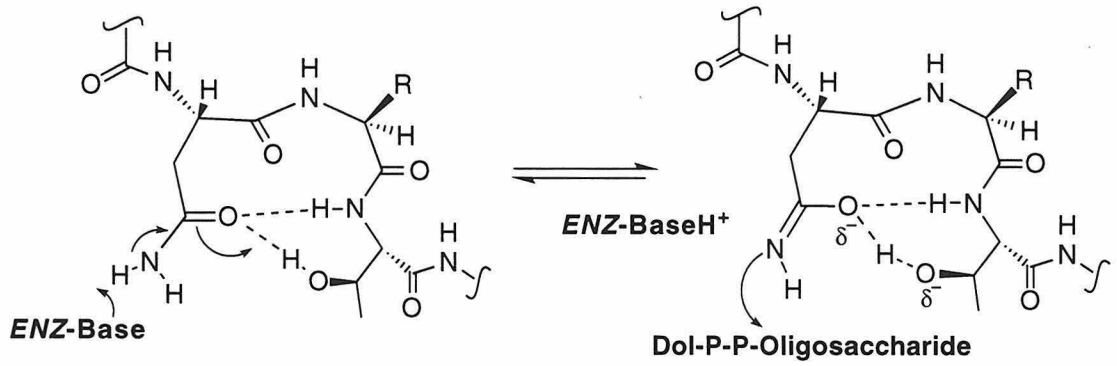

Figure 2-1. The Proposed Mechanism of Action for Oligosaccharyl Transferase.[19]

Decreases in OT activity produced from chemical modifications can be accurately quantified through a radiolabelled assay which measures the

transfer of the tritiated disaccharide chitobiose from Dol-P-P-GlcNAc-[^{3}H]GlcNAc to the tripeptide substrate Bz-Asn-Leu-Thr-NHMe (see Appendix A).[20] The availability of exogenous supplies of both substrates facilitates substrate protection experiments which can be used to pinpoint the positioning of modified residues to either the peptide or oligosaccharide binding sites within the enzyme active site. The oligosaccharide substrate Dol-P-P-GlcNAc-[^{3}H]GlcNAc is prepared through a combination of chemical and enzymatic methods as described in Chapter 1 and in the literature.[21] This method incorporates a tritium label into the C-6 position of the second N-acetylglucosamine; the specific activity of the substrate can be readily adjusted to enable assays at varied substrate concentrations. The tripeptide **3** can be prepared through standard solution phase peptide synthesis protocols.

In addition to kinetic studies, the recent purification of *S. cerevisiae* OT[15,22] has enabled experiments which examine the effect of chemical modification agents on individual subunits by sodium dodecyl sulfate polyacrylamide gel electrophoresis (SDS-PAGE) and Western blot analysis. These techniques are powerful tools and, when combined with detailed kinetic analyses, can provide additional insight into the exact site of inactivation by specific reagents. An example of the purification of OT from *S. cerevisiae*[15,22] is shown in Figure 2-2 (for more details on the characterization of each subunit, see chapter one).

This chapter describes an investigation of the active site of OT through chemical modification studies; these experiments were designed to probe for the proposed active site base. A series of chemical modification reagants were screened for their ability to inactivate OT. Those modifiers which produced a decrease in enzyme activity were further characterized through substrate protection experiments to determine if the modified amino acid was located

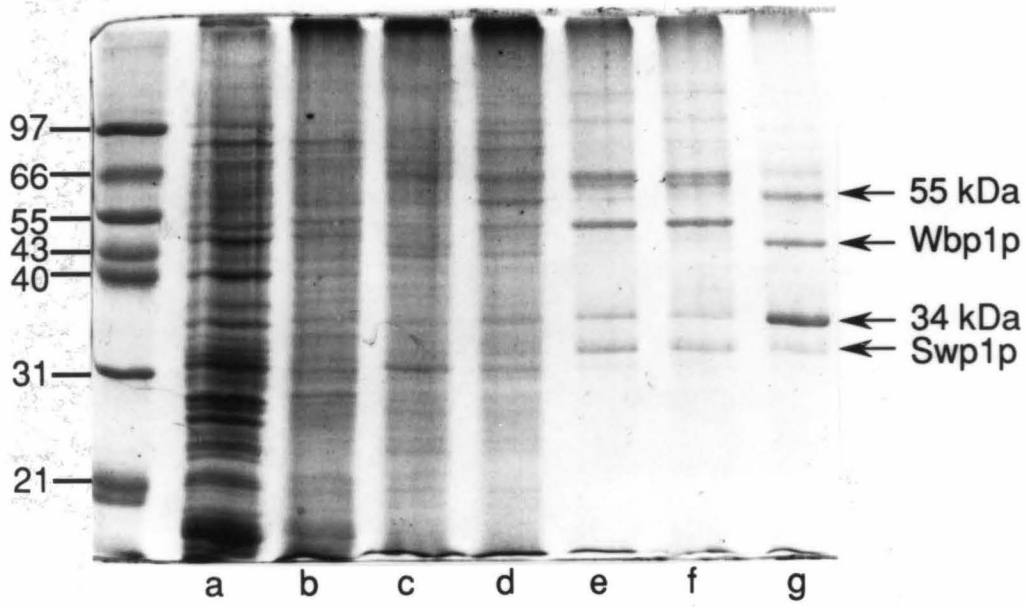

Figure 2-2. Purification of *S. cerevisiae* Oligosaccharyl Transferase.[15] Lanes represent the following protein fractions: a) yeast microsomes; b) NP-40 solubilized microsomes; c) concanavalin A eluate; d) heparin-agarose eluate; e) Q-sepharose eluate; f) hydroxyapatite eluate; and g) hydroxyapatite eluate digested with 0.5 unit PNGaseF. The deglycosylated oligosaccharyl transferase complex is composed of subunits with apparent molecular weights of 55 kDa (Nlt1p), 43 kDa (Wbp1p), 34 kDa (Ost3p), and 32 kDa (Swp1p); PNGaseF comigrates with the 34 kDa subunit.

in either the peptide or the oligosaccharide binding site. Specifically, these experiments identified a reactive cysteine residue at or near the oligosaccharide donor binding site. Through the development and application of a novel biotinylated chemical modification reagent, this residue, and therefore the sugar binding site, was localized to the Wbp1p subunit of OT.

2.2 Results and Discussion

2.2.1 Inactivation of OT with Commercially Available Modification Agents

The kinetic response of solubilized *Saccharomyces cerevisiae* OT was characterized following treatment with several different chemical modifiers, including MMTS, DTNB, *p*-chloromercuribenzenesulfonic acid (PCMBS), *N*-ethylmaleimide (NEM), iodoacetic acid (IAA), iodoacetamide (IAM), DEPC, benzoic anhydride (BzAnh), acetic anhydride (AcAnh) and succinic anhydride (SuccAnh) (Figure 2-3). These compounds were all chosen for their ability to modify potential active site basic residues including cysteine, lysine and histidine. Particular attention was paid to compounds designed to react with sulfhydryl groups, based on the observation that OT activity decreased following exposure to the chemical oxidant *m*-chloroperbenzoic acid (*m*-CPBA). MMTS, DTNB and PCMBS have strong affinities for free sulfhydryl groups, independent of the nucleophilicity of the cysteine side chain. The remainder of the compounds investigated rely on the presence of a nucleophilic moiety, so although they preferentially react with cysteine (with the exception of DEPC which prefers histidine), they will also react with lysine, histidine and extremely activated serines. Traditionally, IAA and IAM are both examined, even though they have similar reactivities, as IAM favors

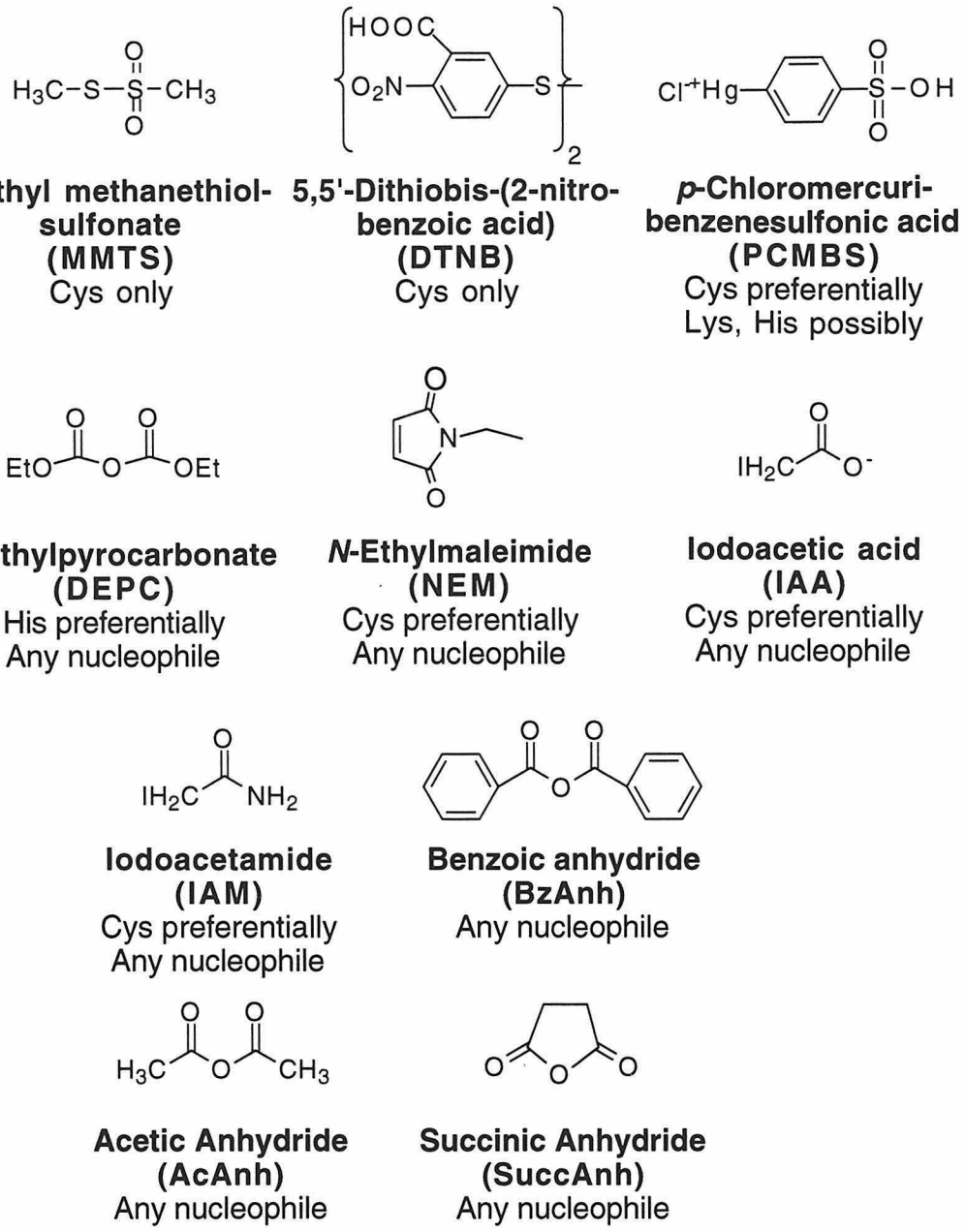

Figure 2-3. Chemical Structures and Target Amino Acids of the Commercially Available Modifiers Used to Characterize Oligosaccharyl Transferase.

more hydrophobic environments whereas IAA favors hydrophilic environments.

Several experiments were performed with each modifier using crude solubilized OT. First, different concentrations were examined to determine the level required to produce a 50% decrease in enzymatic activity following a 2 minute preincubation. Second, the rate of inactivation over time was examined to verify that the loss in activity was time dependent and not due to simple, reversible competitive inhibition. Third, each inactivator was reexamined with OT that had been preincubated with either the peptide or the sugar substrate. These substrate protection experiments were designed to determine if the location of the modified residue was in either of the two substrate binding sites. The results from these experiments are summarized in Table 2-1. Finally, when appropriate, the inactivated enzyme complex was treated with dithiothreitol (DTT, for MMTS and DTNB studies) or hydroxylamine (for DEPC studies) to examine whether the inactivation was reversible.

OT activity was inactivated by incubation with MMTS, PCMBS, DTNB, DEPC and BzAnh at low to mid micromolar concentrations (90 μM - 750 μM). However, NEM was a poor inactivator with 50% inactivation being observed at 10 mM; IAA,IAM, AcAnh and SuccAnh did not inactivate the enzyme at all. Several trends emerged from this study. First, the sulfhydryl modifiers, PCMBS and MMTS, were the most effective inactivators of OT, and activity was also strongly effected by DTNB, the only other compound which is completely selective for cysteine. Inactivation by DTNB and MMTS was fully reversible upon treatment with DTT, confirming the modification of a cysteine residue. When analyzed for substrate protection, the effectiveness of all three of these compounds as inactivators decreased when the enzyme was pretreated with Dol-P-P-$GlcNAc_2$; this substrate protection was observed for

Table 2-1. Susceptibility of OT Activity to Chemical Modifiers.

Chemical Reagent	50% Inactivation	Time Dependent	Substrate Protection	
			Peptide	Sugar
MMTS	100 μM	Yes	Yes	Yes
PCMBS	90 μM	Yes	Partial	Partial
DTNB	425 μM	Yes	No	Yes
NEM	10000 μM	Yes	Partial	Partial
IAA	No inhibition	NA	NA	NA
IAM	No inhibition	NA	NA	NA
DEPC	200 μM	No	No	No
BzAnh.	750 μM	No	ND	ND
AcAnh	No inhibition	NA	NA	NA
SuccAnh	No inhibition	NA	NA	NA

ND - Not determined; NA - Not applicable; 50% Inactivation represents the concentration which produced a 50% decrease in activity relative to a control after a 2 minute incubation.

MMTS even when the inactivator concentration was increased to 500 μM (see Figure 2-4). MMTS and PCMBS were also partially deterred by pretreatment with the peptide substrate Bz-NLT-NHMe; however, this peptide substrate protection disappeared when the concentration of MMTS was increased (see Figure 2-5). These results confirmed the presence of a cysteine residue in or near the oligosaccharide binding site.

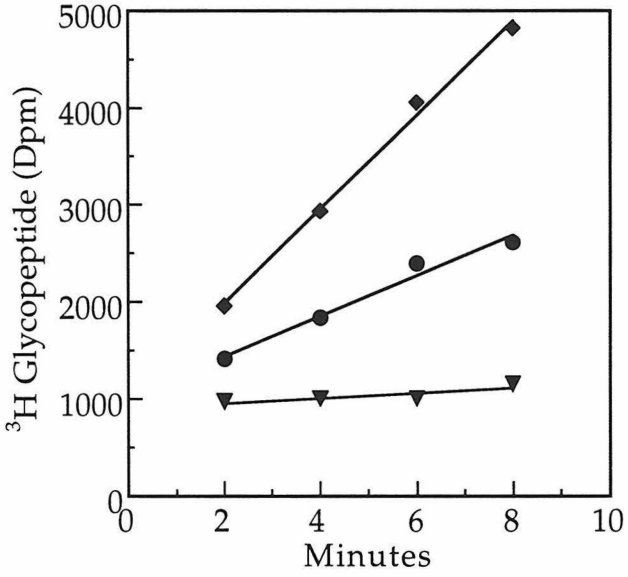

Figure 2-4. Oligosaccharide Substrate Protection from Inactivation of Crude Oligosaccharyl Transferaseby MMTS. Enzyme activity was measured after 2 minutes. Preincubation conditions: ● - MeOH, no substrate; ▼ - 500 μM MMTS, 4.4 μM Dol-PP(GlcNAc)$_2$; ◆ - 500 μM MMTS, no substrate.

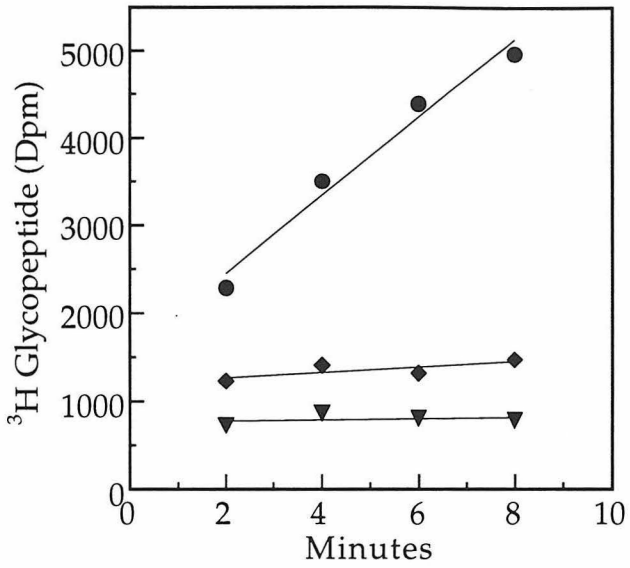

Figure 2-5. Peptide Substrate Protection from Inactivation of Crude Oligosaccharyl Transferase by MMTS. Enzyme activity was measured after 2 minutes. Preincubation conditions: ● - MeOH, no substrate; ▼ - 500 μM MMTS, 1.2 mM Bz-NLT-NHMe; ◆ - 500 μM MMTS, no substrate.

OT activity was only slightly affected by NEM, and no inactivation was observed with IAA or IAM. These inactivators all target nucleophilic residues and are therefore particularly useful for cysteine modification, as the side chain sulfur is commonly extremely nucleophilic. Although a cysteine residue is clearly localized at or near the active site based on the results discussed above, this residue does not appear to be nucleophilic, based on its reactivity towards these three compounds. The possibility that the decrease in nucleophilicity of the cysteine was the result of ligation to the required manganese metal cofactor was considered. To examine this hypothesis, OT was exhaustively treated with EDTA and *O*-phenanthroline to remove all

metal cations (confirmed by a complete loss in OT activity). The apoenzyme was treated with each of the three inactivators and then reconstituted with manganese and examined kinetically. No increase in inactivation was observed, demonstrating that the poor reactivity of the cysteine towards these inactivators was not due to interference by chelation of the cysteine to a metal cation. It appears that the cysteine is unusually non-reactive towards electrophiles, for reasons that have not yet been identified, and the enzyme is only inactivated by MMTS, DTNB, and PCMBS because of their high affinities for sulfur.

In contrast to the poor inactivation by NEM, OT activity was strongly affected by treatment with BzAnh, a modifier which will also react with any strong nucleophile. Further examination revealed that this inhibition was due to competition and not covalent modification of an amino acid; dilution of the enzyme inactivator complex resulted in restoration of enzyme activity. It has previously been observed that the peptide substrate Bz-NLT-NHMe is much more effective than Ac-NLT-NHMe, suggesting that OT has a specific preference for aromatic groups in this position.[20] It is possible that BzAnh competitively inhibits OT by accessing this aromatic binding pocket; this hypothesis is further supported by the inability of AcAnh and SuccAnh, non-aromatic anhydrides, to inhibit OT activity either competitively or irreversibly.

In general, DEPC reacts preferentially with histidine, to generate an ethoxyformylated histidine; this modification can be readily reversed by the addition of hydroxylamine. DEPC is unstable at pH 7.5, the optimum pH for OT, thus the pH was reduced to 6.0 to sufficiently enhance the stability of the modifier without seriously altering the overall activity of the enzyme. OT activity did decrease with DEPC treatment; however, substrate protection

experiments by pretreatment with either the peptide or oligosaccharide substrate revealed that the modified residue was not in either binding site. This inactivation may be caused by placing an obstruction at the entrance to the active site, or a modification which is well removed from the active site, but which disrupts the overall conformation of the enzyme. Attempts to regenerate OT activity through the addition of hydroxylamine were unsuccesful as the substrate Dol-P-P-$GlcNAc_2$ was labile to this reagent.

2.2.2 Design and Synthesis of *N*-biotinoyl(aminoethane)thiolsulfonate

The successful modification of a cysteine residue in the Dol-P-P-$GlcNAc_2$ binding site provided the opportunity for further characterization of OT by examining the specific site of modification. Of the reagents which adequately and predictably reacted with this cysteine, MMTS was the most readily modified to incorporate a detectible tag while maintaining the reactive portion of the molecule. An analog of MMTS was designed which contains the reactive thiosulfonate moiety covalently attached to a biotin reporter group. This reagent, methyl *N*-biotinoyl-(aminoethane)-thiolsulfonate (BMTS, Figure 2-6), should react with the same cysteine that is modified by MMTS. The biotin group will provide the ability to visualize the site of modification by separating the subunits of the inactivated protein by SDS-PAGE and analyzing for biotin through a Western blot with an avidin-horseradish peroxidase conjugation system (Biorad). The synthesis of *S*-(aminoethyl) methanethiolsulfonate hydrobromide has previously been reported.[23] BMTS was readily prepared from the condensation of this reagent with the *p*-nitrophenyl ester of biotin in the presence of mild base. Recrystallization from methanol afforded pure product.

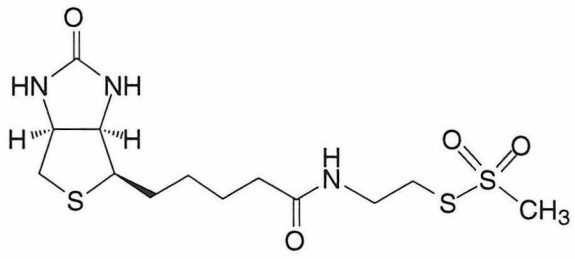

Figure 2-6. The Chemical Modification Reagent Methyl N-Biotinoyl(amino-ethane)thiolsulfonate (BMTS).

2.2.2 BMTS Modification and Visualization of Wbp1p Subunit

Complete kinetic evaluations of the inhibitory properties of BMTS and MMTS were performed with pure OT isolated from *S. cerevisiae*. The purified enzyme complex exhibits slightly different properties than the crude enzyme previously characterized. Most notably, the purified enzyme requires the addition of 140 mM sucrose and 0.5 mg/mL phosphatidylcholine for stabilization, during both the purification and the kinetic assays. Presumably, these additives stabilize the enzyme by interacting with the Dol-P-P-$GlcNAc_2$ binding site; in fact, the presence of these compounds also appears to protect OT from inactivation from MMTS or BMTS in a manner which is analogous to substrate protection by Dol-P-P-$GlcNAc_2$. This hypothesis was confirmed by investigating the ability of DTNB to inactivate solubilized OT under analogous conditions, and indeed, the DTNB concentration had to be increased from 425 μM to greater than 2 mM for inactivation to be observed when the enzyme mixture contained sucrose and PC. In a like manner, treatment of crude OT with 500 μM MMTS resulted in a complete loss of enzyme activity after only two minutes (Figure 2-4); however, when inactivation of pure OT was examined, significantly higher concentrations and longer incubation times were required to achieve similar levels of inactivation (Figure 2-7). Following MMTS inactivation, enzyme activity

could be slowly regenerated over time by treatment with 40 mM DTT at 4°C (Figure 2-8). Attempts to more quickly restore enzyme activity using the reagent tributylphosphine were also made.[24] This reagant is less hydrophilic than DTT and was chosen because it may be able to more readily access hydrophobic regions of the modified enzyme. However, these experiments were unsuccessful due to the lability of the enzyme in the presence of tributylphosphine.

As predicted, BMTS caused a decrease in OT activity in a manner which was very similar to that of MMTS. At a concentration of 2.5 mM, BMTS exhibited time dependent inactivation of OT (Figure 2-9) and substrate protection when the enzyme was pretreated with the substrate Dol-P-P-$GlcNAc_2$ (Figure 2-10). To visualize this modification, aliquots of modified pure enzyme were first treated with a small burst of MMTS, to limit any non-specific BMTS interactions. These samples were then incubated with BMTS for 0.5, 2, 5, and 30 minutes and quenched with cysteine (to react with the remaining BMTS); an additional sample was treated with BMTS for 30 minutes and then brought to 40 mM DTT. The quenched solutions were divided into two parts and loaded onto 12% polyacrylamide gels for electrophoresis and transfer to nitrocellulose as described.[15]One membrane was probed with the avidin-biotinylated alkaline phosphatase complex (Pierce); the second membrane was treated with anti-Wbp1p antiserum (provided by M. Aebi, Zurich).[25] The results of these Western blots are shown in Figure 2-11. Although OT is a multimeric protein complex (see Figure 2-2), treatment of OT with BMTS resulted in the modification of exclusively the Wbp1p subunit. The time dependence of this inactivation is clearly visible by the increase in the intensity of the biotin label; in addition,

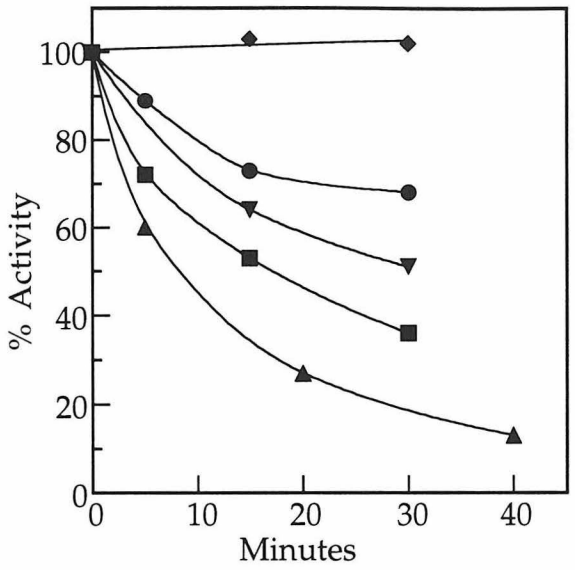

Figure 2-7. Inactivation of Pure Oligosaccharyl Transferase by MMTS. Enzyme activity was monitored at various concentrations of MMTS (◆ - control; ● - 0.5 mM; ▼ - 1.0 mM; ■ - 2.0 mM; ▲ - 4.0 mM).

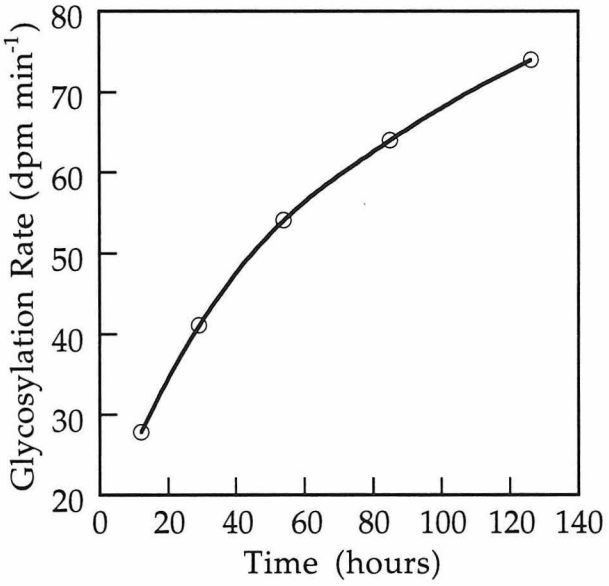

Figure 2-8. DTT Regeneration of Oligosaccharyl Transferase Activity Following Inactivation by MMTS.

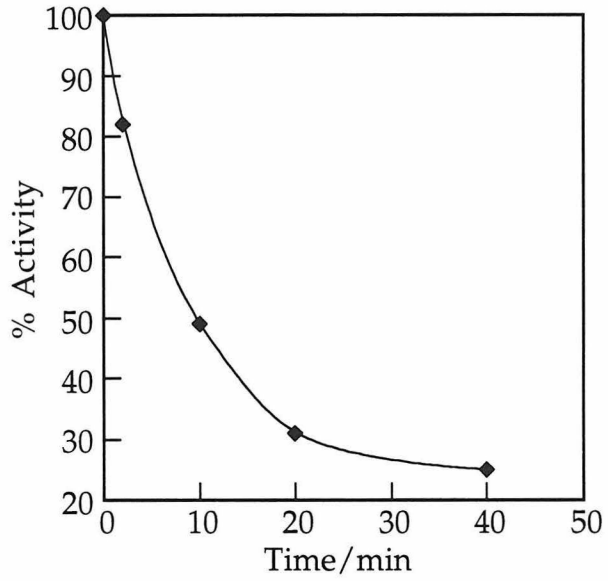

Figure 2-9. Inactivation of Pure Oligosaccharyl Transferase by BMTS. Enzyme activity was monitored at various times after the addition of 2.5 mM BMTS.

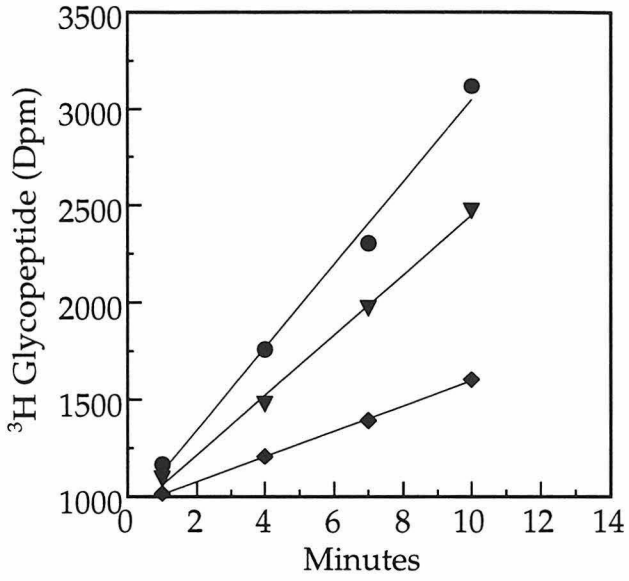

Figure 2-10. Substrate Protection of BMTS Inactivation with Pure Oligosaccharyl Transferase. Enzyme activity was measured after 15 minutes. Preincubation conditions: ● - MeOH, no substrate; ▼ - 2.5 mM BMTS, 4.4 μM Dol-PP$(GlcNAc)_2$; ◆ - 2.5 mM BMTS, no substrate.

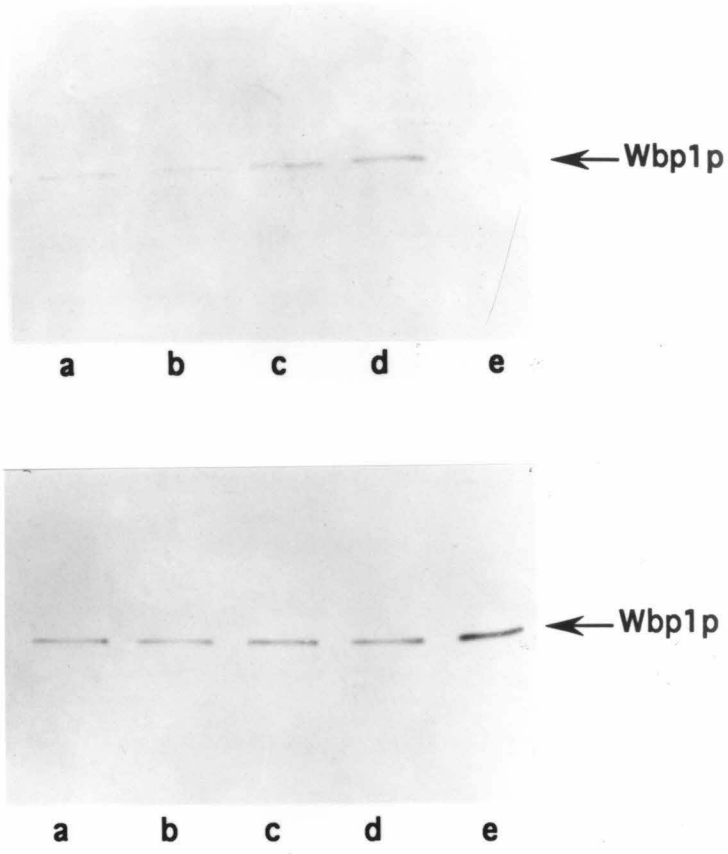

Figure 2-11. Labeling of Oligosaccharyl Transferase Wbp1p Subunit by BMTS. Top: Time-dependent labeling of oligosaccharyl transferase with 2.5 mM BMTS. Aliquots of the BMTS-treated enzyme were prepared and visualized as described in the text. Each lane contains an aliquot quenched after a different time interval: a) 0.5 minutes, b) 2.0 minutes, c) 5.0 minutes, d) 30.0 minutes, and e) 30.0 minutes (treated with DTT).

Bottom: Anti-Wbp1p staining of BMTS-treated aliquots. Identical amounts of the same samples were probed with antiserum raised against Wbp1p[25] and developed with an anti-rabbit IgG alkaline phosphatase conjugate. The samples are: a) 0.5 minutes, b) 2.0 minutes, c) 5.0 minutes, d) 30.0 minutes, and e) 30.0 minutes (treated with DTT).

the biotin reporter group is completely removed upon treatment with DTT (Figure 2-11A). When combined with the fact that pretreatment of OT with the substrate Dol-P-P-GlcNAc$_2$ produces substantial substrate protection, these results suggest that the sugar substrate binding site can be found on the Wbp1p subunit, or at the interface of this subunit and the rest of the protein complex.

2.3 Conclusions

Overall, characterization of OT through the use of commercially available chemical modification agents has revealed that a cysteine residue is located at or near the binding site for the substrate Dol-P-P-GlcNAc$_2$. It remains to be determined if this cysteine is catalytically important. In addition, BMTS was designed and synthesized and successfully inactivated the purified oligosaccharyl transferase complex. Visualization of this inactivation placed the site of modification, and consequently the sugar substrate binding site, on the Wbp1p subunit.

These studies were initially designed to probe for an active site base at or near the peptide binding site. However, the only reactive residue which was identified was placed in the oligosaccharide binding site. Inactivation due to the modification of this cysteine was not affected by pretreatment of the enzyme with Bz-NLT-NHMe suggesting that this residue is too far removed from the peptide binding site to be the active site base. This observation does not preclude the presence of an active site base for several reasons. First, the residue may not be reactive towards the reagents used in this study. This possibility could be examined through further modification studies. For example, an aspartic or glutamic acid side chain could function as an active site base. These residues would be most readily detected by

treatment of the enzyme with a carbodiimide and glycine to modify the carboxylate side chains. Second, the base required for deprotonation of the imidate may not be provided by an amino acid side chain, and instead may be the result of the activation of a water molecule via metal coordination. And finally, this catalytic residue may be inactive prior to treatment of the enzyme with the peptide substrate. These last two possibilities are most readily examined through the use of affinity labels, compounds which resemble the peptide substrate but have been altered to contain highly reactive electrophilic groups. The synthesis and kinetic evaluation of affinity labels for OT will be discussed in detail in chapter five.

2.4 Acknowledgements

Rahul Pathak developed the procedures used to solubilize and purify OT from *Saccharomyces cerevisiae.* He also provided a sample of purified OT for the BMTS experiments. Keith Rickert performed some preliminaray chemical modification experiments. Professor Barbara Imperiali synthesized BMTS and characterized the purified enzyme complex with BMTS and MMTS. Portions of the work presented in this chapter have appeared in the following publication: Pathak, R., Hendrickson, T. L., Imperiali, B. (1995). Sulfhydryl Modification of the Yeast Wbp1p Inhibits Oligosaccharyl Transferase Activity. *Biochemistry* **34**, 4179-4185.

2.5 Experimental

2.5.1 Materials

Solubilized microsomes and pure OT were isolated from *Saccharomyces cerevisiae* by Rahul Pathak as previously described.[15] PCMBS, MMTS, DEPC, IAA, IAM and NEM were purchased from Sigma. BzAnh and

SuccAnh were purchased from Aldrich. AcAnh was purchased from Fisher. DTNB was purchased from Calbiochem.

2.5.2 Chemical Modification of Crude Oligosaccharyl Transferase

General Enzyme Assay

In a typical assay, 50,000 dpm [^{3}H]-dolichylpyrophosphoryl-N,N'-diacetylchitobiose (specific activity 36.5 Ci/mmol) were dried down in a micro-centrifuge tube. The radiolabelled sugar[21] was redissolved in 10 µL of a DMSO solution of 2.5 mM Bz-NLT-NHMe and 90 µL assay buffer (50 mM Tris-HCl, pH 7.5, 1.2% Triton X-100, 10 mM MnCl). The reaction was initiated by the addition of 100 µL of an enzyme solution prepared by diluting the solubilized microsomes (25 µL) to 150 µL with 7.5 µL DMSO and assay buffer. Reaction aliquots (4 x 40 µL) were removed at two minute intervals and quenched into 1.2 mL of 3:2:1 chloroform/methanol/4 mM $MgCl_2$. The tritiated glycopeptide was separated from the unreacted glycolipid through a series of extractions. The upper aqueous layer of the quenched reaction mixture was removed and the organic layer was extracted twice with 0.6 mL Theoretical Upper Phase with salt (TUP: 12/192/186/2.69 chloroform/ methanol/ water/0.25 M $MgCl_2$). The combined aqueous layers were quantitated for tritium content in 5.5 mL Ecolite (ICN) as disintegrations per minute.

Concentration Dependence Assay

Stock solutions of PCMBS, NEM, DTNB, IAA, IAM, and the three anhydrides were prepared in DMSO; solutions of MMTS were prepared in methanol; DEPC solutions were prepared fresh daily in DMSO. Solubilized microsomes (25 µL) were combined with 117.5 µL assay buffer and 7.5 µL of

the appropriate inactivator solution and incubated at room temperature. (An MES/KOH buffer at pH=6.0, with 140 mM sucrose and 1.2% Triton-X, was used for all DEPC experiments, rather than the standard buffer described above). After two minutes, 100 µL of this mixture were transferred to a solution containing the radiolabelled sugar donor and Bz-NLT-NHMe and the assay was completed as described above. A corresponding control assay was performed for each inactivator in which 7.5 µL DMSO (or MeOH for MMTS) was added to the enzyme solution. Each inactivator was examined over a range of final concentrations from 50 µM to 10 mM and percent inactivation was determined relative to the control. Unless otherwise stated, all further experiments were performed at the inactivator concentration which produced a 50% drop in enzymatic activity under these conditions.

The concentration dependence of DTNB was also evaluated under conditions where the standard assay buffer had the following additions: 140 mM sucrose and 0.5 mg/mL or 140 mM sucrose alone or 0.5 mg/mL PC alone.

Time Dependence of Inactivation

Solubilized microsomes (50 µL) were combined with 15 µL PCMBS, NEM, DTNB, or MMTS solution and 235 µL assay buffer. This solution was incubated at room temperature and 100 µL aliquots were removed after 2 and 15 minutes. Aliquots were assayed as described above. Time dependence was determined relative to a control experiment.

Peptide Substrate Protection - Bz-NLT-NHMe

Solubilized microsomes (25 µL), 110 µL assay buffer and 7.5 µL 20 mM Bz-NLT-NHMe in DMSO were combined and incubated at room temperature for several minutes. An aliquot of inactivator (7.5 µL) was added. After two

minutes, 100 μL of this mixture was transferred to a solution of Dol-P-P-$GlcNAc_2$ (50,000 dpm, 36.5 Ci/mmol) in 10 μL DMSO and 90 μL assay buffer; the assay was completed as described above. Two controls were performed for each inactivator. First, the inactivator was replaced by 7.5 μL DMSO (or MeOH). Second, the Bz-NLT-NHME was omitted from the enzyme preincubation and the Dol-P-P-$GlcNAc_2$ (50,000 dpm, 36.5 Cimmol) was dissolved in 10 μL 10 mM Bz-NLT-NHMe in DMSO and 90 μL assay buffer prior to initiation of the assay.

Preparation of Dol-P-P-$GlcNAc_2$ with Low Specific Activity

Dol-P-P-[^{3}H]-$GlcNAc_2$ (^{3}H labeled at C-6 position of the β-1,4 linked GlcNAc) was prepared as described previously.[21] Material of the desired specific activity for each experiment was obtained by the dilution of high specific activity UDP-[^{3}H]GlcNAc (36.5 Ci/mmol, NEN) with unlabelled UDP-GlcNAc, prior to the biosynthetic preparation of the lipid-linked disaccharide.

Sugar Substrate Protection - Dol-P-P-$GlcNAc_2$

Aliquots of Dol-P-P-[^{3}H]-$GlcNAc_2$ (200,000 dpm, 0.22 Ci/mmol) were dried down under nitrogen, redissolved in 10 μL DMSO and 110 μL assay buffer and combined with solubilized microsomes (25 μL). Two solutions were combined with 5 μL of either the appropriate inactivator solution (in DMSO or MeOH) or DMSO or MeOH. After an incubation time of two minutes, the assays were initiated by the addition of 50 μL of a prepared solution of 50 μL 2.5 mM Bz-NLT-NHMe and 200 μL assay buffer. As a control, 20 μL DMSO, 220 μL assay buffer, 50 μL solubilized microsomes and 10 μL inactivator were combined and, after a two minute incubation, 150 μL of this mixture was transferred to a solution of Dol-P-P-[^{3}H]-$GlcNAc_2$ (200,000

dpm, 0.22 Ci/mmol) in 10 μL 2.5 mM DMSO solution of Bz-NLT-NHMe and 40 μL assay buffer. Aliquots of each assay were removed and quenched as described above.

2.5.3 Synthesis of Methyl *N*-Biotinoyl-(aminoethane)thiolsulfonate (BMTS)

Methyl aminoethanethiolsulfonate hydrobromide (44 mg, 0.19 mmol)[23] and (+)-biotin *p*-nitrophenyl ester (70 mg, 0.19 mmol) were dissolved in 0.4 mL anhydrous dimethylformamide and cooled to 0°C. Triethylamine (24μL, 0.19 mmol) was then added dropwise with stirring. After 2 hours at this temperature, an additional portion of methyl aminoethanethiolsulfonate hydrobromide (10 mg, 0.05 mmol) was added. The reaction was then stirred for 2 hours at which time the solvent was removed under low pressure at room temperature. The crude residue was then redissolved in a minimal volume of warm methanol, filtered and cooled to 0°C. The coupled product crystallized readily from the filtrate. BMTS was further purified by two additional recrystallizations from methanol. The reaction afforded 50 mg (70% yield) of pure white crystalline product.

Mp 108-109°C. MS: [MH^+] calcd. for $C_{13}H_{23}N_3O_4S_3$, 382 obsd. 382. ^1H NMR (d_7-DMF) δ: 1.36-1.76 (m, 6H), 2.19 (t, 2H, J =7.4 Hz), 2.82 (AB, 2H, J = 0, 4.9 and 12.4 Hz), 3.18 (m, 1H), 3.37 (t, 1H, J = 6.3 Hz), 3.52 (t, 1H, J = 6.0 Hz), 3.58 (s, 3H), 4.28 (m, 1H), 4.45 (m, 1H), 6.38 (s, 1H), 6.47 (s, 1H), 8.14 (t, 1H, J = 5.2 Hz). ^{13}C NMR (d_7-DMF) δ: 26.1, 29.0, 29.1, 36.0, 36.3, 39.1, 40.7, 50.6, 56.4, 60.5, 62.1, 163.7, 173.5.

2.5.4 Chemical Modifications of Pure Oligosaccharyl Transferase

General Enzyme Assay

Modification of the purified yeast oligosaccharyl transferase with MMTS was performed in 50 mM HEPES, pH 7.5, 140 mM sucrose, 0.6% Nonidet P-40, 10 mM $MnCl_2$ and 0.5 mg/mL phosphatidylcholine at 25°C and a protein concentration of 23.6 µg/mL. MMTS in 6 µL methanol was added to 114 µL pure enzyme solution to yield final reagent concentrations of 0 mM, 0.5 mM, 1.0 mM, 2.0 mM, and 4.0 mM. At various time intervals after MMTS addition, 30 µL of the preincubation mixture was diluted to 200 µL into the assay buffer containing Bz-NLT-NHMe (10 µL 2.5 mM in DMSO) and Dol-P-P-$GlcNAc_2$ (200,000 dom, 0.22 Ci/mmol). Enzyme activity was quantitated as described above for the solubilized microsomes and the loss of catalytic activity was monitored over 40 minutes. In the absence of MMTS the enzyme maintained full activity over this time period.

Regeneration of Activity with Dithiothreitol

Pure oligosaccharyl transferase was treated with MMTS as described above and then diluted to 40 mM DTT and stored at 4°C. The regeneration of activity was monitored over time by removing aliquots every 24h and performing the assay as described above. Unmodified oligosaccharyl transferase activity was not affected by the addition of DTT. Attempts to completely regenerate enzymatic activity with tributylphosphine[24] were hindered due to the lability of the enzyme in the presence of this reagent at 1 mM concentrations.

Inactivation of Pure Oligosaccharyl Transferase with BMTS

BMTS inactivation was carried out as described for MMTS at a final concentration of 2.5 mM. Inactivation was also performed in the presence of Dol-P-P-$GlcNAc_2$ in order to demonstrate substrate protection by preincubating 100 µL of the purified enzyme complex with $1x10^6$ dpm [^{3}H] Dol-P-P-$GlcNAc_2$ (0.22 Ci/mmol) for ten minutes. After this time, BMTS (2.5 mM in MeOH) was added. At 15 minutes, 20 µL of the incubation mixture was assayed for transferase activity in 180 µL assay buffer containing 10 µL 2.5 mM Bz-NLT-NHME in DMSO. As a control, the Dol-P-P-$GlcNAc_2$ in the incubation mixture was omitted and an equivalent amount of this substrate was added to the assay buffer.

Visualization of Subunit Containing the Biotin Modification

An aliquot of purified oligosaccharyl transferase was modified with BMTS until the enzyme was completely inactivated. The biotinoylated subunit was visualized as previously described.[15]

2.6 References

1. Means, G. E.; Feeney, R. E. *Chemical Modifications of Proteins*; Holden-Day, Inc.: San Fansisco, 1971.

2. Vallee, B. L.; Riordan, J. F. "Chemical Approaches to the Properties of active Sties of Enzymes," *Ann. Rev. Biochem.* **1969**, *707*, 733-794.

3. Kenyon, G. L.; Bruice, T. W. "Novel Suflhydryl Reagents," *Meth. Enzym.* **1977**, *47*, 407-430.

4. Burstein, Y.; Walsh, K. A.; Neurath, H. "Evidence of an Essential Histidine Residue in thermolysin," *Biochemistry* **1974**, *13*, 205-210.

5. Holbrook, J. J.; Ingram, V. A. "Ionic Properties of an Essential Histidine Residue in Pig Heart Lactate Dehydrogenase," *Biochem. J.* **1973**, *131*, 729-738.

6. Brocklehurst, K.; Little, G. "Reactions of Papain and of Low-Molecular-Weight Thiols with some Aromatic Disulphides," *Biochem. J.* **1973**, *133*, 67-80.

7. Smith, D. J.; Kenyon, G. L. "Nonessentiality of the Active Sulfhydryl Group of Rabbit Muscle Creatine Kinase," *J. Biol. Chem.* **1974**, *249*, 3317-3318.

8. Berliner, L. J.; Grunwald, J.; Hankovszky, O.; Hideg, K. "A Novel Reversible Thiol-Specific Spin Label: Papain Active Site Labeling and Inhibition," *Anal. Biochem.* **1982**, *119*, 450-455.

9. Leavis, P. C.; Lehrer, S. S. "A Sulfhydryl-Specific Fluorescent Label, S-Mercuric N-DansylCysteine. Titrations of Glutathione and Muscle Proteins," *Biochemistry* **1974**, *13*, 3042-3048.

10. Bloxham, D. P.; Cooper, G. K. "Formation of a Polymethylene Bis(disulfide)Intersubunit Cross-Link Between Cysteine-281 Residues in Rabbit Muscle Glyceraldehyde-3-phosphte Dehydrogenase Using Octamethylene Bis(methane[^{35}S]thiosulfonate)," *Biochemistry* **1982**, *21*, 1807-1812.

11. Kumar, V.; Korza, G.; Heinemann, F. S.; Ozols, J. "Human Oligosaccharyltransferase: Isolation, Characterization, and the Complete Amino Acid Sequence of 50-kDa Subunit," *Arch. Biochem. Biophys.* **1995**, *320*, 217-223.

12. Kelleher, D. J.; Kreibich, G.; Gilmore, R. "Oligosaccharyltransferase Activity Is Associated with a Protein Complex Composed of Ribophorins I and II and a 48 kD Protein," *Cell* **1992**, *69*, 55-65.

13. Breuer, W.; Bause, E. "Oligosaccharyl Transferase is a Constitutive Component of an Oligomeric Protein Complex From Pig Liver Endoplasmic Reticulum," *Eur. J. Biochem.* **1995**, *228*, 689-696.

14. Kumar, V.; Heinemann, F. S.; Ozols, J. "Purification and Characterization of Avian Oligosaccharyltransferase: Complete Amino Acid Sequence of the 50 kDa Subunit," *J. Biol. Chem.* **1994**, *269*, 13451-13457.

15. Pathak, R.; Hendrickson, T. L.; Imperiali, B. "Sulfhydryl Modification of the Yeast Wbp1p Inhibits Oligosaccharyl Transferase Activity," *Biochemistry* **1995**, *34*, 4179-4185.

16. Kelleher, D. J.; Gilmore, R. "The *Saccharomyces cerevisiae* Oligosaccharyltransferase Is a Protein Complex Composed of Wbp1p, Swp1p, and Four Additional Polypeptides," *J. Biol. Chem.* **1994**, *269*, 12908-12917.

17. Knauer, R.; Lehle, L. "The N-oligosaccharyltransferase Complex From Yeast," *FEBS Lett.* **1994**, *344*, 83-86.

18. Michel, H. "Crystallization of Membrane Proteins," *Trends in Biol. Sci.* **1983**, *8*, 56-59.

19. Imperiali, B.; Shannon, K. L.; Unno, M.; Rickert, K. W. "A Mechanistic Proposal for Asparagine-Linked Glycosylation," *J. Am. Chem. Soc.* **1992**, *114*, 7944-7945.

20. Imperiali, B.; Shannon, K. L. "Differences Between Asn-Xaa-Thr Containing Peptides: A Comparison of Solution Conformation and Substrate Behavior with Oligosaccharyltransferase," *Biochemistry* **1991**, *30*, 4374-4380.

21. Imperiali, B.; Zimmerman, J. W. "Synthesis of Dolichylpyrophosphate-Linked Oligosaccharides," *Tetrahedron Lett.* **1990**, *31*, 6485-6488.

22. Pathak, R.; Parker, C. S.; Imperiali, B. "The Essential Yeast NLT1 Gene Encodes the 64kDa Glycoprotein Subunit of the Oligosaccharyl Transferase," *FEBS Lett.* **1995**, *362*, 229-234.

23. Bruice, T. W.; Kenyon, G. L. "Novel Alkyl Alkanethiolsulfonate Sulfhydryl Reagents. Modification of Derivatives of L-Cysteine," *J. Prot. Chem.* **1982**, *1*, 47-58.

24. Nishimura, J. S.; Kenyon, G. K.; Smith, D. J. "Reversible Modification of the Sulfhydryl Groups of *Escherichia coli* Succinic Thiokinase with Methanethiolating Regents, 5,5'-Dithio-bis(2-Nitrobenzoic Acid), *p*-Hydroxymercuribenzoate, and Ethylmercurithiosalicylate," *Arch. Biochem. Biophys.* **1975**, *170*, 461-467.

25. te Heesen, S.; Rauhut, R.; Aeversold, R.; Abelson, J.; Aebi, M.; Clark, M. W. "An Essential 45 kDa Yeast Transmembrane Protein Reacts With Anti-Nuclear Pore Antibodies: Purification of the Protein Immunolocalization and Cloning of the Gene," *Eur. J. Cell. Biol.* **1991**, *56*, 8-18.

Chapter 3. Asparagine-Linked Glycosylation: Metal Ion Dependence

3.1 Introduction

Oligosaccharyl transferase catalyzes the glycosylation of specific asparagine residues within nascent peptides as they emerge into the endoplasmic reticulum (ER).[1] The ER contains various metal ions and cofactors which can be used by OT to facilitate catalysis; this type of cofactor participation often provides enzymes with reactivity not normally available from the 20 natural amino acids. Because of the potential mechanistic importance of cofactor participation, a complete evaluation of the *N*-linked glycosylation process rests on the elucidation of the role of these constituents, including metal ions.

OT manifests an absolute requirement for certain divalent metal cations for activity. In the native enzyme, Mn(II) is considered to be the endogenous metal ion;[2] however, in reconstitution experiments, magnesium can be substituted for manganese with the regeneration of approximately one-third of the native activity.[3] Manganese-dependent enzymes fall into two categories: those which contain a tightly bound manganese and those which are loosely associated with their metal cofactor.[4] For the latter class of enzymes, which includes OT, stimulation of enzyme activity is often observed with the addition of exogenous manganese to the enzyme solution. In some cases, other similar metal cations may also effect enzyme activity. In light of the potential utility of manganese as a spectroscopic probe, particularly in EPR experiments,[5] it is important to establish if the metal cofactor plays an implicit chemical role in OT catalysis, or if it serves simply in a structural capacity.

A powerful tool for assessing the potential role of a metal ion in enzyme catalysis involves the parallel kinetic analyses of substrates and substrate analogs that differ only in the metal-coordinating properties of the heteroatoms at or near the reacting center. This approach has been used in the presence of different metal ions to provide valuable information on the direct catalytic role of the

cofactors in the hammerhead RNA self cleavage reaction[6] and in carboxypeptidase mediated amide hydrolysis.[7] In these cases, substrate analogs, in which an oxygen near the reactive site was replaced by a sulfur atom, were prepared. Kinetic analyses in the presence of different metal ions revealed a direct relationship between the identity and thiophilicity of the metal and the effectiveness of the substrate, thereby demonstrating that the metal and substrate interact during catalysis.

It has recently been reported that the incorporation of thioasparagine, in place of asparagine, affords competent substrates for the glycosylation reaction catalyzed by OT.[8] The kinetic constants for the tripeptide substrates Bz-Asn-Leu-Thr-NHMe (**1**) and Bz-Asn(γS)-Leu-Thr-NHMe (**2**) were determined with porcine liver OT. These two substrates exhibited similar binding constants (K_M); however, the thioasparagine tripeptide **2** was a less efficient substrate with an approximate tenfold drop in maximum velocity (V_{max}) when compared to the V_{max} of **1**.[8] Because **2** is an adequate substrate for OT and because sulfur and oxygen exhibit different metal binding affinities, this subtle replacement provides an ideal platform for the examination of the role of the required metal cofactor.

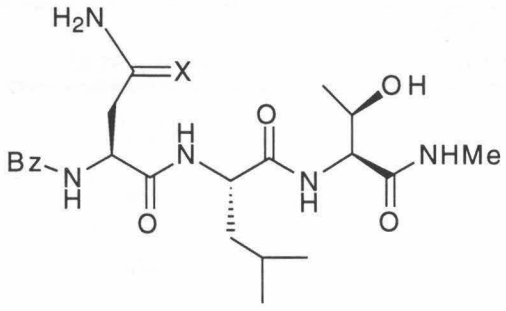

1: X=O
2: X=S

This chapter describes a series of experiments designed to identify and elucidate interactions between the peptide substrate and the required metal cofactor during OT mediated catalysis. Comparative kinetic analyses were performed on Bz-Asn-Leu-Thr-NHMe (**1**) and Bz-Asn(γS)-Leu-Thr-NHMe (**2**) with OT that had been independently reconstituted with four different metal cations. These studies revealed that specific features of the metal cofactor, particularly the ionic radius and thiophilicity, directly affect the substrate behavior of the peptide. In addition, a detailed analysis of the glycosylation products of **2** confirmed that glycosylation occurs predominantly or exclusively on the nitrogen of the thioasparagine side chain suggesting that, in natural systems, OT may play a specific role in directing the regiochemistry of glycosylation.

3.2 Results and Discussion

3.2.1 Oligosaccharyl Transferase Metal Cation Cofactor Requirements

The metal cofactor requirements for oligosaccharyl transferase, isolated from both porcine liver and *S. cerevisiae* sources, were investigated (Table 3-1).

Table 3-1. Oligosaccharyl Transferase Activity with Various Metal Cations.

Metal	*S. cerevisiae* Activity (%)	Porcine Liver Activity (%)
Mn2+	100	100
Fe2+	84	50
Co2+	32	0
Mg2+	32	20
Ca2+	13	34

The ability of various metal cations to reconstitute OT activity was examined by adding exogenous metal stocks to solubilized apoenzyme and assaying for OT activity with the standard peptide Bz-Asn-Leu-Thr-NHMe (**1**). For these studies, the *S. cerevisiae* enzyme was solubilized as previously described;[9] the porcine enzyme was solubilized by a modification of the procedure described for the canine pancreas enzyme.[10] Each apoenzyme was prepared by treating the solubilized enzyme with the chelating resin Chelex (BioRad) until a standard assay for OT activity (see Appendix A) revealed that a complete loss in enzyme activity had been achieved. Chelex is a resin bound form of EDTA, and its use removed the need for dialysis and greatly increased the availability of apoenzyme, particularly with the porcine enzyme which was unstable during extensive dialysis. Wild type enzyme activity could be regenerated by the addition of exogenous manganese. After solubilization in a detergent buffer with sucrose and phosphatidylcholine, the two sources of apoenzyme were stable for several months at -80°C.

In each case, a final metal cation concentration of 10 mM was utilized to insure maximum enzyme activity. Wild type activity was observed with manganese ion concentrations ranging from 1 mM to 20 mM. The addition of several divalent metal cations, including magnesium, iron, cobalt, and calcium, resulted in the reconstitution of enzyme activity (see Table 3-1). Surprisingly, cobalt effectively reconstituted *S. cerevisiae* OT activity; however, it was ineffective with the porcine liver enzyme; the cause of this variation is currently unknown. Divalent zinc, nickel, cadmium, mercury, copper, lead and trivalent aluminum were also examined. However, these cations did not reconstitute enzyme activity. These studies suggest that OT has a distinct preference for metal cations which can adopt octahedral coordination geometries.

3.2.2 Kinetic Constants for 1 and 2 with Reconstituted Oligosaccharyl Transferase

The kinetic constants for compounds **1** and **2** have previously been determined with porcine liver *oligosaccharyl transferase* in the presence of manganese.[8] Compound **1** is also an excellent substrate for yeast OT;[11] however, analysis of the thioamide **2** with the yeast enzyme revealed that **2** is not glycosylated and instead behaves as a competitive inhibitor with an approximate K_i of 100 μM. This observation is consistent with the observed differences in kinetic responses of the two enzyme sources. Typically, peptide substrates bind the *S. cerevisiae* enzyme more tightly (lower K_M) than the porcine enzyme; however, they are glycosylated less efficiently (lower V_{max}). Although the thioamide **2** is recognized by the yeast enzyme, its V_{max} is too low to be detected (as manifested by the competitive inhibition kinetics). Because of the poor substrate behavior of **2** with yeast OT, all further studies were performed with the porcine liver enzyme.

To examine interactions between the metal cation and the peptide substrate during OT mediated catalysis, kinetic analyses on **1** and **2** were performed in the presence of four different divalent metal ions: Mn^{2+}, Fe^{2+}, Mg^{2+}, and Ca^{2+}. These metals were chosen because they produce significant rates of turnover with **1** (Table 3-1) and they represent a wide range of ionic radii (0.64Å to 0.99Å), as well as different affinities for sulfur ($Fe^{2+}>Mn^{2+}>>Mg^{2+}\approx Ca^{2+}$). Each enzyme assay was run at a final metal concentration of 10.5 mM which was well within the range of maximum activity for each of the four metals. Since the kinetic experiments did not control for Fe^{2+} oxidation, the possible effects of Fe^{3+} were also considered. Control experiments indicate that enzyme activity is not reconstituted with Fe^{3+}. Furthermore, in the presence of 10 mM Fe^{2+}, concentrations of Fe^{3+} below 0.5 mM did not inhibit

enzyme activity. Partial inhibition of OT activity due to the oxidation of Fe^{2+} to Fe^{3+} was observed after 6 - 8 hours of incubation in the preparative product synthesis; this inhibition would not be significant on the 20 minute time scale of the kinetic experiments.

Each set of kinetic data was obtained from the same stock of apoenzyme to allow for comparison between data sets. The concentration of Dol-P-P-GlcNAc-[^{3}H]-GlcNAc was maintained at 12.6 nM for each kinetic experiment. This concentration is well below the reported K_M of 1.2 μM for the lipid-linked substrate.[3] The possibility that the K_M could vary when the enzyme was reconstituted with the various metals was considered. However, when the Dol-P-P-GlcNAc-[^{3}H]-GlcNAc concentration was increased to 41.3 μM (above K_M) for the glycopeptide synthesis, similar trends in relative velocities were observed.

Kinetic constants were calculated based on data obtained from a Hanes plot (S/V vs. S where S equals the peptide concentration and V is the relative maximum velocity observed at each concentration).[12] These constants were not calculated when peptide **2** was examined with OT and magnesium or calcium, because under these conditions, the substrate behavior was too poor. Figures 3-1 through 3-8 show representative kinetic data for each peptide and metal cation combination. In addition to the kinetic analyses of **1** and **2**, background rates for each metal were assessed in the absence of peptide substrate. These rates were very low and may be due either to glycosylation of endogenous proteins or to metal mediated breakdown of the glycosyl donor. Control experiments indicated that the background rates are suppressed in the presence of the tripeptide substrates; therefore, the rate data were used directly for calculation of the kinetic constants without correction.

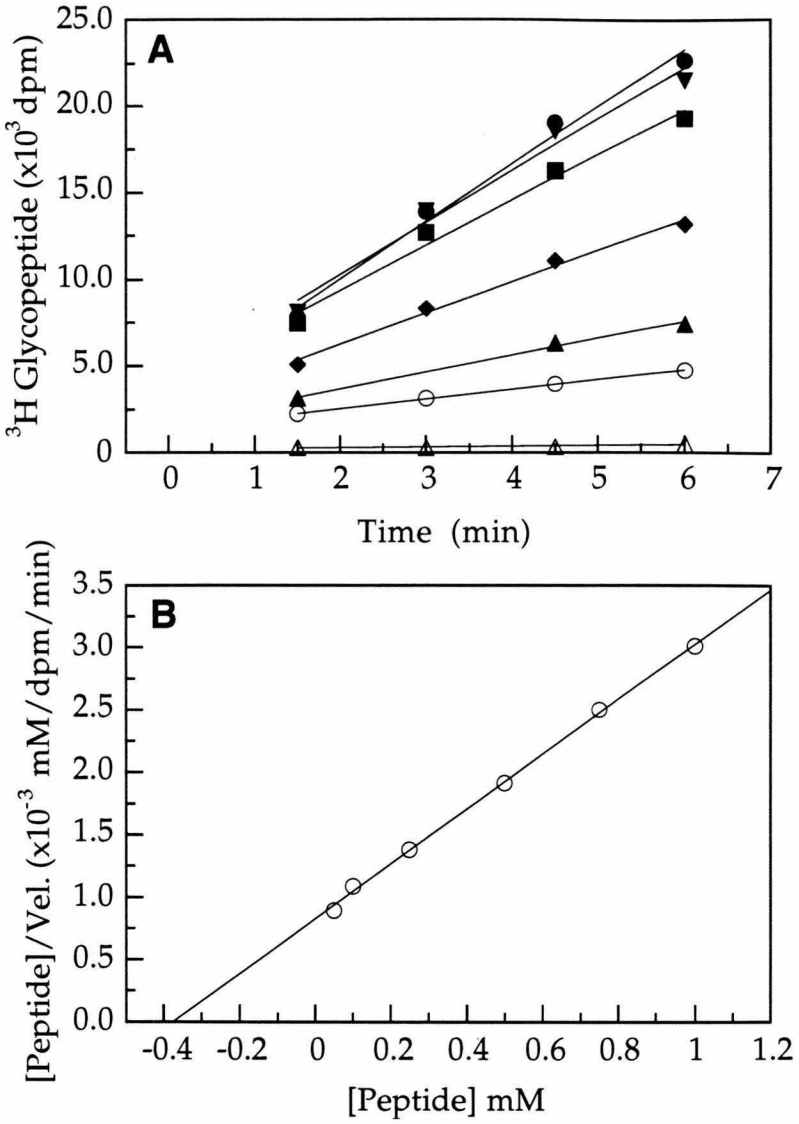

Figure 3-1. Kinetic Analysis of Bz-Asn-Leu-Thr-NHMe (**1**) with $MnCl_2$. (A) Relative rates of glycosylation with increasing concentrations of **1** (○, 0.05 mM; ▲, 0.10 mM; ◆, 0.25 mM; ■, 0.5 mM; ▼, 0.75 mM; ●, 1.0 mM) in the presence of 10.5 mM $MnCl_2$. Apoenzyme was also assayed without added metal cations (△, 0.5 mM Bz-Asn-Leu-Thr-NHMe (**1**)). (B) Hanes plot of **1** with $MnCl_2$.

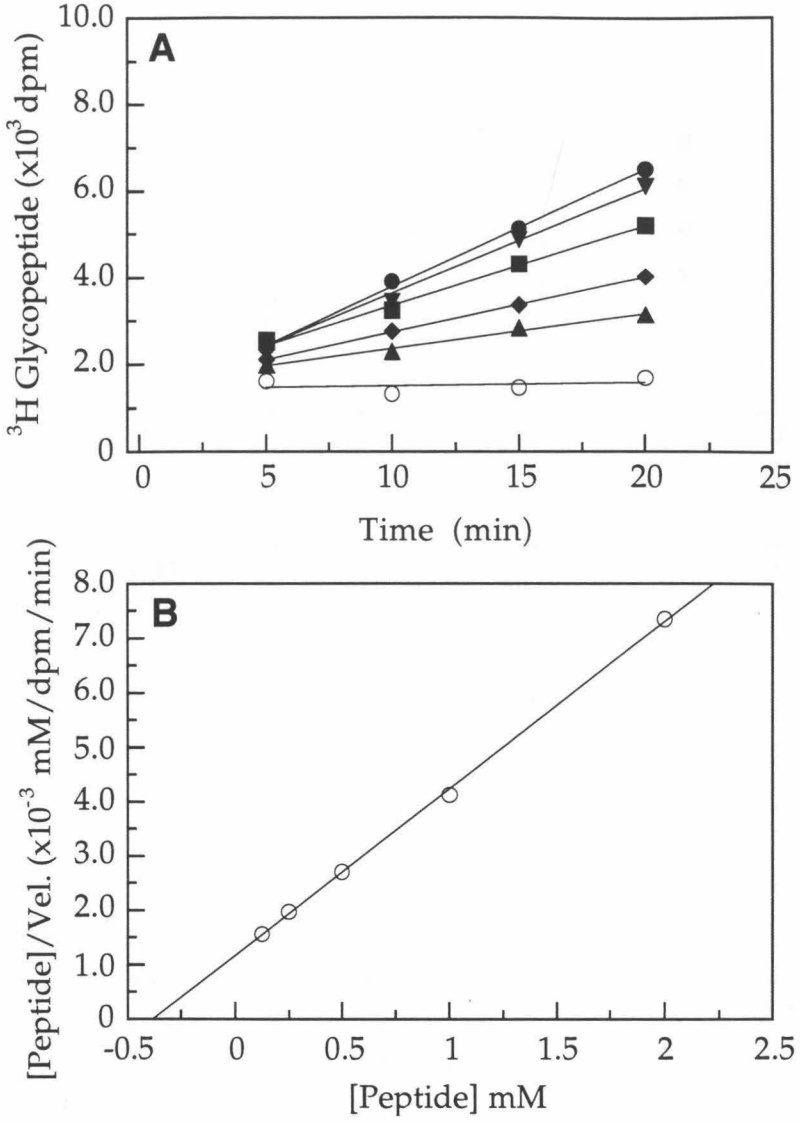

Figure 3-2. Kinetic Analysis of Bz-Asn(γS)-Leu-Thr-NHMe (**2**) with $MnCl_2$. (A) Relative rates of glycosylation with increasing concentrations of **2** (○, 0 mM; ▲, 0.125 mM; ◆, 0.25 mM; ■, 0.5 mM; ▼, 1.0 mM; ●, 2.0 mM) in the presence of 10.5 mM $MnCl_2$. (B) Hanes plot of **2** with $MnCl_2$.

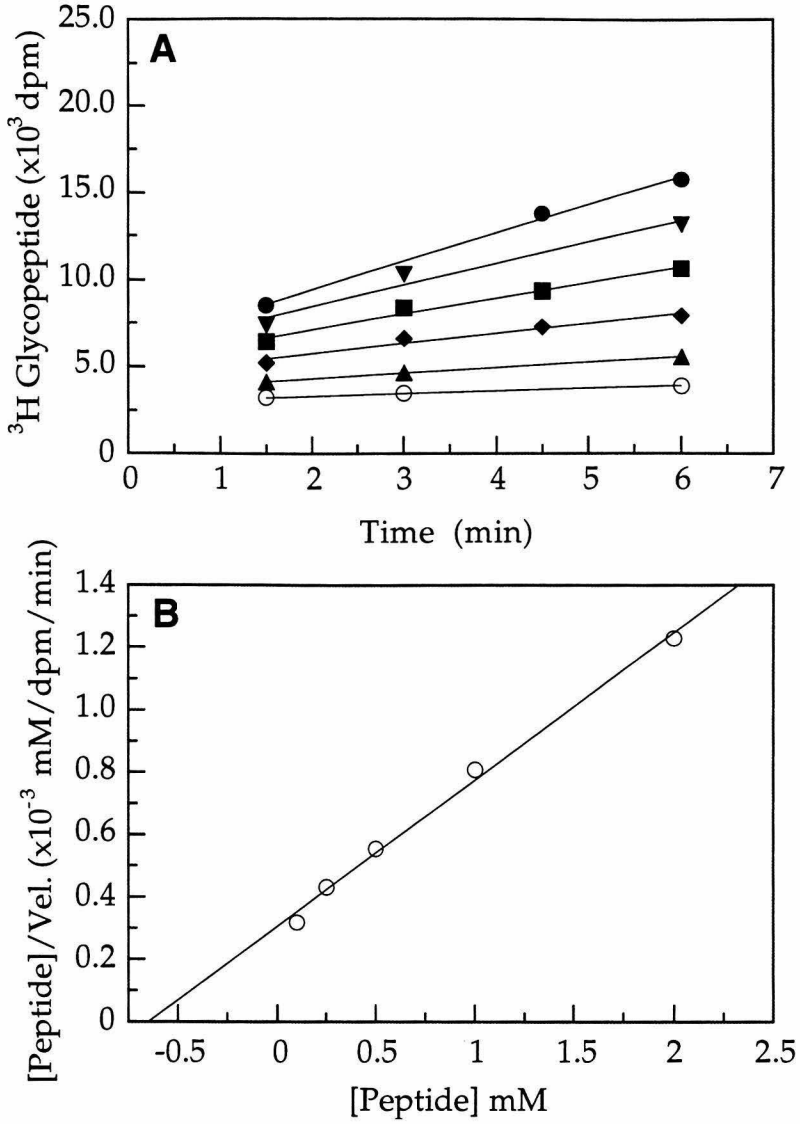

Figure 3-3. Kinetic Analysis of Bz-Asn-Leu-Thr-NHMe (**1**) with $Fe(NH_4)_2(SO_4)_2$. (A) Relative rates of glycosylation with increasing concentrations of **1** (○, 0 mM; ▲, 0.10 mM; ◆, 0.25 mM; ■, 0.5 mM; ▼, 1.0 mM; ●, 2.0 mM) in the presence of 10.5 mM $Fe(NH_4)_2(SO_4)_2$. (B) Hanes plot of **1** with $Fe(NH_4)_2(SO_4)_2$.

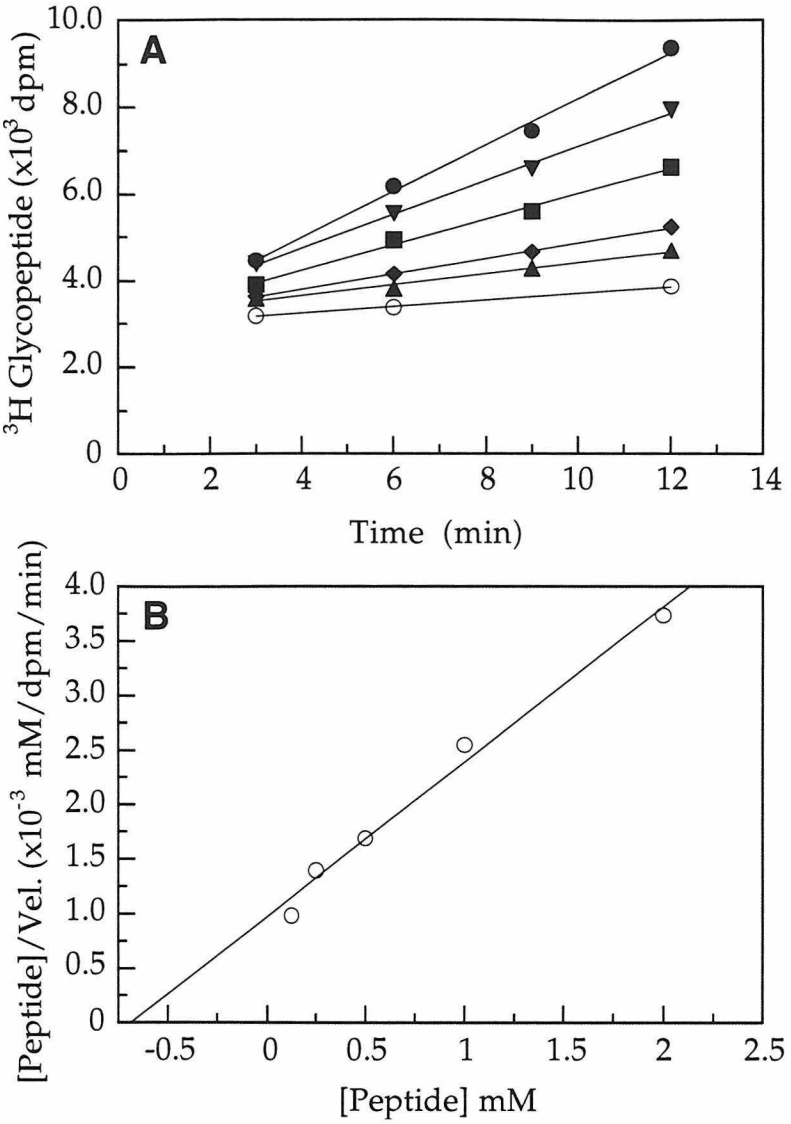

Figure 3-4. Kinetic Analysis of Bz-Asn(γS)-Leu-Thr-NHMe (**2**) with $Fe(NH_4)_2(SO_4)_2$. (A) Relative rates of glycosylation with increasing concentrations of **2** (○, 0 mM; ▲, 0.125 mM; ◆, 0.25 mM; ■, 0.5 mM; ▼, 1.0 mM; ●, 2.0 mM) in the presence of 10.5 mM $Fe(NH_4)_2(SO_4)_2$. (B) Hanes plot of **2** with $Fe(NH_4)_2(SO_4)_2$.

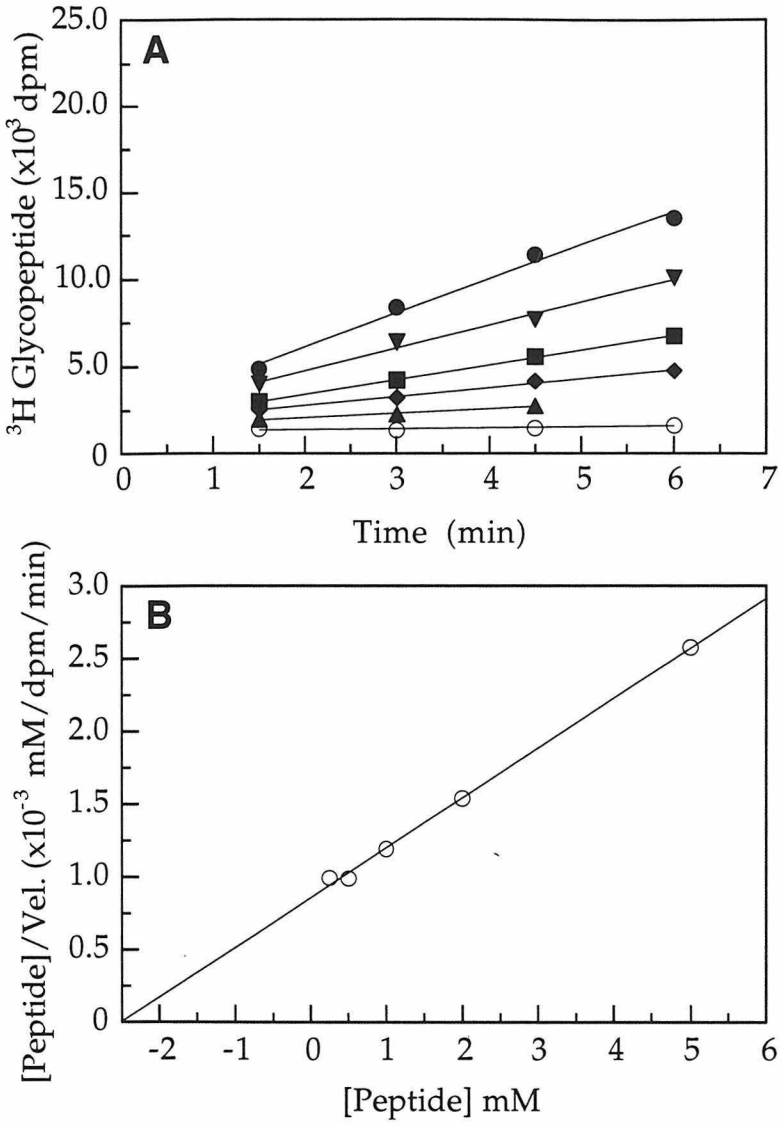

Figure 3-5. Kinetic Analysis of Bz-Asn-Leu-Thr-NHMe (**1**) with $MgCl_2$. (A) Relative rates of glycosylation with increasing concentrations of **1** (○, 0 mM; ▲, 0.25 mM; ◆, 0.5 mM; ■, 1.0 mM; ▼, 2.0 mM; ●, 5.0 mM) in the presence of 10.5 mM $MgCl_2$. (B) Hanes plot of **1** with $MgCl_2$.

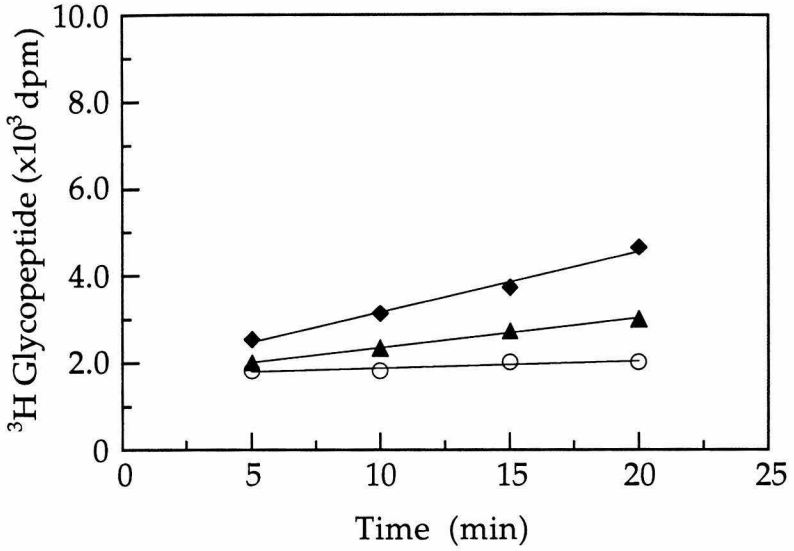

Figure 3-6. Kinetic Analysis of Bz-Asn(γS)-Leu-Thr-NHMe (**2**) with $MgCl_2$. Relative rates of glycosylation with increasing concentrations of **2** (○, 1.0 mM; ▲, 2.0 mM; ◆, 5.0 mM) in the presence of 10.5 mM $MgCl_2$.

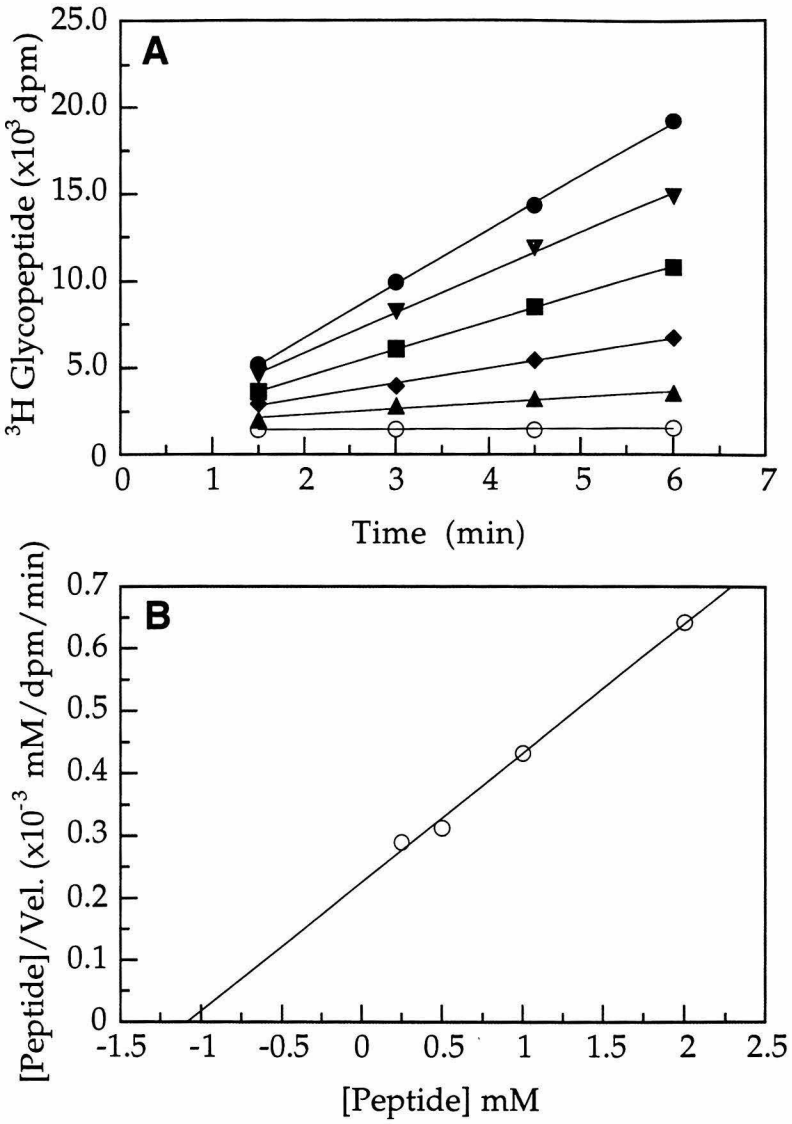

Figure 3-7. Kinetic Analysis of Bz-Asn-Leu-Thr-NHMe (**1**) with $CaCl_2$. (A) Relative rates of glycosylation with increasing concentrations of **1** (○, 0 mM; ▲,0.10 mM; ◆, 0.25 mM; ■, 0.5 mM; ▼, 1.0 mM; ●, 2.0 mM) in the presence of 10.5 mM $CaCl_2$. (B) Hanes plot of **1** with $CaCl_2$.

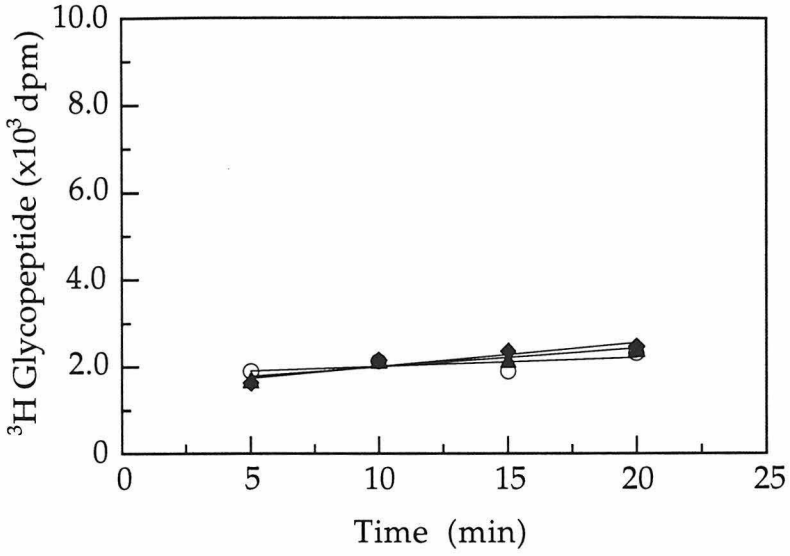

Figure 3-8. Kinetic Analysis of Bz-Asn(γS)-Leu-Thr-NHMe (**2**) with $CaCl_2$. (A) Relative rates of glycosylation with increasing concentrations of **2** (○, 1.0 mM; ▲, 2.0 mM; ◆, 5.0 mM) in the presence of 10.5 mM $CaCl_2$.

The Michaelis-Menten constants for both **1** and **2**, with OT and each metal ion, are listed in Table 3-2 for comparison. These results represent constants obtained from a typical set of experiments.

Table 3-2. Kinetic Parameters for Bz-Asn-Leu-Thr-NHMe (**1**) and Bz-Asn(γS)-Leu-Thr-NHMe (**2**) with OT Reconstituted with Various Divalent Metal Cations.

	Bz-Asn-Leu-Thr-NHMe (**1**)		Bz-Asn(γS)-Leu-Thr-NHMe (**2**)	
Metal Ion	Apparent K_M (μM)	V_{max} (dpm/min)	Apparent K_M (μM)	V_{max} (dpm/min)
Mn^{2+}	380	4550	380	326
Fe^{2+}	650	2120	680	703
Ca^{2+}	1100	4800	NA	No Rate
Mg^{2+}	2500	2930	>5000	<100

NA - Not applicable

The substrate behaviors of **1** and **2** with OT and the various metal cations were very distinct (Figure 3-9). Oligosaccharyl transferase activity, when regenerated with manganese, produces the optimum kinetic parameters with compound **1**. However, the K_M values obtained for **1** and **2** in the presence of Mn^{2+} were found to be similar (380 μM each); thioamide **2** was a less effective substrate because its V_{max} is approximately one order of magnitude lower than that of the corresponding oxygen containing peptide **1**. When enzymatic activity was restored with iron, **1** and **2** still exhibited similar binding constants (650 μM and 680 μM, respectively). Notably, thioamide **2** was turned over at a rate which was only three times slower than **1**, and in fact, the relative maximum velocity for **2** doubled when manganese was replaced with iron. The trend in the kinetic parameters for calcium and magnesium is even more dramatic. While the amide

substrate **1** is turned over with reasonable efficiency in the presence of each of these metals, the thioasparagine peptide **2** is not glycosylated at all in the presence of calcium and is very poorly glycosylated in the presence of magnesium (Figure 3-9).

The kinetic constants calculated for each peptide in the presence of the four different divalent metal cations followed distinct trends (Table 3-1). The metal ion substitution studies reveal that the asparagine-containing tripeptide is efficiently turned over in the presence of several metal cations (Mn^{2+}, Fe^{2+}, Mg^{2+}, and Ca^{2+}). For the thioasparagine peptide (**2**), the thiophilicity of the metal cation directly correlates with the efficiency of turnover. Both iron and manganese resulted in active complexes, and iron, the most thiophilic metal, yielded the highest relative rates. In contrast, when the enzyme is reconstituted with the oxophilic cations, magnesium and calcium, the thioasparagine peptide is very poorly glycosylated. The kinetic constants also appear to be correlated with the size of the metal cation. With peptide **1**, iron and magnesium (ionic radii of 0.66 and 0.64 Å, respectively) produced the lowest turnover rates and calcium and manganese (0.99 and 0.80 Å, respectively) produced the highest rates. A different effect was observed with peptide **2** and this may be due to the fact that sulfur substitution imposes its own steric perturbations. Both the heteroatom covalent radius and the carbon-heteroatom bond length increase by about 25% on changing from oxygen to sulfur.[13] In the case of calcium and peptide **2**, both binding and turnover were undetectable and this may be due to both steric effects between the bulky sulfur and the calcium ion as well as the low thiophilicity of the metal. When these trends are examined together, they suggest that the metal cation and the peptide substrate are in proximity and may directly interact during the catalytic process of *N*-linked glycosylation.

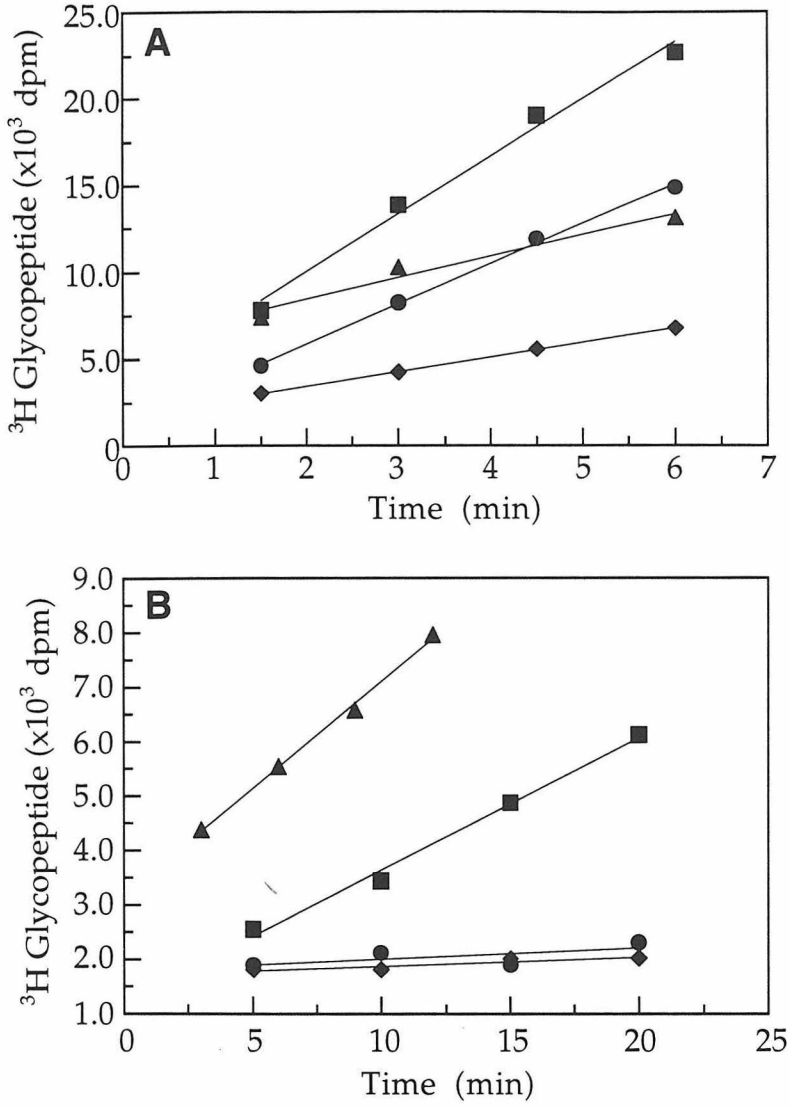

Figure 3-9. Relative Rates of Bz-Asn-Leu-Thr-NHMe (**1**) and Bz-Asn(γS)-Leu-Thr-NHMe (**2**) with Different Metal Cations. Final metal concentrations were 10.5 mM (▲ - $Fe(NH_4)_2(SO_4)_2$; ■ - $MnCl_2$; ◆ - $MgCl_2$; ● - $CaCl_2$). Peptide concentrations were 1.0 mM. (A) Relative rates of Bz-Asn-Leu-Thr-NHMe (**1**). (B) Relative rates of Bz-Asn(γS)-Leu-Thr-NHMe (**2**). Peptide concentration was 1.0 mM.

3.2.3 Regiochemistry of Asparagine-Linked Glycosylation

The kinetic experiments on peptides **1** and **2**, described above, suggest that the metal cation is in direct proximity to the peptide substrate during catalysis. The conclusions drawn from these experiments relied on the assumption that glycosylation of the thioasparagine **2** produced a glycopeptide product (**4a**) which is directly analogous to **3**, the glycopeptide product of **1**. However, it has previously been proposed that, during the *N*-linked glycosylation process, the peptide substrate underogoes a tautomerization to an imidol (see Figure 1-7), and this nucleophilic species completes the glycosylation reaction.[8] The analogous tautomerization of **2** produces a thioimidol (Figure 3-10), with two reactive nucleophiles and the potential to complete the glycosylation process through alkylation at two different sites, the nitrogen or the sulfur.

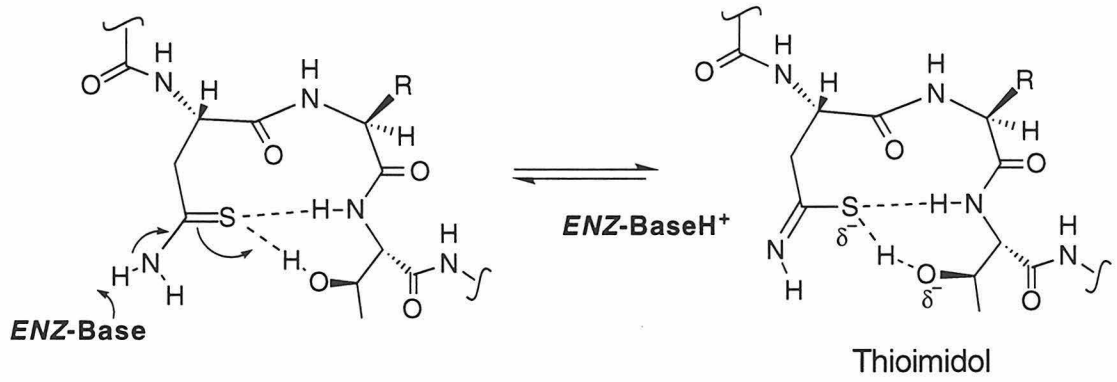

Figure 3-10. Proposed Tautomerization of Bz-Asn(γS)-Leu-Thr-NHMe (**2**) within the Active Site of Oligosaccharyl Transferase.

Because of the potential ambiguity introduced by tautomerization of the thioamide side chain, the possibility that glycosylation of **2** occurred on the sulfur of the thioamide substrate, rather than the nitrogen, had to be considered; this unusual modification would produce the glycopeptide product **4b** (Figure 3-11).

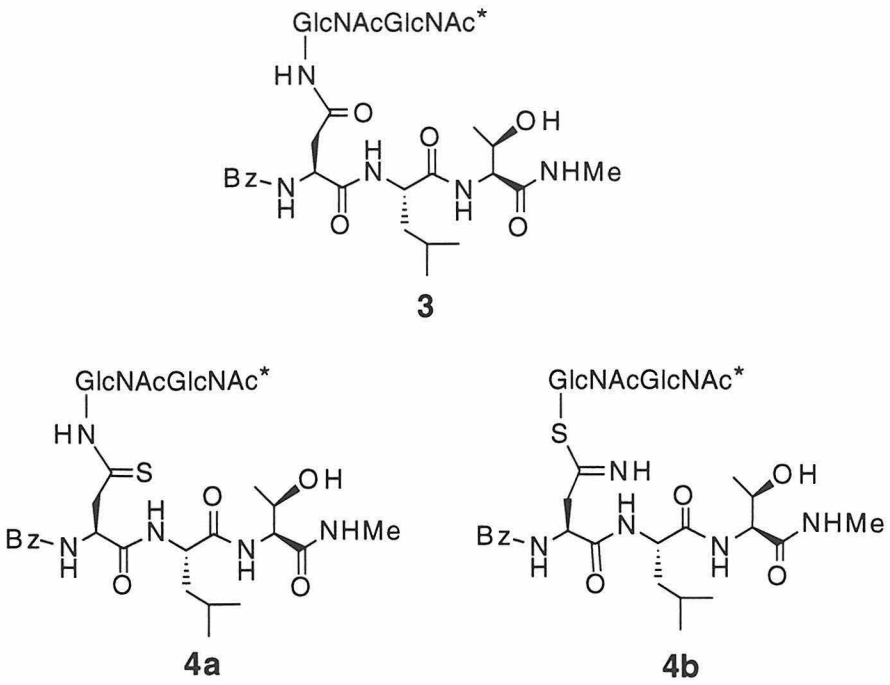

Figure 3-11. Predicted Glycosylation Products for Oxoamide **1** and Thioamide **2**. GlcNAcGlcNAc indicates chitobiose; asterisk indicates the presence of a tritium radiolabel.

Several experiments were designed and implemented to confirm the identities of glycopeptides **3** and **4** (**a** or **b**). Prior to analysis, each glycopeptide was synthesized on a preparative scale by incubating the appropriate peptide with OT and low specific activity Dol-P-P-GlcNAc-[^{3}H]GlcNAc. The products were purified and characterized by HPLC. The enzymatic synthesis of **3** yielded a chromatogram with only two peaks, the starting material **1** and the product **3**. The radiolabeled product eluted approximately 2 minutes earlier than the starting material. The retention time and the presence of the tritium label were consistent with the formation of a glycosylated product. Mass spectral analysis confirmed the identity of the product peak.

For the turnover of peptide **2**, products resulting from glycosylation at both sulfur and/or nitrogen were considered. For clarity, the isolated material is designated as **4**, and the two potential products are designated as **4a** for nitrogen glycosylation and **4b** for sulfur glycosylation (Figure 3-11). Enzymatic synthesis of **4** produced an HPLC chromatogram which contained the desired glycopeptide as well as several small side products and starting material. The radioactivity quantitatively eluted with the glycopeptide peak approximately 4 minutes earlier than the corresponding peptide. These results were independent of the divalent metal ion (Mn^{2+} or Fe^{2+}) used to prepare the glycopeptide. Control experiments, in the absence of enzyme, indicated that the observed side products result from the normal decomposition of **2**; this breakdown is most likely due to succinimide formation with the amide nitrogen of the adjacent amino acid.[14] The rate of decomposition was insignificant on the time scale of the kinetic experiments and was only observed during the longer glycopeptide synthesis and isolation procedures. Mass spectral analysis of the purified product afforded the correct molecular weight but could not be used to distinguish between the two possible products (**4a** and **4b**) which have the same molecular formula. Capillary zone electrophoresis of **4** yielded one major peak (94%).

Since **4** was only available in microgram quantities, the glycosylation regiochemistry had to be assessed through the use of analytical methods which were amenable to HPLC and TLC characterization. Treatment of **4** with mercuric acetate and with Raney nickel were chosen as promising options, because each of the reaction products obtained from these conditions could be predicted and were synthetically accessible for comparison. The chemical transformations that were investigated and the predicted products following treatment of compounds **4a** or **4b** are summarized in Figure 3-12 and Figure 3-13.

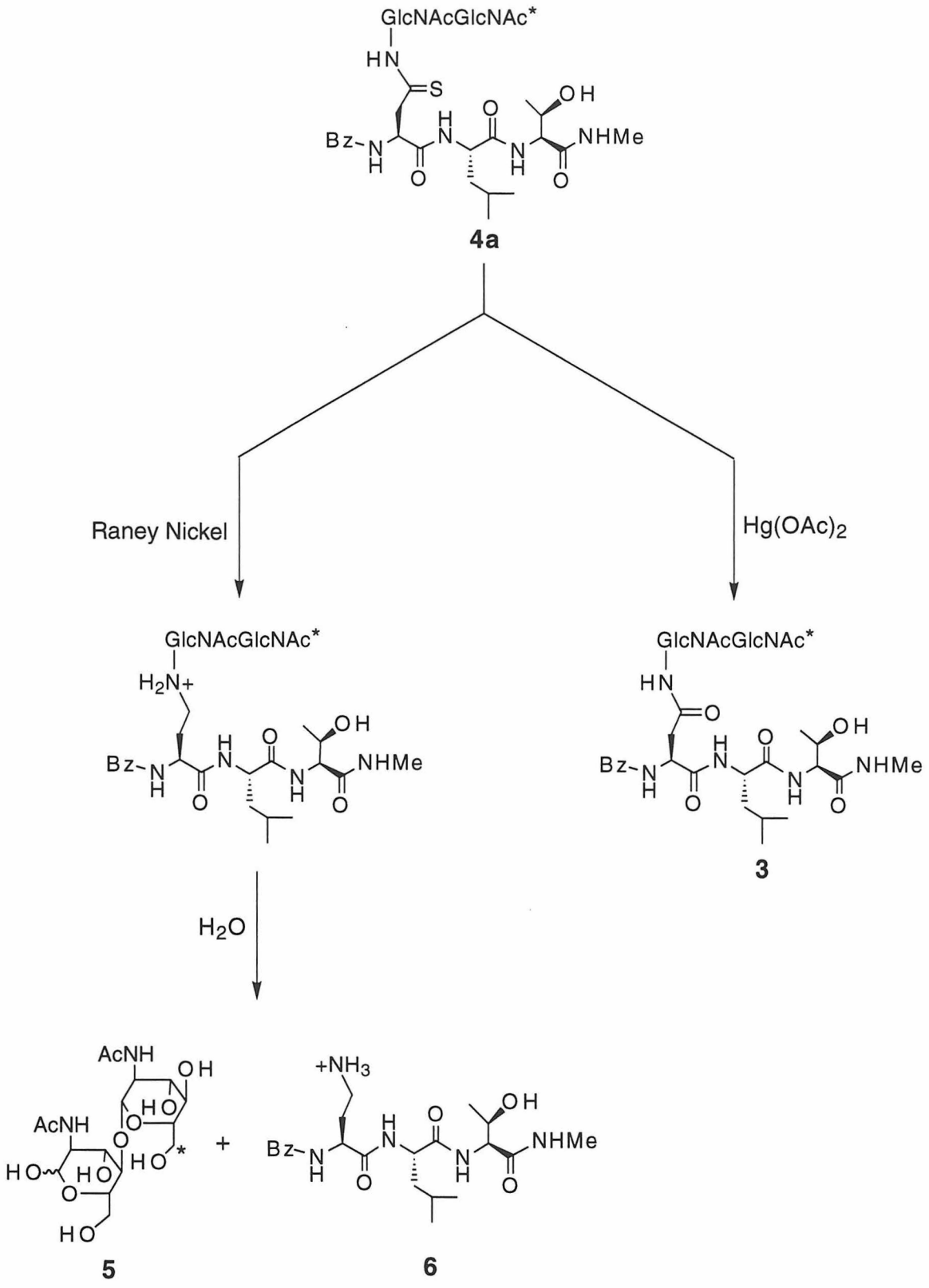

Figure 3-12. Predicted Chemical Reactivity of Glycopeptide **4a**. GlcNAcGlcNAc indicates chitobiose; asterisk indicates the presence of a tritium radiolabel.

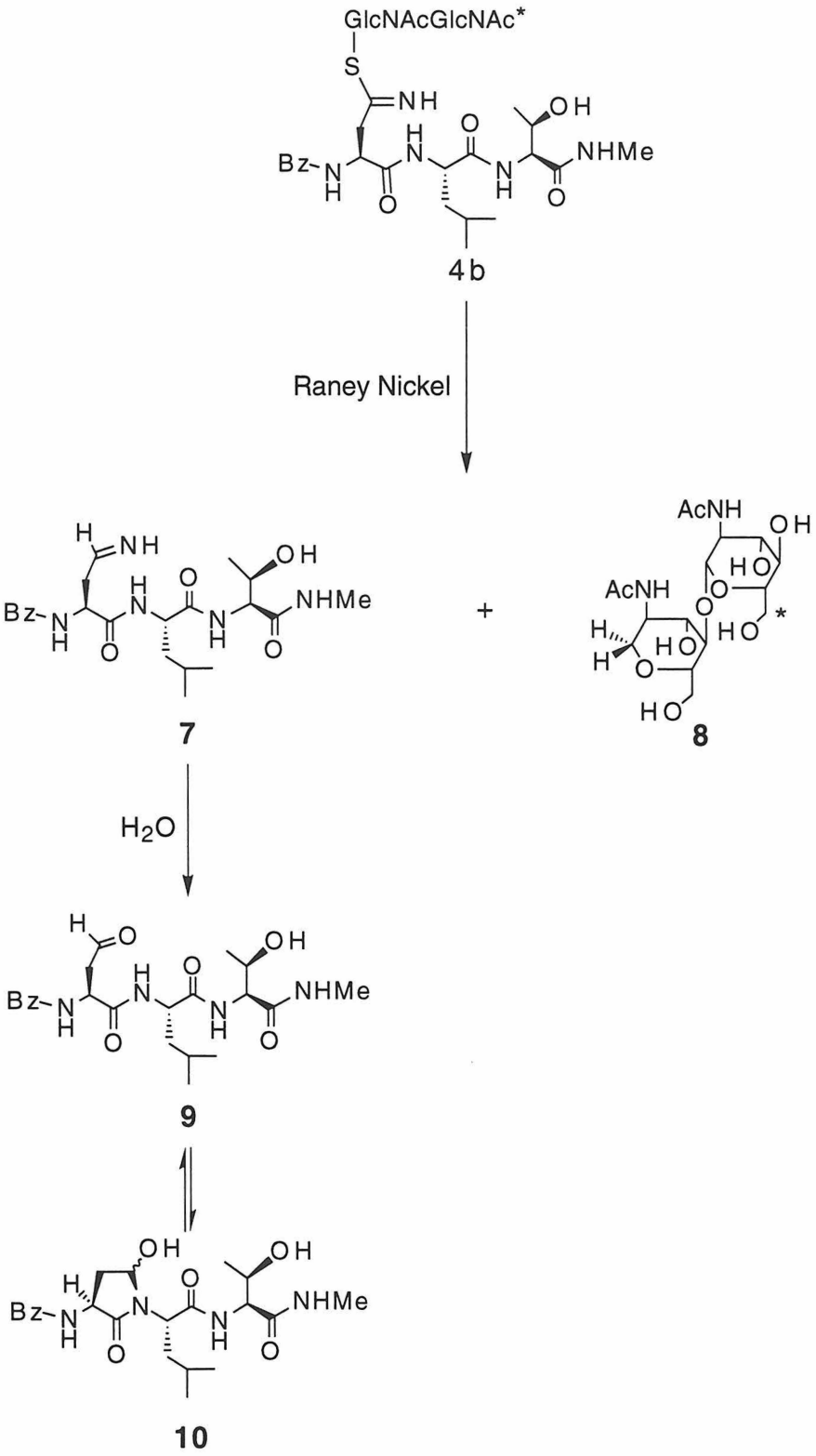

Figure 3-13. Predicted Chemical Reactivity of Glycopeptide **4b**. GlcNAcGlcNAc indicates chitobiose; asterisk indicates the presence of a tritium radiolabel.

Mercuric acetate has previously been shown to convert thioamides to their corresponding oxoamides in organic solvents;[15,16] model reactions on N-ethylthioacetamide indicated that mercuric acetate would effect the same conversion in water. As determined by HPLC analysis (Figure 3-14), treatment with mercuric acetate converted compound **4** to glycopeptide **3** (Figure 3-14C). When the radioactivity was quantified, 71% of the tritium label was found to coelute with the product glycopeptide (**3**). The remaining 29% or the radioactivity eluted in a broad peak which was not visible at 228 or 254 nm, suggesting the presence of a carbohydrate fragment. As a control, compound **3** was also treated with mercuric acetate. In this case, no reaction occurred and the radiolabel quantitatively eluted with **3**. These results are consistent with at least 71% of the glycosylation occurring on the nitrogen of the thioasparagine side chain (**4a**). The reactivity of **4b** in the presence of mercuric acetate was not predicted.

Raney nickel reductively cleaves carbon-sulfur bonds in both aqueous and organic media. As illustrated in Figure 3-12, treatment of **4a** with Raney nickel would be expected to afford a labile product which, in the presence of water, would hydrolyze to chitobiose (**5**, Sigma) and Bz-Amb-Leu-Thr-NHMe (**6**, Amb: α-aminobutyrine). HPLC analysis (Figure 3-15) of the Raney nickel products indicated the presence of **6**, when compared to an authentic sample.[8] Furthermore, TLC analysis indicated that 40-50% of the radiolabel was converted from **4** to chitobiose (**5**). In addition, the Raney nickel treatment resulted in the production of 15-25% glycopeptide **3**, presumably through a mechanism similar to that of mercuric acetate in which the thiocarbonyl is converted to an oxocarbonyl. The desulfurization of **4b** by Raney nickel would be expected to yield two products (**7** and **8**, Figure 3-12). The imine, **7**, if formed, should hydrolyze to the aldehyde **9** which is in equilibrium with the cyclic

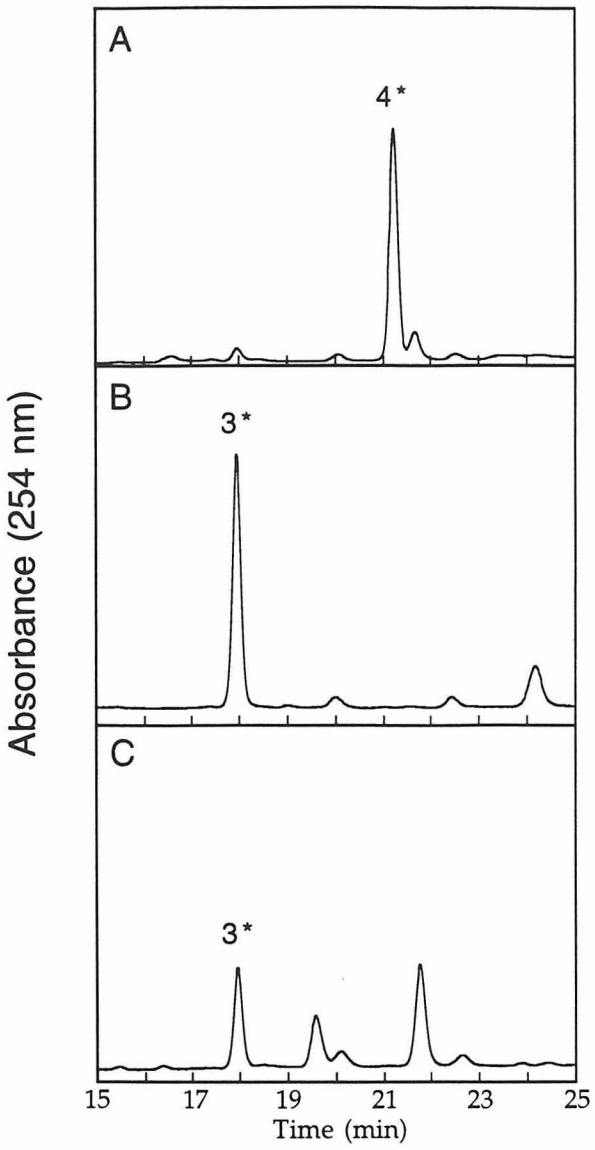

Figure 3-14. HPLC Analysis Following Treatment of **4** with Mercuric Acetate. Aliquots were counted for radioactivity at one minute intervals. Asterisk denotes radiolabel. (A) Bz-Asn(γS)[GlcNAcGlcNAc]-Leu-Thr-NHMe (**4**). (B) Bz-Asn[GlcNAcGlcNAc]-Leu-Thr-NHMe (**3**). (C) Treatment of Bz-Asn(γS)[GlcNAc-GlcNAc]-Leu-Thr-NHMe (**4**) with mercuric acetate.

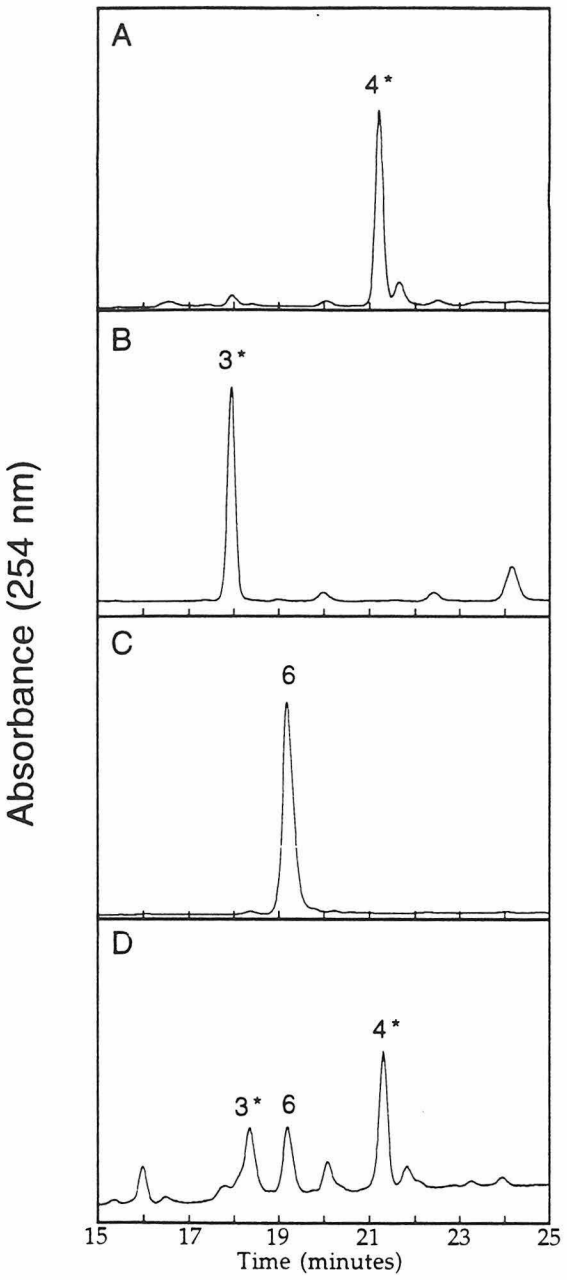

Figure 3-15. HPLC Analysis Following Treatment of **4** with Raney Nickel. Asterisk denotes radiolabel. (A) Bz-Asn(γS)[GlcNAcGlcNAc]-Leu-Thr-NHMe (**4**). (B) Bz-Asn[GlcNAcGlcNAc]-Leu-Thr-NHMe (**3**). (C) Bz-Amb-Leu-Thr-NHMe (**6**). (D) Treatment of Bz-Asn(γS)[GlcNAcGlcNAc]-Leu-Thr-NHMe (**4**) with Raney nickel.

aminal **10**. The second product would be 1-deoxychitobiose (**8**).[17] Both **8** and **10** were synthesized for comparison. Compound **10** was not visible by HPLC analysis. In the TLC analysis, compound **8** was not observed; however, an unidentified radiolabeled product was present which accounted for 25-35% of the radioactivity. Again, these results are consistent with **4a** as the predominant glycosylation product.

Mercuric acetate and Raney nickel analysis of **4** indicates that at least 70% of the glycosylation product is alkylated at the nitrogen (**4a**). The identity of the remaining 30% has yet to be confirmed. The possibility that the product **4b** was produced, but was labile under the reaction conditions, was also considered. This reaction course would be manifested by the appearance of increased levels of peptide **1** or the corresponding glycopeptide **3**. HPLC analysis revealed that hydrolysis of **4** to afford **1** or **3** did not occur. This observation, in combination with the chemical reactivity studies, confirmed that **4a**, with alkylation occurring at the nitrogen, is the predominant glycosylation product of **2**.

In general, amide functional groups can undergo alkylation on the nitrogen or the oxygen to afford amide or imidate products respectively. In solution, the relative distributions of these two products vary depending on the nature of the electrophile and the reaction conditions.[18] In model systems, electrophilic attack on thioamides occurs preferentially at sulfur.[19] In the "normal" asparagine-linked glycosylation process, it is clear that the reaction is predominantly localized at nitrogen. In nature, this regiochemical control is important because the corresponding *O*-alkylated imidate products would be too labile to be viable in a physiological context. Therefore, in these experiments it was imperative to establish whether the regiochemical control with the unnatural thioamide substrate paralleled that of the amide substrate. A detailed analysis of the glycosylated thioasparagine-containing peptide did not indicate the presence

of sulfur alkylation products as would be manifested either by the production of a labile product that spontaneously hydrolyzed to the corresponding asparagine-containing tripeptide or by formation of a stable product that could be converted to known authentic samples *via* Raney nickel or mercuric acetate treatment. In fact, at least 70% of the glycosylated species was directly identified as the *N*-linked glycopeptide. The results from these regiochemical studies suggest that the catalytic machinery of OT participates in directing glycosylation to the appropriate site on the asparagine side chain, to generate stable and physiologically viable glycoprotein products.

3.3 Conclusions

In enzyme catalyzed glycosylation of asparagine, the distinct preference for manganese over magnesium argues against a specific role for the metal cation in coordination to the pyrophosphoryl moiety of the lipid-linked carbohydrate substrate.[20] The results of the comparative studies on asparagine and thioasparagine-containing tripeptides discussed in this chapter provide the first compelling evidence that the metal cofactor is proximal to the peptide binding site. This observation suggests the intriguing possibility that the metal cation is an integral part of the catalytic machinery of OT. In the future, connections between the divalent metal cation and catalysis can be further investigated by using the manganese center as a spectroscopic probe for EPR experiments to evaluate the interactions of the enzyme with asparagine and thioasparagine substrates. This information will be important in future considerations of the mechanism of asparagine-linked glycosylation.

It has recently been reported that the fidelity of asparagine-linked glycosylation may be related to the ability of the peptide substrates to adopt an Asx-turn conformation.[11] The hydrogen bonding network seen in this motif,

along with participation of the enzyme, are believed to direct the modification to the nitrogen of the bidentate functional group in the natural substrates. Although thioamides preferentially undergo sulfur alkylation in model systems,[19] the observation that enzyme-catalyzed thioamide glycosylation proceeds predominantly or exclusively at the nitrogen is consistent with the environment of the functional group playing an important role in targeting the alkylation to the correct heteroatom despite the inherent chemical tendencies of the system. Thus, it appears that the environment provided by OT acts in concert with the peptide substrate and the metal cofactor to control the regiochemistry of *N*-linked glycosylation while concomitantly catalyzing this complicated process.

3.4 Acknowledgements

Rahul Pathak characterized the metal cofactor requirements for *S. cerevisiae* OT (Table 3-1). A significant portion of the material presented in this chapter appeared in the following publication: Hendrickson, T. L.; Imperiali, B. (1995). Metal-Ion Dependence of Oligosaccharyl Transferase: Implications for Catalysis. *Biochemistry*, **34**, 9444-9450.

3.5 Experimental Methods

3.5.1 Enzyme Assays and Determination of Kinetic Constants

General Methods

Unless otherwise noted, mass spectral analyses were determined by the University of California-Riverside Mass Spectroscopy Facility using standard Fast Atom Bombardment (FAB) protocols. Tritium quantification was obtained in disintegrations per minute (dpm) on a Beckman LS-5000TD scintillation counter. HPLC purification and analysis were on a Beckman Dual Channel System operating with Sytem Gold software with an analytical grade, C-18

reverse phase column (25cm x 4.6mm). Proton NMR spectra were acquired on a Bruker AM-500 MHz spectrometer.

Buffers and Solutions

Buffer A contained 50 mM Hepes, pH 7.4, 1.2% Triton X-100. Buffer B contained 50 mM Hepes, pH 7.4, 140 mM sucrose, 1% NP-40, 0.5 mg/mL PC. Buffer C contained 50 mM Hepes, pH 7.4, 1 mM DTT, 500 mM NaCl, 140 mM sucrose, 0.1 mM AEBSF, 2 μg/mL leupeptin and 4 μg/mL pepstatin. Buffer D contained 50 mM Hepes, pH 7.4, 1 mM DTT, 50 mM NaCl, 140 mM sucrose, 0.1 mM AEBSF, 2 μg/mL leupeptin, 4 μg/mL pepstatin and 0.1% NP-40. Buffer E contained 50 mM Hepes, pH 7.4, 1 mM DTT, 500 mM NaCl, 140 mM sucrose, 1% NP-40, 1 mg/mL PC, 0.1 mM AEBSF, 2 μg/mL leupeptin and 4 μg/mL pepstatin. Theoretical Upper Phase (TUP, 12:192:186:2.69 chloroform/methanol/water/0.25 M $MgCl_2$) [21].

Peptide Synthesis

Peptides **1** and **2** were synthesized by standard solution phase coupling methods. Bz-Asn(γS)-Leu-Thr-NHMe (**2**) was prepared as previously described by converting β-cyanoalanine to thioasparagine by sequential treatment with saturated ammonia in ethanol followed by hydrogen sulfide.[8]

Glycolipid Synthesis

Dol-P-P-[^{3}H]-GlcNAc-GlcNAc (^{3}H labeled at C-6 position of the β-1,4 linked GlcNAc) was prepared as described previously.[22] Material of the desired specific activity for each experiment was obtained by appropriate dilution of high specific activity UDP-[^{3}H]GlcNAc (ca. 36 Ci/mmol, NEN) prior to the biosynthetic preparation of the lipid-linked disaccharide.

Glycopeptide Synthesis

Five samples of Dol-P-P-GlcNAc-[^{3}H]-GlcNAc (200,000 dpm, 0.011 Ci/mmol) were each dissolved in 20 μL 5 mM Bz-Asn-Leu-Thr-NHMe in DMSO. Buffer B was added to each sample in 75 μL aliquots. The glycosylation reaction was initiated by the addition of 100 μL solubilized porcine apoenzyme (see below) and 5 μL 600 mM $MnCl_2$. After agitation for four hours at room temperature, the five reactions were quenched together into 6 mL 3/2/1 chloroform/methanol/4 mM $MgCl_2$. The aqueous layer was removed and the organic layer washed with 2 x 3 mL TUP. The combined aqueous layers were washed with 1 mL chloroform and then dried under a stream of nitrogen. The resulting residue was partially purified by gradient elution with acetonitrile from a SepPak cartridge (C-18, Millipore). The product was detected by monitoring for radioactivity which typically eluted from the cartridge between 15% and 25% acetonitrile in water. Final purification was accomplished by reverse phase HPLC (on a C-18 analytical column, 25 cm x 4.6 mm) with a 0.1% TFA/acetonitrile/water gradient from 15% - 20% acetonitrile over 25 minutes. Typically, 1,000,000 dpm Dol-P-P-GlcNAc-[^{3}H]-GlcNAc afforded 250,000 dpm pure Bz-Asn(GlcNAc-[^{3}H]-GlcNAc)-Leu-Thr-NHMe(**3**).

A similar procedure was utilized for the preparation of Bz-Asn(γS)(GlcNAc-[^{3}H]-GlcNAc)-Leu-Thr-NHMe (**4**). Dol-P-P-GlcNAc-[^{3}H]-GlcNAc was dissolved in 5 μL DMSO and 15 μL of a 10 mM DMSO solution of **2** and combined with 75 μL Buffer B and 100 μL of the solubilized porcine apoenzyme. The reaction was initiated by the addition of 5 μL 600 mM $MnCl_2$ or 600 mM $Fe(NH_4)_2(SO_4)_2$. The reactions were agitated for 12 hours at room temperature and then quenched and purified as described above. HPLC analysis indicated the preparation of one radiolabeled product (**4**) and several non-

radiolabeled side products. Utilization of the two different divalent metals yielded identical HPLC chromatograms.

The syntheses of non-radiolabeled glycopeptides **3** and **4** were accomplished as described above. Dol-P-P-GlcNAc-GlcNAc was prepared enzymatically from UDP-GlcNAc and Dol-P-P-GlcNAc by using protocols identical to those developed for the synthesis of radiolabeled material.[22] The progress of the reaction was estimated by monitoring a parallel reaction using radiolabeled UDP-[^{3}H]GlcNAc at identical concentrations. Products were purified by HPLC and elution times were identical to the corresponding radiolabeled analogs. The product identities were further verified by mass spectroscopy. Molecular weights for the two unlabeled glycosylated peptides, **3** and **4**, were determined by MALDI-Time of Flight mass spectroscopy using a 2,5-dihydroxybenzoic acid matrix. Calculated molecular weight for **3**: 869.9 (MNa^+: 892.9). Observed MNa^+: 893.5. Calculated molecular weight for **4**: 885.9 (MNa^+: 908.9). Observed MNa^+: 909.6. The purified glycopeptide **4** was also analyzed for purity by capillary zone electrophoresis. The results indicate that the sample obtained in the HPLC purification migrates as predominantly (94%) one peak.

The solution state stabilities of **2** and **4** under the reaction conditions used throughout these experiments were assessed as follows. Four control experiments, A-D, were prepared by combining 5 μL 600 mM $MnCl_2$, 5 μL DMSO and 155 μL Buffer A. Experiments A-C contained 15 μL 10 mM **2** in DMSO and experiment D contained 15 μL 10 mM **1** in DMSO. Experiment A was initiated by the addition of 20 μL solubilized apoenzyme. Experiment B was initiated by the addition of 20 μL Buffer A. Experiment C was prepared in the presence of 50,000 dpm Dol-P-P-GlcNAc-[^{3}H]-GlcNAc, and was also initiated by the addition of 20 μL solubilized apoenzyme. Experiment D was again initiated by the addition of 20 μl solubilized apoenzyme. Experiments A-D were agitated

for 12 hours, quenched and purified as described above. HPLC traces for all four reactions were obtained.

Mercuric Acetate Reactions

Pure, radiolabeled glycopeptides **3** and **4** (50,000 dpm each, 0.011 Ci/mmol) were dissolved in 20 μL acetonitrile and mercuric acetate (80 μL of a 1 mg/mL water solution) was added to each glycopeptide. The reactions were agitated overnight and filtered through microcentrifuge filters (5000 rpm x 40 minutes). Filtered samples were used immediately or stored at -80°C until ready for HPLC analysis.

Raney Nickel Reactions

The glycopeptide (**3** or **4**, 50,000 dpm, 0.011 Ci/mmol) was dissolved in 150 μL water and excess activated Raney nickel in ethanol was added (20 μL of an approximately 1:1 Raney nickel:ethanol slurry). After three hours of agitation, a second aliquot of Raney nickel (20 μL) was added and the reaction was shaken for an additional 3 hours. The reaction was centrifuged briefly to settle the catalyst and the supernatant was removed. The catalyst was washed four times with 200 μL 20% acetonitrile in water. The supernatants were pooled and any remaining catalyst was removed through centrifugation. The final supernatant was dried under a stream of nitrogen and redissolved in water for HPLC and TLC analysis.

HPLC Analysis

Mercuric acetate and Raney nickel reactions were examined by analytical HPLC. Fractions were collected over one minute intervals and quantitated for ^{3}H content. Absorbances were monitored at 228 nm and 254 nm.

TLC Analysis

Raney nickel reactions were applied to TLC plates (250 μM, glass, EM Science) in 10,000 dpm fractions and dried under vacuum. The plate was developed six times in 65/35/4/4 chloroform/methanol/water/15M ammonium hydroxide.[23] Compound **3** ($R_f \approx 0.6$), chitobiose (**5**, $R_f = 0.33$) and 2-acetamido-1,5-anhydro-4-O-(2-acetamido-2-deoxyglucopyranosyl)-2-deoxy-glucitol (**8**, $R_f = 0.53$)[17] were included on the same TLC plate for comparison. The plate was analyzed for ^3H content by removing the silica in 0.5 cm portions. Each sample was suspended in 1 mL water and counted in 6 mL Ecolite. Non-radiolabeled lanes were visualized by heating the TLC plate after immersion in a 5% H_2SO_4 methanolic solution.

Saccharomyces cerevisiae Oligosaccharyl Transferase

A solubilized preparation of the yeast enzyme was prepared as previously described.[9] Prior to assaying, the crude enzyme was diluted seven-fold with buffer A and the $MnCl_2$ concentration was brought to 10 mM. A 200,000 dpm aliquot of Dol-P-P-GlcNAc-[^3H]-GlcNAc (specific activity 36.5 Ci/mmol) was brought to dryness in a microcentrifuge tube. The lipid-linked donor was then redissolved in 10 μL DMSO, 10 μL 20 mM Bz-Asn(γS)-Leu-Thr-NHMe (**2**) in DMSO and 30 μL buffer A. The assay was initiated by the addition of 150 μL of the diluted enzyme. Four time points were obtained by removing 40 μL aliquots at 2 minute intervals. Each aliquot was quenched in a solution of 1.2 mL 3/2/1 chloroform/methanol/4 mM $MgCl_2$. The aqueous layer was removed and the organic layer was washed twice with 0.6 mL TUP. The aqueous layers were combined and counted (dpm) in 5 mL Ecolite (ICN).

In order to determine whether **2** is a competitive inhibitor for OT activity, three samples of Dol-P-P-[^3H]-GlcNAc-GlcNAc (50,000 dpm, 36.5 Ci/mmol)

were each redissolved in 10 μL 1 mM Bz-Asn-Leu-Thr-NHMe in DMSO and 155 μL buffer B (with 10 mM $MnCl_2$). An additional 10 μL of DMSO or of a 1 mM or a 10 mM DMSO solution of Bz-Asn(γS)-Leu-Thr-NHMe were added to each of the three reaction mixtures to bring the final concentration of **2** to 0 mM, 50 μM and 500 μM, respectively. Each assay was initiated by the addition of 20 μL undiluted, solubilized yeast OT. Time points were obtained as described above.

Porcine Liver Oligosaccharyl Transferase

Crude porcine liver microsomes were prepared from fresh pig liver [23] and solubilized by a modified version of the procedure published for the solubilization of canine pancreatic microsomes.[10] Crude liver microsomes (30 mL, 30% v/v glycerol suspension) were diluted to 150 mL with buffer C. This mixture was incubated at 0°C for 20 minutes and centrifuged for 60 minutes at 2.5×10^5 g. The pellets were resuspended in 150 mL buffer D. This mixture was incubated for 20 minutes at 0°C and then centrifuged for 60 minutes at 2.5×10^5 g. The pellets were resuspended in 50 mL buffer E and centrifuged, following a 20 minute incubation, for 60 minutes at 1.4×10^5 g. The supernatant was divided into two portions (25 and 20 mL) and stored at -80°C.

Apoenzyme for metal reconstitution experiments was prepared as follows. The solubilized porcine microsomes (25 mL) were gently thawed and treated twice with Chelex resin (BioRad) at 4°C for five minutes each. A brief centrifugation (2 minutes at 2000 rpm) facilitated the separation of the resin from the supernatant. The solution was then brought to a final concentration of 5 mM EDTA and incubated for 5 minutes at 4°C. This solution was dialyzed twice against 500 mL buffer E for 30 minutes each time. The apoenzyme could be stored at -80°C for several months without loss of activity. Regeneration of activity was obtained by the addition of exogenous $MnCl_2$, $MgCl_2$, $CaCl_2$ or

$Fe(NH_4)_2(SO_4)_2$ at concentrations in excess of 2 mM. Other divalent metal cations, including $ZnCl_2$, $NiCl_2$, $CdCl_2$ and $CoCl_2$, failed to restore activity. A two-fold dilution of this enzyme was used for all experiments. This dilution resulted in 56% conversion of Bz-Asn-Leu-Thr-NHMe (**1**) to **3** in 8 minutes with a peptide concentration of 1 mM and 200,000 dpm Dol-P-P-GlcNAc-[^{3}H]-GlcNAc (specific activity 36.5 Ci/mmol).

*Determination of Kinetic Constants for **1** and **2***

In a typical experiment, six aliquots of Dol-P-P-GlcNAc-[^{3}H]-GlcNAc (200,000 dpm, specific activity 36.5 Ci/mmol) were blown dry under a stream of nitrogen in small eppendorf tubes. A DMSO solution of Bz-Asn(γS)-Leu-Thr-NHMe was added in 20 µL aliquots to each of five of the eppendorfs to yield final peptide concentrations of 2 mM, 1 mM, 500 µM, 250 µM and 125 µM. A blank was prepared in the same manner using 20 µL DMSO. Buffer A was added to each tube in 75 µL aliquots. The solubilized porcine apoenzyme (700 µL) was combined with 35 µL of a 400 mM solution of $MnCl_2$, $MgCl_2$, $CaCl_2$ or $Fe(NH_4)_2(SO_4)_2$ and 105 µL of this solution was used to initiate each assay. Aliquots (40 µl each) were removed after appropriate intervals and were treated as described above. The organic layers were dried and the remaining proteinaceous residue was redissolved in 200 µL Solvable (NEN), agitated for 30 minutes and counted in 6 mL Formula 989 (New England Nuclear). The amount of radioactivity present in the aqueous extracts was normalized against the total radioactivity (aqueous and organic) for each sample. Each set of kinetic values (K_M and V_{max}) was determined separately from the same batch of solubilized apoenzyme and peptide concentrations were varied as needed.

3.5.2 Synthetic Protocols and Physical Data - Bz-aminal-Leu-Thr-NHMe (10)

Synthesis of Boc-Hse(OBn)-Leu-Thr-NHMe :

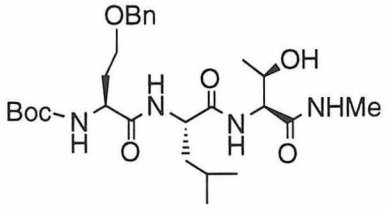

Boc-Hse(OBn) (50.3 mg, 163 μmoles) was dissolved in 600 μL THF. DCC (36.7 mg, 178 μmoles, 1.1 eq) and *p*-nitrophenol (25.8 mg, 186 μmoles, 1.14 eq) were added. The solution was stirred for four hours and then filtered to remove DCU. The activated ester was briefly purified via silica gel chromatography and used immediately (53.6 mg, 125 μmoles). TFA-Leu-Thr-NHMe (51.4 mg, 149 μmoles, 1.2 eq) was dissolved in 600 μL DMF and combined with triethylamine (39 μL, 282 μmoles, 2.2 eq). This solution was added to the activated Boc-Hse(OBn) *p*-nitrophenol ester and stirred for 16 hours. The resultant tripeptide was purified by silica gel chromatography to yield 65 mg (121 μmoles, 68% yield) Boc-Hse(OBn)-Leu-Thr-NHMe. TLC: R_f = 0.45 in 5/1 chloroform/methanol. MS calculated for $C_{27}H_{44}N_4O_7$ (MH^+) 537.6, observed 537.3. ^{1}H-NMR δ_H (500 MHz, $CDCl_3$): 7.31 (m, 5H), 7.23 (d, 1H, J = 8.2 Hz), 7.09 (d, 1H, J = 6.7 Hz), 6.91 (d, 1H, J = 5.3 Hz), 4.48 (s, 2H), 6.06 (d, 1H, J = 3.4 Hz), 4.36 (d, 2H, J = 7.1 Hz), 4.23 (dd, 1H, J = 11.6 Hz, 5.2 Hz), 3.61 (m, 1H), 3.66 (m, 1H), 2.08 (m, 1H), 2.77 (d, 3H, J = 4.8 Hz), 1.99 (m, 1H), 1.63 (m, 2H), 1.25 (s, 1H), 1.43 (s, 9H), 1.49 (m, 1H), 1.12 (d, 3H, J = 6.4 Hz), 0.89 (dd, 6H, J = 9.3 Hz, 6.3 Hz).

Synthesis of Bz-Hse(OBn)-Leu-Thr-NHMe:

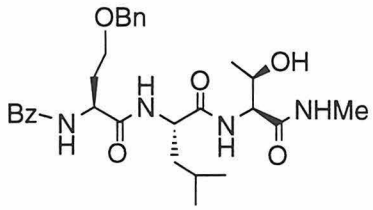

Boc-Hse(OBn)-Leu-Thr-NHMe (61.8 mg, 115 μmoles) was dissolved in 2 mL dichloromethane and 2 mL trifluoroacetic acid and stirred for 20 minutes. The TFA was removed under a stream of nitrogen and the resultant oil was lyophilized from water to afford a fluffy white powder which was redissolved in 550 μL DMF. The *p*-nitrophenyl ester of benzoic acid was added (33 mg, 136 μmoles, 1.2 eq) along with triethylamine (23 μL, 166 μmoles, 1.5 eq). The reaction was complete after 6 hours at which time the DMF was removed under vacuum. The product was purified by silica gel chromatography to yield 48 mg (84.9 μmoles, 76% yield) Bz-Hse(OBn)-Leu-Thr-NHMe. TLC: R_f = 0.5 in 5/1 chloroform/methanol. MS calculated for $C_{29}H_{40}N_4O_6$ (MH^+) 541.6, observed 541.3. ^{1}H-NMR δ_H (500 MHz, $CDCl_3$): 8.10 - 6.95 (m, 14H), 4.71 (dd, 1 H, J = 5.1 Hz, 12.0 Hz), 4.51 (s, 2H), 4.52-4.45 (m, 1H), 4.39 (m, 2H), 4.10 (m, 1H), 3.84 (m, 1H), 3.74 (m, 1H), 2.78 (d, 3H, J = 4.8 Hz), 2.22 (m, 2H), 1.69 (m, 1H), 1.60 (m, 1H), 1.51 (m, 1H), 1.14 (d, 3H, J = 6.4 Hz), 0.88 (d, 3H, J = 6.5 Hz), 0.86 (d, 3H, 6.4 Hz).

Synthesis of Bz-Hse-Leu-Thr-NHMe:

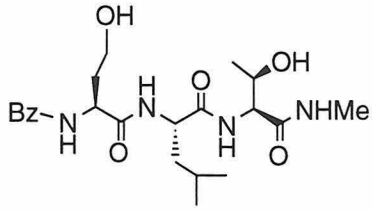

Bz-Hse(OBn)-Leu-Thr-NHMe (14 mg, 26 μmoles, 1 eq) was dissolved in 1 mL methanol. The flask was purged with nitrogen. Approximately 2 mg palladium over carbon were introduced to the flask and the flask was purged

again and evacuated. Hydrogen gas was introduced into the flask from a balloon and the reaction was stirred for 30 minutes. The solution was filtered over celite and dried down to afford 10 mg (22.2 μmoles, 86% yield) Bz-Hse-Leu-Thr-NHMe. TLC: R_f = 0.46 in 5/1 chloroform/methanol. MS calculated for $C_{22}H_{32}N_4O_6$ (MH^+) 450.5 observed 451.3. ^{1}H-NMR δ_H (500 MHz, $CDCl_3$): 8.10 (d, 1H, J = 6.7 Hz), 7.75 (m, 3H), 7.53 (d, 1H, J = 8.2 Hz), 7.49-7.37 (m, 4H), 7.24 (m, 1H), 4.71 (m, 1H), 4.34 (m, 1H), 4.25 (m, 2H), 3.68 (m, 2H), 2.72 (d, 3H, J = 4.7 Hz), 2.1 (m, 1H), 1.9 (m, 1H), 1.67 - 1.53 (m, 3H), 1.1 (m, 3H), 0.88 (d, 3H, J = 4.4 Hz), 0.83 (d, 3H, J = 4.2 Hz).

Synthesis of Bz-Hse(OBn)-Leu-Thr(TBDMS)-NHMe:

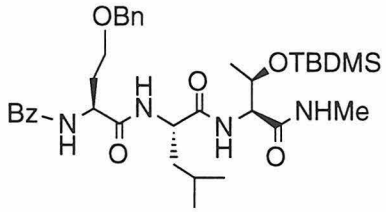

Bz-Hse(OBn)-Leu-Thr-NHMe (48 mg, 88.8 μmoles, 1 eq) was dissolved in 1 mL anhydrous acetonitrile. The solution was chilled in an ice bath and pyridine (34 μL, 422 μmoles, 5 eq) and TBDMS-triflate (48 μL, 209 μmoles, 2.5 eq) were added. The reaction was slowly warmed to room temperature and stirred for 90 minutes. The reaction was then quenched with saturated ammonium chloride and the product was extracted into chloroform. The product was purified by silica gel chromatography to yield Bz-Hse(OBn)-Leu-Thr(TBDMS)-NHMe (40 mg, 61.1 μmoles, 69% yield). TLC: R_f = 0.32 in 10/1 chloroform/methanol. MS calculated for $C_{35}H_{54}N_4O_6Si$ (MH^+) 655.9, observed 655.4. ^{1}H-NMR δ_H (500 MHz, $CDCl_3$): 7.87 - 6.77 (m, 14 H), 4.66 (m, 1H), 4.45 (s, 2H), 4.43 (m, 1H), 4.15 (m, 2H), 3.95 (m, 1H), 3.71 (m, 1H), 2.71 (d, 3H, J = 4.7 Hz), 2.17 (m, 1H), 2.11 (m, 1H), 1.60 - 1.41 (m, 3H), 1.01 (d, 3H, J = 6.3 Hz), 0.81 - 0.74 (m, 15 Hz), 0.02 (s, 3H), -0.02 (s, 3H).

Synthesis of Bz-Hse-Leu-Thr(TBDMS)-NHMe:

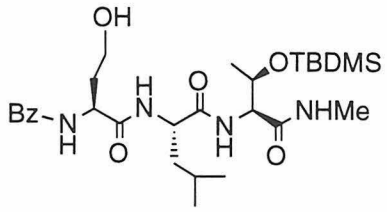

Bz-Hse(OBn)-Leu-Thr(TBDMS)-NHMe (13 mg, 19.9 μmoles) was dissolved in approximately 1 mL methanol. Reaction vessel was purged with nitrogen and $Pd(OH)_2$ was added. Reaction vessel was purged again and evacuated. Hydrogen gas was introduced from a balloon for one hour with stirring. The reaction was monitored by TLC and, when complete, filtered over celite and dried down to afford Bz-Hse-Leu-Thr(TBDMS)-NHMe (10 mg, 17.7 μmoles, 89.0% yield). TLC: R_f = 0.56 in 9/1 ethyl acetate/methanol. MS calculated for $C_{28}H_{48}N_4O_6Si$ (MH^+) 565.8, observed 565.3. ^{1}H-NMR δ_H (500 MHz, $CDCl_3$): 7.83 - 7.44 (m, 6H), 6.85 (d, 1H, J = 4.8 Hz), 4.95 (m, 1H), 4.41 (m, 1H), 4.33 (m, 1H), 3.85(m, 1H), 3.77 (m, 1H), 2.80 (d, 3H, J = 4.8 Hz), 2.25 (m, 1H), 1.94 (m, 1H), 1.70 (m, 3H), 1.06 (d, 3H, J = 6.3 Hz), 0.89 (m, 15 H), 0.13 (s, 3H), 0.11 (s, 3H).

*Synthesis of **9** and **10**:*

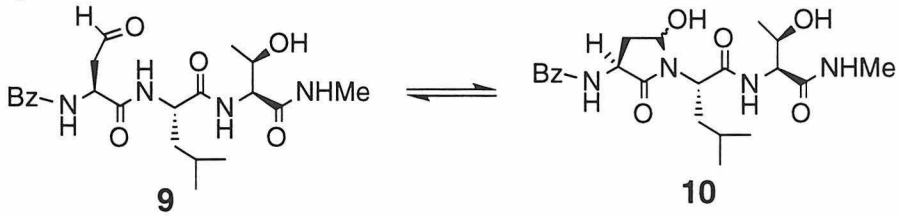

Chromium (VI) trioxide (23.3 mg, 233 μmoles, 13.1 eq) and pyridine (35 μL, 434 μmoles, 24.5 eq) were combined with 0.5 mL anhydrous dichloromethane and chilled to 0°C. The yellow-brown mixture was stirred for 15 minutes and a 0.5 mL solution of Bz-Hse-Leu-Thr(TBDMS)-NHMe (10.0 mg, 17.7 μmoles, 1 eq) in anhydrous dichloromethane was added via cannula. The solution turned

black and was allowed to stir for 20 minutes at 0°C. The solution was immediately passed over several columns of silica gel in 9/1 ethyl acetate/methanol to completely remove the chromium. The remaining residue (3.1 mg) was dissolved in 30 µL acetonitrile and a 2% HF solution in acetonitrile (11.6 µL) was added. After 60 minutes, an additional 5.5 µL HF solution was added. The reaction was stirred for 90 minutes and then brought to dryness. The product was purified by analytical HPLC on a 10% to 30% gradient of acetonitrile in water (0.1% TFA). MS calculated for $C_{27}H_{44}N_4O_7$ (MH^+) 449.5, observed 449.

Additionally, the impure product (1 mg, 2.2 µmoles, 1eq) was treated with excess sodium borohydride (0.88 mg, 23 mmoles) in methanol for 45 minutes and reexamined by HPLC. The product was quantitatively reduced to Bz-Hse-Leu-Thr-NHMe.

3.5.3 Synthetic Protocols and Physical Data - Reduced Chitobiose (8)

Synthesis of 2-acetamido-3,6-Di-O-acetyl-4-O-(2-acetamido-3,4,6-tri-O-acetyl-2-deoxygluco-pyranosyl)-1-chloro-1-deoxy-D-glucopyranoside:

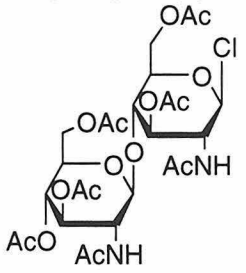

The disaccharide 2-acetamido-3,6-Di-O-acetyl-1-chloro-1-deoxy-4-O-(2-acetamido-3,4,6-tri-O-acetyl-2-deoxyglucopyranosyl)-D-glucopyranoside was prepared from octaacetyl-chitobiose (56.5 mg, 83.7 µmoles) as previously described.[17] Further purification was performed on silica gel for a final yield of 26 mg (39.8 µmoles, 47.5% yield). TLC: R_f = 0.49 in 9/1 ethyl acetate/methanol. ^{1}H-NMR δ_H (500 MHz, $CDCl_3$): 6.15 - 6.10 (m, 2 H, H-1 and N-H'), 5.94 (d, 1H, J

= 7.5 Hz, N-H), 5.29 (m, 1H, H-3), 5.21(m, 1H, H-3'), 5.03 (m, 1H, H-4'), 4.61 (m, 1H, H-1'), 4.45 - 4.35 (m, 4H, H-2, H-6A, H-6B, H-6A'), 4.18 (m, 1H, H-5), 4.02 (m, 1H, H-6B'), 3.87 - 3.77 (m, 2H, H-2' and H-4), 3.65 (m, 1H, H-5'), 2.15 - 1.94 (m, 21H, acetyl CH_3's).

Synthesis of 2-acetamido-3,6-Di-O-acetyl-1,5-anhydro-4-O-(2-acetamido-3,4,6-tri-O-acetyl-2-deoxyglucopyranosyl)-2-deoxy-D-glucitol:

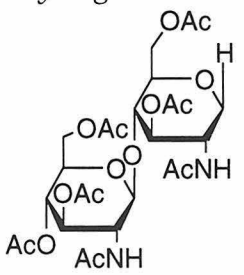

The heptaacetyl chloride (5.4 mg, 8.3 μmoles) was dissolved in dry toluene (1.1 mL) with 2 mg AIBN. Tributyl tin hydride (64 μL) was added and the reaction was heated at 90 °C for 11 hours. Toluene was removed and the product was separated from remaining starting material by silica gel chromatography for a final yield of 1.5 mg (2.4 μmoles, 29.2% yield). TLC: R_f = 0.30 in 9/1 ethyl acetate/methanol. ^{1}H-NMR δ_H (500 MHz, $CDCl_3$): 5.99 (d, 1H, J = 9.0 Hz, N-H'), 5.87 (d, 1H, J = 7.4 Hz, N-H), 5.16 (m, 1H, H-3'), 5.06 (m, 1H, H-4'), 4.93 (m, 1H, H-3), 4.51 (d, 1H, J = 8.4 Hz, H-1'), 4.39 - 4.27 (m, 3H, H-6A, H-6B, H-6A'), 4.14 - 4.10 (m, 2H, H-6B', H-2), 4.03 (d, 1H, J = 12.4 Hz, H-1A), 3.93 (m, 1H, H-2'), 3.64 (m, 2H, H-4, H-5'), 3.48 (m, 1H, H-5), 3.12 (m, 1H, H-1B), 2.19 - 1.94 (m, 21H, acetyl CH_3's).

Synthesis of 2-acetamido-1,5-anhydro-4-O-(2-acetamido-2-deoxyglucopyranosyl)-2-deoxy-glucitol: (8)

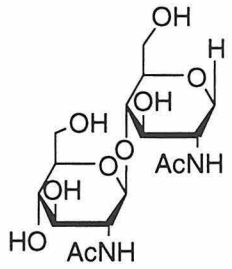

8

The protected disaccharide 2-acetamido-3,6-Di-O-acetyl-1,5-anhydro-4-O-(2-acetamido-3,4,6-tri-O-acetyl-2-deoxyglucopyranosyl)-2-deoxy-D-glucitol (1.5 mg, 2.4 μmoles) was dissolved in 0.5 mL 3/2 chloroform/methanol. A 50 μL aliquot of an anhydrous solution of sodium methoxide (750 mM) was added to the disaccharide solution. After 20 minutes, the reaction was complete by TLC. The solution was neutralized with Dowex-50 pyridinium-HCl, filtered and brought to dryness to quantitatively yield the deprotected disaccharide. TLC: R_f = 0.08 in 65/35/4/4 chloroform/methanol/water/15 M ammonium hydroxide. MS calculated for $C_{16}H_{28}N_2O_{12}$ (MH^+) 409, (MNa^+) 431, observed 409 and 431. ^{1}H-NMR δ_H (500 MHz, d6-DMSO): 7.74 (d, 1H, J = 7.83 Hz, N-H), 7.68 (d, 1H, J = 9.52 Hz, N-H'), 4.29 (d, 1H, J = 8.51 Hz, H-1'), 3.74 - 3.17 (br. m, 11H), 3.03 (m, 2H), 2.91 (m, 1H, H-1B), 1.74 (s, 3H, acetyl CH_3), 1.71 (s, 3H, acetyl CH_3). ^{1}H NMR Chemical Shifts obtained from Double Quantum Filtered COSY, d_6-DMSO, (δ ppm): 7.74 (N-H), 7.68 (N-H'), 4.29 (H-1'), 3.64 (H-1A), 3.55 (H-2), 3.41 (H-2'), 3.38 (H-3), 2.84 (H-1B).

3.6 References

1. Nilsson, I.; von Heijne, G. "Determination of the Distance between the Oligosaccharyltransferase Active Site and the Endoplasmic Reticulum Membrane," *J. Biol. Chem.* **1993**, *268*, 5798-5801.

2. Kaufman, R. J.; Swaroop, M.; Murtha-Riel, P. "Depletion of Manganese within the Secretory Pathway Inhibits O-Linked Glycosylation in Mammalian Cells," *Biochemistry* **1994**, *33*, 9813-9819.

3. Sharma, C. B.; Lehle, L.; Tanner, W. "*N*-Glycosylation of Yeast Proteins: Characterization of the Solubilized Oligosaccharyl Transferase," *Eur. J. Biochem.* **1981**, *116*, 101-108.

4. McEuen, A. R. "Manganese Metalloproteins and Manganese-Activated Enzymes," *Inorg. Biochem.* **1982**, *3*, 314-343.

5. Campbell, I. D.; Dwek, R. A. In *Biological Spectroscopy*; The Benjamin/Cummings Publishing Company, Inc.: London, 1984; pp 179-216.

6. Dahm, S. C.; Uhlenbeck, O. C. "Role of Divalent Metal Ions in the Hammerhead RNA Cleavage Reaction," *Biochemistry* **1991**, *30*, 9464-9469.

7. Mock, W. L.; Chen, J.-T.; Tsang, J. W. "Hydrolysis of a Thiopeptide by Cadmium Carboxypeptidase A," *Biochem. Biophys. Res. Commun.* **1981**, *102*, 389-396.

8. Imperiali, B.; Shannon, K. L.; Unno, M.; Rickert, K. W. "A Mechanistic Proposal for Asparagine-Linked Glycosylation," *J. Am. Chem. Soc.* **1992**, *114*, 7944-7945.

9. Pathak, R.; Hendrickson, T. L.; Imperiali, B. "Sulfhydryl Modification of the Yeast Wbp1p Inhibits Oligosaccharyl Transferase Activity," *Biochemistry* **1995**, *34*, 4179-4185.

10. Kelleher, D. J.; Kreibach, G.; Gilmore, R. "Oligosaccharyltransferase Activity is Associated with a Protein Complex Composed of Ribophorins 1 and 2 and a 48 kD Protein," *Cell* **1992**, *69*, 55-65.

11. Imperiali, B.; Spencer, J. R.; Struthers, M. D. "Structural and Functional-Characterization of a constrained Asx-turn Motif," *J. Am. Chem. Soc.* **1994**, *116*, 8424-8425.

12. Cornish-Bowden, A. In *Fundamentals of Enzyme Kinetics*; Butterworths: London, 1979; pp 16-38.

13. Sherman, D. B.; Spatola, A. F. "Compatibility of Thioamides with Reverse Turn Features: Synthesis and Conformational Analysis of Two Model Cyclic Pseudopeptides Containing Thioamides as Backbone Modifications," *J. Am. Chem. Soc.* **1990**, *112*, 433-441.

14. Brennan, T. V.; Clarke, S. In *Deamidation and Isoaspartate Formation in Peptides and Proteins*; D. W. Aswad, Ed.; CRC Press: Boca Raton, 1995; pp 65-90.

15. Davies, S. G.; Mortlock, A. A. "Bifunctional Chiral Auxiliaries 2: The Synthesis of 1,3-Diacylimidazolidin-2-ones from 1,2-Diamines," *Tetrahedron Lett.* **1991**, *32*, 4791-4794.

16. Davies, S. G.; Mortlock, A. A. "Bifunctional Chiral Auxiliaries 5: The Synthesis of 1,3-Diacylimidazolidine-2-thiones and 1,3-Diacylimidazolidin-2-ones from 1,2-Diamines," *Tetrahedron* **1993**, *49*, 4419-4438.

17. Hiraizumi, S.; Spohr, U.; Spiro, R. G. "Characterization of Endomannosidase Inhibitors and Evaluation of Their Effect on *N*-Linked Oligosaccharide Processing during Glycoprotein Biosynthesis," *J. Biol. Chem.* **1993**, *268*, 9927-9935.

18. Challis, B. C.; Challis, J. In *The Chemistry of Amides*; J. Zabicky, Ed.; Wiley Interscience: London, 1970; pp 731-858.

19. Walter, W.; Voss, J. In *The Chemistry of Amides*; J. Zabicky, Ed.; Wiley Interscience: London, 1970; pp 383-476.

20. Frausto da Silva, J. J. R.; Williams, R. J. P. In *The Biological Chemistry of the Elements*; Clarendon Press: Oxford, 1991; pp 250-254.

21. Behrens, N. H.; Tabora, E. "Dolichol Intermediates in the Glycosylation of Proteins," *Methods Enzymol.* **1978**, *50*, 402-435.

22. Imperiali, B.; Zimmerman, J. W. "Synthesis of Dolichylpyrophosphate-linked Oligosaccharides," *Tetrahedron Lett.* **1990**, *31*, 6485-6488.

23. Imperiali, B.; Shannon, K. L. "Differences Between Asn-Xaa-Thr- Containing Peptides: A Comparison of Solution Conformation and Substrate Behavior with Oligosaccharyltransferase," *Biochemistry* **1991**, *30*, 4374-4380.

Chapter 4. Design and Evaluation of Potent Inhibitors of Asparagine-Linked Glycosylation

4.1 Introduction

One of the most powerful tools in the field of mechanistic enzymology is the analysis of substrate analogs as a means of probing an enzyme active site. A great deal of information can be acquired by monitoring changes in kinetic behavior following the introduction of seemingly minute alterations into the chemical structure of an enzyme substrate. For example, as demonstrated in chapter three of this dissertation, the generation of alternate, non-native substrates and their subsequent kinetic evaluation can be used to contribute to a picture of an enzyme's active site environment during the catalytic process. Similarly, knowledge of substrate specificities can be used to design compounds which no longer behave as substrates and potentially inhibit enzyme activity. By kinetically examining the mode of inhibition, these compounds can provide further information about an enzyme active site and its mechanistic machinery.

In addition to providing information about the mode of action of a specific enzyme, inhibitors are often invaluable as therapeutic and biotechnological agents.[1] Compactin, which targets the enzyme 3-hydroxy-3-methylglutaryl coenzyme A reductase (HMG-CoA reductase) is a prime example.[2] HMG-CoA reductase catalyzes the rate determining step in *de novo* cholesterol biosynthesis; compactin specifically targets and inhibits this enzyme and is therefore a potentially powerful anti-hypercholesterolemic agent.[2, 3] In addition to its therapeutic benefits, compactin has been used to produce inhibitor resistant cell lines which dramatically overexpress HMG-CoA reductase, thus enabling further biochemical studies.[4]

Protein glycosylation has recently gained attention as a critical biological modification[5-7] with diverse ramifications including effects on protein stability and folding,[8] cellular targeting and sorting,[9] and intercellular

recognition.[6] Asparagine-linked glycosylation[10] is the predominant protein-carbohydrate modification in eukaryotic cells.[11] Because of the widespread and varied roles played by *N*-linked glycoproteins, inhibitors which interfere with the biosynthesis of these biomolecules would have immediate potential as biotechnological tools and potential chemotherapeutic agents.[12]

The biosynthetic pathway which leads to the development of functional asparagine-linked glycoproteins is catalyzed by a series of enzymes within the endoplasmic reticulum and the golgi apparatus.[13] These enzymes can be divided into three different functions: Those involved in the biosynthesis of the lipid-linked tetradecasaccharide donor Dol-P-P-$GlcNAc_2$-Man_9-Glc_3 (I, Figure 4-1), 2) that which catalyzes the transfer of this tetradecasaccharide to an asparagine within a nascent protein (II, Figure 4-1), and 3) those involved in the modification of the oligosaccharide following transfer to the protein (III, Figure 4-2). Each individual step in this biosynthetic pathway represents a potential target for inhibition. Several inhibitors of specific enzymes in the assembly of the lipid-linked donor and in the processing of *N*-linked glycoproteins have been identified and characterized; some of these compounds are illustrated in conjunction with the relevant enzymatic steps in Figures 4-1 and 4-2.

Enzyme inhibitors classically fall into two different categories: irreversible inactivators and reversible, competitive inhibitors.[1] An irreversible inactivator binds to and then reacts with the substrate binding site to form a covalent bond between the inactivator and the enzyme. Covalent modification results in time-dependent, irreversible inactivation of the enzyme activity. (The use of this type of inactivatior to investigate oligosaccharyl transferase will be discussed in chapter five of this dissertation.) Alternatively, a reversible, competitive inhibitor typically binds

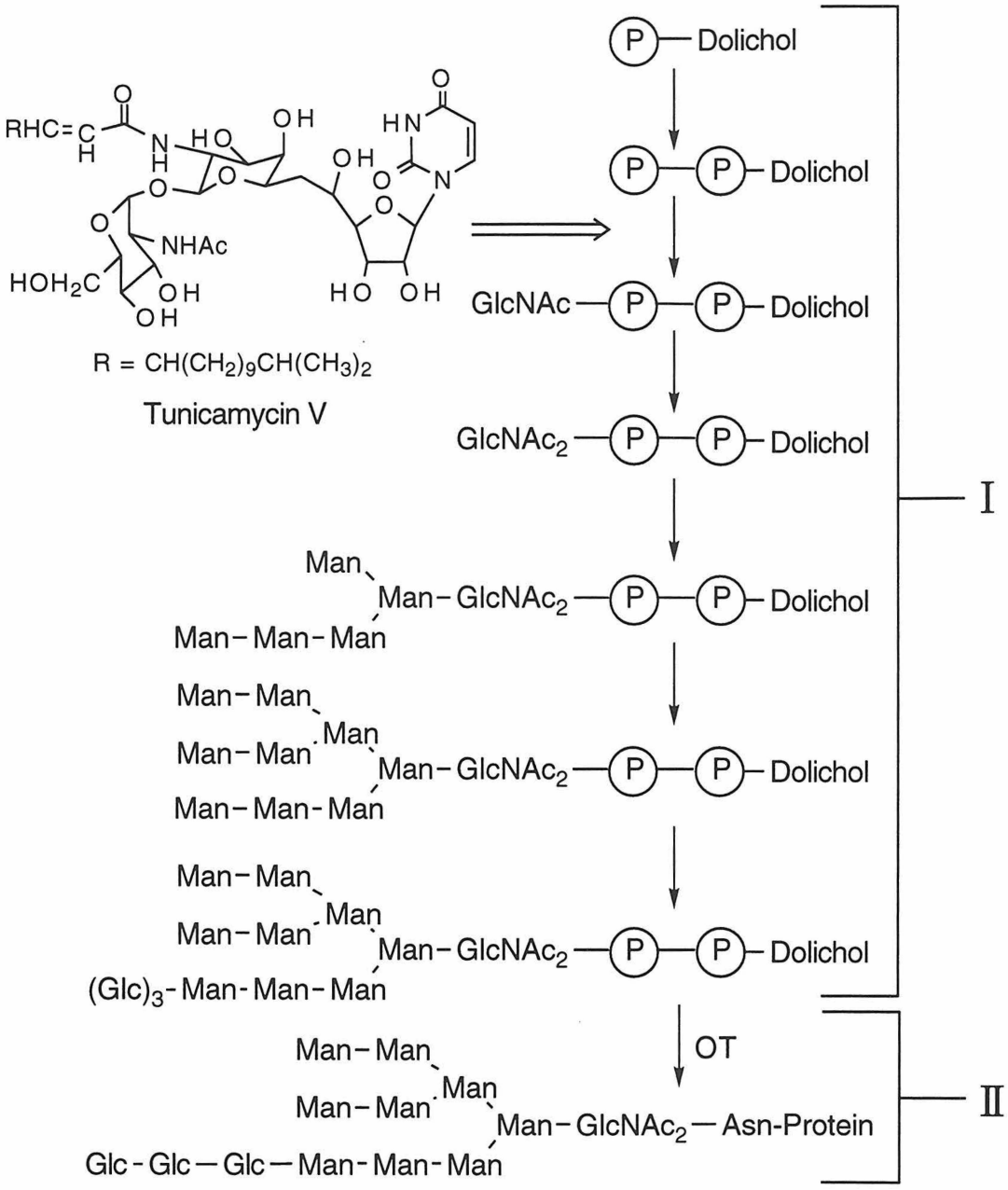

Figure 4-1. Biosynthesis of Asparagine-Linked Glycoproteins and the Site of Inhibition for the Tunicamycin Family of Compounds (adapted from Elbein).[14] I. Biosynthesis of the donor Dol-P-P-$GlcNAc_2$-Man_9-Glc_3; each step is catalyzed by a different glycosyl transferase. II. Oligosaccharyl transferase catalyzed transfer of $GlcNAc_2$-Man_9-Glc_3 to an asparagine residue.

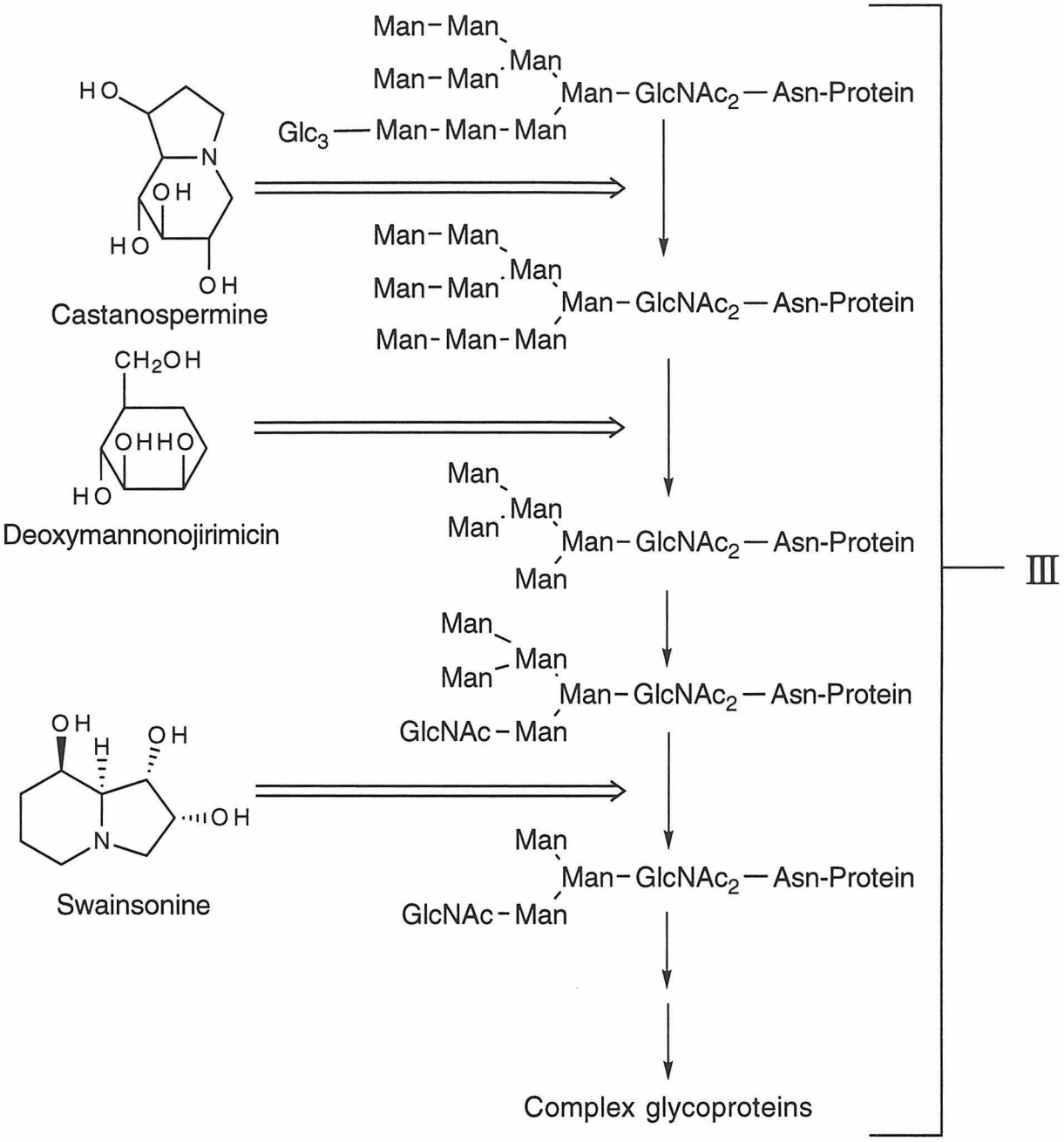

Figure 4-2. Processing of Asparagine-Linked Glycoproteins and the Specific Enzymatic Steps Targetted by Several Inhibitors (adapted from Kaushal and Elbein).[15] III. Reactions catalyzed by processing enzymes; the processing of oligosaccharides may require as many as 100 - 200 glycosyl transferases and hydrolases to generate the sequence diversity observed in nature.[16-18]

to an enzyme active site with a binding affinity similar to, or more effective than, that of the native substrate. Competitive inhibition can often be reduced by an increase in the concentration of the competing substrate, by dilution of the enzyme-inhibitor complex, or by dialysis to remove the inhibitor. The inhibitors of protein glycosylation shown in Figures 4-1 and 4-2 are all reversible, competitive inhibitors, with varying degrees of affinity for their specific enzymes. These compounds effectively compete for the substrate binding site, resulting in a reduction in enzyme activity without covalent modification.

Currently, the only pre-transfer inhibitor of *N*-linked protein glycosylation that demonstrates activity at a practical concentration is the microbial product tunicamycin (I, Figure 4-1).[19, 20] Tunicamycin does not specifically target OT, but rather functions by inhibiting the first step in the assembly of the complex, lipid-linked oligosaccharide donor (Dol-P-P-$(GlcNAc)_2$-$(Man)_9$-$(Glc)_3$) that provides the oligosaccharide moiety for all asparagine-linked glycoproteins.[21] Although tunicamycin is active at low nanomolar concentrations, its use is limited because several cell cycles are required before the supply of the lipid-linked donor is sufficiently depleted to arrest protein glycosylation. Therefore, the effect of tunicamycin on protein glycosylation is neither specific nor immediate. The processing inhibitors shown in Figure 4-2 inhibit specific enzymes which manipulate the oligosaccharide sequence following protein synthesis and therefore do not completely abolish the glycosylation process. These inhibitors can be used to produce glycoproteins with elongated or truncated oligosaccharide chains that are not normally found in mature glycoproteins. The clinical potential of several of these inhibitors is currently being investigated.[12]

Despite the centrality of asparagine-linked glycosylation, no potent inhibitors for oligosaccharyl transferase, the enzyme that catalyzes the first committed step in this process, have been reported (II, Figure 4-1). Two peptidyl inhibitors for this step have previously been synthesized; however, characterization of their inhibitory constants revealed that they were only poor inhibitors of OT.[22, 23] Appropriately designed inhibitors of this enzyme would be particularly useful because they could provide further insight into the mechanism of action of OT; they could be used to induce the overexpression of the active OT complex, a target which has remained elusive;[24] and they could facilitate further investigations into the complex roles of glycoproteins by enabling the preparation of oligosaccharide depleted proteins. In addition, inhibitors of this process could provide new leads for the development of novel therapeutic strategies.[12, 25]

This chapter describes the development of a new class of reversible, competitive inhibitors for oligosaccharyl transferase. These constrained peptidyl compounds exhibit nanomolar binding constants and slow, tight binding inhibition, suggesting that they may ressemble the transition state of the *N*-linked glycosylation reaction. In addition, these compounds were examined for their ability to specifically inhibit OT isolated from different sources and these studies revealed that they are selective for OT which has been isolated from the yeast *S. cerevisiae*.

4.2 Results and Discussion

4.2.1 Design and Synthesis of Cyclic Inhibitors For Oligosaccharyl Transferase

During the process of *N*-linked glycosylation, oligosaccharyl transferase catalyzes a reaction between two different substrates, a nascent polypeptide and a lipid-linked tetradecasaccharide; analogs of either of these two

substrates could be potential inhibitors. Unlike the compounds shown in Figures 4-1 and 4-2 which are all sugar analogs, the two reported inhibitors for OT are both peptidyl compounds.[22, 23] The most effective of these two inhibitors is the tripeptide Bz-Amb-Leu-Thr-NHMe (**1**).[23] In this peptide, the required asparagine residue, within the consensus sequence Bz-Asn-Leu-Thr-NHMe, has been replaced with a γ-aminobutyrine (Amb) amino acid; this modification increases the acidity of the side chain amine; however, it no longer contains the carbonyl group required to complete the hydrogen bonding array of the Asx-turn, the conformation that has been implicated in conferring substrate ability to peptides (see Figure 1-4).[23]

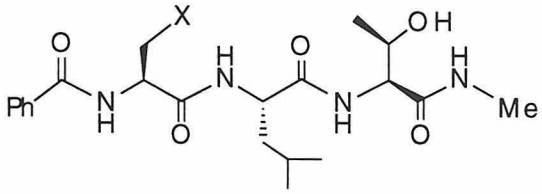

1: X = $CH_2NH_3^+$
2: X = $C(O)NH_2$

Peptide **1** inhibits porcine liver OT with a K_i (~1 mM) that is slightly lower than the K_M of the competing substrate Bz-Asn-Leu-Thr-NHMe (250 μM, **2**).[23] This decrease in affinity is most likely associated with the second peptide's inability to adopt a formal Asx-turn. The absence of the side chain carbonyl in the Amb residue does not preclude access to an Asx-turn-like form, but it does remove the crucial and defining stabilization factor. However, the observation that inhibition occurs, albeit weakly, when an asparagine residue is replaced with an Amb residue provided a starting point for the design of a more potent inhibitor of OT.

Previously, it has been reported that the incorporation of a constrained Asx-turn into a tripeptide substrate (**3**) results in a tenfold improvement in binding affinity (K_M) for OT.[26] In an effort to improve the inhibitory behavior of **1**, it was of interest to introduce a similar constraint into an Amb containing tripeptide. The cyclic, constrained peptide **4**, in which the asparagine side chain of **3** was replaced with an Amb residue was therefore designed and synthesized for biochemical studies.

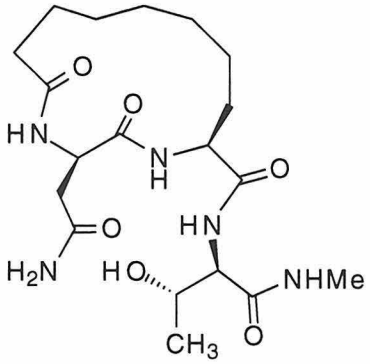

3

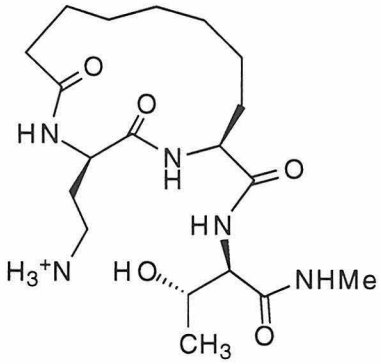

4

The syntheses of **3** and **4** proceed through the incorporation of the unnatural amino acid α-aminodecanedioic acid (Add) into the appropriate tripeptide prior to cyclization; the synthesis of **3** has been previously reported.[26] The ring closure, which introduces the required constraint, is effected by activating the Add side chain carboxylic acid as a pentafluorophenyl ester for base-induced condensation with the amino terminus of the tripeptide. Following synthesis and purification, tripeptides **3** and **4** were each analyzed with OT isolated from *S. cerevisiae*; peptide **3** is a substrate with a K_M of 78 μM, whereas **4** is an effective competitive inhibitor of the enzyme with a K_i of 50 μM. Thus, the introduction of the cyclic constraint produced an inhibitor **4** that can obtain a conformation which resembles an Asx-turn and therefore exhibits an improved K_i (as compared to

1) which is essentially identical to the binding affinity of the analogous substrate **3**.

Several additional modifications were considered in an effort to further develop peptide **4**. These alterations were specifically designed to improve the synthetic accessibility of the inhibitor while simultaneously enhancing its binding affinity for OT. Most notably, it was believed that an increase in the length of the tripeptide backbone of **4** to a hexapeptide would offer several advantages. OT recognizes an extended peptide chain during *in vivo* glycosylation, and statistical studies of *N*-linked glycoproteins suggest that glycosylation is modulated by the identity of the residues flanking the consensus sequence.[27] These observations suggest that interactions between OT and extended binding substrate determinants can be exploited to improve binding affinity. Thus, the preparation of a cyclic hexapeptide, analogous to **4**, should generate a structure which exhibits improved recognition by OT and is therefore more effective as an inhibitor.

The decision to increase the length of the peptide inhibitor prompted the need for the development of a solid phase synthesis method. The cyclic constraint could be incorporated through the introduction of an orthogonally protected cysteine residue and a bromohexanoyl cap on the *N*-terminus of the hexapeptide (Figure 4-3). Deprotection of the cysteine thiol and subsequent nucleophilic displacement of the bromine would yield the desired product,[28] with a conservative thioether replacement for one of the methylene groups in **4**. The cyclic hexapeptide *cyclo*[SHex-Amb-Cys]-Thr-Val-Thr-Nph-NH_2 (**5**, Nph = *p*-nitrophenylalanine) was chosen as the most promising inhibitor for evaluation with OT. This peptide contains the inhibitory portion of **4** with the addition of three residues on the *C*-terminal side of the original sequence. Val and Thr were selected to follow the consensus sequence based on the

statistical analysis of Gavel and von Heijne[27] which suggests that these residues are prevalent in these two positions in native glycoproteins. The Nph residue was included to provide a diagnostic chromophore to facilitate purification and quantification of the final cyclic compound. In a deviation from **4**, the formation of a thioether was selected to introduce the cyclic constraint.

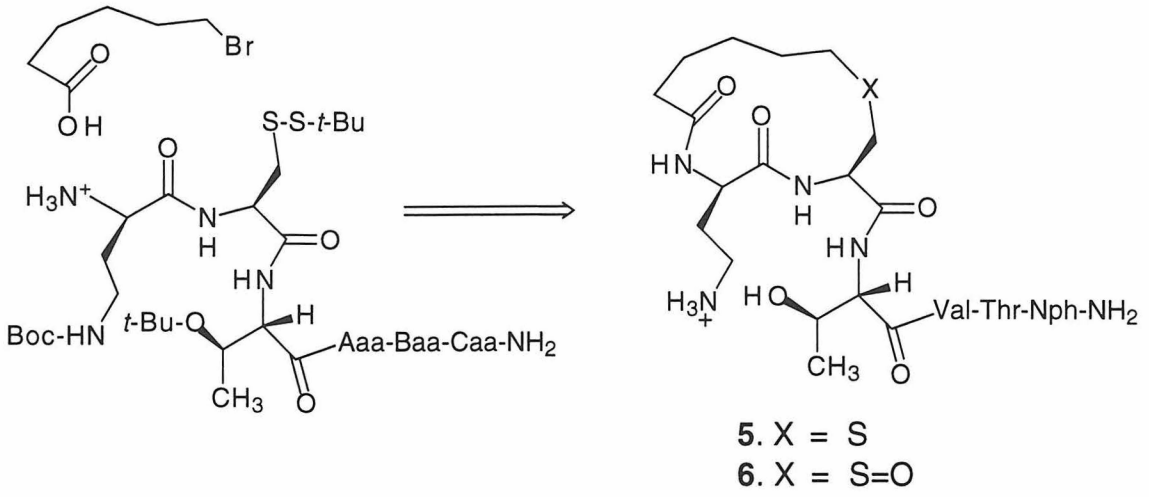

Figure 4-3. Scheme for the Solid Phase Preparation of **5** and **6**.

Two additional potential inhibitors were prepared for further evaluation and for comparison to **5**. The thioether of **5** was oxidized to a sulfoxide (**6**) as it has previously been demonstrated that constrained thioethers and sulfoxides can favor different conformations and may therefore exhibit different inhibitory properties.[29] The possibility that two diastereomeric sulfoxides were generated during this reaction was considered; however, only one product was observed by HPLC analysis, suggesting that a single diastereomer was formed. The unconstrained analog **7**, with the

peptide sequence N^{α}-hexanoyl-Amb-Cys(S-S-*tert*-butyl)-Thr-Val-Thr-Nph-NH_2 (**7**, not shown), was also synthesized.

Compounds **5** and **6** were readily prepared using standard Fmoc-based solid phase peptide synthesis procedures (Figure 4-4). The Amb residue was incorporated into the peptide as Fmoc-Amb(Boc). This amino acid can be prepared from Fmoc-Gln in one step *via* a Hofmann rearrangement using $Pb(OAc)_4$ in *tert*-butanol.[30] In order to introduce the required conformational constraint, an orthogonally protected cysteine residue Fmoc-Cys(S-S-*tert*-butyl) was incorporated into each peptide[28] and the *N*-terminus of the completed peptide was capped with 6-bromohexanoic acid. The cysteine side chain was deprotected by treatment with tributylphosphine and the cyclization was affected *via* alkylation at the C-6 carbon of the hexanoic acid. Direct cleavage from the resin at this stage afforded peptide **5**. The related product, **6**, was generated by mild oxidation (H_2O_2) prior to cleavage from the solid support.[29] The linear analog **7** was prepared through standard methods and the *N*-terminus was capped with hexanoic acid; the cysteine side chain remained fully protected. Each peptide was readily purified by HPLC and the identity was confirmed by mass spectroscopy and amino acid analysis. Peptide **5** was also examined by proton NMR; the ten methylene protons of the hexanoic acid all appeared as diastereotopic protons thereby establishing the introduction of the cyclic constraint.

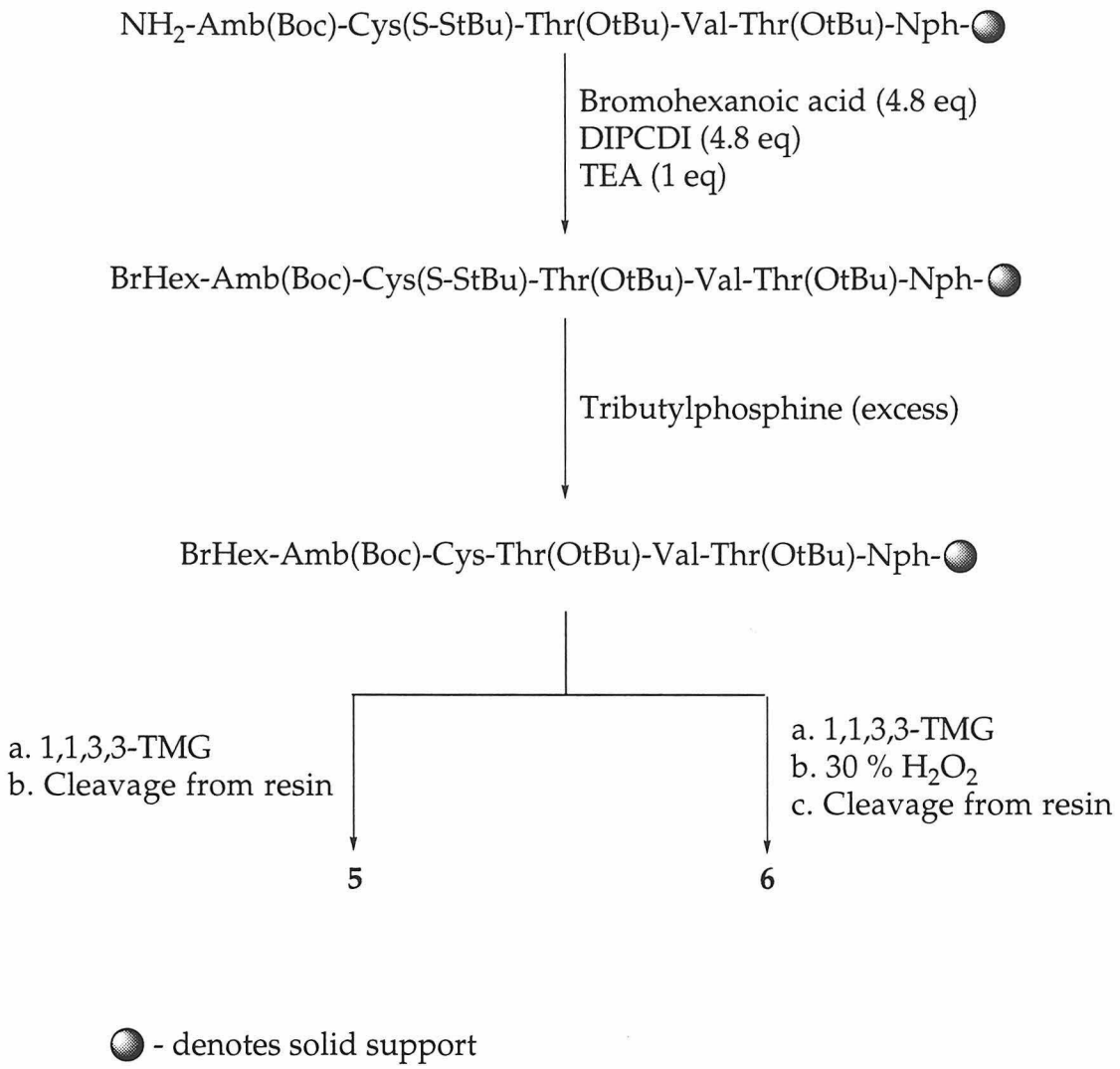

Figure 4-4. Solid Phase Synthesis and Cyclization of **5** and **6**. Compounds **5** and **6** were purified by reverse phase HPLC on a C_{18} column with a water/ acetonitrile/0.1 % TFA gradient; (1,1,3,3 -TMG: 1,1,3,3-tetramethylguanidine).

4.2.2 Kinetic Evaluation of 5, 6 and 7

Each of the compounds (**5 - 7**) was evaluated using *Saccharomyces cerevisiae* oligosaccharyl transferase in a series of competitive assays with the standard tripeptide substrate Bz-Asn-Leu-Thr-NHMe (**2**).[31] For each experiment, the precise concentration of each inhibitor was determined through quantitative amino acid analysis of stock solutions. Initial experiments revealed that all three peptides exhibit slow, tight binding kinetic behavior against OT, as evidenced by the curvature of the data in Figure 4-5. This kinetic phenomenon is unusual and is often associated with a slow, structural reorganization of the enzyme/inhibitor complex to a species that may more closely resemble the transition state in the reaction coordinate.[32] Two different possibilities may account for this behavior with peptides **5 - 7**. It has been proposed that asparagine glycosylation occurs following tautomerization with concomitant deprotonation of the asparagine side chain (see Figure 1-7).[23] This process requires an active site base positioned in proximity to the asparagine side chain; the pK_a of the Amb side chain (~ 9) is significantly reduced from that of an asparagine carboxamide and the slow binding behavior of peptides **5 - 7** may be due to deprotonation of the side chain to the neutral amine. Alternatively, or simultaneously, the unusual kinetic behaviors of these three peptides may be due to the peptides slowly accessing a more appropriate conformational space, perhaps analogous to an Asx-turn.

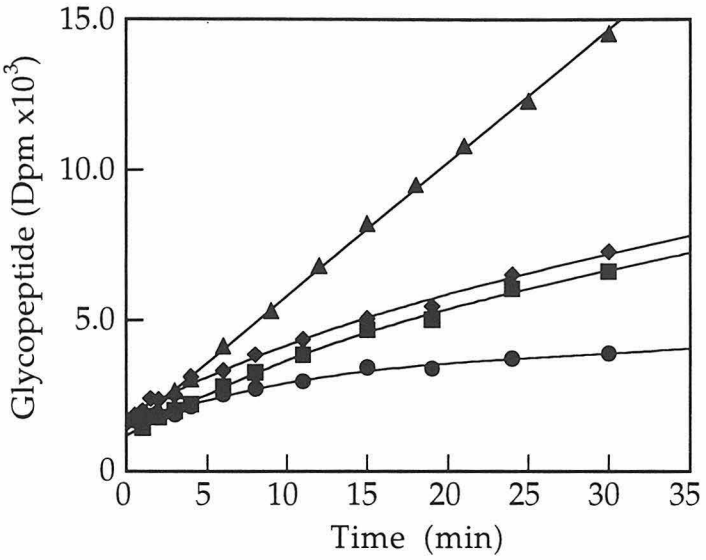

Figure 4-5. Inhibition of Oligosaccharyl Transferase by Compounds **5** - **7** (▲ - no inhibitor; ◆ - 800 nM linear inhibitor **7**; ■ - 200 nM cyclic sulfoxide inhibitor **6**; ● - 200 nM cyclic thioether inhibitor **5**).

Each K_i was determined by preincubating OT with the appropriate peptide inhibitor at 4 °C for 30 minutes prior to the competitive assay. The slow binding kinetic behavior of these peptides necessitated this preincubation to allow the inhibitors and the enzyme to completely equilibrate prior to analysis. Several concentrations were examined for each inhibitor (Figures 4-6, 4-7 and 4-8). From this data, a concentration was selected which induced a moderate drop (~50%) in OT activity (as measured by the rate of glycosylation) in the presence of 50 μM of the competing substrate Bz-Asn-Leu-Thr-NHMe (**1**, $2xK_M$). The values for K_i were calculated for **6** and **7** as described by Segel[33] by inserting this concentration ([I]) into equation 3-1. This equation is most accurate under conditions where the enzyme rate is decreased by 50% (i = 0.50) in the presence of the inhibitor.

$$K_i = \frac{[I] - i[I]}{i + ([S]i/K_M)} \qquad (3\text{-}1)$$

i represents the percent inhibition as compared to the rate of a control.

[I] represents the inhibitor concentration.

[S] represents the concentration of the competing substrate ([S] = 50 μM).

K_M represents the binding constant for the competing substrate **2** (K_M = 25 μM).

A summary of the kinetic data for peptides **5** - **7** is given in Table 4-1; several related compounds have been included for comparison. The calculated K_i for **5** (37 nM) shows that this constrained peptide is at least three orders of magnitude more potent than any previously reported inhibitor of OT,[22, 23] including **1**[23] and **4**. This enhancement in potency is due to the collective exploitation of the specific structural features which were incorporated into the design, including the introduction of the cyclic

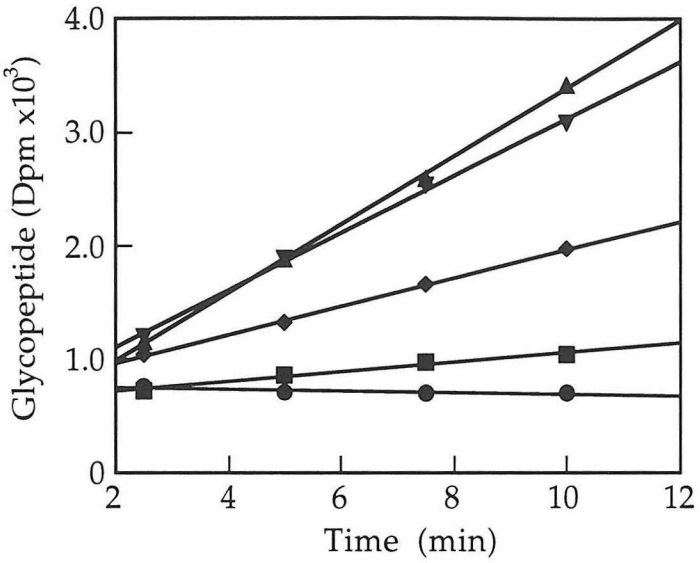

Figure 4-6. Concentration Dependence of **5** with Oligosaccharyl Transferase and Bz-Asn-Leu-Thr-NHMe (Concentration of **5**: ▲ - 0 nM; ▼ - 7.5 nM; ■ - 75 nM; ◆ - 750 nM; ● - 7.5 μM).

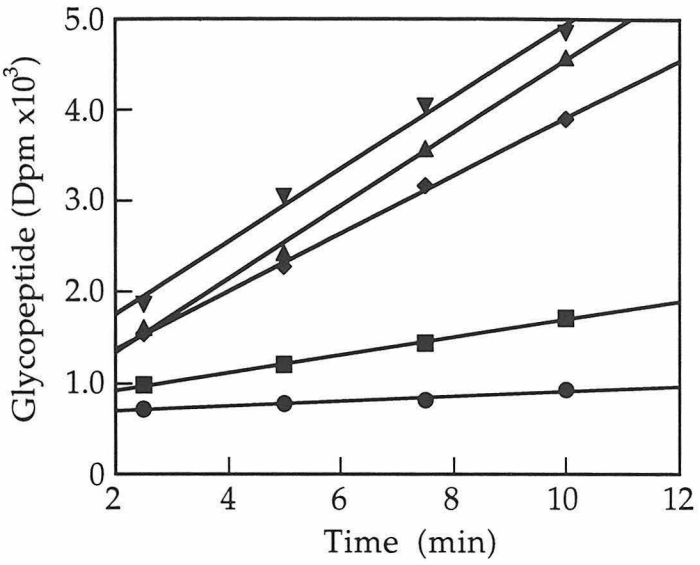

Figure 4-7. Concentration Dependence of **6** with Oligosaccharyl Transferase and Bz-Asn-Leu-Thr-NHMe (Concentration of **6**: ▲ - 0 nM; ▼ - 9.7 nM; ■ - 97 nM; ◆ - 970 nM; ● - 9.7 μM).

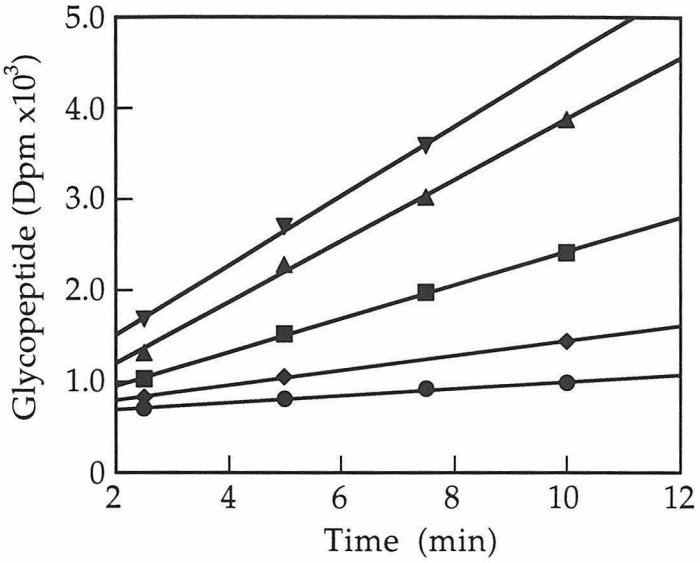

Figure 4-8. Concentration Dependence of **7** with Oligosaccharyl Transferase and Bz-Asn-Leu-Thr-NHMe (Concentration of **7**: ▲ - 0 nM; ▼ - 10 nM; ■ - 100 nM; ◆ - 1 μM; ● - 10 μM).

constraint and the exploitation of extended binding sites. The 3.5-fold difference in affinity between **5** and the cyclic sulfoxide **6** is attributed to the unique conformational preferences of the thioether **5**.

Table 4-1. Kinetic Constants for Inhibitors of OT

Peptide	K_M (μM)	K_i (nM)
Bz-NLT-NHMe (**2**)	25	
1[23]		1000000
4		50000[a]
5		37[b]
6		130[c]
7		360[c]

[a] Not slow binding. [b] K_i was determined from a progress curve analysis (see text), $k_{on} = 2.4 \times 10^4\ s^{-1}\ M^{-1}$, $k_{off} = 8.9 \times 10^{-4}\ s^{-1}$; for comparison, a value of 18 nM was obtained using equation 1. [c] K_is were determined using equation 1.

As the most potent inhibitor, the slow binding kinetic behavior of **5** was more precisely delineated through a detailed kinetic evaluation using a progress curve analysis (Figures 4-9) for the determination of k_{on} and k_{off}.[34] These constants were determined by examining the rate of inhibition of **5** at several different concentrations. (Figure 4-9A shows a representative set of slow binding data; these curves were obtained from a single experiment.) A value for k_{obsd} was determined for each concentration by fitting the data in Figure 4-9 (and other experiments) to equation 3-2.[34]

$$\text{Dpm} = \frac{\upsilon_f t - (\upsilon_f - \upsilon_i)[1 - \exp(-k_{obsd} t)]}{k_{obsd}} + \text{Dpm}_0 \qquad \text{(3-2)}$$

Dpm represents disintegrations per minute.

Dpm_0 represents dpm at t = 0.

υ_f and υ_i represent the final and initial velocities (estimated from the data for each individual experiment).

Values for K_{on} and K_{off} were determined from a replot of the calculated k_{obsd} *vs.* inhibitor concentration, using equation (3-3).

$$k_{obsd} = k_{off} + \frac{k_{on}[I]}{1 + [S]/K_M} \qquad \text{(3-3)}$$

[I] = [**5**].

[S] = [**2**] = 37.5 μM.

K_M = 25 μM.

The value for K_i given in Table 4-1 is the ratio of the K_{off} and K_{on}[34] and was determined from average values for k_{obsd} over several experiments (Figure 4-9B, 1 - 4 measurements were made at each inhibitor concentration). The low nanomolar K_i for **5** makes it the most potent inhibitor of OT identified to date. In addition, the slow binding kinetic behavior of this compound may, in the future, shed light on the mechanism of action of asparagine-linked glycosylation.

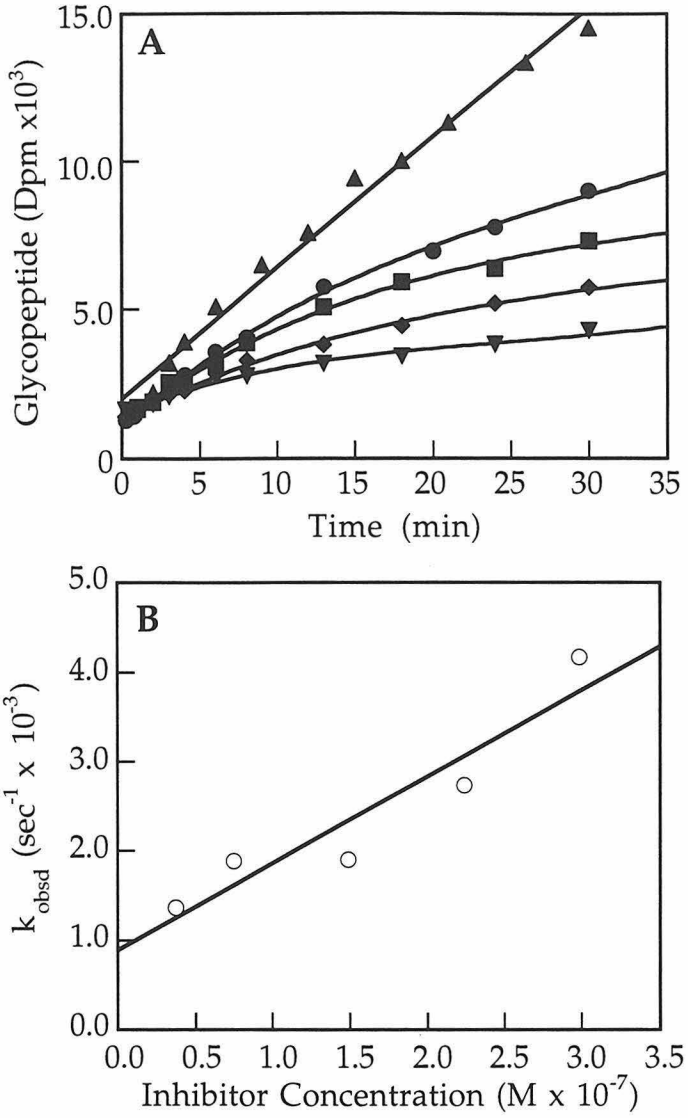

Figure 4-9. Characterization of the Slow, Tight Binding Inhibition of Oligosaccharyl Transferase by **5**. A. Inhibition of OT Activity by Compound **5** (▲ - no inhibitor; ● - 37.5 nM inhibitor; ■ - 75 nM inhibitor; ◆ - 150 nM inhibitor; ▼ - 300 nM inhibitor). B. Plot of k_{obsd} (calculated from part A) *vs.* inhibitor concentration.

Peptides **5** and **6** represent a new class of potent inhibitors for oligosaccharyl transferase, with the cyclic thioether **5** being the most effective. These compounds represents the culmination of a logical plan designed to systematically improve the affinity of **1** (K_i = 1 mM). The binding affinities for the two cyclic peptides have been enhanced to nanomolar levels through the incorporation of several different experimental observations. Most notably, the combination of the cyclic constraint and the extension in length to a hexapeptide seem to act in concert to produce compounds which are substantially more effective than their truncated linear (**1**) or cyclic (**4**) analogs.

4.2.3 Species Selectivity and Enzyme Specificity

The enzyme oligosaccharyl transferase has been characterized from several different species and shows structural homology throughout eukaryotic evolution.[35] It was therefore of interest to examine whether inhibitors **5** and **6** demonstrate any species selectivity. The two constrained peptides were examined as inhibitors against *S. cerevisiae* and porcine liver OT (Figures 4-10 and 4-11, respectively). The percent inhibition was determined by measuring any decrease in the rate of OT mediated glycosylation in the presence of various concentrations of each inhibitor. Notably, in each case, inhibition of yeast OT was approximately three-fold more effective. Since extended binding interactions from the C-terminal residues contribute significantly to enzyme binding,[27] these results suggest that it may be possible to manipulate and enhance this species selectivity by simple changes in the inhibitor primary sequence. This possibility is currently being investigated in the Imperiali group.

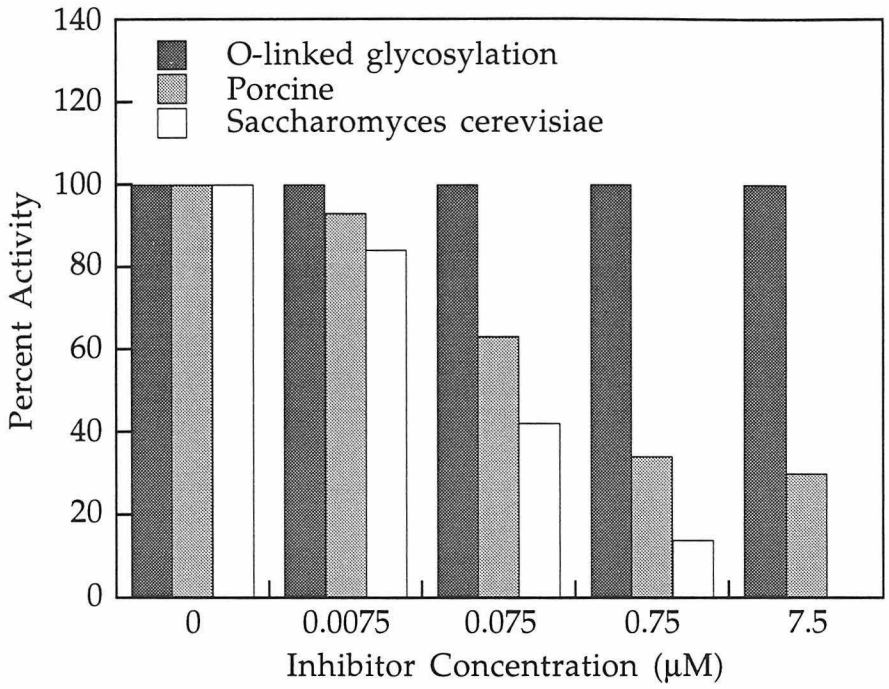

Figure 4-10. Species-Selectivity and Enzyme-Specificity of **5**. Cyclic peptide **5** was examined as an inhibitor against OT isolated from *S. cerevisiae* and porcine liver sources to determine its species selectivity. Enzyme specificity was examined through an assay of GalNAc-transferase[36] in the presence of **5**.

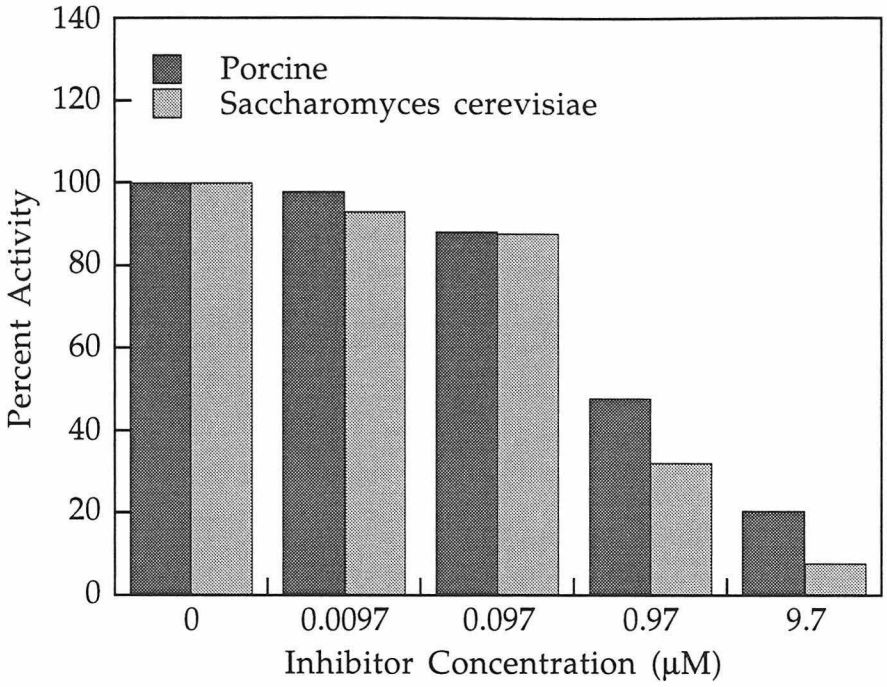

Figure 4-11. Species-Selectivity of **6**. Cyclic peptide **6** was examined as an inhibitor against OT isolated from *S. cerevisiae* and porcine liver sources to determine its species selectivity.

As a final control, the ability of **5** to specifically inhibit *N*-linked rather that *O*-linked glycosylation was assessed by monitoring its activity against the common *O*-linked glycosylation enzyme, polypeptide *N*-acetyl galactosaminyltransferase (GalNAc-transferase).[36] This enzyme catalyzes the transfer of GalNAc from UDP-GalNAc to threonine residues within peptides; a consensus sequence has not been identified. As **5** contains two threonine residues, it was also evaluated for substrate activity. As expected, the inhibitor **5** showed no measurable activity against this enzyme even at elevated concentrations (Figure 4-10).

4.3 Conclusions

The investigations presented in this chapter all represent *in vitro* analyses of a new class of cyclic inhibitors, using solubilized sources of oligosaccharyl transferase; the *in vivo* efficacies of the compounds remain unevaluated. One problem that has not yet been addressed experimentally is the possibility that compounds such as **5** and **6** will not be able to access OT *in vivo*. OT is sequestered on the lumenal side of the endoplasmic reticulum (ER)[13] and is therefore likely to be inaccessible to extracellular antagonists. Thus, for this new class of inhibitors to be effective for *in vivo* studies, they must be able to cross the cell wall and be transported into the ER. Variations of the core structure of **5** are currently under consideration in the Imperiali group in an effort to design an inhibitor which gains access to the ER.

Glycoproteins play critical biological roles in all eukaryotic cells. Because of the importance of these glycoconjugates, potent and specific inhibitors of *N*-linked protein glycosylation may find diverse applications. This chapter has described the design and evaluation of a new class of slow, tight binding inhibitors that exhibit nanomolar binding constants for the

enzyme oligosaccharyl transferase. The modular nature of these inhibitors provides immediate opportunities for structural diversification through combinatorial synthesis,[37-39] making this class of cyclic peptides the first example of a readily available and adaptable family of potent protein glycosylation inhibitors. These compounds present a platform which can be easily modified for the further development of specific glycosylation inhibitors as diagnostic tools to evaluate the role of glycoproteins in biological systems and as potential therapeutic agents.[25] These compounds may prove to be valuable tools for future studies designed to elucidate the roles of glycosylation in complex cellular processes.

4.4 Acknowledgements

The research discussed in this chapter is the result of a fruitful collaboration between three different people in the Imperiali group. Dr. Jeffrey Spencer designed, synthesized and characterized the original cyclic, constrained tripeptide inhibitor (**4**) which formed the foundation for this project; for completeness, the synthetic protocols for this compound, which were developed by Dr. Spencer, have been included at the end of the experimental methods section of this chapter. He also developed the protocol for the synthesis of Fmoc-Amb(Boc) and made the first cyclic hexapeptide with a nanomolar K_i for OT. Mihoko Kato prepared and purified the linear hexapeptide (**7**), and prepared additional quantities of starting materials and intermediates along the way. A substantial portion of the results presented in this chapter have been submitted for publication: Hendrickson, T. L.; Spencer, J. R.; Kato, M.; Imperiali, B. (1996). Design and Evaluation of Potent Inhibitors of Asparagine-Linked Protein Glycosylation.

4.5 Experimental Methods

4.5.1 Solid Phase Synthesis of Cyclic Inhibitors 5 and 6

Synthesis of Fmoc-Amb(Boc)

A heterogeneous mixture of Fmoc-Gln-OH (2.3 mmol, 0.85 g) and anhydrous *tert*-butanol (15 mL) was placed in a dry flask, degassed under reduced pressure and placed under nitrogen. The mixture was warmed to 75 °C and lead tetraacetate (4.6 mmol, 2.05 g) was added. The dark orange mixture was allowed to stir at 75 °C for 1 hour and was warmed to 80 - 85 °C for an additional 45 min, during which time the color lightened to pale brown. To the cooled (20 °C) mixture was added ether (50 mL) and $NaHCO_3$ (1 g). The suspension was allowed to stir for 20 min. The solids and salts were removed by filtration through a plug of silica gel followed by rinsing with $CHCl_3$/MeOH/AcOH : 96/4/1. The foam obtained upon removal of the solvent was purified by silica gel chromatography ($CHCl_3$/MeOH/AcOH : 96/4/1, R_f 0.25). The product was obtained as a white powder (0.437 g, 43%) upon removal of solvent and crystallization in petroleum ether: mp 73.5 - 75.5 °C, $[\alpha]_D^{25}$ + 3.9 ° (c 1.0, $CHCl_3$), R_f 0.36 ($CHCl_3$/MeOH/AcOH : 95/5/1); ^{1}H-NMR δ_H (300 MHz, $CDCl_3$) 7.78 (d, 2H, J = 7.7 Hz, Fmoc arom), 7.60 (d, 2H, J = 6.8 Hz, Fmoc arom), 7.39 (t, 2H, J = 7.7 Hz, Fmoc arom), 7.32 (t, 2H, J = 7.7 Hz, Fmoc arom), 6.65 - 5.17 (four br s, 2H, NH^{α} and NH^{γ}), 4.40 (m, 3H, CH^{α} and Fmoc CH_2), 4.23 (t, 1H, J = 6.6 Hz, Fmoc 9-CH), 3.50 - 3.00 (m, 2H, CH_2^{β}), 2.36, 2.00 (m,m, 2H, CH_2^{γ}), 1.46 (s, 9H, Boc CH_3); ^{13}C-NMR δ (75 MHz, $CDCl_3$) 143.7, 141.3, 127.7, 127.1, 125.1, 120.0, 80.3, 67.1, 66.9, 51.4, 47.2, 36.7, 28.3. IR ν_{max} (thin film, NaCl) 3327, 2969, 1702, 1518, 1445, 1361, 1249, 1165, 1054, 908, 735. HRMS calcd for $C_{24}H_{27}N_2O_6$ (MH^-) 439.187 g/mol, found 439.187.

Fmoc-Thr(OtBu)-Val-Thr(OtBu)-Pal-Peg Resin

The *C*-terminal tetrapeptide for compounds **5** and **6** was prepared using standard solid phase synthesis protocols and 9-fluorenylmethoxycarbonyl (Fmoc) protecting group chemistry on a Millipore 9050 Peptide Synthesizer with Enhanced Monitoring. Unless otherwise stated, all Fmoc protected amino acids were purchased from Perseptive Biosystems (USA). The peptide was generated on Pal-Peg Resin (1.0 g, 0.170 meq/g) to afford a *C*-terminal carboxamide upon cleavage. Each coupling cycle was conducted with 3 equivalents of each amino acid and HOBT coupling chemistry. The final deprotection cycle was omitted to generate Fmoc-Thr(OtBu)-Val-Thr(OtBu)-Pal-Peg Resin.

Fmoc-Cys(SStBu)-Thr(OtBu)-Val-Thr(OtBu)-Pal-Peg Resin

Fmoc-Thr(OtBu)-Val-Thr(OtBu)-Pal-Peg resin (34 μmoles) was washed twice (30 seconds) with DMF and then treated twice with 20% piperidine/DMF (3 minutes). Following an extensive wash with DMF, a solution of Fmoc-Cys(SStBu)-OH (48.8 mg, 113 μmoles, 3 eq, CalBiochem, USA), HOBT (19.1 mg, 125 μmoles, 3.6 eq) and diisopropylcarbodiimide (DIPCDI, 16.5 μL, 112 μmoles, 3.3 eq) in 2 mL DMF was added to the resin and agitated for 2 hours. The resin was washed with DMF and treated twice with 10 mL of the following capping solution: 180 mL DMF, 20 mL dichloromethane, 5.7 mL acetic anhydride (29 mM) and 8.13g HOBT (26 mM). The resin was rinsed twice with DMF and twice with dichloromethane.

Fmoc-Amb(Boc)-Cys(SStBu)-Thr(OtBu)-Val-Thr(OtBu)-Pal-Peg Resin

Fmoc-Cys(SStBu)-Thr(OtBu)-Val-Thr(OtBu)-Pal-Peg resin (34 μmoles) was washed twice (30 seconds) with DMF and then treated twice with 20%

piperidine/DMF (3 minutes). Following an extensive wash with DMF, a solution of Fmoc-Amb(Boc)-OH (46.8 mg, 110 μmoles, 3.2 eq), HOBT (16.7 mg, 109 μmoles, 3.2 eq) and diisopropylcarbodiimide (DIPCDI, 16.5 μL, 112 μmoles, 3.3 eq) in 2 mL DMF was added to the resin and agitated for 2 hours. The resin was washed with DMF and then treated twice with the capping solution described in the previous solution. Following capping of all unreacted amino groups, the resin was washed twice with DMF and twice with dichloromethane.

BrHex-Amb(Boc)-Cys(SStBu)-Thr(OtBu)-Val-Thr(OtBu)-Pal-Peg Resin

Fmoc-Amb(Boc)-Cys(SStBu)-Thr(OtBu)-Val-Thr(OtBu)-Pal-Peg resin (34 μmoles) was washed twice (30 seconds) with DMF and then treated twice with 20% piperidine/DMF (3 minutes). Following an extensive wash with DMF, the resin was combined with a solution of bromohexanoic acid (32 mg, 164 μmoles, 4.8 eq), DIPCDI (24 μL, 163.5 μmoles, 4.8 eq) and triethylamine (22 μL, 159 μmoles, 4.7 eq) in 3 mL DMF for 1.5 hours. Resin was filtered and recombined with a solution of bromohexanoic acid (33.6 mg, 172 μmoles, 5.0 eq), DIPCDI (24 μL, 163.5 μmoles, 4.8 eq) in 2 mL DMF and agitated overnight. Resin was filtered and washed with DMF and dichloromethane.

Solid Phase Cyclization of Hexapeptides

Cyclization was afforded according to the method of Virgilio and Ellman.[28] A 5/3/2 solution (15 mL) of *n*-propanol/DMF/water was prepared and bubbled with nitrogen for 15 minutes. A 10 mL aliquot of this solution was combined with the resin bound BrHex-Amb(Boc)-Cys(SStBu)-Thr(OtBu)-Val-Thr(OtBu)-Pal-Peg resin (34 μmoles) for ten minutes and then removed *via* filtration. The S-*t*-butyl protecting group was removed under a nitrogen

atmosphere by combining the resin with an additional 15 mL of the deoxygenated *n*-propanol solution and 375 μL tributyl phosphine. After 6 hours, the resin was filtered and the filtrate was quenched with a bleach solution. The resin was washed twice with methanol and twice with dichloromethane. A solution of DMF was bubbled under a stream of nitrogen. Cyclization was afforded by washing the resin with 10 mL DMF and then combining the resin with an additional 15 mL DMF and 375 μL 1,1,3,3-tetramethylguanidine and agitating the mixture for 20 hours. Resin was washed extensively with DMF and dichloromethane to yield *cyclo*[SHex-Amb(Boc)-Cys]-Thr(*O*tBu)-Val-Thr(*O*tBu)-Nph-Pal-Peg resin.

Cleavage and Deprotection

Cleavage and deprotection was accomplished by shaking *cyclo*[SHex-Amb(Boc)-Cys]-Thr(*O*tBu)-Val-Thr(*O*tBu)-Nph-Pal-Peg resin with 95/5/5 trifluoroacetic acid/dimethyl sulide/water (1 mL) for four hours. The resin was filtered and rinsed with TFA. The filtrate was concentrated under a stream of nitrogen and then triturated 3 times with ether to remove the excess dimethyl sulfide. The impure peptide (6 mg) was lyophilized overnight from water. The peptide was purified by HPLC with a acetonitrile/water/0.1%TFA gradient ranging from 35% to 55% acetonitrile over 20 minutes. The product was detected by monitoring absorbance changes at 228 nm and 280 nm. *Cyclo*[SHex-Amb-Cys]-Thr-Val-Thr-Nph-NH_2 **5** eluted with a retention time of 8.4 minutes. The product was pure by HPLC and proton NMR. Final yield was approximately 400 μg. ^{1}H-NMR δ_H (500 MHz, DMSO-d_6) 8.45 (d, 1H, J = 8.4 Hz, NH), 8.09 (d, 2H, J = 8.3 Hz, Nph arom), 8.00 (d, 1H, J = 8.4 Hz, NH), 7.92 (d, 1H, J = 8.6 Hz, NH), 7.65 (m, 6H, three NH and NH_3^+), 7.49 (d, 2H, J = 8.4 Hz, Nph arom), 7.45 (s, NH_2), 7.22 (s, NH_2), 4.94

(br s, 1H, Thr OH), 4.84 (br s, 1H, Thr OH), 4.65 (m, 1H, CH^{α}), 4.52 (m, 2H, two CH^{α}), 4.28 (m, 1H, CH^{α}), 4.29 (m, 2H), 3.93 (br s, 2H), 3.19 (d, 1H, J = 4.0 Hz), 3.17 (d, 1H, J = 4.3 Hz), 2.93 (dd, 1H, J = 13.7, 9.1 Hz), 2.85 (dd, 1H, J = 13.9, 7.1 Hz), 2.78 (br m, 3H), 2.35 - 2.42 (br m, obscured by solvent), 2.18 (m, 1H), 2.11 (m, 1H), 2.02 (m, 1H), 1.92 (m, 1H), 1.78 (m, 1H), 1.68 (br s, 1H), 1.48 - 1.22 (m, ~8H), 0.98 (m, 6H), 0.75 (m, 6H). HRMS calcd for $C_{35}H_{55}N_9O_{11}S$ (MH^+) 810.3820 g/mol, found 810.3858 g/mol. Quantitative amino acid analysis confirmed the presence of each amino acid (except cysteine) in the appropriate ratios (see below).

*Oxidation of Cyclic Thioether **5** to Cyclic Sulfoxide **6***

Cyclo[SHex-Amb(Boc)-Cys]-Thr(*O*tBu)-Val-Thr(*O*tBu)-Nph-Pal-Peg resin (approximately 10 mg) was combined with 75 µL *n*-propanol, 75 µL dichloromethane and 30 µL 30% hydrogen peroxide. Mixture was agitated for five hours, washed with water and dichloromethane and cleaved as described above with 200 µL 95/5/5 trifluoroacetic acid/dimethyl sulide/water. Following trituration and lyophilization, the reaction products were analyzed by HPLC on an analytical column with a gradient of acetonitrile from 20% to 30% over 20 minutes. The sulfoxide product eluted with a retention time of 10.9 minutes, compared to a retention time of 17.1 minutes for the thioether starting material. Only one new peak was observed following oxidation suggesting that only one diastereomer is generated or the two diastereomers coelute under these conditions. Approximately 150 µg of the sulfoxide **6** were purified. LRMS calcd for $C_{35}H_{55}N_9O_{12}S$ (MH^+) 826 g/mol, found 826 g/mol. Quantitative amino acid analysis verified the presence of each amino acid (except cysteine) in the appropriate ratios (see below).

*Hexanoyl-Amb(Boc)-Cys(SStBu)-Thr(OtBu)-Val-Thr(OtBu)-NH_2 (**7**)*

Fmoc-Amb(Boc)-Cys(SStBu)-Thr(OtBu)-Val-Thr(OtBu)-Pal-Peg resin (50 μmoles) was washed twice (30 seconds) with DMF and then treated twice with 20% piperidine/DMF (3 minutes). Following an extensive wash with DMF, the resin was combined with a solution of hexanoic acid (30 μL, 240 μmoles, 4.8 eq), DIPCDI (35 μL, 240 μmoles, 4.8 eq) and triethylamine (7 μL, 50 μmoles, 1 eq) in 3 mL DMF and agitated overnight. The resin was filtered and washed with DMF and dichloromethane and cleaved from the resin as described above. Peptide was purified by HPLC. Quantitative amino acid analysis verified the presence of each amino acid (except cysteine) in the appropriate ratios (see below).

4.5.2 Enzymatic Evaluation of Cyclic Inhibitors

Determination of Peptide Solution Concentrations by Quantitative Amino Acid Analysis

Following HPLC purification, the water/acetonitrile solutions of cyclic peptides **5** and **6** were quantitated by measuring the solutions absorbance between 250 nm and 300 nm on a Beckman DU7500 Spectrophotometer in a 1 cm cell. Using an extinction coefficient of 9340 mol^{-1} cm^{-1}, the concentration of each solution was estimated using Beer's Law. Based on this concentration, the cyclic peptides were aliquoted into microcentrifuge vials in 10 nmole portions.

For the final concentration determination, a 10 nmole aliquot of each cyclic peptide was redissolved in 100 μL 50% acetonitrile/water/0.1%TFA. The linear peptide **7** was dissolved in 200 μL DMSO to yield an approximate concentration of 840 μM as determined by UV analysis. An aliquot of this solution (10 μL, 7.56 μg) was dried under vacuum and redissolved in 100 μL 50% acetonitrile/water/0.1%TFA. These three solutions were submitted to

Kristine Swiderick at the amino acid analysis facility at the City of Hope for analysis. The concentration was determined by quantitative amino acid analysis for valine. The 10 nmole aliquot of **5** contained 6.04 μg peptide (7.5 nmoles); the 10 nmole aliquot of **6** contained 8.0 μg peptide (9.7 nmoles); The 9 nmole aliquot of the linear peptide **7** contained 4.70 μg peptide (5.6 nmoles).

Solutions of the two unnatural amino acids, Fmoc-Amb(Boc) and Fmoc-Nph, were also analyzed as standards by the amino acid analysis facility at the City of Hope. The results from these experiments were combined with the analyses of peptides **5 - 7** to confirm the presence of each of the amino acids in the expected ratios (1 Amb, 2 Thr, 1 Val, 1 Nph); cysteine is not readily observed by quantitative amino acid analysis.

General Assay for Competitive Inhibition - Oligosaccharyl Transferase

Final peptide concentrations ranged from 7.5 nM to 7.5 μM for peptide **5**; from 9.7 nM to 9.7 μM for peptide **6**; and from 10 nM to 10 μM for peptide **7**. Assays were compared to control experiments which did not contain the inhibitor peptides. Porcine liver and *S. cerevisiae OT* were isolated as previously described.[31, 36, 40] The solubilized yeast (150 μL) and the crude porcine (20 μL) OT were diluted to final volumes of 1200 μL with assay buffer (50 mM Hepes, pH 7.5, 140 mM sucrose, 1% Triton X-100, 0.5 mg/mL phosphatidylcholine, 10 mM $MnCl_2$). Solutions of each peptide were prepared in DMSO at concentrations which would yield the appropriate final concentration following the 20-fold dilution of the assay.

A 200 μL portion of each enzyme was combined with 13.3 μL Bz-NLT-NHMe (10 mM and 1 mM stock solutions in DMSO for porcine and *S. cerevisiae* assays, respectively), 13.3 μL of the appropriate inhibitor solution or DMSO (control) and 13.4 μL assay buffer. These solutions were equilibrated

on ice for 30 minutes. The assays were initiated by transferring 180 μL of the equilibrated enzyme solution into eppendorfs containing 50,000 dpm dolichol-PP-$GlcNAc_2$ (36.5 Ci/mmol) and 20 μL assay buffer. Following initiation, aliquots were treated as previously described.[31]

General Assay for Competitive Inhibition - Polypeptide N-Acetyl-galactosaminyl Transferase

Solubilized GalNAc-transferase (100 μL) was suspended in 112.5 μL of buffer (100 mM imidazole/HCl, pH 7.5, 1% Triton-X). Ac-PDAATAAPL-NH_2 was added (12.5 μL of a 8 mM solution) with 12.5 μL inhibitor or DMSO (control). Following preincubation, the assay was initiated by the addition of 12.5 μL of a 2.5 mM solution UDP-GalNAc (0.1 μCi) and completed as previously described.[36]

Determination of Kinetic Constants - Approximate K_i

The IC_{50}, or the concentration of each peptide which produced a 50% decrease in OT activity, was determined through standard competitive assays in the presence of 50 μM Bz-NLT-NHMe (2x K_M). The values for K_i were calculated as described by Segel[33] by inserting the results from these experiments into the following equation: $K_i = ([I]-i[I])/(i + [S]i/K_M)$; [I] = concentration of inhibitor peptide; i = percent observed inhibition; [S] = 50 μM; K_M = 25 μM. This equation is most accurate when i = 0.5.

Determination of Kinetic Constants - Precise K_i, K_{on} and K_{off}

Peptide **5** was further evaluated for slow binding inhibition of oligosaccharyl transferase. OT (*S. cerevisiae* solubilized microsomes,[40] 210 μL) was diluted with 3.57 mL assay buffer (50 mM Hepes, pH 7.5, 140 mM

sucrose, 1% Triton X-100, 0.5 mg/mL phosphatidylcholine, 10 mM $MnCl_2$). Radiolabeled dolichol-P-P-$GlcNAc_2$ (DPPC) was prepared as previously described (1.2 x 10^6 dpm, 60 Ci/mmol per assay).[41] Each aliquot was diluted with unlabeled DPPC and dissolved in 540 µL enzyme solution. The final DPPC concentration was 160 nM. Assays were initiated by the addition of 60 µL of a DMSO solution containing 375 µM Bz-NLT-NHMe and the appropriate concentration of **5**. Following initiation, aliquots of each assay were quenched and quantitated as previously described.[31] Compound **5** was examined over a range of concentrations from 37.5 nM to 300 nM.

Values for k_{obsd} were calculated for each peptide concentration by fitting the data to the equation $Dpm = \upsilon_f t - (\upsilon_f - \upsilon_i)[1-\exp(-k_{obsd}t)]/k_{obsd} + Dpm_0$.[34] Values for K_{on} and K_{off} were determined from a replot of the calculated k_{obsd} *vs.* inhibitor concentration, using the equation $k_{obsd} = k_{off} + k_{on}[I]/(1 + [S]/K_m)$.[34]

4.5.3 Solution Phase Synthesis of *cyclo*[Amb-Add]-Thr-NHMe (4)

The experimental protocols described in this section were developed and accomplished by Dr. Jeffrey R. Spencer and have been included for completeness.

Synthesis of Boc-Gln-Add(All)-OH (SIII.97)

A chilled (- 20 °C) solution of HCl•H-L-Add(All)-OH (2.3 mmol, 0.67 g) and HOBt (2.5 mmol, 0.34 g) in DMF (9 mL) was treated with NMM (2.3 mmol, 0.25 mL). An additional 0.15 mL (1.4 mmol) of NMM was added to adjust the mixture pH to 7-8. The ester Boc-Gln-ONp (2.5 mmol, 0.93 g) was added, and the reaction was allowed to proceed 20 min at - 20 °C and 18 hours at 20 °C. The mixture was then chilled (0 °C), treated with additonal Boc-Gln-ONp (0.27 mmol, 0.10 g) and allowed to proceed 8 hours more. This step was

repeated. After removal of the solvent under reduced pressure, the residue obtained was suspended in AcOEt (400 mL) and washed with several portions (10 mL) of 1 N $NaHSO_4$ and H_2O (2x10 mL) and dried ($MgSO_4$). The residue obtained upon removal of the solvent under reduced pressure was purified by silica gel chromatography ($CHCl_3$/MeOH/AcOH : 90/10/1 → 85/15/1). The dipeptide was obtained as a white powder (0.71 g, 64%) after the addition and removal under reduced pressure of toluene and hexanes: mp 65.5 - 68 °C, $[\alpha]_D^{25}$ + 7.1 ° (c 0.3, $CHCl_3$), R_f 0.14 ($CHCl_3$/MeOH/AcOH : 90/10/1); ^{1}H-NMR δ_H (300 MHz, DMSO-d_6) 7.60 (br s, 1H, NH), 7.03 (d, 2H, J = 165 Hz, Gln NH_2^d), 6.98 (d, 1H, J = 8.2 Hz, NH), 5.88 (m, 1H, CH_2-C*H*=CH_2), 5.23 (ddd, 2H, J = 26.8, 20.7, 1.8 Hz, CH_2-CH=C*H*$_2$), 4.53 (d, 2H, J = 6.1 Hz, C*H*$_2$-CH=CH_2), 4.00 (m, 1H, CH^α), 3.85 (m, 1H, CH^α), 2.29 (t, 2H, J = 7.4 Hz, Add CH_2^θ), 2.07 (m, 2H, Gln CH_2^γ), 1.83 (m, 1H, Gln $CH^{\beta d}$), 1.65 (m, 1H, Gln $CH^{\beta u}$), 1.65-1.50 (m, 4H, Add CH_2^β and CH_2^γ), 1.37 (s, 9H, Boc CH_3), 1.22 (br s, 8H, Add CH_2); ^{13}C-NMR δ (75 MHz, DMSO-d_6) 174.0, 172.5, 171.0, 155.2, 132.8, 117.6, 78.0, 64.2, 54.0, 52.8, 33.4, 31.9, 31.6, 28.8, 28.7, 28.5, 28.2, 27.7, 24.9, 24.5. IR ν_{max} (thin film NaCl) 3306, 2930, 1733, 1661, 1569, 1451, 1418, 1367, 1247, 1170. FAB MS m/z: 508 (MNa^+); FAB HRMS calcd for $C_{23}H_{39}N_3O_8Na$ (MNa^+) 508.2635, found 508.2653.

Synthesis of Boc-Gln-Add(All)-Thr(tBu)-NHMe (SIII.99)

To a solution of Cbz-Thr(tBu)-NHMe (0.93 mmol, 0.30 g) in MeOH/1% HOAc (10 mL) was added 10% Pd/C (0.045 g). Hydrogen was introduced at atmospheric pressure at 20 °C, and the mixture allowed to react 1 hour. The catalyst was removed by filtration and the solvent removed under reduced pressure. Toluene (2 x 10 mL) was added and removed under reduced pressure. A mixture of the amino component and Boc-Gln-Add(All)-OH (0.83 mmol, 0.40 g) in DMF (3.3 mL) was chilled to - 40 °C under nitrogen.

The mixture was treated with NMM (0.83 mmol, 0.091 mL) and after 5 min, HOAt (0.81 mmol, 0.11 g) and EDC (0.83 mmol, 0.16 g) were added. After 30 min at - 40 °C, the reaction was allowed to warm to 20 °C and proceed for 18 hours. The solvent was removed under reduced pressure. The residue obtained was suspended in 400 mL of AcOEt and washed with 0.5 M $NaHCO_3$ (10 mL), saturated $NaHCO_3$ (3 x 10 mL), H_2O (10 mL), 1 N $NaHSO_4$ (3 x 10 mL), saturated NaCl (3 x 10 mL) and dried (Na_2SO_4). The solvent was removed under reduced pressure, and the tripeptide was obtained as a white powder (0.45 g, 83%): mp 174 - 176.5 °C, $[\alpha]_D^{25}$ +2.3° (c 0.2, $CHCl_3$), R_f 0.62 ($CHCl_3$/MeOH/AcOH : 85/15/3); ^{1}H-NMR δ_H (300 MHz, DMSO-d_6) 7.95 (d, 1H, J = 8.3 Hz, NH), 7.58 (d, 1H, J = 4.8 Hz, N*H*CH_3), 7.48 (d, 1H, J = 8.9 Hz, NH), 7.00 (d, 2H, J = 138 Hz, Gln NH_2^{δ}), 6.98 (d, 1H, J = 8.3 Hz, NH), 5.89 (m, 1H, CH_2-C*H*=CH_2), 5.23 (ddd, 2H, J = 26.2, 19.2, 1.7 Hz, CH_2-CH=C*H*$_2$), 4.53 (d, 2H, J = 5.6 Hz, C*H*$_2$-CH=CH_2), 4.31 (m, 1H, CH^{α}), 4.14 (dd, 1H, J = 8.6, 2.9 Hz, CH^{α}), 3.90 (m, 2H, CH^{α} and Thr CH^{β}), 2.58 (d, 3H, J = 4.6 Hz, NC*H*$_3$), 2.30 (t, 2H, J = 7.6 Hz, Add CH_2^{θ}), 2.07 (m, 2H, Gln CH_2^{γ}), 1.80 (m, 1H, Gln $CH^{\beta d}$), 1.65 (m, 1H, Gln $CH^{\beta u}$), 1.65-1.50 (m, 4H, Add CH_2^{β} and CH_2^{γ}), Add 1.36 (s, 9H, Boc CH_3), 1.23 (br s, 8H, Add CH_2), 1.08 (s, 9H, tBu CH_3), 0.95 (d, 3H, J = 6.5 Hz, Thr CH_3^{γ}); ^{13}C-NMR δ (75 MHz, DMSO-d_6) 173.7, 172.5, 172.0, 171.5, 169.9, 155.2, 132.8, 117.6, 78.0, 73.5, 67.0, 64.2, 57.7, 54.1, 52.5, 33.3, 31.7, 31.6, 28.6, 28.4, 28.2, 28.1, 28.0, 27.6, 25.6, 25.0, 24.5, 19.5. IR ν_{max} (thin film, NaCl) 3293, 2929, 1732, 1641, 1550, 1522, 1390, 1236, 1172, 1095. FAB MS m/z: 656 (MH^+); FAB HRMS calcd for $C_{32}H_{58}N_5O_9$ (MH^+) 656.4235, found 656.4238.

Synthesis of *Boc-Gln-Add(OH)-Thr(tBu)-NHMe (SIII.100)*

A mixture of Boc-Gln-Add(All)-Thr(tBu)-NHMe (0.50 mmol, 0.33 g) and AcOH (2.4 mmol, 0.14 mL) in anhydrous THF (5 mL) was treated with $PdCl_2(PPh_3)_2$ (0.016 mmol, 0.011 g). The heterogeneous, bright yellow mixture became homogeneous and darker upon the rapid addition of nBu_3SnH (0.52 mmol, 0.14 mL). After 30 min, a white precipitate began forming and increased as the reaction was allowed to proceed another 5 hours. Additional nBu_3SnH (0.056 mmol, 0.015 mL) was added. After 1 hour, the solvent was removed under reduced pressure and hexanes was added and removed. A pale yellow solid was isolated by filtration from a suspension in hexanes. The carboxylic acid was purified by recrystallization from hot AcOEt/hexanes and obtained as a white powder (0.23 g, 77%): mp 172.0 - 175.0 °C, $[\alpha]_D^{25}$ - 13.7 ° (c 0.3, MeOH), R_f 0.10 ($CHCl_3$/MeOH/AcOH : 95/5/3); ^{1}H-NMR δ_H (300 MHz, DMSO-d_6) 11.95 (s, 1H, COOH), 7.92 (d, 1H, J = 7.9 Hz, NH), 7.50 (m, 2H, NH and N*H*CH_3), 7.08 (d, 2H, J = 117 Hz, Asn NH_2^{γ}), 7.00 (d, 1H, J = 7.9 Hz, Asn NH), 4.24 (m, 2H, two CH^{α}), 4.12 (m, 1H, CH^{α}), 3.92 (m, 1H, Thr CH^{β}), 2.58 (d, 3H, J = 4.8 Hz, NHC*H*$_3$), 2.35 (m, 2H, Asn CH_2^{β}), 2.17 (m, 2H, Ada CH_2^{θ}), 1.53 (m, 4H, two Ada CH_2), 1.36 (s, 9H, Boc CH_3), 1.22 (m, 8H, four Ada CH_2), 1.07 (s, 9H, tBu CH_3), 0.96 (d, 3H, J = 6.6 Hz, Thr CH_3^{γ}); ^{13}C-NMR δ (75 MHz, DMSO-d_6) 174.5, 174.0, 171.5, 171.4, 169.9, 155.1, 78.2, 73.5, 66.9, 57.8, 52.7, 51.3, 37.1, 33.7, 31.8, 28.6, 28.5, 28.4, 28.1, 28.0, 25.7, 25.0, 24.5, 19.6. IR ν_{max} (KBr) 3310, 2905, 1687, 1639, 1538, 1453, 1389, 1219. FAB MS m/z: 602 (MH^+); FAB HRMS calcd for $C_{28}H_{52}N_5O_9$ (MH^+) 602.3765, found 602.3784.

Synthesis of cyclo[Gln-Add]-Thr-NHMe (SIV.05-06, 09)

A mixture of Boc-Gln-Add(OH)-Thr(tBu)-NHMe (0.30 mmol, 0.185 g) and DMF (1.0 mL) was chilled (- 15 °C) under nitrogen. To the mixture was

added DCC (0.46 mmol, 0.094 g). After 15 min at - 15 °C, the mixture was treated with a solution of pentafluorophenol (0.76 mmol, 0.14 g) in AcOEt (0.15 mL), and the reaction was allowed to proceed for 30 min at - 15 °C and another 12 hours at 20 °C. After the solvent was removed under reduced pressure, a solid material containing DCU was obtained. The pentafluorophenyl ester was extracted by suspension of the solid material in AcOEt followed by removal of the solid by filtration. Additional pentafluorophenyl ester was recovered by recrystallizing the solid in warm AcOEt/$CHCl_3$ and retaining the liquid phase. The organic layers were pooled and a pale yellow residue was obtained upon removal of the solvent under reduced pressure. The pentafluorophenyl ester was obtained as a white solid (0.233 g, with trace DCU impurities) following crystallization in 1/1 : ether/hexanes and filtration: TLC R_f 0.28 ($CHCl_3$/MeOH/AcOH : 95/5/3).

To a heterogeneous mixture of the protected compound Boc-Gln-Add(OPfp)-Thr(tBu)-NHMe (0.13 mmol, 0.10 g) and CH_2Cl_2 (5 mL) was added TFA (5 mL) with dissolving of the solid material. The homogeneous mixture was allowed to stir 1.75 hours at 20 °C. After the solvents were removed under a stream of nitrogen, additional CH_2Cl_2 (2 x 30 mL) was added and removed under reduced pressure to assist in removing excess TFA. The residue obtained was stored under reduced pressure for 4 hours.

The residue was then chilled (0 °C) under nitrogen and dissolved in chilled (0 °C), freshly distilled DMF (125 mL). After 15 min at 0 °C, the mixture was allowed to warm to 4 - 6 °C and stir for 6 days. A 0.64 M TEA solution was prepared from freshly distilled TEA (0.089 mL) and freshly distilled DMF (0.911 mL). After the first 24 hours, the reaction mixture was treated at 24 hours intervals with 0.050 mL of the TEA solution (0.032 mmol TEA). The progress of the reaction was monitored by RP HPLC (analytical, 10

→ 80% MeCN/H_2O, 0.1% TFA over 25 min., retention time 9.4 min). The solvent was removed under reduced pressure. A solid material (0.065 g) was obtained after the residue was suspended in and centrifuged out of ether (three times) to assist in crystallization and removal of pentafluorophenol. The crude material was fractionated in batches of 17 mg with a pre-packed reversed phase (C_{18}) column (Waters, SepPak) employing a gradient elution of 0 → 40% MeCN/H_2O. The cyclic compound eluted in the range of 5 → 12% MeCN/H_2O. After removal of solvent by lyophilization, the purified cyclic compound was obtained as a fluffy white powder (0.048 g, 74%): mp 287 - 290 °C dec., analytical HPLC (10 → 80% MeCN/H_2O, 0.1% TFA over 25 min.) retention time 9.4 min, R_f 0.19 ($CHCl_3$/MeOH/AcOH : 85/15/3); ^{1}H-NMR δ_H (300 MHz, DMSO-d_6) 8.31 (d, 1H, J = 9.0 Hz, NH), 7.74 (d, 1H, J = 5.1 Hz, N*H*-Me), 7.66 (d, 1H, J = 9.0 Hz, NH), 7.63 (d, 1H, J = 9.0 Hz, NH), 7.02 (d, 2H, J = 150 Hz, Gln NH_2^{δ}), 4.85 (br s, 1H, Thr OH), 4.35 (m, 2H, two CH^{α}), 4.10 (dd, 1H, J = 8.6, 5.0 Hz, CH^{α}), 3.90 (m, 1H, Thr CH^{β}), 2.57 (d, 3H, J = 4.9 Hz, N-CH_3), 2.10, 1.90 (m,m, 2H, Add CH_2^{β}), 2.04 (t, 2H, J = 7.9 Hz, Add CH_2^{θ}), 1.90, 1.68 (m,m, 2H, Gln CH_2^{γ}), 1.68 - 1.05 (m, 12H, five Add CH_2 and Gln CH_2^{β}), 0.98 (d, 3H, J = 6.0 Hz, Thr CH_3^{γ}). FAB MS m/z: 442 (MH^+); FAB HRMS calcd for $C_{20}H_{36}N_5O_6$ (MH^+) 442.2666, found 442.2691.

*Synthesis of cyclo[Amb-Add]-Thr-NHMe (**4**, SIV.13)*

A heterogeneous mixture of the cyclic compound *cyclo*[Gln-Add]-Thr-NHMe (0.017 mmol, 7.6 mg) in 2/1: MeCN/H_2O (0.10 mL) was treated at 20 °C with [bis(trifluoroacetoxy)iodo]benzene (0.026 mmol, 11.0 mg). The reaction was allowed to proceed at 20 °C for 1 hour and was warmed to 50 °C for 15 min. After more 2/1 : MeCN/H_2O (0.020 mL) was added, the mixture was allowed another 3.5 hours at 50 °C. The mixture was then treated with an

additional portion of [bis(trifluoroacetoxy)iodo]benzene (0.0093 mmol, 4.0 mg) and 2/1 : MeCN/H_2O (0.060 mL) and warmed (50 °C) for 2 hours more. To the cooled mixture was added 0.1 M HCl (1 mL). The acidic layer was washed with ether (3 x 1 mL) to remove [bis(trifluoroacetoxy)iodo]benzene and iodobenzene. A solid material was removed from the aqueous layer by centrifugation, and the crude compound was obtained following removal of the aqueous solvent by lyophilization. The crude solid was fractionated with a pre-packed reversed phase (C_{18}) column (Waters SepPak) employing a gradient elution of 0 → 20% MeCN/H_2O. The cyclic compound eluted in the range of 5 → 7.5% MeCN/H_2O. After removal of the solvent by lyophilization, the purified cyclic compound was obtained as a fluffy white powder (3.1 mg, 44%): mp 245.5 - 247.5 °C dec., analytical HPLC (10 → 80% MeCN/H_2O, 0.1% TFA over 25 min.) retention time 8.5 min, R_f 0.39 ($CHCl_3$/MeOH/AcOH : 6/4/1); ^{1}H-NMR δ_H (300 MHz, DMSO-d_6) 8.43 (d, 1H, J = 8.4 Hz, NH), 7.74 (m, 6H, three NH and NH_3^+), 4.85 (d, 1H, J = 5.5 Hz, Thr OH), 4.43 (m, 2H, two CH^{α}), 4.10 (dd, 1H, J = 8.3, 4.1 Hz, CH^{α}), 3.92 (m, 1H, Thr CH^{β}), 2.75 (t, 2H, J = 10.7 Hz, Dab CH_2^{γ}), 2.57 (d, 3H, J = 5.2 Hz, N-CH_3), 2.29, 1.80 (m,m, 2H, Add CH_2^{β}), 1.97 (m, 4H, Add CH_2^{θ} and Dab CH_2^{β}), 1.65 - 1.20 (m, 10H, five Add CH_2), 0.98 (d, 3H, J = 6.4 Hz, Thr CH_3^{γ}). FAB MS m/z: 414 (MH^+); FAB HRMS calcd for $C_{19}H_{36}N_5O_5$ (MH^+) 414.2716, found 414.2716.

4.6 References

1. Silverman, R. B. in *Enzyme Inhibition and Inactivation*; Academic Press, Inc., San Diego, 1992; pp 147-218.

2. Endo, A. "Compactin (ML-236B) and Related Compounds as Potential Cholesterol-Lowering Agents That Inhibit HMG-CoA Reductase," *J. Med. Chem.* **1985**, *28*, 401-405.

3. Endo, A.; Hasumi, K. "HMG-CoA Reductase Inhibitors," *Natural Product Reports* **1993**, *10*, 541-549.

4. Hasumi, K.; Yamada, A.; Shimizu, Y.; Endo, A. "Overaccumulation of 3-Hydroxy-3Methylglutaryl-Coenzyme-A Reductase in a Compactin (ML-236B)-Resistant Mouse-Cell Line With Defects in the Regulation of its Activity," *Eur. J. Biochem.* **1987**, *164*, 547-552.

5. Opdenakker, G.; Rudd, P. M.; Ponting, C. P.; Dwek, R. A. "Concepts and Principles of Glycobiology," *Faseb J.* **1993**, *7*, 1330-1337.

6. Varki, A. "Biological Roles of Oligosaccharides: All of the Theories are Correct," *Glycobiology* **1993**, *3*, 97-130.

7. Dwek, R. A. "Glycobiology: More Functions for Oligosaccharides" *Science* **1995**, *269*, 1234-1235.

8. Wyss, D. F.; Choi, J. S.; Li, J.; Knoppers, M. H.; Willis, K. J.; Arulanandam, A. R. N.; Smolyar, A.; Reinherz, E. L.; Wagner, G. "Conformation and Function of the N-Linked Glycan in the Adhesion Domain of Human CD2," *Science* **1995**, *269*, 1273-1278.

9. Scheiffele, P.; Peranen, J.; Simons, K. "N-Glycans as Apical Sorting Signals in Epithelial Cells," *Nature* **1995**, *378*, 96-98.

10. Hubbard, S. C.; Ivatt, R. J. "Synthesis and Processing of Asparagine-Linked Oligosaccharides" *Ann. Rev. Biochem.* **1981**, *50*, 555-583.

11. Jentoft, N. "Why are Proteins O-Glycosylated?" *Trends in Biochemical Sciences* **1990**, *15*, 291-294.

12. Jacob, G. S. "Glycosylation Inhibitors in Biology and Medicine," *Curr. Opin. Struct. Biol.* **1995**, *5*, 605-611.

13. Hirschberg, C. B.; Snider, M. D. "Topography of Glycosylation in the Rough Endoplasmic Reticulum and Golgi Apparatus," *Ann. Rev. Biochem.* **1987**, *56*, 63-87.

14. Elbein, A. D. "Inhibitors of the Biosynthesis and Processing of *N*-Linked Oligosaccharide Chains," *Ann. Rev. Biochem.* **1987**, *56*, 497-534.

15. Kaushal, G. P.; Elbein, A. D. "Glycosidase Inhibitors in Study of Glycoconjugates," *Meth. Enzymol.* **1994**, *230*, 316-329.

16. Paulson, J. C.; Colley, K. J. "Glycosyltransferases: Structure, Localization, and Control of Cell Type-Specific Glycosylation," *J. Biol. Chem.* **1989**, *264*, 17615-17618.

17. Roseman, S. "The Synthesis of Complex Carbohydrates by Multiglycosyltransferase Systems and Their Potential Function in Intercellular Adhesion," *Chem. Phys. Lipids* **1970**, *5*, 270-297.

18. Gleeson, P. A.; Teasdale, R. D.; Burke, J. "Targeting of Proteins to the Golgi Apparatus," *Glycoconjugate J.* **1994**, *11*, 381-394.

19. Elbein, A. D. "The Tunicamycins-Useful Tools For Studies on Glycoproteins," *Trends in Biochemical Sciences* **1981**, *6*, 291-293.

20. Tamura, G. *Tunicamycin*; Japan Scientific Society Press: 1982.

21. Keller, R. K.; Boon, D. Y.; Crum, F. C. "*N*-Acetylglucosamine-1-Phosphate Transferae from Hen Oviduct: Solubilization, Characterization, and Inhibition by Tunicamycin," *Biochemistry* **1979**, *18*, 3946-3952.

22. Rathod, P. K. ;. Tashjian, A. H. Jr.; Abeles, R. H. "Incorporation of β-Fluoroasparagine into Peptides Prevents N-Linked Glycosylation," *J. Biol. Chem.* **1986**, *261*, 6461-6469.

23. Imperiali, B.; Shannon, K. L.; Unno, M.; Rickert, K. W. "A Mechanistic Proposal for Asparagine-Linked Glycosylation," *J. Am. Chem. Soc.* **1992**, *114*, 7944-7945.

24. Pathak, R.; Parker, C. S.; Imperiali, B. "The Essential Yeast NLT1 Gene Encodes the 64kDa Glycoprotein Subunit of the Oligosaccharyl Transferase," *FEBS Lett.* **1995**, *362*, 229-234.

25. Goss, P. E.; Baker, M. A.; Carver, J. P.; Dennis, J. W. "Inhibitors of Carbohydrate Processing: A New Class of Anticancer Agents," *Clinical Cancer Research* **1995**, *1*, 935-944.

26. Imperiali, B.; Spencer, J. R.; Struthers, M. D. "Structural and Functional Characterization of a Constrained Asx-Turn Motif," *J. Am. Chem. Soc.* **1994**, *116*, 8424-8425.

27. Gavel, Y.; von Heijne, G. "Sequence Differences Between Glycosylated and Non-glycosylated Asn-X-Thr/Ser Acceptor Sites: Implications for Protein Engineering," *Protein Eng.* **1990**, *3*, 433-442.

28. Virgilio, A. A.; Ellman, J. A. "Simultaneous Solid-Phase Synthesis of β-Turn Mimetics Incorporating Side-Chain Functionality," *J. Am. Chem. Soc.* **1994**, *116*, 11580-11581.

29. Barker, P. L.; Bullens, S.; Bunting, S.; Burdick, D. J.; Chan, K. S.; Deisher, T.; Eigenbrot, C.; Gadek, T. R.; Gantzos, R.; Lipari, M. T.; Muir, C. D.; Napier, M. A.; Pitti, R. M.; Padua, A.; Quan, C.; Stanley, M.; Struble, M.; Tom, J. Y. K.; Burnier, J. P. "Cyclic RGD Peptide Analogues as Antiplatelet Antithrombotics," *J. Med. Chem.* **1992**, *35*, 2040-2048.

30. Burgess, K.; Ho, K. "Assymetric Syntheses of all 4 Stereoisomers of 2,3-Methanomethionine," *J. Org. Chem.* **1992**, *57*, 5931-5936.

31. Imperiali, B.; Shannon, K. L. "Differences Between Asn-Xaa-Thr Containing Peptides: A Comparison of Solution Conformationand Substrate Behavior with Oligosaccharyltransferase" *Biochemistry* **1991**, *30*, 4374-4380.

32. Morrsion, J. F.; Walsh, C. T. "The behavior and significance of slow-binding enzyme-inhibitors" *Adv. Enzymol.* **1988**, *61*, 201-301.

33. Segel, I. H. *Enzyme Kinetics*; John Wiley and Sons: New York, 1975.

34. Cha, S. "Tight Binding Inhibitors - 1" *Biochem. Pharmacol.* **1975**, *24*, 2177-2185.

35. Imperiali, B.; Hendrickson, T. L. "Asparagine-Linked Glycosylation: Specificity and Function of *Oligosaccharyl Transferase*" *Bioorg. Med. Chem.* **1995**, *3*, 1565-1578.

36. Wang, Y.; Abernathy, J. L.; Eckhardt, A. E.; Hill, R. L. "Purification and Characterization of UDP-N-acetylgalatosamine:polypeptide N-acetylgalactosaminyltransferase Specific for Glycosylation of Threonine Residues" *J. Biol. Chem.* **1992**, *267*, 12709-12716.

37. Lam, K. S.; Salmon, S. E.; Hersh, E. M.; Hruby, V. J.; Karmierski, W. M.; Knapp, R. J. "A New Type of Synthetic Peptide Library for Identifying Ligand-Binding Activity" *Nature* **1991**, *354*, 82-83.

38. Houghten, R. A.; Pinilla, C.; Blondelle, S. E.; Appel, J. R.; Dooley, C. T.; Cuervo, J. H. "Generation and Use of Synthetic Peptide Combinatorial Libraries for Basic Research and Drug Discovery" *Nature* **1991**, *354*, 84-86.

39. Gallop, M. A.; Barrett, R. W.; Dower, W. J.; Fodor, S. P. A.; Gordon, E. M. "Applications of Combinatorial Technologies to Drug Discovery. 1. Background and Peptide Combinatorial Libraries" *J. Med. Chem.* **1994**, *37*, 1233-1251.

40. Pathak, R.; Hendrickson, T. L.; Imperiali, B. "Sulfhydryl Modification of the Yeast Wbp1p Inhibits Oligosaccharyl Transferase Activity" *Biochemistry* **1995**, *34*, 4179-4185.

41. Imperiali, B.; Zimmerman, J. W. "Synthesis of Dolichylpyrophosphate-Linked Oligosaccharides" *Tetrahedron Lett.* **1990**, *31*, 6485-6488.

Chapter 5. Affinity Labels for Oligosaccharyl Transferase: Future Directions

5.1 Introduction

The 20 natural amino acids provide enzymes with different reactive functionalities which are used to construct the catalytic machinery of enzymes. As demonstrated in chapter two, these amino acid side chains can often be identified and localized to an enzyme active site through the use of nonspecific chemical modification reagents. A related and frequently more powerful approach is to synthetically introduce an electophilic site into a natural substrate to generate a selective affinity label. Affinity labels are compounds which resemble the natural substrate sufficiently to bind to the enzyme active site with near native affinity. However, the introduction of an electrophilic moiety provides the opportunity for alkylation of a reactive amino acid within the enzyme active site.[1] When combined with site-directed mutagenesis or digestion by limited proteolysis and sequencing of the modified protein, affinity labels can often be used to identify amino acids which are directly involved in enzyme-mediated catalysis.

In the design of affinity labels, the most common form of modification includes the introduction of a halo- or diazo-ketone as the reactive electrophile; these modifications produce labels which are ideal for the identification of active site bases or nucleophiles. For example, 3-bromo, 3-chloro and 3-iodo-1-hydroxy-2-propanone phosphate (Figure 5-1, **1**), halogenated analogs of the substrate dihydroxyacetone phosphate (Figure 5-1, **2**), were used to characterize triosephosphate isomerase (TIM).[2] These three compounds irreversibly inactivated the enzyme; the site of alkylation was identified as a highly reactive glutamate (Glu-165) and it was later confirmed that this residue is directly involved in TIM mediated catalysis.[3] Similarly, the compound 6-diazo-5-oxonorleucine (Figure 5-1, DON, **3**) has been used to characterize several of a family of amidotransferases which catalyze the

transfer of ammonia from glutamine to other substrates.[4] DON is a direct analog of glutamine (Figure 5-1, **4**) wherein the carboxamide side chain has been replaced by a reactive diazoketone; it irreversibly inactivates many of these enzymes by alkylating a crucial cysteine residue.[5, 6] Figure 5-1 shows the chemical structure of each of these inactivators adjacent to the relevant substrate; the effectiveness of these labels can be directly attributed to their structural similarity to the corresponding substrate.

Triosephosphate Isomerase

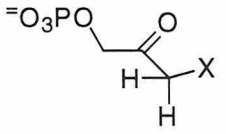

Affinity Label
X = Br, Cl, I
3-Halo-1-hydroxy-2-propanone phosphate
1

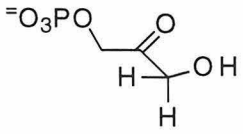

Substrate
Dihydroxyacetone phosphate
2

Glutamine Amidotransferases

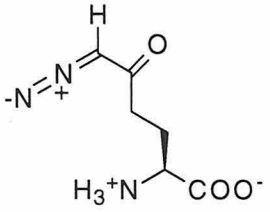

Affinity Label
6-Diazo-5-oxonorleucine (DON)
3

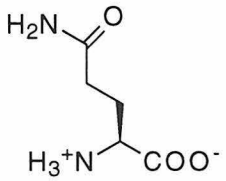

Substrate
Glutamine
4

Figure 5-1. Structural Similarities Between Substrates and Affinity Labels for Two Different Enzyme Systems.

Modification of oligosaccharyl transferase by peptide affinity labels has been attempted and reported in the literature on two occasions with mixed results. Lennarz and coworkers synthesized a tripeptide photoaffinity label based on the OT substrate Ac-Asn-Xaa-Thr-NHMe.[7] In their label, Xaa consisted of a lysine residue which had been modified at the ε-amino group with *p*-azidobenzoic acid (**5**). Upon irradiation at 254 nm to generate the reactive nitrene, this compound selectively modified one protein within the endoplasmic reticulum. However, further scrutiny revealed that protein disulfide isomerase had been targeted and identified instead of OT.[8]

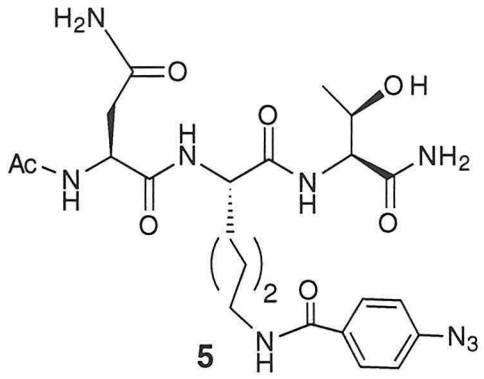

5

Although *p*-azidobenzoyl groups are frequently used as photoaffinity labels, the placement of this moiety in **5** has several drawbacks which, when considered together, significantly decrease the chances of selectively modifying OT. First, the consensus sequence for OT is -Asn-Xaa-Thr/Ser- with very little sequence specificity for the central amino acid. Thus, the photoreactive functionality of **5** is placed in a position which does not appear to specifically interact with the OT peptide binding site. Second, tripeptides with an acetylated *N*-terminus typically exhibit poor affinities for OT.[9] In addition, the use of a lysine side chain further lengthens the distance between the enzyme binding site and the photolabile group. The stringent sequence

specificity of OT and the bulky nature of the *p*-azidobenzoyl group preclude the positioning of this moiety in place of the asparagine or threonine residues of the consensus sequence.

A second affinity label for OT has been reported which replaces the threonine residue in the consensus sequence with an epoxide ring to yield Arg-Asn-Gly-Asn-Gly-Vepx-Ala-Val-OMe (**6**, Vepx = vinyl glycine based epoxide).[10] The epoxide moiety was introduced into the peptide by oxidative treatment with *m*-chloroperoxybenzoic acid (*m*-CPBA). This modification is significantly more specific than that of **5**, in that the reactive group is placed in one of the two positions of high sequence selectivity and it introduces only minimal structural perturbations. Time dependent inhibition of oligosaccharyl transferase was observed when OT was treated with an impure form of this peptide. Further attempts to purify and characterize the inhibitor resulted in peptide cleavage on the *C*-terminal side of the epoxide ring; the possibility that inhibition was being induced by a contaminant, such as *m*-CPBA, was never eliminated.

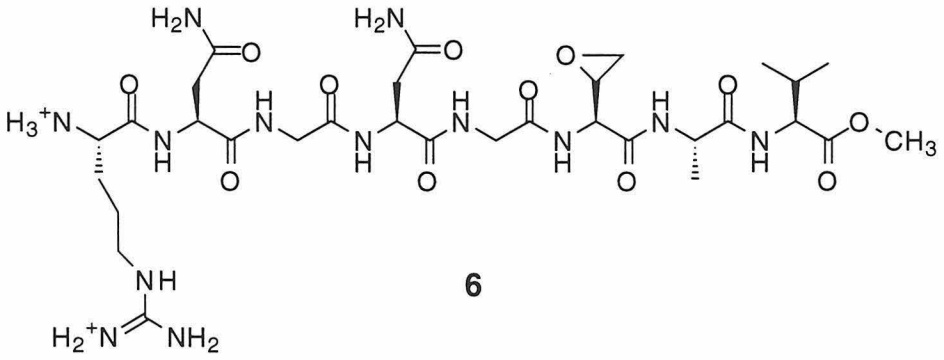

6

Currently, the favored mechanism for oligosaccharyl transferase catalyzed protein glycosylation (see chapter one) involves deprotonation of an asparagine side chain by an active site base (Figure 5-2).[11] Based on this

mechanism, successful glycosylation would occur only if this putative base is in direct proximity to the asparagine side chain during the catalytic process. As of yet, affinity labels which have been designed to probe this region have not been reported. Tripeptide affinity labels, which incorporate electrophilic modifications into the asparagine side chain of the consensus sequence, are ideal compounds to facilitate the investigation and identification of this active site base.

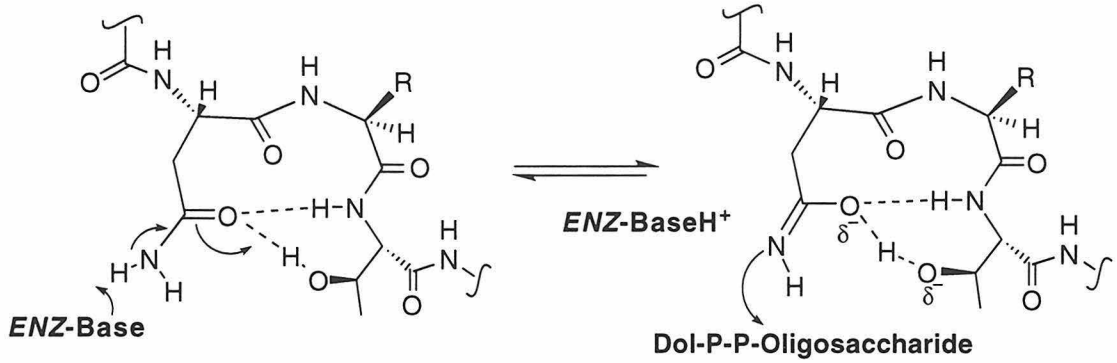

Figure 5-2. Proposed Mechanism of Action of Oligosaccharyl Transferase with Positioning of an Active Site Base Near the Asparagine Side Chain.

This chapter describes the design and investigation of several different peptidyl affinity labels for oligosaccharyl transferase which may be divided into three separate groups: α-methyl substituted ketones, epoxides and peptides incorporating an organomercurial functionality. The synthesis of the α-methyl ketone analogs proved futile because the introduction of electrophilic groups to the side chain of asparagine resulted in side chain to main chain cyclization. This cyclization generated peptides which were no longer effective analogs of the consensus sequence and were therefore no longer potential affinity labels. The second series of affinity labels (epoxides)

was prepared and kinetically evaluated without success; however, these compounds contained less conservative structural modifications and less reactive electrophilic centers than the original designs. The third set of affinity labels (organomercurial containing peptides) were prepared and evaluated. These compounds were unsuccessful as affinity labels of OT. However, the reactivity of this type of compound is limited by being highly specific for cysteine residues. Finally, a discussion has been included which addresses possible explanations for the lack of reactivity of residues within the peptide binding site as well as prospects for the synthesis of more potent affinity labels.

5.2 Results and Discussion

5.2.1 Analogs of -Asn-Xaa-Thr-: α-Methyl Ketone Substituted Affinity Labels

Initially, three different synthetic targets were chosen as potential affinity labels for OT. Compounds **7**, **8**, and **9** are all analogs of the substrate Bz-Asn-Leu-Thr-NHMe (**10**) which have been modified at the asparagine carboxamide to contain an α-diazomethyl, an α-chloromethyl or an α-fluoromethyl ketone as a reactive electrophilic group.

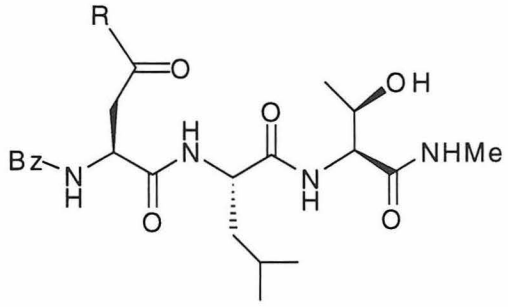

7: R = CHN_2
8: R = CH_2Cl
9: R = CH_2F

10: R = NH_2

The proposed synthesis for each of these tripeptides is shown in Figure 5-3. Bz-Asp-Leu-Thr-NHMe (**11**) was treated with oxalyl chloride to yield the aspartic acid chloride **12**. It was predicted that this reactive tripeptide could be treated with diazomethane to yield **7**[12] which could be quenched with chloride ions or pyridinium poly (HF)[13] to afford the two halomethyl ketones **8** and **9**, respectively. Analysis of the oxalyl chloride reaction revealed that **12** underwent cyclization with the peptide backbone to form the succinimide **13** in greater than 35% yield. In addition to **13**, several other side products were observed which most likely result from further hydrolysis of the succinimide. Treatment of this reaction mixture with diazomethane did not induce the formation of **7**.

The ability of asparagine and aspartic acid side chains to cyclize with the peptide backbone has been well documented in the literature and has been implicated in the normal aging process of proteins.[14, 15] This process often results in the deamidation of asparagine and the generation of aspartatic acid and isoaspartic acid containing peptides. In nature, this structural breakdown occurs slowly with peptides often having half lives of years.[14] Activation of the aspartic acid side chain to generate **12** appears to have greatly accelerated this process, inducing rapid cyclization in high yields, thereby prohibiting the formation of **7**, **8** and **9**. In addition, it is probable that if peptides **7**, **8** and **9** could be prepared without the intermediacy of **12**, they would immediately cyclize to form six-membered rings (rather than the five-membered succinimide ring formed from the acid chloride). Regardless, these cyclic compounds are not potential affinity labels as they no longer resemble the substrate **10** and the electrophilic center has been removed.

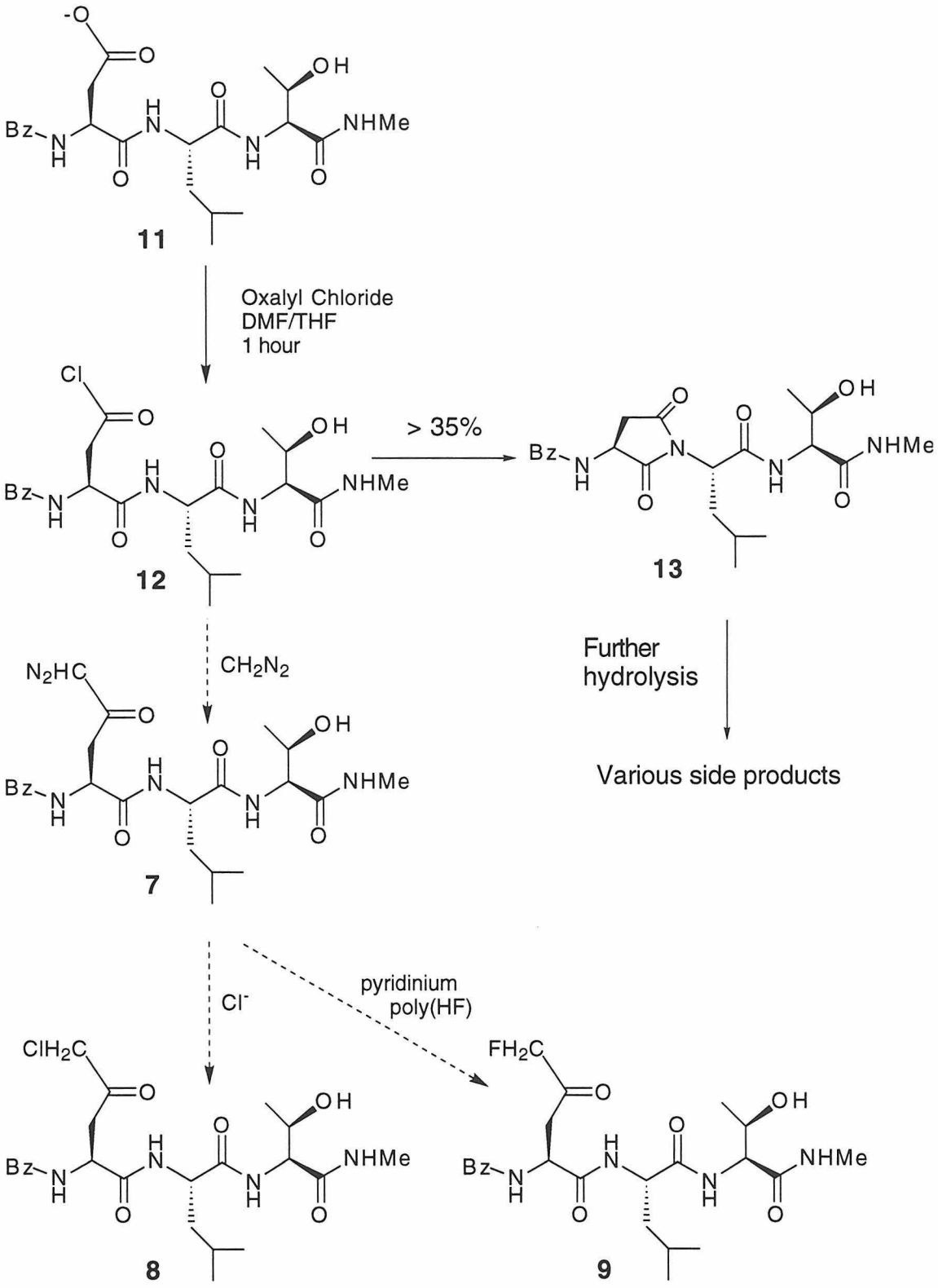

Figure 5-3. Synthetic Scheme for Affinity Labels **7**, **8**, and **9**.

5.2.2 Analogs of -Asn-Xaa-Thr-: Epoxide Affinity Labels

Because of the problems encountered during the synthesis of **7**, **8** and **9**, a new family of potential affinity labels, containing an epoxide as the electrophile, was designed and evaluated. Typically, epoxides are less reactive than the corresponding acid halides and α-substituted ketones discussed above and are therefore less potent as affinity labelling reagents. However, they are readily synthesized and are still reactive towards strong nucleophiles such as the thiol group of cysteine or the ε-amino group of lysine. In the design of affinity labels for OT, where the electrophile needs to be incorporated into an amino acid side chain, it was believed that the less reactive epoxide moiety would prove to be an asset by prohibiting unfavorable cyclizations between the peptide backbone and the electrophilic amino acid side chain.

Four epoxide peptides were selected for the initial investigations with oligosaccharyl transferase (**14** - **17**). Each of these peptides contains an epoxy amino acid in place of the asparagine or threonine residue in the OT consensus sequence (-Asn-Xaa-Thr-). Two different amino acids were selected (Epx and Vepx) with side chains that differ by only one methylene group. It was predicted that by using both of these amino acids in similar peptide affinity labels, slightly different regions of the enzyme's peptide binding site could be investigated; this could substantially increase the chance of successful enzyme inactivation by one of the compounds. To introduce the epoxides, the non-natural amino acids allyl glycine and vinyl glycine were chosen to be synthetically incorporated into the desired position of the peptide sequence. Oxidation of these residues would generate the two epoxide amino acids, in a mixture of diastereomers (Epx and Vepx, respectively).

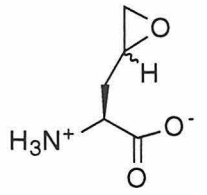

Epx

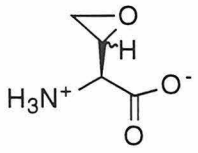

Vepx

The first three inhibitors were designed to examine the asparagine position of the consensus sequence. Bz-Epx-Leu-Thr-NHMe (**14**) is a direct analog of the tripeptide substrate Bz-Asn-Leu-Thr-NHMe (**10**). Ac-Ser-Phe-Epx-Leu-Thr-Val-Thr-NH2 (**15**) contains the consensus sequence flanked by four amino acids (two on each side); these residues were selected based on the statistical analysis of Gavel and von Heijne[16] and were chosen to enhance recognition of the inhibitor by OT. Finally, Bz-Vepx-Leu-Thr-Phe-OMe (**16**) was prepared in case the active site base is not appropriately positioned to react with **14**. The fourth epoxide peptide contains a more conservative modification which replaces the required threonine with Vepx (Bz-Asn-Leu-Vepx-Phe-OMe, **17**); this peptide was designed to reexamine the previously reported inhibition of OT by **6**.[10]

Prior to oxidation, the precursor peptides to **14**, **16** and **17** were prepared through standard solution phase synthesis protocols; the precursor to peptide **15** was prepared by solid phase synthesis methods. Two different methods for the oxidation of the allyl glycine and vinyl glycine residues were evaluated. Initially, *m*-CPBA was utilized as described by Bause.[10] This method presented two complications. During *m*-CPBA oxidation to generate **15**, the peptide fragment Leu-Thr-Val-Thr-NH_2, where the *N*-terminal amine of the leucine had been oxidized, was isolated indicating that peptide backbone cleavage had occurred. Cleavage of the peptide backbone appeared to progress

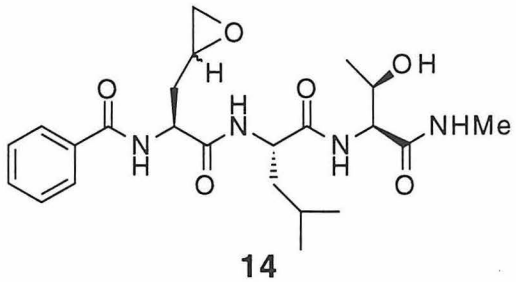

14

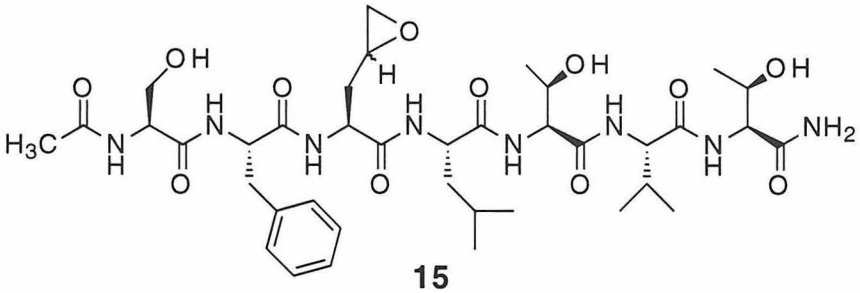

15

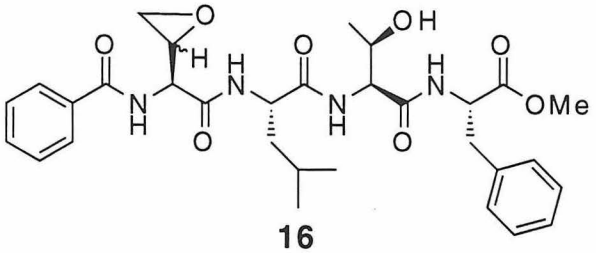

16

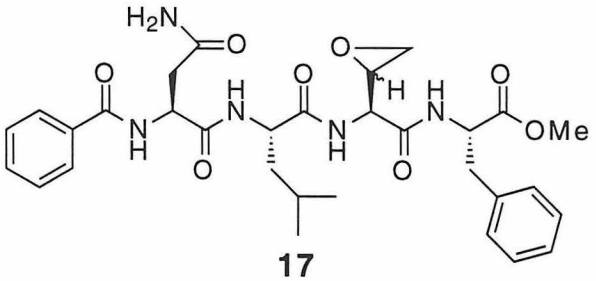

17

during purification, similar to the breakdown reported by Bause.[10] Kinetic evaluation of the impure peptide was hindered by the presence of intact *m*-CPBA which effectively inactivates the enzyme (presumably by oxidizing the cysteine residue in the sugar substrate binding site, see chapter two). Because of this complication, dimethyldioxirane (DMDO),[17, 18] which decomposes to acetone during purification,[19] was examined as an alternative oxidant. The conditions for DMDO oxidation are neutral and mild and, in each case, the reaction proceeded in nearly quantitative yield to produce pure product.

Peptides **14 - 17** were evaluated as inhibitors of oligosaccharyl transferase. Each epoxide was combined with the enzyme (prior to addition of the substrate **10**) and the enzyme was analyzed for activity after several different incubation times. To maximize potential inactivation, the inhibitors were examined at high concentrations (2.5 mM - 5.0 mM) relative to the competing substrate **10** (200 μM). The rate of inactivation was determined by comparing the OT activity of these enzyme mixtures to an analogous control experiment that did not contain any of the inhibitors. In each case, the enzyme activity remained constant over time, indicating that the epoxide inhibitors do not effectively inactivate OT. Figure 5-4 shows a comparison of the rates obtained when OT was treated with peptide **15** versus the relevant control; nearly identical results were obtained with the other three epoxide peptides (**14**, **16** and **17**).

The most remarkable result obtained from this series of inhibitors was the inability of **17** to inactivate the enzyme. This peptide contained a Vepx residue in place of the threonine, a conservative modification which has been previously reported to result in the inactivation of OT.[10] However, in a direct contradiction to the previous report, **17** did not inactivate the enzyme. The

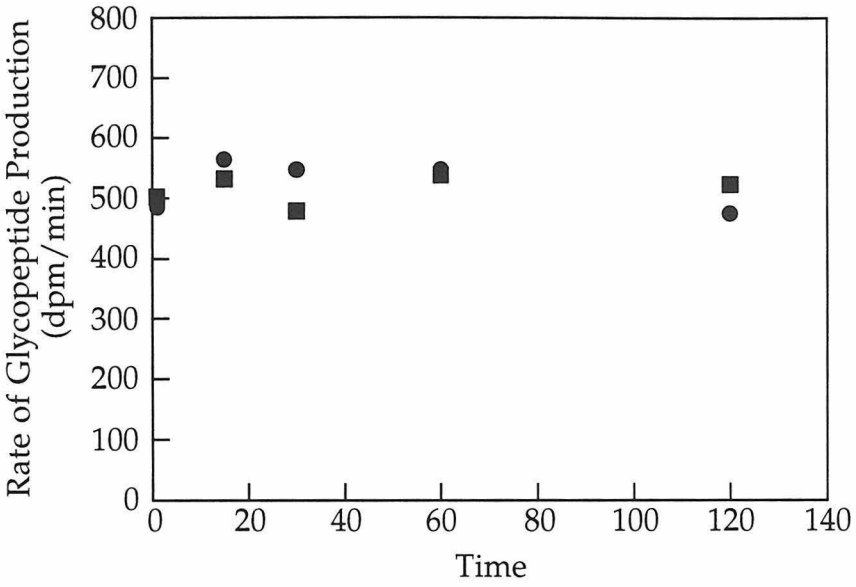

Figure 5-4. Treatment of OT with Epoxide Peptide **15** (■, 2.5 mM **15** during preincubation; ●, control, no inhibitor).

compound examined by Bause (**6**) was utilized in an impure form immediately following oxidation; one possible explanation for the earlier results is that inactivation was induced by residual *m*-CPBA and not by alkylation of an active site nucleophile upon epoxide ring opening. This hypothesis is supported by the observation that treatment of OT with pure *m*-CPBA does result in a substantial loss in enzyme activity over time. A reexamination of the precise peptide sequence previously evaluated, using DMDO as the oxidant, would need to be accomplished to confirm this hypothesis.

The epoxide peptides proved disappointing as affinity labels for OT; however, these results suggest that the previous claims are not valid. Most importantly, Epx and Vepx are not good analogs of asparagine and it is therefore likely that they are not bound by OT with appreciable affinity. In addition, the epoxide is not highly reactive and ring opening would most likely only occur if a cysteine or a highly nucleophilic lysine was present in the peptide binding site, a possibility that is not supported by the results of the chemical modification studies presented in chapter two. The lack of reactivity of these epoxide affinity labels towards OT does not rule out the presence of a histidine or an aspartic or glutamic acid as the active site base.

5.2.3 Analogs of -Asn-Xaa-Thr-: *S*-Mercury Affinity Labels

One final series of potential affinity labels was prepared based on a report that cysteine residues could be modified by compounds which contain an appropriately positioned organomercurial group ($R\text{-}S\text{-}Hg^{+}$).[20] When incubated with an enzyme, the high affinity of mercury for sulfur can induce a reaction with cysteine side chains to form R-S-Hg-S-Cys-Enz. Competition studies can be used to determine whether the cysteine side chain resides in

the enzyme active site. Two peptides were chosen to test against OT, in which either the asparagine or the threonine of the consensus triad was replaced with a cysteine. These peptides were synthesized through standard solid phase synthesis procedures and, following cleavage and purification, treated with mercuric nitrate to generate **18** and **19**.

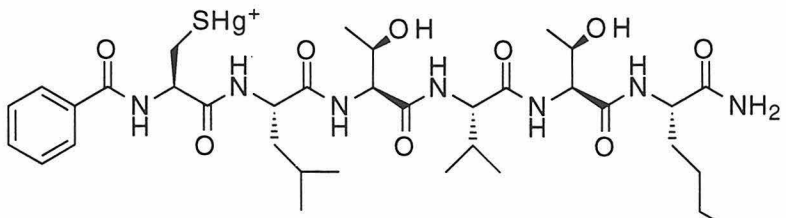

18

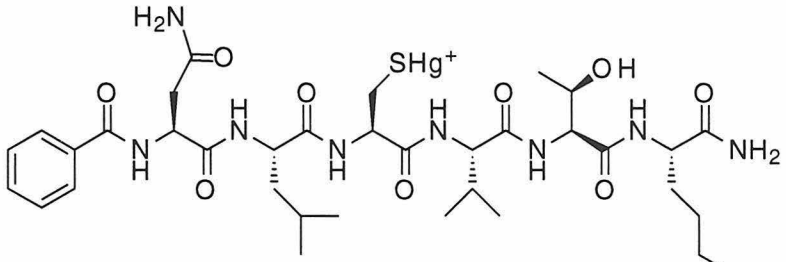

19

Peptides **18** and **19** were evaluated as potential inhibitors of oligosaccharyl transferase. Competing interactions between chloride anions and the mercury cation in each peptide were observed to interfere with the ability of these compounds to react with enzymic cysteine residues by the formation of R-S-HgCl. Thus, following an initial evaluation, an OT preparation was developed which contained dramatically decreased levels of chloride anions. This enzyme source was used for all further studies.

Inhibition of OT activity was observed when the enzyme was treated with each mercury peptide; however, enzyme activity did not decrease with

time and different preparations of the peptides produced dramatic variations in the degree of inhibition observed. Further evaluation revealed that this inhibition was due to competition for the manganese binding site by residual mercury (II) nitrate and not the direct result of the mercury-containing peptides. Again, the fact that these peptides were ineffective as affinity labels is not surprising as peptides **18** and **19** do not closely mimic the consensus triad and therefore may not even be recognized by OT. Additionally, this type of affinity label is designed to specifically target cysteine side chains and the chemical modification studies presented in chapter two strongly suggest that a reactive cysteine is not located in or near the peptide binding site of OT.

5.3 Conclusions and Future Directions

The design and evaluation of nine different affinity labels has been accomplished. Of the inhibitors that were successfully prepared, none produced a significant decrease in OT activity, even when examined at elevated concentrations. Unfortunately, these compounds were all limited in reactivity and their final structures were significantly removed from that of the consensus sequence normally recognized by OT.[21] With the high degree of substrate specificity exhibited by OT,[22] it is not surprising that these compounds were unsuccessful as potential affinity labels. The α-substituted methyl ketone containing peptides **7**, **8** and **9** were the most promising of the affinity labels considered. Their structures contained straightforward and subtle modifications based on the simple substrate **10**. However, these compounds could not be prepared as described and therefore could not be evaluated kinetically. Further structural alterations would need to be considered to develop these peptide analogs into useful affinity labelling reagents.

It has recently been reported that the introduction of a constrained asx-turn into a peptide substrate for OT results in a tenfold enhancement in binding to the enzyme active site.[23] This cyclization has been incorporated into the design of the potent OT inhibitors discussed in chapter four and a solid phase method of synthesis for these compounds has been developed. This method of cyclization could be readily adapted to generate *cyclo*[SHex-Asp-Cys]-Thr-Val-Thr-Nph-NH_2 (**20**) as a precursor to several different affinity labels. The synthetic procedures shown in Figure 5-3 could be used to convert peptide **20** into constrained analogs of **7 - 9** (**21 - 23**, respectively). Steric hindrance caused by the cyclic constraint should eliminate or dramatically decrease succinimide formation, thereby making the preparation of these compounds feasible.

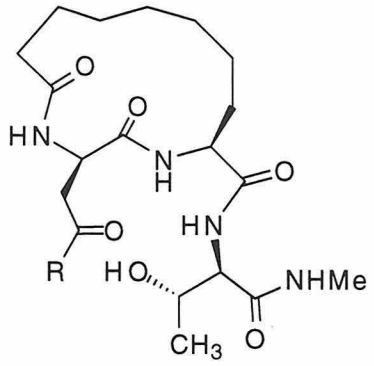

20: R = O^-
21: R = CHN_2
22: R = CH_2Cl
23: R = CH_2F

Cyclic peptides **21 - 23** offer the potential to be powerful affinity labels of oligosaccharyl transferase. These compounds more closely resemble the consensus sequence than any of the other labels designed and presented in this chapter. In addition, the electrophilic modification is located precisely in

the position of interest within the asparagine side chain. Thus, these compounds would be ideally suited to probe for the active site base shown in Figure 5-2.

Modification of this active site base has proven particularly challenging and its identity remains elusive. Chemical modification studies (chapter two) have failed to position any reactive residues within the peptide binding site and the more specific affinity labels have also been unable to provide new information. However, one additional possibility needs to be considered. It has been demonstrated that the required metal cofactor for asparagine-linked glycosylation is positioned in direct proximity to the asparagine carboxamide during catalysis (chapter three); this observation suggests that the divalent manganese may play a distinct role in mediating the glycosylation event. Could the elusive active site base be an activated metal bound water molecule? If this were the case, then irreversible modification of OT by an affinity label or a chemical modification reagent would not be observed because the modified water could be replaced by a new water molecule to regenerate active enzyme. Although unusual, catalytically competent water molecules have been observed in other enzymatic systems[1] and such a possibility is decidedly consistent with the failed attempts to covalently modify a base within the active site of oligosaccharyl transferase.

A metal bound water or hydroxide anion is an interesting mechanistic option that deserves scrutiny. Compounds **21 - 23** could also be used to examine this possibility by incubating these peptides in aqueous solution with and without OT. In the presence of OT, a reactive water or hydroxide ion would manifest itself by increasing the rate at which these peptides are converted to the α-hydroxy ketone. These rates could be readily determined by HPLC analysis of the aqueous peptide solutions. Such experiments could

shed a great deal of light on the mechanistic machinery of oligosaccharyl transferase.

5.4 Acknowledgements

Professor Barbara Imperiali prepared and evaluated the two vinyl glycine epoxide tetrapeptides **16** and **17**.

5.5 Experimental Methods

5.5.1 Analogs of Bz-Asp-Leu-Thr-NHMe - Halomethyl Ketone Affinity Labels

Boc-Leu-Thr-OMe

Boc-Leu-OH (1.4568 g, 5.8 mmol, 1 eq) and Thr-OMe (0.9895 g, 5.8 mmol, 1 eq) were dissolved in 29.2 mL THF. HOBT (5-hydroxybenzotriazole, 0.9416 g, 7.0 mmol, 1.2 eq), dicyclohexylcarbodiimide (DCC, 1.4362 g, 7.0 mmol, 1.2 eq) and triethylamine (1.2 mL, 8.7 mmol, 1.5 eq) were added to this solution. A precipitate of dicyclohexylurea formed and the reaction was left stirring overnight. The mixture was filtered and brought to dryness. Purification was afforded by silica gel chromatography in chloroform. Yield: 1.9559 g, 5.65 mmol, 97%. R_f 0.73 ($CHCl_3$/MeOH: 10/1). ^{1}H-NMR δ_H (500 MHz, $CDCl_3$): 6.85 (br s, 1H), 5.05 (br s, 1H), 4.62 (d, 1H), 4.35 (m, 1H), 4.13 (m, 1H), 3.77 (s, 3H), 1.74 (m, 2H), 1.45 (s, 9H), 1.23 (d, 3H), 0.95 (m, 6H).

Boc-Asp(OBn)-Leu-Thr-OMe

Boc-Leu-Thr-OMe (1.9559 g, 5.65 mmol) was dissolved in 20 mL methylene chloride with 8 mL trifluoroacetic acid. The solution was stirred for 1 hour until the amino terminus was completely deprotected. The solution was dried under a stream of nitrogen and lyophilized from water overnight to quantitatively yield the TFA salt of the dipeptide. This salt was

dissolved in 16 mL DMF. Triethylamine (1.7 mL, 1.8 eq) and the *p*-nitrophenyl ester of Boc-Asp-OH (Boc-Asp-OpNP, 3.3792 g, 7.6 mmol, 1.3 eq) and were added to the solution which was left stirring for 16 hours. The solvent was removed by distillation and the product was purified on a 3/7 ethyl acetate/hexane silica gel column. Yield: 2.5 g, 4.5 mmol, 68%. [Boc Asp-OpNP (0.800 g, 1.8 mmol, 32%) was recovered from the column.] R_f 0.23 ($CHCl_3$/MeOH: 20/1). ^{1}H-NMR δ_H (500 MHz, $CDCl_3$): 7.25(m, 5H), 6.95 (dd, 2H, J = 7.8 Hz), 5.54 (d, 1H, J = 8.5 Hz), 5.03 (s, 2H), 4.5 (dd, 1H), 4.45 (m, 2H), 4.2 (dd, 1H), 2.79 (m, 3H), 1.6 (m, 3H), 1.36 (s, 9H), 1.1 (d, 3H), 0.84, (dd, 6H).

Bz-Asp(OBn)-Leu-Thr-OMe

Boc-Asp(OBn)-Leu-Thr-OMe (0.9037 g, 1.64 mmol) was dissolved in 8 mL methylene chloride and 3 mL trifluoroacetic acid. The solution was stirred for 20 minutes then brought to dryness under a stream of nitrogen to yield a yellow oil. Twice, the oil was redissolved in a 10% toluene in methanol solution and brought to dryness. This step was repeated again with 100% methanol. The oil was dissolved in 8 mL DMF and benzoic anhydride (0.5085 g, 2.2 mmol, 1.4 eq) and triethylamine (425 µL, 3.05 mmol, 2.3 eq) were added. The reaction was stirred for 24 hours. The solvent was removed by distillation and the reaction was purified on a 1/1 ethyl acetate/ hexane silica gel column. Yield: 0.8400 g, 1.5 mmol, 92%. R_f 0.51 ($CHCl_3$/MeOH: 10/1). ^{1}H-NMR δ_H (500 MHz, $CDCl_3$): 7.7 (m, 3H), 7.5 (m, 10H), 5.0 (s, 2H), 4.5 (m, 2H), 4.2 (m, 1H), 3.6 (s, 3H), 2.95 (dd, 1H), 2.8 (dd, 1H), 1.6 (m, 2H), 1.5 (m, 1H), 1.1 (d, 3H), 0.8 (d, 3H), 0.7 (d, 3H).

Bz-Asp-Leu-Thr-OMe

Bz-Asp(OBn)-Leu-Thr-OMe (380 mg, 0.82 mmol, 1 eq) was dissolved in 4 mL methanol. The flask was evacuated and flushed with nitrogen three times. Palladium on activated carbon (10%, 61 mg) was added and the flask was evacuated and flushed with nitrogen again. Hydrogen was added to the reaction from a balloon. The reaction mixture was stirred for 30 minutes. The balloon was regenerated with hydrogen and the reaction was stirred for an additional 30 minutes. The mixture was filtered over celite and dried down to yield Bz-Asp-Leu-Thr-OMe (303 mg, 0.81 mmol, 99 %). R_f 0.17 ($CHCl_3$/MeOH: 5/1).

Bz-Asp-Leu-Thr-NHMe

Bz-Asp-Leu-Thr-OMe (260 mg, 0.70 mmol, 1 eq) was dissolved in a saturated solution of methylamine in anhydrous methanol (~15 mL). The solution was stirred overnight and then dried down under a stream of nitrogen to quantitatively yield Bz-Asp-Leu-Thr-NHMe. R_f 0.11 ($CHCl_3$/MeOH: 5/1).

Examination of Bz-Asp(Cl)-Leu-Thr-OMe Reaction

Bz-Asp-Leu-Thr-NHMe (0.0480 mg, 0.104 mmol, 1 eq) was dissolved in 2 mL dry chloroform. Triethylamine (20.0 µL, 0.145 mmol, 1.4 eq, dried over calcium hydride) was added to the tripeptide solution. Oxalyl chloride (9.0 µL, 0.104 mmol, 1 eq) was added and the solution was stirred for 30 minutes. A diazomethane solution was prepared from diazald as recommended by the manufacturer (Aldrich). This solution was added to the acid chloride solution until a pale yellow color persisted. After 30 minutes, the reaction was quenched with methanol and brought to dryness. The reaction mixture

was purified by preparative TLC in 10:1 chloroform:methanol. Three major products were isolated. NMR analysis revealed that the first product (R_f 0.95) was not peptidyl, the second product was identified as Bz-Asp(OMe)-Leu-Thr-NHMe, and the third product was the succinimide cyclization of Bz-Asp(Cl)-Leu-Thr-NHMe (**13**). Substantial cyclization (>35%) to the succinimide was observed along with other less predominant impurities (not identified). The diazomethyl ketone (**7**) was not detected.

5.5.2 OT Affinity Labels - Epoxide Analogs

Boc-L-Allyl Glycine (Boc-Ag-OH)

Allyl glycine (0.3928 g, 3.4 mmol, 1 eq, Fluka) was dissolved in 6 mL dioxane and 5 mL water. Triethylamine (700 µL, 5.1 mmol, 1.5 eq) and 2-*t*-butoxycarbonyl-oxyimino-2-phenylacetonitrile (BOC-ON, 0.9201g, 3.7 mmol, 1.1 eq, Aldrich) were added to the allyl glycine solution and the reaction was stirred for 90 minutes. After starting material was no longer visible by TLC, the dioxane was removed and the solution was washed with 1/1 ethyl acetate/hexane. Aqueous layer was acidified with a 10% citric acid solution and the impure product was extracted into ethyl acetate. Product was purified on a silica column in chloroform. Yield: 0.7367 g, 3.4 mmol, 99%. R_f 0.55 ($CHCl_3$/MeOH: 10/1); ^{1}H-NMR δ_H (500 MHz, $CDCL_3$): 5.7 (m, 1H), 5.1-5.2 (m, 2H), 4.4 (m, 1H), 2.5-2.6 (m, 2H), 1.5 (s, 9H).

Boc-Ag-Leu-Thr-OMe

Boc-Ag-OH (0.3953 g, 1.8 mmol) was dissolved in 9 mL DMF and the carboxylic acid was activated with HOBT (0.2618 g, 2.1 mmol, 1.15 eq) and HBTU (0.7193 g, 1.89 mmol, 1.05 eq). The TFA salt of Leu-Thr-OMe (0.7249 g, 2.1 mmol, 1.15 eq) was added with triethylamine (370 µL, 2.7 mmol, 1.5 eq).

The solution was stirred at room temperature for 16 hours. The DMF was removed and the product was purified on a silica column in chloroform. Yield: 0.534 g, 1.3 mmol, 70%. R_f 0.60 ($CHCl_3$/MeOH: 10/1). ^{1}H-NMR δ_H (500 MHz, d4-MeOH): 5.78 (m, 1H), 5.08 (dd, 2H), 4.84 (s, 2H), 4.49 (m, 1H), 4.42 (d, 1H), 4.27 (m, 1H), 4.1 (m, 1H), 3.7 (s, 3H), 2.3 - 2.5 (m, 2H), 1.42 (s, 9H), 1.15 (d, 3H), 0.94 (dd, 6H).

TFA-Ag-Leu-Thr-OMe

Boc-Ag-Leu-Thr-OMe (0.2051 g, 0.48 mmol) was dissolved in 3 mL dichloromethane and 3 mL trifluoroacetic acid. The solution was stirred for 30 minutes, blown dry three times from methylene chloride and lyophilized from water overnight to quantitatively yield the deprotected peptide. R_f 0.27 ($CHCl_3$/MeOH: 10/1). ^{1}H-NMR δ_H (500 MHz, D_2O): 5.76 (m, 1H), 5.2 - 5.27 (m, 2H), 4.53 (m, 1H), 4.45 (d, 1H), 3.98 (dd, 1H), 3.72 (s, 1H), 2.56 - 2.68 (m, 2H), 1.61 - 1.65 (m, 3H), 1.15 (d, 3H), 0.95 (dd, 6H).

Bz-Ag-Leu-Thr-OMe

TFA-Ag-Leu-Thr-OMe (0.2052 g, 0.44 mmol) was dissolved in 4.4 mL anhydrous THF and chilled to 0 °C. Anhydrous triethylamine (61 µL, 0.44 mmol, 1 eq) and benzoyl chloride (52 µL, 0.44 mmol, 1 eq) were added. After one hour, the solution was filtered and concentrated. The product was purified on a silica column in 1/1 ethyl acetate/hexane. Yield: 0.1185 g, 0.27 mmol, 60%. R_f 0.24 ($CHCl_3$/MeOH: 10/1). ^{1}H-NMR δ_H (500 MHz, $CDCl_3$): 7.88 - 8.02 (m, 4H), 7.46-7.49 (m, 1H), 7.27-7.38 (m, 2H), 5.7 (m, 1H), 5.07 (d, 1H), 4.98 (m, 2H), 4.63 (m, 2H), 3.76 (s, 3H), 2.54 (m, 2H), 1.59 (m, 1H), 1.58 (m, 1H), 1.52 (m, 1H), 1.15 (d, 3H), 0.72 (dd, 6H).

Bz-Ag-Leu-Thr-NHMe

Bz-Ag-Leu-Thr-OMe (0.1296 g, 0.29 mmol) was dissolved in an anhydrous saturated solution of methylamine in methanol (~15 mL). The solution was stirred for 30 minutes and then blown dry twice from methanol to quantitatively yield the transamidated product *C*-terminal methyl amide. R_f 0.60 ($CHCl_3$/MeOH: 5/1). ^{1}H-NMR δ_H (300 MHz, d4-MeOH): 7.83 (m, 2H), 7.48 (m, 3H), 5.87 (m, 1H), 5.20 (m, 2H), 4.59 (m, 1H), 4.42 (m, 1H), 4.21 (m, 2H), 3.30 (m, 6H), 2.75 (m, 5H), 1.70 (m, 3H), 1.13 (m, 3H), 0.92 (m, 6H).

*Bz-Epx-Leu-Thr-NHMe (**14**) - m-CPBA Oxidation*

Bz-Epx-Leu-Thr-NHMe (0.0864 g, 0.19 mmol) was dissolved in 290 µL chloroform and 40 µL methanol. A solution of *m*-chloroperbenzoic acid (m-CPBA, 0.0539 g, 0.21 mmol, 1.1 eq in 460 µL chloroform) was prepared and added slowly to the peptide solution. Additional *m*-CPBA was added over the next 8 hours (0.1086 g, 0.63 mmol, 3.3 eq). Reaction was quenched with a 10% solution of sodium nitrite and the organic layer was washed with 5% sodium bicarbonate and brine. The organic layer was dried down and the product was purified by preparative TLC in 20/1 chloroform/methanol. TLC analysis revealed that the desired product was formed in very poor yield. Acidic oxidation provided by these reaction conditions induced bond cleavage of the peptide backbone between the allyl glycine residue and leucine to afford the two major products.

Bz-Epx-Leu-Thr-NHMe - Dimethyldioxirane (DMDO) Oxidation

Dimethyldioxirane was generated in acetone from Oxone (Aldrich) as described by the manufacturer. Bz-Epx-Leu-Thr-NHMe (0.00046 g, 10 µmol) was dissolved in 250 µL acetone and the dioxirane solution was added in

excess until a persistant yellow color remained. The solution was stirred for 45 minutes. Evaporation of the solvent yielded the product in quantitative yield. R_f 0.83 ($CHCl_3$/MeOH: 4/1). FAB LRMS calcd for $C_{23}H_{34}N_4O_6$ (MH^+) 462, found 462. ^{1}H-NMR δ_H (500 MHz, d6-DMSO): 7.88 (m, 2H), 7.54 (m, 2H), 7.47 (m, 2H), 4.84 (m, 1H), 4.64 (m, 1H), 4.34 (m, 1H), 4.07 (m, 1H), 3.98 (m, 1H), 3.00 (br s, 1H), 2.67 (m, 1H), 1.97 (m, 2H), 1.62 (m, 1H), 1.49 (m, 2H), 0.97 (d, 3H, J = 6.4 Hz), 0.85 (br dd, 6H).

Fmoc-Allyl Glycine (Fmoc-Ag-OH)

A solution of 9-fluorenylmethoxycarbonyl succinimide ester (Fmoc-OSu, 2.1098 g, 6.3 mmol, 1.2 eq) in 19.5 mL dioxane was added dropwise to a solution of allyl glycine (0.6038 g, 5.2 mmol) in 26 mL 10% sodium carbonate. A precipitate formed. After several hours, the mixture was washed four times with ether. The aqueous layer was chilled to 0 °C and brought to a pH of 2 with concentrated hydrochloric acid. The product precipitated out of solution and was extracted into ethyl acetate. Purification was performed on a silica column in 20/1 chloroform/methanol and recrystallization in chloroform. R_f 0.30 ($CHCl_3$/MeOH: 20/1).

Fmoc-Ser-Phe-Ag-Leu-Thr-Val-Thr-NH_2

The peptide was synthesized by standard solid phase Fmoc protocols using PAL-PEG resin (0.2 meq/g) and Enhanced Monitoring software on a Milligen 9050 automated synthesizer. The final deprotection cycle was omitted to yield the Fmoc protected amino acid. The peptide was cleaved from the resin by treatment with trifluoroacetic acid/thioanisole/ethanedithiol/anisole (90:5:3:2) for 2 hours to yield the carboxy terminus primary amide. The resin was filtered and washed with TFA. The combined

filtrates were concentrated to 2 mL and the peptide was precipitated with 2:1 ether hexane. The peptide was washed with 2:1 ether/hexane several times and lyophilized overnight. To check the purity of the peptide, 1.5 mg were dissolved in 1 mL piperidine and stirred for 15 minutes. Soln was filtered and triturated three times with ether. Characterization was performed by analytical C-18 HPLC with a water/acetonitrile/0.1% TFA solvent system. A single major peak eluted at 26.3 minutes when the acetonitrile was increased from 0% to 60% over 30 minutes.

Fmoc-Ser-Phe-Ag-Leu-Thr-Val-Thr-NH_2

The Fmoc protected heptapeptide (0.0420 g, 42.6 μmol) was dissolved in 400 μL acetic acid and *m*-CPBA (39.1 mg, 226 μmol, 5 eq) was added. The reaction was stirred and an additional 10 - 20 mg *m*-CPBA were added hourly for four hours. The reaction was diluted with 5 mL water and extracted with hexane (20 x 10 mL) and chloroform (10 x 25 mL). The chloroform layer was brought to dryness to yield slightly impure product (31.7 mg, 42 μl, 75% yield). HPLC retention time (linear gradient 0 - 60% ACN, over 30 minutes) 22.5 minutes.

*Ac-Ser-Phe-Epx-Leu-Thr-Val-Thr-NH_2 (**15**)*

Fmoc-Ser-Phe-Ag-Leu-Thr-Val-Thr-Pal-Peg resin was deprotected via treatment with 20% (v/v) piperidine in DMF and the liberated *N*-terminus was acylated with a solution of acetic anhydride and triethylamine in DMF. Cleavage and oxidation were performed as described above. FAB HRMS calcd for $C_{38}H_{60}O_{12}N_8$ (MH+) 821.4409, found 821.4388.

Enzyme Assays - Time Dependence of Inhibition

Yeast oligosaccharyl transferase was solubilized as previously described.[24] The solubilized yeast microsomes (225 μL) was combined with 1575 μL assay buffer (50 mM Hepes, pH 7.5, 0.5 mg/mL PC, 1% Triton-X, 10 mM $MnCl_2$, 0.1 mg/mL PMSF). Each epoxide inhibitor was dissolved in DMSO to yield a 100 mM solution. The inhibitor (45 μL or 22.5 μL) was combined with 855 μL of the enzyme solution to yield an inhibitor concentration of 5 mM or 2.5 mM. These solutions were preincubated at room temperature and aliquots of 150 μL were removed after 1, 15, 30, 60, and 120 minutes. These aliquots were combined with 40 μL assay buffer, 10 μL 4 mM Bz-Asn-Leu-Thr-NHMe (**10**) and 50,000 dpm Dol-P-P-GlcNAc-[^{3}H]GlcNAc (36.5 Ci/mmol).[25] Assays were performed as described in Appendix A of this dissertation. Time dependence was determined relative to a control experiment.

5.5.3 OT Affinity Labels - Mercury Compounds

Peptide Synthesis

Each peptide was synthesized on PAL-PEG resin (Millipore) with a support substitution of 0.140 meq/gram with standard Fmoc protocols and the enhanced monitoring system provided by Millipore. Couplings were performed with a three-fold excess of each amino acid. After attachment of the final residue, the Fmoc protecting group was removed from the N-terminal amino acid, and while still attached to the resin, the *N*-terminus was capped in 4.5 mL DMF, with 105 μL triethylamine and approx. 170 mg benzoic anhydride. This reaction was stirred for two hours or until a negative Kaiser test was obtained. The resin was rinsed extensively with DMF, dichloromethane and MeOH, then dried overnight under reduced pressure

before cleavage. Cleavage from the resin was performed by shaking the resin with Reagant R [trifluoroacetic acid/thioanisole/ethanedithiol/anisole (90:5:3:2)] for four hours. The resin was filtered and rinsed with TFA. The filtrate was concentrated under a stream of nitrogen and then triturated with 2:1 ether:hexane six times to remove the excess cleavage agents. The peptide was lyophilized from water and purity was confirmed by analytical C-18 HPLC. Bz-CLTVTK-NH_2 and Bz-CLTTVK-NH_2 did not require purification. Bz-NLCTVK-NH_2 was purified by loading 20 mg onto a preactivated Sep-Pak and eluting the peptide with a slow gradient of acetonitrile (0.08% TFA) in water (0.1% TFA). The peptide eluted at a concentration of 20% acetonitrile.

Bz-CLTVTK-NH_2: FAB HRMS calcd for $C_{35}H_{59}O_9N_8S$ (MH+) 767.4125, found 767.4111. ^{1}H-NMR δ_H (500 MHz, d6-DMSO): 8.51 (d, 1H, J = 7.9 Hz), 8.20 (d, 1H, J = 7.9 Hz), 7.87 (br d, 3H, J = 7.3 Hz), 7.82 (d, 1H, J = 8.1 Hz), 7.66 - 7.46 (m, 8H), 7.2 (s, 1H), 7.0 (s, 1H), 5.01 (br s, 1H), 4.93 (br s, 1H), 4.56 (m, 1H), 4.37 (m, 1H), 4.32 (m, 1H), 4.26 (m, 1H), 4.13 (m, 2H), 4.03 (m, 1H), 3.97 (m, 1H), 2.93 (m, 1H), 2.84 (m, 1H), 2.74 (m, 2H), 2.07 (m, 1H), 1.62 (m, 2H), 1.49 (m, 5H), 1.26 (m, 4H), 1.03 (m, 6H), 0.87 - 0.81 (m, 14H).

Bz-NLCTVK-NH_2: FAB HRMS calcd for $C_{35}H_{58}O_9N_9S$ (MH+) 780.4078, found 780.4047. ^{1}H-NMR δ_H (500 MHz, d6-DMSO): 8.57 (d, 1H, J = 7.5 Hz), 8.13 (d, 1H, 7.8 Hz), 8.08 (d, 1H, 7.8 Hz), 7.88 (d, 1H, J = 7.9 Hz), 7.83 (m, 3H), 7.59 - 7.44 (m, 8H), 7.19 (s, 1H), 7.01 (s, 1H), 6.96 (s, 1H), 4.92 (d, 1H, J = 5.1 Hz), 4.74 (q, 1H), 4.44 (m, 1H), 4.29 (q, 1H), 4.22 (m, 1H), 4.15 (m, 2H), 4.02 (m, 1H), 2.80 - 2.53 (m, 5-6H, obscured by solvent), 1.99 (m, 1H), 1.61 (m, 2H), 1.49 (m, 5H), 1.28 (m, 2H), 1.02 (d, 3H, J = 6.4 Hz), 0.84 (m, 14H).

*Bz-Cys(SHg$^+$)-Leu-Thr-Val-Thr-Lys-NH$_2$ (**18**)*

The mercury peptides were prepared according to the methods of Leavis and Lehrer.[20] The peptide (0.0114 g, 14.9 μmoles, 1 eq) was dissolved in 3 mL of an aqueous nitric acid solution (pH = 2.9). An Ellman's test was used to determine an accurate peptide concentration (3.4 mM). This peptide solution was added slowly to 7.5 mL 20 mM $Hg(NO_3)_2$ in nitric acid (pH = 2.9). The solution was stirred for 30 minutes, until an Ellman's test indicated that free thiols were no longer present. The solution was passed through an activated Sep-Pak with water to remove any remaining $Hg(NO_3)_2$. The peptide was eluted slowly with a mixture of acetonitrile and water. Yield: 11.1 mg, 11.5 μmoles, 74%. FAB HRMS calcd for $C_{35}H_{59}O_9N_8S$ (MH+) 969.3781, found 967.3700.

*Bz-Asn-Leu-Cys(SHg$^+$)-Thr-Val-Lys-NH$_2$ (**18**)*

The peptide (0.0103 g, 13.2 μmoles, 1 eq) was dissolved in 1.3 mL of an aqueous nitric acid solution (pH = 2.9). The peptide concentration was found to be 4.9 mM by an Ellman's test. This solution was added slowly to 6.6 mL 20 mM $Hg(NO_3)_2$ in nitric acid (pH = 2.9). The solution was stirred for 30 minutes, until an Ellman's test indicated that free thiols were no longer present. Solution was passed through an activated Sep-Pak with water to remove any remaining $Hg(NO_3)_2$. The peptide was eluted slowly with a mixture of acetonitrile and water. Yield: 1.2 mg, 1.3 μmoles, 10%.

Inhibition of OT by Bz-Cys(SHg$^+$)-Leu-Thr-Val-Thr-Lys -NH$_2$

"High Sodium Chloride" Inhibition Studies

Typically, a solution of the solubilized yeast protein (500 mM NaCl) was thawed and combined with the appropriate amount of a 1 M solution of

$MnCl_2$ to afford a final concentration of 10 mM $MnCl_2$. Solutions of the mercuric inhibitors were prepared in DMSO at concentrations of 5 mM, 0.5 mM and 0.05 mM. An aliquot of each of these inhibitor solutions (24 µL) was added to an aliquot of the enzyme solution (95 µL) at time = 0 minutes, with shaking and vortexing to yield final incubation concentrations of 1 mM, 0.1 mM and 0.01 mM. A parallel control was performed where DMSO was added in place of the mercuric peptide. After incubation times of 1, 15, 30 and 60 minutes, 20 µL of each incubation mixture was diluted into a microcentrifuge tube which contained 50000 dpm Dol-P-P-GlcNAc-[^{3}H]GlcNAc, 10 µL 2.5 mM Bz-Asn-Leu-Thr-NHMe and 170 µL assay buffer (50 mM Hepes, pH 7.5, 0.5 mg/mL PC, 1% Triton-X, 10 mM $MnCl_2$). Aliquots of this mixture were removed at specific timepoints and quantitated as described in chapter two of this dissertation. Turnover rates were compared to the relevant control. The conditions described yield sodium chloride concentrations of 500 mM during the preincubation and 50 mM during the enzyme assay.

Preparation of "Low Sodium Chloride" Oligosaccharyl Transferase

Solubilized yeast oligosaccharyl transferase was purified on a concanavilin A column as previously described.[24] The concanavalin A eluate was loaded onto a Mono-S column which had been equilibrated with buffer (140 mM sucrose, 25 mM NaCl, 50 mM succinate, 10 mM $MgCl_2$, 0.4% NP-40, 0.5 mg/mL PC). The protein was eluted with a NaCl gradient from 25 mM to 400 mM over 140 minutes. Active fractions were pooled and dialysed against buffer to achieve the following composition: 140 mM sucrose, 25 mM sodium chloride, 10 mM $MgCl_2$, 50 mM Tris-Cl, 0.4% NP-40, 0.5 mg/ mL PC.

Inhibition of Oligosaccharyl Transferase by ***18*** *and* ***19*** *- "Low Sodium Chloride" Inhibition Studies*

Solutions of the two mercury peptides were prepared in DMSO at concentrations of 25 mM, 5 mM and 0.5 mM. The Mono-S purified oligosaccharyl transferase (54 μL) and 6 μL of each of the inhibitor solutions were combined to yield incubation concentrations of 2.5 mM, 0.5 mM and 0.05 mM. A control was prepared which contained 6 μL DMSO instead of the mercury peptides. After two minutes, 40 μL of each incubation mixture was transferred to a microcentrifuge tube containing 150 μL assay buffer (50 mM Hepes, pH 7.5, 0.5 mg/mL PC, 1% Triton-X, 10 mM $MnCl_2$), 10 μL 2.5 mM Bz-Asn-Leu-Thr-NHMe and 50,000 dpm Dol-P-P-GlcNAc-[^{3}H]GlcNAc. Aliquots of this mixture were removed at specific timepoints and quantitated as described in chapter two of this dissertation. Turnover rates were compared to the relevant control.

Substrate Protection - Bz-Asn-Leu-Thr-NHMe

The incubation mixture was prepared in the same manner as described for the low salt assays except the enzyme solutions contained 1 mM Bz-Asn-Leu-Thr-NHMe. The assay microcentrifuge tube contained 150 μL assay buffer (50 mM Hepes, pH 7.5, 0.5 mg/mL PC, 1% Triton-X, 10 mM $MnCl_2$), 10 μL DMSO and 50,000 dpm Dol-P-P-GlcNAc-[^{3}H]GlcNAc. Experiments were compared to two controls, one which did not contain the mercuric peptide during the preincubation, and the second which did not contain the Bz-Asn-Leu-Thr-NHMe (in this case, the substrate was added to the microcentrifuge tube prior to initiation of the assay). Assays were quantitated as described in Appendix A of this dissertation.

5.6 References

1. Kyte, J. *Mechanism in Protein Chemistry*; Garland Publishing, Inc.: New York, 1995.

2. Hartman, F. C. "Haloacetol Phosphates. Characterization of the Active Site of Rabbit Muscle Triose Phosphate Isomerase," *Biochemistry* **1971**, *10*, 146-154.

3. Davenport, R. C.; Bash, P. A.; Seaton, B. A. "Structure of the Triosephosphate Isomerase Phosphoglycolhydroxamate Complex - An Analog of the Intermediate on the Reaction Pathway," *Biochemistry* **1991**, *30*, 5821-5826.

4. Hartman, S. C. "The Interaction of 6-Diazo-5-oxo-L-norleucine with Phosphoribosyl Pyrophosphate Amidotransferase," *J. Biol. Chem.* **1963**, *238*, 3036-3047.

5. Messenger, L. J.; Zalkin, H. "Glutamine Phosphoribosylpyrophospate Amidotransferase from *Escherichia coli*," *J. Biol. Chem.* **1979**, *254*, 3382-8892.

6. Smith, J. L. "Structures of Gluatamine Amidotransferases from the Purine Biosynthetic Pathway," *Biochem. Soc. Trans.* **1995**, *23*, 894-898.

7. Welply, J. K.; Shenbagamurthi, P.; Nider, F.; Park, H. R.; Lennarz, W. J. "Active Site-Directed Photoaffinity Labeling and Partial Characterization of Oligosaccharyltransferase," *J. Biol. Chem.* **1985**, *260*, 6459-6465.

8. Noiva, R.; Kaplan, H. A.; Lennarz, W. J. "Glycosylation Site-Binding Protein is not Required for *N*-Linked Glycoprotein Synthesis," *Proc. Natl. Acad. Sci. U.S.A.* **1991**, *88*, 1986-1990.

9. Imperiali, B.; Shannon, K. L. "Differences Between Asn-Xaa-Thr Containing Peptides: A Comparison of Solution Conformation and Substrate Behavior with Oligosaccharyltransferase," *Biochemistry* **1991**, *30*, 4374-4380.

10. Bause, E. "Active-Site-Directed Inhibition of Asparagine N-Glycosyltransferases with Epoxy-Peptide Derivatives," *Biochem. J.* **1983**, *209*, 323-330.

11. Imperiali, B.; Shannon, K. L.; Unno, M.; Rickert, K. W. "A Mechanistic Proposal for Asparagine-Linked Glycosylation," *J. Am. Chem. Soc.* **1992**, *114*, 7944-7945.

12. Stone, S. R.; Rennes, D.; Wikstrom, P.; Shaw, E.; Hofsteenge, J. "Peptidyldiazomethanes: A Novel Method of Interaction with Prolyl Endopeptidase," *Biochem. J.* **1992**, *283*, 871-876.

13. Olah, G. A.; Welch, J. "Synthetic Methods and Reactions XV. Convenient Dediazoniative Hydrofluorination and Halofluorination of Diazoalkanes and Diazoketones in Pyridinium Polyhydrogen Fluoride Solution," *Synthesis Communications* **1974**, *12*, 896-898.

14. Brennan, T. V.; Clarke, S. in *Deamidation and Isoaspartate Formation in Model Synthetic Peptides: The Effects of Sequence and Solution Environment*; Aswad, D. W.; CRC Press, Boca Raton, 1995; pp 65-90.

15. Lura, R.; Schirch, V. "Role of Peptide Conformation in the Rate and Mechanism of Deamidation of Asparaginyl Residues," *Biochemistry* **1988**, *27*, 7671-7677.

16. Gavel, Y.; von Heijne, G. "Sequence Differences Between Glycosylated and Non-glycosylated Asn-X-Thr/Ser Acceptor Sites: Implications for Protein Engineering," *Protein Eng.* **1990**, *3*, 433-442.

17. Adam, W.; Curci, R.; Edwards, J. O. "Dioxiranes: A New Class of Powerful Oxidants," *Acc. Chem. Res.* **1989**, *22*, 205-211.

18. Murray, R. W.; Jeyaraman, R. "Dioxiranes: Synthesis and Reactions of Methyldioxiranes," *J. Org. Chem.* **1985**, *50*, 2847-2853.

19. Adam, W.; Chan, Y. Y.; Cremer, D.; Gauss, J.; Scheutzow, D.; Schindler, M. "Spectral and Chemical Properties of Dimethyldioxirane as Determined By Experiment and *ab Initio* Calculations," *J. Org. Chem.* **1987**, *52*, 2800-2803.

20. Leavis, P. C.; Lehrer, S. S. "A Sulfhydryl-Specific Fluorescent Label, *S*-Mercuric *N*-Dansylcysteine. Titrations of Glutathione and Muscle Proteins," *Biochemistry* **1974**, *13*, 3042-3048.

21. Marshall, R. D. "The Nature and Metabolism of the Carbohydrate-Peptide Linkages of Glycoproteins," *Biochem. Soc. Symp.* **1974**, *40*, 17-26.

22. Imperiali, B.; Hendrickson, T. L. "Asparagine-Linked Glycosylation: Specificity and Function of Oligosaccharyl Transferase," *Bioorganic and Medicinal Chemistry* **1995**, *3*, 1565-1578.

23. Imperiali, B.; Spencer, J. R.; Struthers, M. D. "Structural and Functional Characterization of a Constrained Asx-Turn Motif," *J. Am. Chem. Soc.* **1994**, *116*, 8424-8425.

24. Pathak, R.; Hendrickson, T. L.; Imperiali, B. "Sulfhydryl Modification of the Yeast Wbp1p Inhibits Oligosaccharyl Transferase Activity," *Biochemistry* **1995**, *34*, 4179-4185.

25. Imperiali, B.; Zimmerman, J. W. "Synthesis of Dolichylpyrophosphate-Linked Oligosaccharides," *Tetrahedron Lett.* **1990**, *31*, 6485-6488.

Appendix A. Oligosaccharyl Transferase Assay

A.1 General Oligosaccharyl Transferase Assay

A basic assay for oligosaccharyl transferase has been developed which can be modified to accommodate a wide variety of different kinetic experiments.[1] The fundamentals of this assay have been used throughout this dissertation; specific variations have been described in detail in the relevant experimental sections of each chapter.

In vivo, OT catalyzes the transfer of a triantennary branched tetradecasaccharide from a lipid-linked donor to an asparagine residue in a nascent polypeptide chain. *In vitro*, a simpler substrate, Dol-P-P-GlcNAc-GlcNAc, can be used as the oligosaccharide donor with similar efficiencies.[2] This disaccharide donor can be prepared through a combination of synthetic and enzymatic steps,[3] with the incorporation of a tritium radiolabel at the C-6 position of the second GlcNAc. This radiolabel serves as a tag for facile quantification of OT activity.

The OT assay used in this dissertation relies on the different solubility properties of the tripeptide glycopeptide product, Bz-Asn(GlcNAc-GlcNAc)-Leu-Thr-NHMe, and the oligosaccharide donor, Dol-P-P-GlcNAc-GlcNAc. Briefly, the enzyme is combined with the two substrates under appropriately buffered conditions. At various time points, an aliquot is removed and quenched into a biphasic aqueous/organic solvent system. The product and the unreacted oligosaccharide starting material are separated through a series of extractions. The lipid-linked donor remains in the organic phase, while aqueous washes remove the glycopeptide product. The tritium content of each phase is determined using a scintillation counter to calculate disintegrations per minute (dpm). A plot of dpm *vs.* time can be used to determine the glycosylation rate for each assay. This rate can be compared to other experiments performed under analogous conditions.

This assay is straightforward and can be manipulated to examine different aspects of the OT system. For example, the enzyme may be preincubated with exogenous compounds prior to the addition of one or both of the substrates; this type of experiment allows the specific binding sites of the two substrates to be examined separately (see chapter two). In addition, the concentrations of the two substrates can be altered for the determination of kinetic constants or for the examination of unnatural substrates (see chapter three). Also, the concentration of the enzyme can be adjusted to enable longer kinetic experiments (see chapter four). The assay conditions given below have been designed to yield an active and stable enzyme solution which demonstrates linear kinetics over a ten minute experiment.

A.2 Experimental Method

In a typical experiment, an aliquot of Dol-P-P-GlcNAc-[^{3}H]-GlcNAc (50,000 dpm, specific activity 36.5 Ci/mmol)[3] was blown dry under a stream of nitrogen in a small microcentrifuge tube. The radiolabelled carbohydrate substrate was redissolved in 10 µL of a DMSO solution of Bz-Asn-Leu-Thr-NHMe (5 mM). An additional 10 µL DMSO were added with 160 µL assay buffer (50 mM Hepes, pH 7.5, 140 mM sucrose, 1.2% Triton X-100, 0.5 mg/mL PC, 10 mM $MnCl_2$). The assay was initiated by adding 20 µL of the gently thawed *S. cerevisiae* OT enzyme to the substrate solution. During the course of the experiment, the enzyme mixture was gently agitated. Reaction aliquots (4 x 40 µL) were removed at two minute intervals and quenched into 1.2 mL of 3:2:1 chloroform/methanol/4 mM $MgCl_2$. The tritiated glycopeptide was separated from the unreacted glycolipid through a series of extractions. The upper aqueous layer of the quenched reaction mixture was removed and the organic layer was extracted twice with 0.6 mL Theoretical Upper Phase with salt (TUP:

12/192/186/2.69 chloroform/methanol/water/0.25 M $MgCl_2$). The combined aqueous layers were quantitated for tritium content in 5.5 mL Ecolite (ICN) as disintegrations per minute. The organic layers were dried and the remaining proteinaceous residue was redissolved in 200 μL Solvable (NEN), agitated for 30 minutes and counted in 6 mL Formula 989 (New England Nuclear). The amount of radioactivity present in the aqueous extracts was normalized against the total radioactivity (aqueous and organic) for each sample. OT activity was determined by plotting the normalized value for tritium in the aqueous phase *vs.* time.

A.3 References

1. Imperiali, B.; Shannon, K. L. "Differences Between Asn-Xaa-Thr Containing Peptides: A Comparison of Solution Conformation and Substrate Behavior with Oligosaccharyltransferase," *Biochemistry* **1991**, *30*, 4374-4380.

2. Sharma, C. B.; Lehle, L.; Tanner, W. "N-Glycosylation of Yeast Proteins: Characterization of the Solubilized Oligosaccharyl Transferase," *Eur. J. Biochem.* **1981**, *116*, 101-108.

3. Imperiali, B.; Zimmerman, J. W. "Synthesis of Dolichylpyrophosphate-Linked Oligosaccharides," *Tetrahedron Lett.* **1990**, *31*, 6485-6488.

Appendix B. Synthesis and Evaluation of Bz-Amk-Leu-Thr-NHMe

B.1 Introduction

The asparagine-linked glycosylation reaction is unusual in that the carboxamide side chain of an asparagine residue appears to act as a nucleophile. Within the consensus sequence -Asn-Xaa-Thr/Ser-, this residue attacks the electrophilic oligosaccharide donor. Several mechanisms have been proposed which attempt to explain this surprising enhancement in nucleophilicity (see chapter one). The most recent of these stems from the observation that the Asx-turn is the conformational motif most likely recognized by oligosaccharyl transferase.[1, 2] This conformation includes hydrogen bonds between the carbonyl of the asparagine side chain, the amide backbone and the required threonine or serine residue. The hydrogen bonding array of the Asx-turn and the catalytic machinery of OT may act in concert to promote tautomerization of the asparagine carboxamide to an imidol; this nucleophilic species may then complete the glycosylation event (Figure B-1).[3] Tautomerization to the imidol requires the presence of an active site base, and identification of this base has been the main driving forces behind several of the experiments presented in this dissertation.

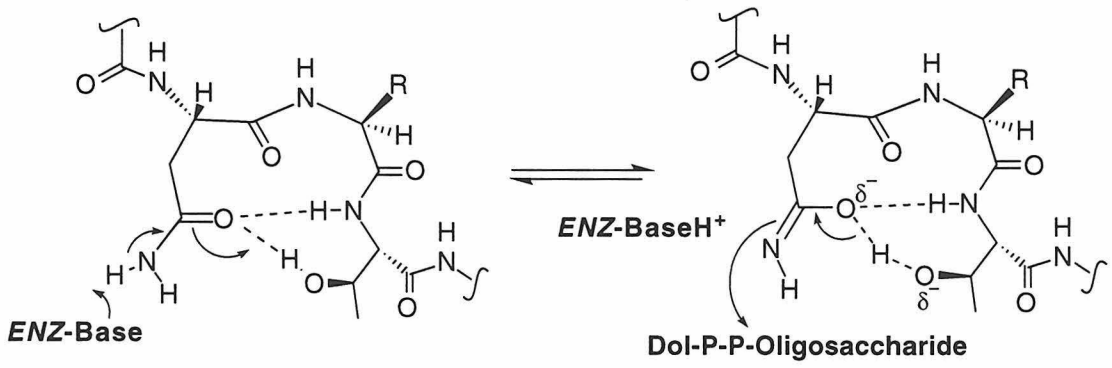

Figure B-1. Proposed Tautomerization of the Peptide Substrate During Asparagine-Linked Glycosylation.[3]

While investigating the presence of an active site base, a parallel study was designed to further characterize the tautomerization of the asparagine side chain. To accomplish this end, the compound Bz-Amk-Leu-Thr-NHMe (**2**) was designed. This peptide is an analog of the substrate Bz-Asn-Leu-Thr-NHMe (**1**) in which the Asn carboxamide is replaced by a methyl ketone.

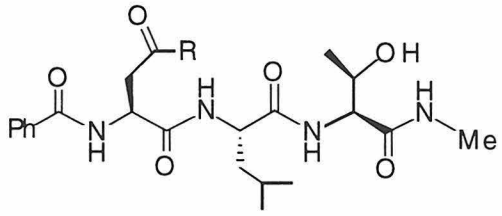

1. R = NH_2
2. R = CH_3

The goal of this project was to incubate **2** with catalytic amounts of OT under deuterated or tritiated solvent conditions and to subsequently monitor **2** for isotope incorporation into the methyl ketone (by NMR or scintillation counts). It was predicted that when **2** was bound to the OT active site, the same active site machinery that induces the amide to imidol tautomerization shown in Figure B-1 would induce the analogous ketone to enol tautomerization of the Amk side chain. This enolization, under deuterated or tritiated conditions, would greatly facilitate isotope incorporation by promoting proton exchange between the methyl group of the side chain and the exchangeable protons of the active site base and the threonine hydroxide (Figure B-2). With a catalytic amount of enzyme present, NMR experiments could be performed on the reaction mixture, without the need for isolation of **2**. Quantification of the amount of tritium incorporation, by means other than NMR, would require isolation of **2** and extensive washes to remove all the rapidly exchangeable protons prior to analysis.

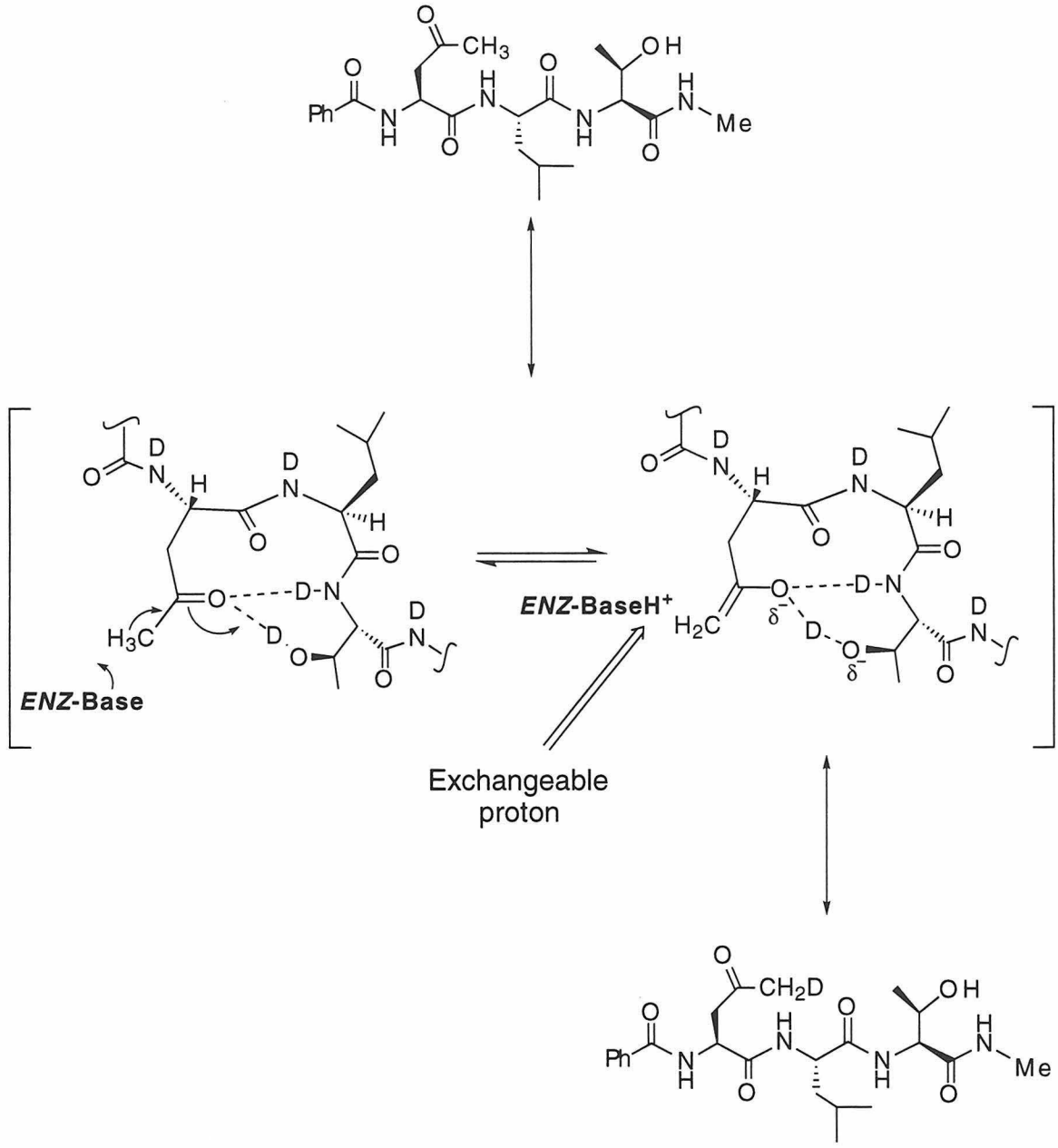

Figure B-2. Proposed Method of Deuterium Incorporation into Bz-Amk-Leu-Thr-NHMe (**2**).

B.2 Results and Discussion

The synthesis of a methyl ketone analog of glutamine has recently been reported,[4] and this method was used for the preparation of Cbz-Amk-OH. Briefly, Cbz-Asp-OH is condensed with formaldehyde to form the oxazolidinone prior to functional group manipulation on the amino acid side chain. The side chain carboxylate is then converted to the acid chloride and treated with diazomethane and hydroiodic acid.[4] The α-amino acid is regenerated from the oxazolidinone by treatment with anhydrous sodium methoxide to produce the corresponding methyl ester; saponification affords the desired product (Cbz-Amk-OH, **3**).

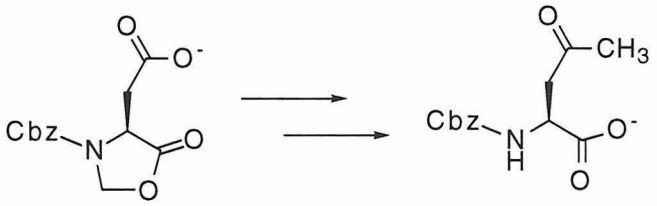

3

Unfortunately, incorporation of **3** into a tripeptide proved difficult and proceeded in poor yield. The Cbz- protected *N*-terminus had to be reprotected with a benzoyl group because enzyme assays of Cbz-Asn-Leu-Thr-NHMe revealed that the Cbz group substantially decreases the substrate affinity of this peptide for OT. Once the synthesis of **2** was completed, NMR analysis revealed the presence of diastereomeric products. The diastereomers proved to be difficult to separate, further decreasing the yields of the preparation. Additional analysis confirmed that significant racemization had occurred during ring opening of the oxazolidinone, prior to peptide synthesis.

An enzyme assay of the diastereomeric mixture confirmed that **2** is a competitive inhibitor for OT; however, its binding affinity was very low and

inhibition was not observed until **2** was present at low millimolar concentrations (as compared to low micromolar concentrations of the competing substrate **1**). The correct diastereomer of **2** is probably a slightly better inhibitor, since OT is unlikely to recognize the D-Amk containing tripeptide; however, neither isomer was isolated in pure form. Because of the poor affinity of OT for **2**, this investigation was discontinued.

B.3 Conclusions and Future Directions

Because peptide **2** was never prepared in significant quantities nor to optical purity, it was never thoroughly examined as an inhibitor for OT and the NMR based isotope experiments described above were not undertaken. However, the fact that **2** is a competitive inhibitor of OT is remarkable and may deserve further scrutiny. Future efforts would require a separation method for the two enantiomers of the Amk amino acid prior to peptide incorporation. Probably the most straightforward approach would be to manipulate the protecting groups of the Amk amino acid so that an enzymatic resolution could be performed. Once accomplished, the overall synthesis of an Amk containing peptide could be streamlined by using solid phase synthesis methods. Such an approach would improve the yields of the peptide synthesis and, as an Fmoc protected amino acid, Amk could be incorporated into the cyclic structure described in chapter four to enhance binding to OT.

B.4 Experimental Methods

B.4.1 Synthesis of Bz-Amk-Leu-Thr-NHME (2)

(S)-3-Benzyloxycarbonyl-5-oxo-4-oxazolidinineacetic Acid

N-Benzyloxycarbonyl-L-aspartic acid (10.3728 g, 38.8 mmol, 1eq), paraformaldehyde (2.3491 g, 78.3 mmol, 2 eq) and *p*-toluenesulfonic acid (0.4437 g, 2.33 mmol, 0.06 eq) were combined in 290 mL benzene. The reaction mixture was heated at reflux with a Dean-Stark Trap for 90 minutes. The solution was cooled and combined with 60 mL ethyl acetate. The organic solution was washed with 5% sodium bicarbonate (10 mL) and water (3 x 10 mL). The organic layer was brought to dryness to yield a clear oil which slowly recrystallized at 4 °C. Yield: 9.53 g, 34.0 mmol, 88%. R_f 0.29 ($CHCl_3$/MeOH: 10/1). ^{1}H-NMR δ_H (500 MHz, $CDCl_3$): 7.30-7.41 (m, 5H), 5.48 (d, 1H), 5.12-5.48 (m, 3H), 4.88 (s, 1H), 4.40 (s, 1H), 2.9-3.3 (m, 2H).

(S)-3-Benzyloxycarbonyl-4-(2-oxopropyl)-5-oxazolidinone

(S)-3-Benzyloxycarbonyl-5-oxo-4-oxazolidinineacetic acid (1.655 g, 5.9 mmol, 1 eq) was dissolved in 11 mL dry, ethanol free chloroform. Oxalyl chloride (616 µl, 7.1 mmol, 1.2 eq) was added with a catalytic amount of DMF (30 µL). After 1 hour, an additional 50 µL oxalyl chloride was added. The reaction was brought to dryness and the remaining residue was dissolved in 10 mL dry THF, chilled in an ice bath and kept under nitrogen. A freshly prepared ether solution of diazomethane was added until the yellow color of excess diazomethane remained. The excess diazomethane was quenched with a small amount of acetic acid and the reaction was dried and stored at -20 °C for 24 hours. The diazomethyl intermediate was redissolved in 50 mL anhydrous $CHCl_3$ and quenched by the slow addition of a solution of 6 mL HI (47% in $CHCL_3$). After ten minutes, the brown solution was combined with

62 mL Chloroform and 31 mL water. The organic layer was further extracted with water to incompletely remove the iodine. The product was purified by silica gel chromatography first with 9/1 ethyl acetate/hexane and then with CHCl3. Yield: 1.10 g, 3.9 mmol, 66.8%. R_f 0.16 ($CHCl_3$). FAB HRMS calcd for $C_{14}H_{15}O_5N$ (MH+) 278.103, found 278.103. ^{1}H-NMR δ_H (500 MHz, $CDCl_3$): 7.37-7.19 (br m, 5H), 5.48 (br s, 1H), 5.26 (s, 1H), 5.19 (br s, 1H), 5.13 (s, 1H), 5.10 (s, 1H), 4.23 (s, 1H), 3.52 (br d, 1H, J = 6.2 Hz), 3.24 (br s, 1H), 3.09 (br d, 1H, J = 8.0 Hz), 2.15 (br s, 3H).

CBZ-Amk-OMe

(S)-3-Benzyloxycarbonyl-4-(2-oxopropyl)-5-oxazolidinone (0.5993 g, 2.2 mmol, 1 eq) was dissolved in 40 mL anhydrous methanol. An anhydrous sodium methoxide solution was prepared by dissolving sodium pellets (0.1212 g, 5.3 mmol, 2.4 eq) in 10 mL methanol. This solution was chilled in a salt/ice bath (-10 °C) and the ketone solution was added *via* cannula transfer. The reaction was stirred for 2 hours and slowly warmed to room temperature. HCl (1N, ~50 mL) was added and the MeOH was removed by evaporation. The aqueous layer was washed with hexanes and then the desired product was extracted into ethyl acetate. The organic solution was washed with a 5% sodium bicarbonate solution, dried with sodium sulfate and brought to dryness. No further purification was necessary. Yield: 0.440 g, 1.7 mmol, 77.5%. R_f 0.55 ($CHCl_3$/MeOH: 20/1). FAB HRMS calcd for $C_{14}H_{17}O_5N$ (MH+) 280.1185, found 280.1185. ^{1}H-NMR δ_H (500 MHz, $CDCl_3$): 7.35 (m, 5H), 5.78 (br s, 1H), 5.1 (s, 2H), 4.52 (m, 1H), 3.72 (s, 3H), 3.22 (dd, 1H), 2.99 (dd, 1H), 2.18 (s, 3H).

CBZ-Amk-OH (3)

CBZ-Amk-OMe (0.415 g, 1.5 mmol, 1 eq) was dissolved in 3.9 mL dioxane and 3.9 mL water and the solution was chilled to -10 °C. A solution of 1N NaOH (1.6 mL, 1.6 mmol, 1.1 eq) was added slowly and the reaction was stirred for 75 minutes. The reaction was quenched with 1.6 mL 1N HCl and the dioxane was removed by evaporation. The aqueous solution was washed three times with chloroform and the organic layer was dried down to afford the pure product. Yield: 0.3811 g, 1.44 mmol, 97%. R_f 0.12 ($CHCl_3$/MeOH: 10/1). FAB HRMS calcd for $C_{13}H_{15}O_5N$ (MH-) 266.1041, found 266.1028. ^{1}H-NMR δ_H (500 MHz, $CDCl_3$): 7.34 (m, 5H), 5.81 (d, 1H), 5.11 (s, 2H), 4.59 (m, 1H), 3.01 (dd, 1H), 2.99 (dd, 1H), 2.16 (s, 1H).

Cbz-Amk-Leu-Thr-NHMe (p-Nitrophenol Ester Coupling)

CBZ-Amk-OH (0.0812 g, 0.29 mmol) was dissolved in 290 µl DMF. *p*-nitrophenol (0.0425 g, 0.31 mmol, 1.05 eq) and dicyclohexylcarbodiimide (0.0625 g, 0.031 mmol, 1.05 eq) were added. After 3 hours, the precipitated dicyclohexylurea (DCU) was removed by filtration. The TFA salt of Leu-Thr-OMe (0.130 g, 0.37 mmol, 1.3 eq), triethylamine (60 µl, 0.45 mmol, 1.5 eq) and 1.2 mL DMF were added to the *p*-nitrophenyl ester of CBZ-Amk-OH. After 14 hours, the DMF was removed and the product was purified by silica gel chromatography in $CHCl_3$. Yield: 20 mg, 15% yield. R_f 0.46 (EtOAc/MeOH: 9/1).

Cbz-Amk-Leu-Thr-NHMe (Isobutylchloroformate Coupling)

CBZ-Amk-OH and the TFA salt of Leu-Thr-NHMe were dried from toluene under vacuum. CBZ-Amk-OH (0.155 g, 0.585 mmol) was dissolved in 5.85 mL dry THF with N-methylmorpholine (NMM, 64 µl, 0.585 mmol, 1 eq).

The solution was chilled to -23 °C and isobutylchloroformate (IBCF, 76 µl, 0.585 mmol, 1 eq) was added. After five minutes, a chilled solution of the TFA-Leu-Thr-NHMe (0.235 g, 0.683 mmol, 1.17 eq) in 6.85 mL dry THF with NMM (64 µl, 0.585 mmol, 1 eq) was transferred *via* cannula into the CBZ-Amk-OH solution. After one hour, the solution was brought to dryness, redissolved in chloroform and washed with 10% citric acid. The product was purified on silica gel in ethyl acetate. Yield: 181 mg, 0.37 mmol, 62%. R_f 0.1 in ethyl acetate. FAB HRMS calcd for $C_{24}H_{36}O_7N_4$ (MH+) 493.266, found 466.268. ^{1}H-NMR δ_H (500 MHz, $CDCl_3$): 7.35 (m, 5H), 6.98 (br s, 1H), 6.63 (s, 1H), 5.77 (d, 1H), 5.11 (s, 2H), 4.55 (br s, 1H), 4.42 (d, 1H), 4.30 (m, 2H), 3.13 (dd, 1H), 2.90 (dd, 1H), 2.76 (d, 3H), 2.18 (s, 3H), 1.17 (m, 3H), 1.12 (d, 3H), 0.95 (d, 3H), 0.89 (d, 3H).

Bz-Amk-Leu-Thr-NHMe

Cbz-Amk-Leu-thr-NHMe (0.527 g, 0.107 mmoles, 1 eq) was dissolved in 1 mL MeOH. The flask sealed, evacuated and flushed with nitrogen. Palladium on activated carbon (10%, 10 mgs) was added to the solution and hydrogen was released into the flask from a balloon. After 1 hour, the solution was filtered over celite and evaporated to dryness to yield 25.7 mg (72 µmoles) of the deprotected tripeptide. This peptide was redissolved in 400 µL DMF and combined with the *p*-nitrophenyl ester of benzoic acid (0.0210 g, 86 µmoles, 1.2 eq) and TEA (15 µL, 108 µmoles, 1.5 eq). After approximately 16 hours, the DMF was removed. The peptide product was purified by reverse phase C-18 HPLC with an elution system of 30% acetonitrile/70% water/0.1% TFA (isocrat). FAB HRMS calcd for (MH+) 463.2550, found 463.2557. ^{1}H-NMR δ_H (500 MHz, d6-DMSO): 8.58 (1H, d, J = 7.2 Hz), 8.13 (d, 1H, J = 8.1 Hz), 7.82 (m, 2H), 7.54 (m, 3H), 7.46 (m, 3H), 4.79 (m, 1H), 4.29 (m, 1H), 4.07 (m, 1H),

4.00 (m, 1H), 2.95 (m, 2H), 2.59 (d, 4.6 Hz), 2.12 (s, 3H), 1.61-1.45 (m, 3H), 0.98 (d, 3H, 6.3 Hz), 0.84 (d, 3H, J = 6.6 Hz), 0.80 (d, 3H, J = 6.5 Hz).

Analysis of Racemization

The optical rotations for two different preparations of CBZ-Amk-OH were examined. Prior to analysis, each sample was dissolved in enough $CHCl_3$ to yield a 3 mg/mL solution. The rotation of each sample was measured five times in a 10 dm cell and the average value was used for all calculations. Preparation 1 (165.8 mg) was dissolved in 5.0 mL $CHCl_3$ and a 180.8 µL aliquot was diluted to 2.00 mL; the optical rotation was determined at 25 °C. $[\alpha]_{Na} = 100(0.0274)/0.3(1) = 9.13$. Preparation 2 (453 mg) was dissolved in 14.0 mL $CHCl_3$ and a 185.4 µL aliquot was diluted to 2.00 mL; the optical rotation was determined at 25 °C. $[\alpha]_{Na}^{25} = 100(0.0038)/0.3(1) = 1.27$.

B.4.2 Synthesis of Cbz-Asn-Leu-Thr-NHME

CBZ-Asn-Leu-Thr-OMe

CBZ-Asn-OpNP (0.3399g, 0.88 mmol, 1.1 eq) was dissolved in 3.9 mL DMF. The TFA salt of Leu-Thr-OMe (0.269 g, 0.78 mmol, 1 eq) and triethylamine (162 µl, 1.32mmol, 1.5eq) were added. The solution was stirred overnight. DMF was removed and the residue was washed with ethyl acetate. Product was collected by filtration. Yield: 0.2289 g, 0.46 mmol, 59.5%. R_f 0.43 ($CHCl_3$/MeOH: 5/1). ^{1}H-NMR δ_H (500 MHz, $CDCl_3$): 8.0 (d, 1H), 7.9 (d, 1H), 7.4 (d, 1H), 7.3 (m, 6H), 6.9 (s, 1H), 5.0 (m, 3H), 4.4 (m, 2H), 4.2 (m, 1H), 4.1 (m, 1H), 3.6 (s, 3H), 2.3 - 2.5 (m, 2H), 1.6 (m, 1H), 1.45 (m, 2H), 1.1 (d, 3H), 0.8 (dd, 6H).

CBZ-Asn-Leu-Thr-NHMe

CBZ-Asn-Leu-Thr-OMe (0.0327 g, 0.067 mmol, 1 eq) was dissolved in 15 mL saturated methylamine in methanol with sonication. The solution was stirred for 15 hours. Product precipitated out of solution and was collected by centrifuge. The precipitate was washed three times with chloroform to yield the desired product. Yield: 13 mg, 0.023 mmol, 39%. R_f 0.30 ($CHCl_3$/MeOH: 5/1). ^{1}H-NMR δ_H (500 MHz, d4-MeOH): 7.3 (m, 5H), 5.08 (s, 2H), 4.5 (m, 1H), 4.32 (m, 1H), 4.23 (m, 2H), 2.79 - 2.83 (dd, 1H), 2.72 (s, 3H), 2.63 - 2.68 (dd, 1H), 1.64 - 1.71 (m, 3H), 1.16 (d, 3H), 0.86 - 0.94 (dd, 6H).

B.5 References

1. Imperiali, B.; Shannon, K. L.; Unno, M.; Rickert, K. W. "Role of Peptide Conformation in Asparagine-Linked Glycosylation" *J. Am. Chem. Soc.* **1992**, *114*, 7942-7944.

2. Imperiali, B.; Spencer, J. R.; Struthers, M. D. "Structural and Functional Characterization of a Constrained Asx-Turn Motif" *J. Am. Chem. Soc.* **1994**, *116*, 8424-8425.

3. Imperiali, B.; Shannon, K. L.; Unno, M.; Rickert, K. W. "A Mechanistic Proposal for Asparagine-Linked Glycosylation" *J. Am. Chem. Soc.* **1992**, *114*, 7944-7945.

4. Scholtz, J. M.; Bartlett, P. A. "A Convenient Differential Protection Strategy for Functional Group Manipulation of Aspartic and Glutamic Acids" *Synthesis Communications* **1989**, *7*, 542-544.

Appendix C. Design and Synthesis of Crosslinking Reagents for Oligosaccharyl Transferase

C.1 Design and Synthesis of Crosslinking Reagents

Chapter two of this dissertation described the identification of a cysteine residue located at or near the oligosaccharide binding site of OT. This cysteine residue is highly reactive towards the alkyl alkanethiolsulfonate family of thioalkylating agents, including methyl methanethiolsulfonate (MMTS). Based on this observation, a novel biotinylated MMTS analog (BMTS) was prepared and used to characterize the Wbp1p subunit of OT (see chapter two).[1] The unusual reactivity of this cysteine makes it an ideal target for experiments designed to further characterize the enzyme.

OT is a multisubunit, membrane bound protein; Wbp1p is just one of as many as six different subunits and the organization of these subunits, relative to each other, is currently unknown (see chapter one).[2] Chemical crosslinking agents are commonly used to demonstrate that two subunits are in proximity with each other in an intact protein. With the observation that the Wbp1p polypeptide encompasses all or part of the oligosaccharide binding site (and possibly the active site), it is of interest to identify which other subunits directly interact with Wbp1p; adjacent polypeptides could be involved in completing the enzyme active site machinery. With this goal in mind, several novel crosslinking reagents were designed which connect the reactive portion of MMTS to a benzophenone or *p*-azidobenzoic acid photoaffinity label (Figure C-1, **1** - **3**). Each of these compounds contains a aminoethanethiolsulfonate group which has been condensed either immediately with the carboxylic acid of the photoactive moiety (**1**) or extended by a hexanoic linker prior to addition of the photoreactive group (**2** - **3**). The preparation of these compounds was straightforward and they are ready for analysis with OT.

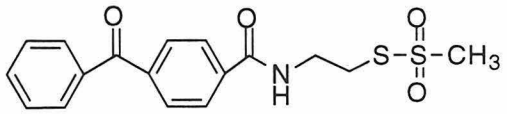

1

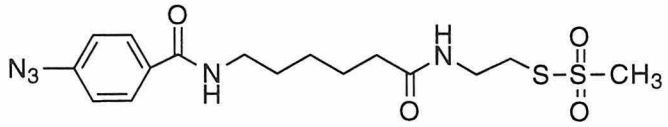

2

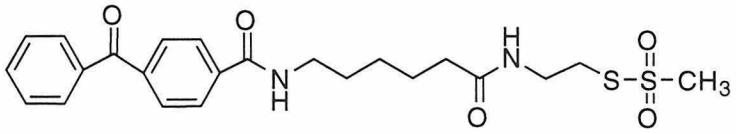

3

Figure C-1. Chemical Structures of New Crosslinking Agents.

C.2 Experimental Methods

p-Benzoyl benzoyl-OpNP

p-Benzoyl benzoic acid (0.2049 g, 0.91 mmoles, 1 eq) was dissolved in 2.5 mL THF with *p*-nitrophenol (0.195 mg, 0.95 mmoles, 1.05 eq). Dicyclohexylcarbodiimide (DCC, 0.1501 g, 0.11 mmoles, 1.2 eq) was added. After three hours, an addition 0.010 g *p*-nitrophenol and 0.010 g DCC were added. The reaction was stirred for an additional hour. The dicyclohexylurea (DCU) was removed via filtration and the reaction product was used without further preparation.

*p-BzBz-aminoethanethiolsulfonate (**1**)*

Methyl aminoethanethiolsulfonate hydrobromide (44 mg, 0.19 mmol)[3] and *p*-benzoyl benzoyl-OpNP (0.0400 g, 0.173 mmoles, 1 eq) were dissolved in 750 µL

anhydrous DMF with sonication. The solution was chilled in an ice bath and TEA (35 μL, 253 μmoles, 1.5 eq) was added slowly. After one hour, an additional 0.0320 g *p*-benzoyl benzoyl-OpNP (92 μmoles, 0.47 eq) were added. The reaction was left overnight. The DMF was removed by distillation and the reaction product was purified by silica gel chromatography in 1/1 ethyl acetate/hexanes. Yield: 53.7 mg, 148 μmoles, 85%. R_f 0.11 (ethyl acetate/ hexanes: 1/1). ^{1}H-NMR δ_H (300 MHz, $CDCl_3$): 7.96 - 7.76 (m, 6H), 7.63 (t, 1H), 7.51 (t, 2H), 7.09 (br s, 1H), 3.88 (q, 2H), 3.46 (t, 2H), 3.39 (s, 3H).

Boc-6-aminohexanoyl-aminoethanethiolsulfonate

Boc-6-aminohexanoic acid (0.1978 g, 0.855 mmoles) was dissolved in 1.0 mL DMF with DCC (0.1951 g, 0.947 mmoles) and *p*-nitrophenol (0.1313 g, 0.942 mmoles). The solution was stirred for three hours and 0.25 eq DCC (0.0444 g, 0.216 mmoles) was added. After an additional hour, the DCU precipitate was removed by filtration. Methyl aminoethanethiolsulfonate hydrobromide (86.7 mg, 0.375 mmol, 1 eq)[3] was dissolved in 500 μL DMF and combined with 500 μL of the activated ester solution of Boc-6-aminohexanoic acid. The solution was chilled in an ice bath and TEA (77 μL, 0.557 mmoles, 1.5 eq) was added slowly. Two additional 100 μL aliquots of the activated Boc-6-aminohexanoic acid ester were added over three hours. The reaction was stirred for approximately 16 hours and the DMF was removed under reduced pressure. The reaction product was purified by silica gel chromatography: Mixture was loaded in 1/1 ethyl acetate/hexanes and the product was eluted with pure ethyl acetate. R_f 0.4 (ethyl acetate). Yield: 98.5 mg, 266 μmoles, 71%. ^{1}H-NMR δ_H (500 MHz, $CDCl_3$): 6.2 (br s, 1H), 3.60 (dd, 2H, J = 9.3, 6.1 Hz), 3.36 (s, 3H), 3.31 (t, 2H, J = 6.4 Hz), 3.09 (t, 2H, J = 6.9 Hz), 2.19 (t, 2H, J = 7.5 Hz), 1.64 (m, 2H), 1.46 (m, 2H), 1.43 (s, 9H), 1.34 (m, 2H).

TFA-6-aminohexanoyl-aminoethanethiolsulfonate

Boc-6-aminohexanoyl-aminoethanethiolsulfonate (98.5 mg, 0.266 mmoles, 1 eq) was dissolved in methylene chloride (~5 mL) and TFA (~2 mL) was added. The reaction was stirred until TLC analysis indicated that the starting material was no longer visible. Solution was dried down under a stream of nitrogen, redissolved in methylene chloride and brought to dryness again. The product was dissolved in water (~5 mL) and shell frozen. Lyophilization yielded the desired product in quantitative yield. Rf 0.08 (ethyl acetate).

*p-azidoBz-6-aminohexanoyl-aminoethanethiolsulfonate (**2**)*

TFA-6-aminohexanoyl-aminoethanethiolsulfonate (240 μmoles) was dissolved in 1.2 mL anhydrous DMF. An aliquot of this solution (300 μL, 60 μmoles) was chilled in an ice bath and combined with the succinic acid ester of *p*-azidobenzoic acid (0.0182 g) and TEA (12 μL, 86.7 μmoles, 1.4 eq). The reaction was slowly warmed to room temperature. After three hours, an additional 0.5 equivalents of the succinic acid ester of *p*-azidobenzoic acid (0.0087 g) and TEA (4 μL) were added. After two more hours, the DMF was removed under reduced pressure. The product was purified by silica gel chromatography in ethyl acetate. Yield: 34.4 mg. ^{1}H-NMR δ_H (500 MHz, d4-MeOH): 7.63 (d, 2H), 7.12 (d, 2H), 3.5 (t, 2H), 3.35 (m, 2H), 2.41 (t, 2H), 1.64 (m, 4H), 1.40 (m, 2H).

*p-BzBz-6-aminohexanoyl-aminoethanethiolsulfonate (**3**)*

TFA-6-aminohexanoyl-aminoethanethiolsulfonate (240 μmoles) was dissolved in 1.2 mL anhydrous DMF. An aliquot of this solution (300 μL, 60 μmoles) was chilled in an ice bath and combined with *p*-Benzoyl benzoyl-OpNP (0.0254 g, 73.2 μmoles, 1.2 eq) and TEA (12 μL, 86.7 μmoles, 1.4 eq). The reaction was slowly warmed to room temperature. After three hours, an additional 0.5 equivalents*p*-Benzoyl benzoyl-OpNP (0.0102 g, 29.4 μmoles) were added. After three more hours, the DMF was removed

under reduced pressure. The product was purified by silica gel chromatography in 20/1 chloroform/methanol. Yield: 33.7 mg, 71 μmoles, > 100 %, contains traces of *p*-nitrophenol. R_f 0.34 ($CHCl_3$/MeOH: 20/1). ^{1}H-NMR δ_H (300 MHz, $CDCl_3$): 8.02 - 7.78 (m, 7H), 7.63 (t, 1H), 7.51 (t, 2H), 6.80 (br t, 1H), 6.41 (br t, 1H), 3.61 (dd, 2H, J = 12.0, 6.0 Hz), 3.52 (dd, 2H, J = 12.9, 6.6 Hz), 3,36 (s, 3H), 3.33(t, 2H), 2.26 (t, 2H, J = 7.2 Hz), 1.70 (m, 4H), 1.44 (m, 2H).

C.5 References

1. Pathak, R.; Hendrickson, T. L.; Imperiali, B. "Sulfhydryl Modification of the Yeast Wbp1p Inhibits Oligosaccharyl Transferase Activity," *Biochemistry* **1995**, *34*, 4179-4185.

2. Imperiali, B.; Hendrickson, T. L. "Asparagine-Linked Glycosylation: Specificity and Function of Oligosaccharyl Transferase," *Bioorg. Med. Chem.* **1995**, *3*, 1565-1578.

3. Bruice, T. W.; Kenyon, G. L. "Novel Alkyl Alkanethiolsulfonate Sulfhydryl Reagents. Modification of Derivatives of L-Cysteine," *J. Prot. Chem.* **1982**, *1*,

Appendix D. Selected NMR Spectra

Chapter Two

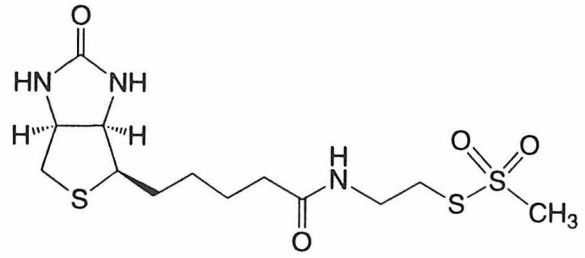

N-Biotinoyl(aminoethane)thiolsulfonate (BMTS)

Chapter Three

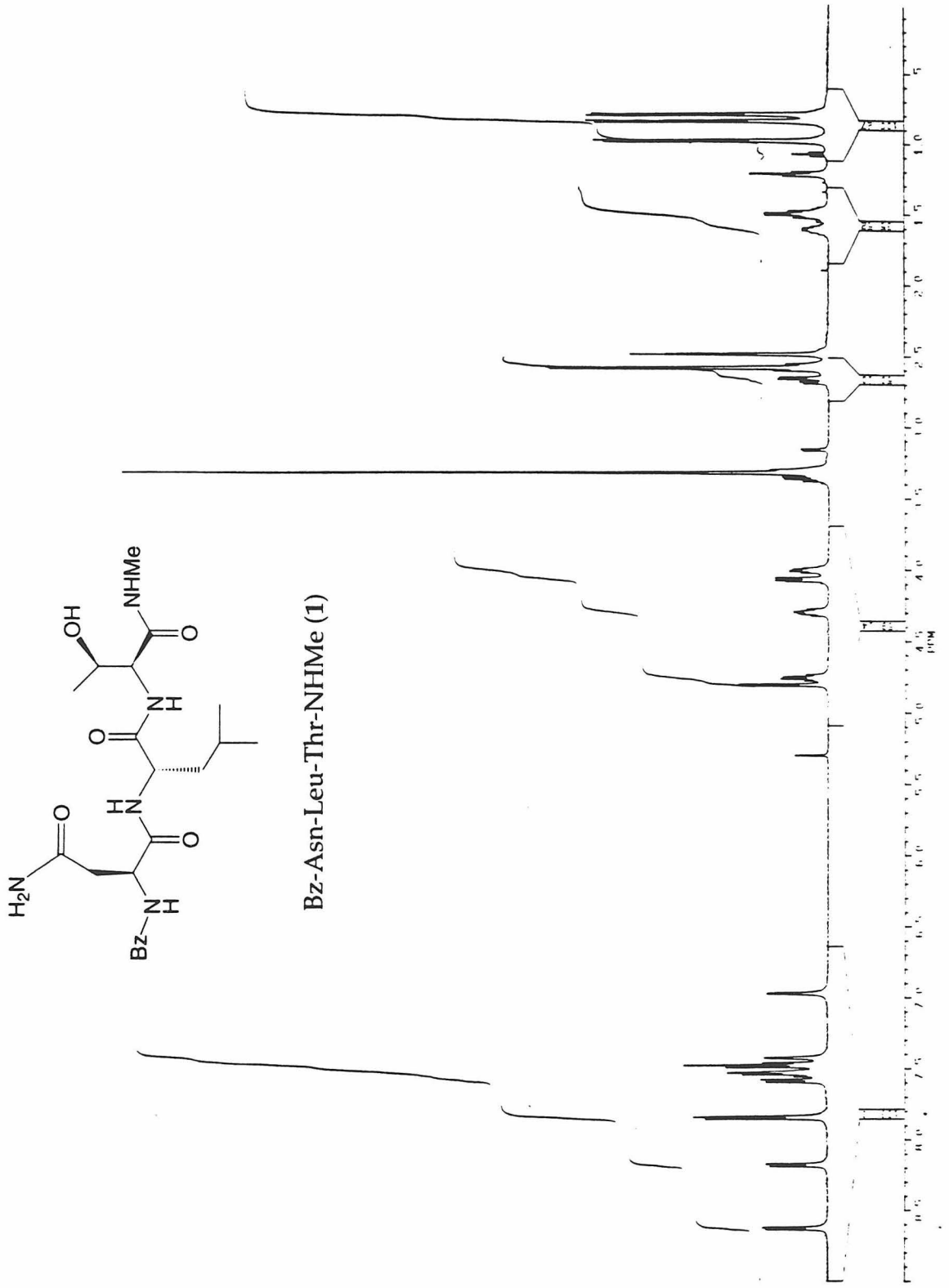
Bz-Asn-Leu-Thr-NHMe (1)
PPM

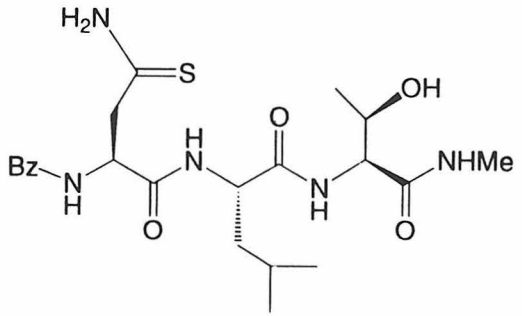

Bz-Asn(γS)-Leu-Thr-NHMe (**2**)

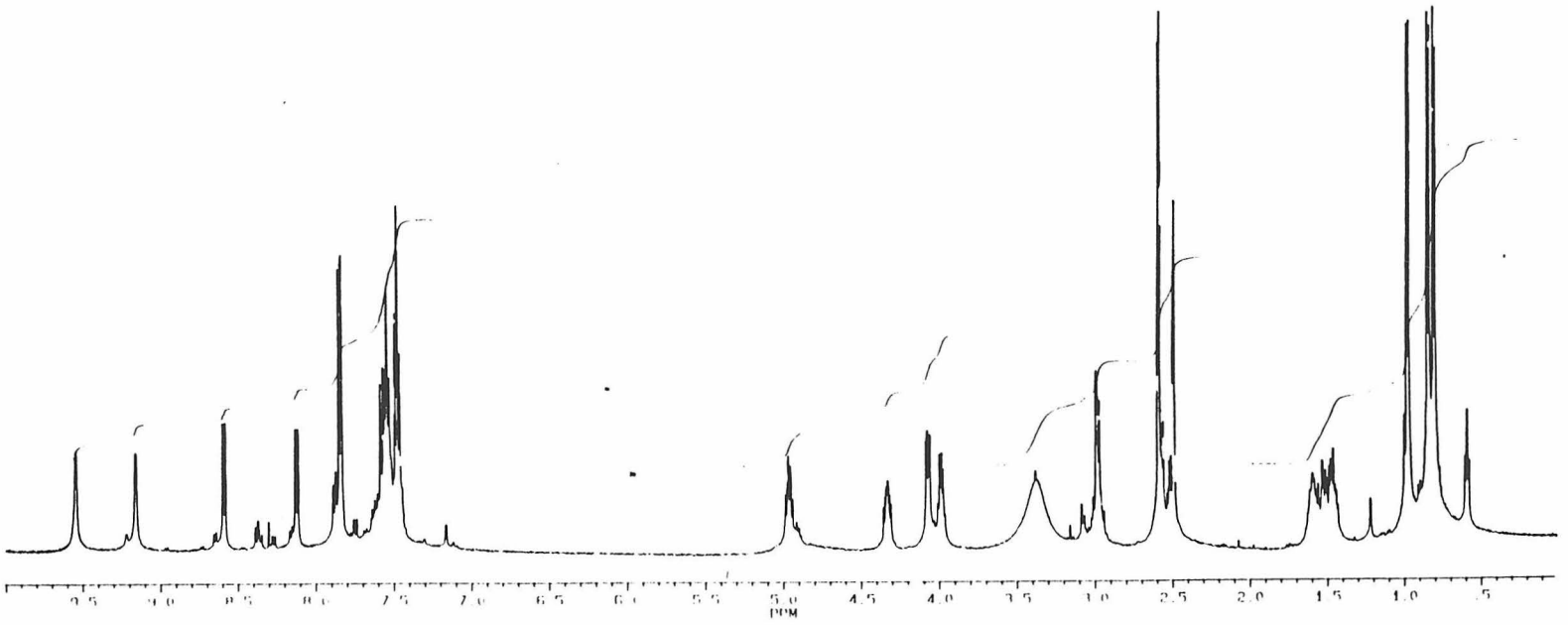

Boc-Hse(OBn)-Leu-Thr-NHMe

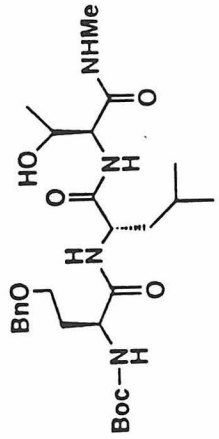

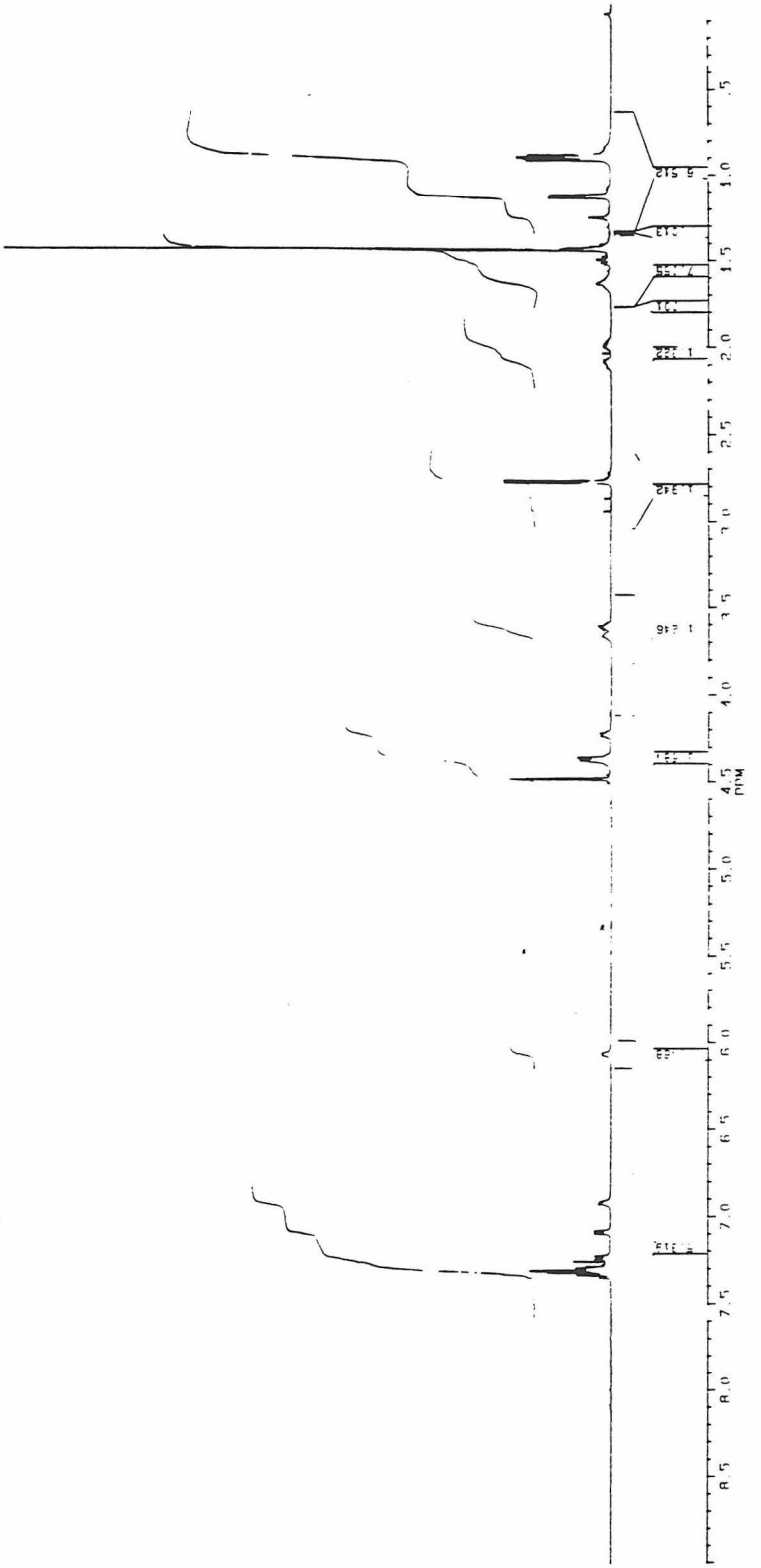

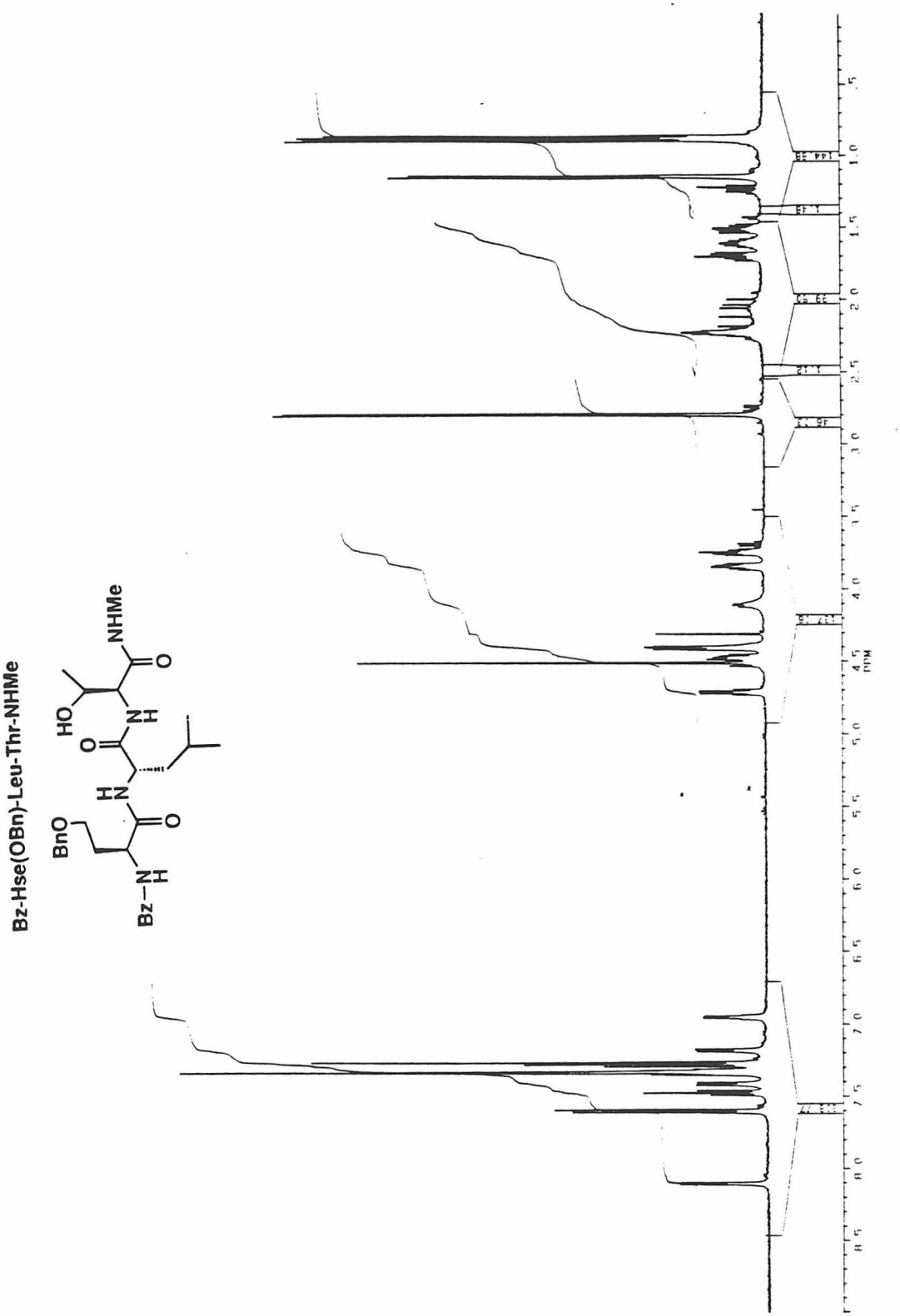
Bz-Hse(OBn)-Leu-Thr-NHMe
BnO
HO
NHMe
Bz
ppm

Bz-Hse-Leu-Thr-NHMe

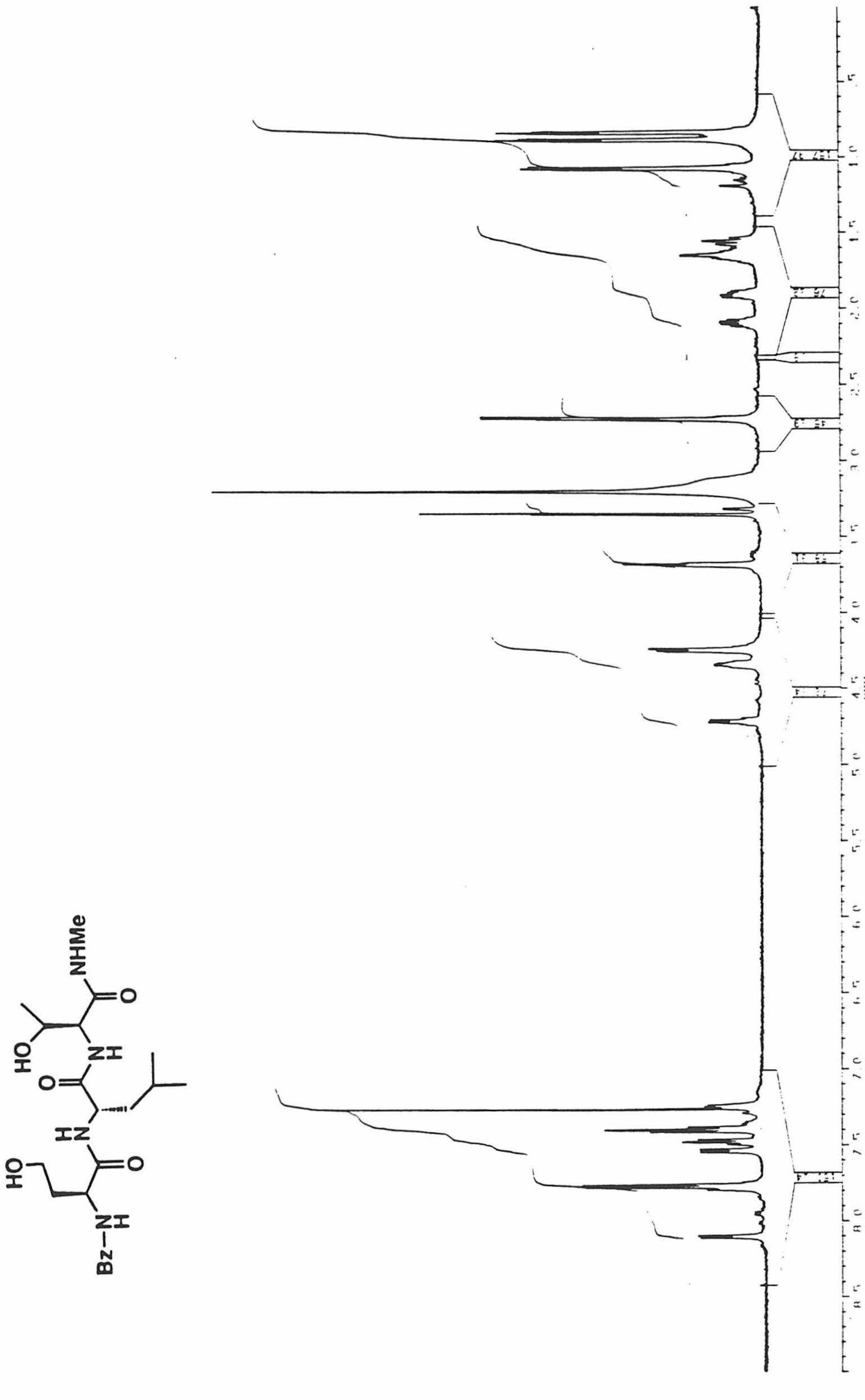

Bz-Hse(OBn)-Leu-Thr(TBDMS)-NHMe

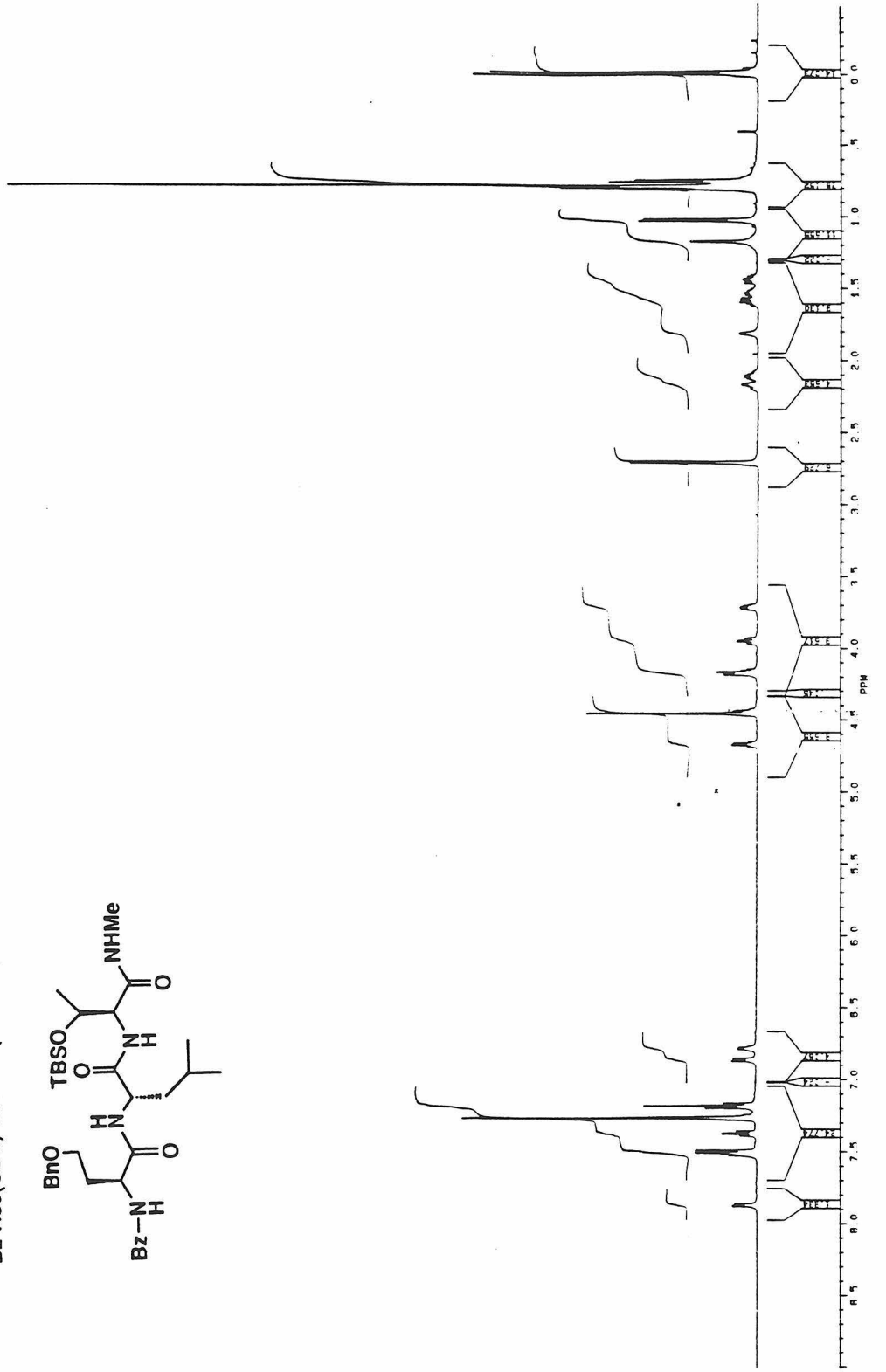

Bz-Hse-Leu-Thr(TBDMS)-NHMe

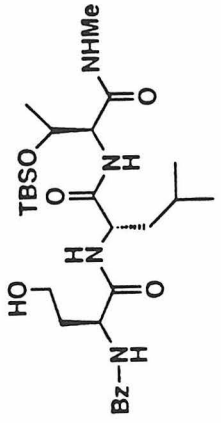

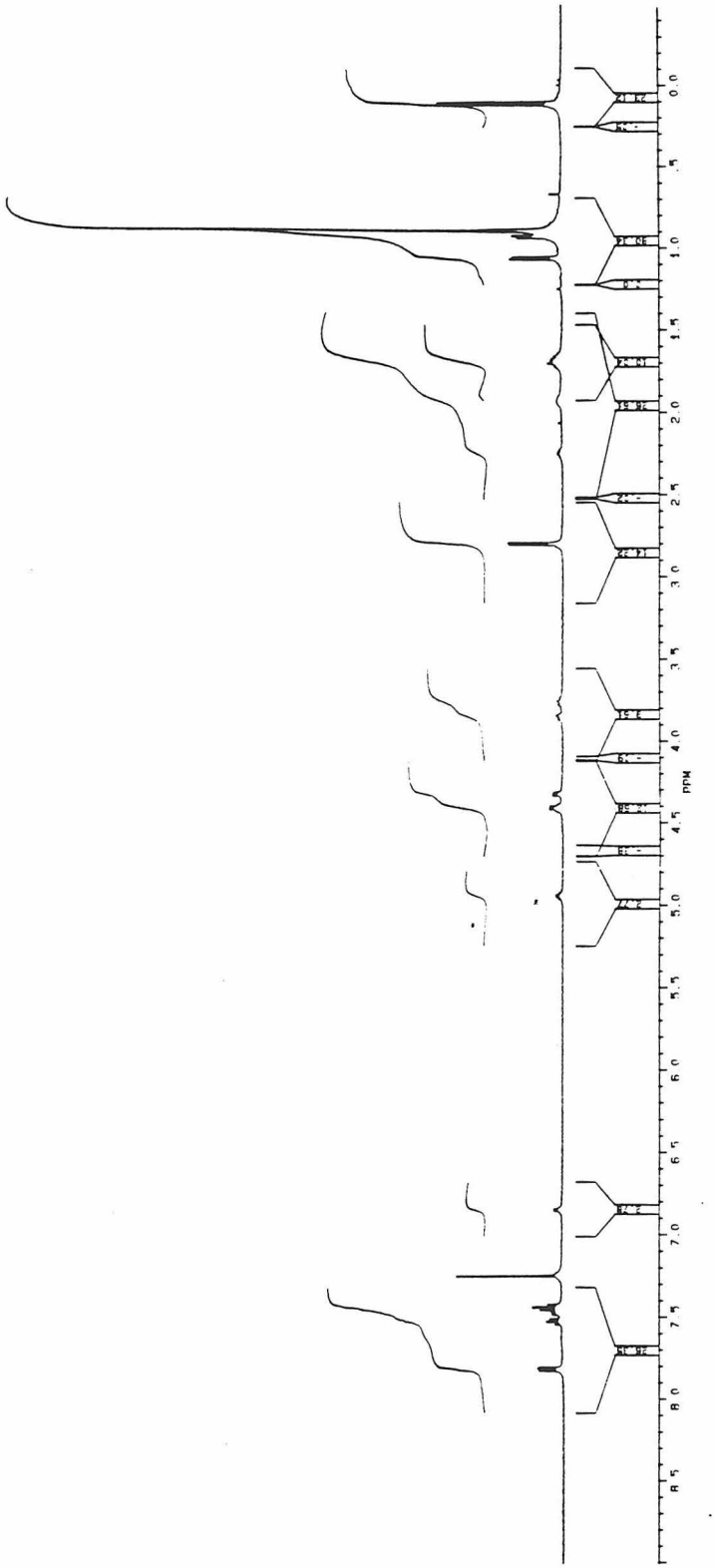

2-Acetamido-3,6-Di-O-acetyl-4-O-(2-acetamido-3,4,6-tri-O-acetyl-2-deoxygluco-pyranosyl)-1-chloro-1-deoxy-D-glucopyranoside

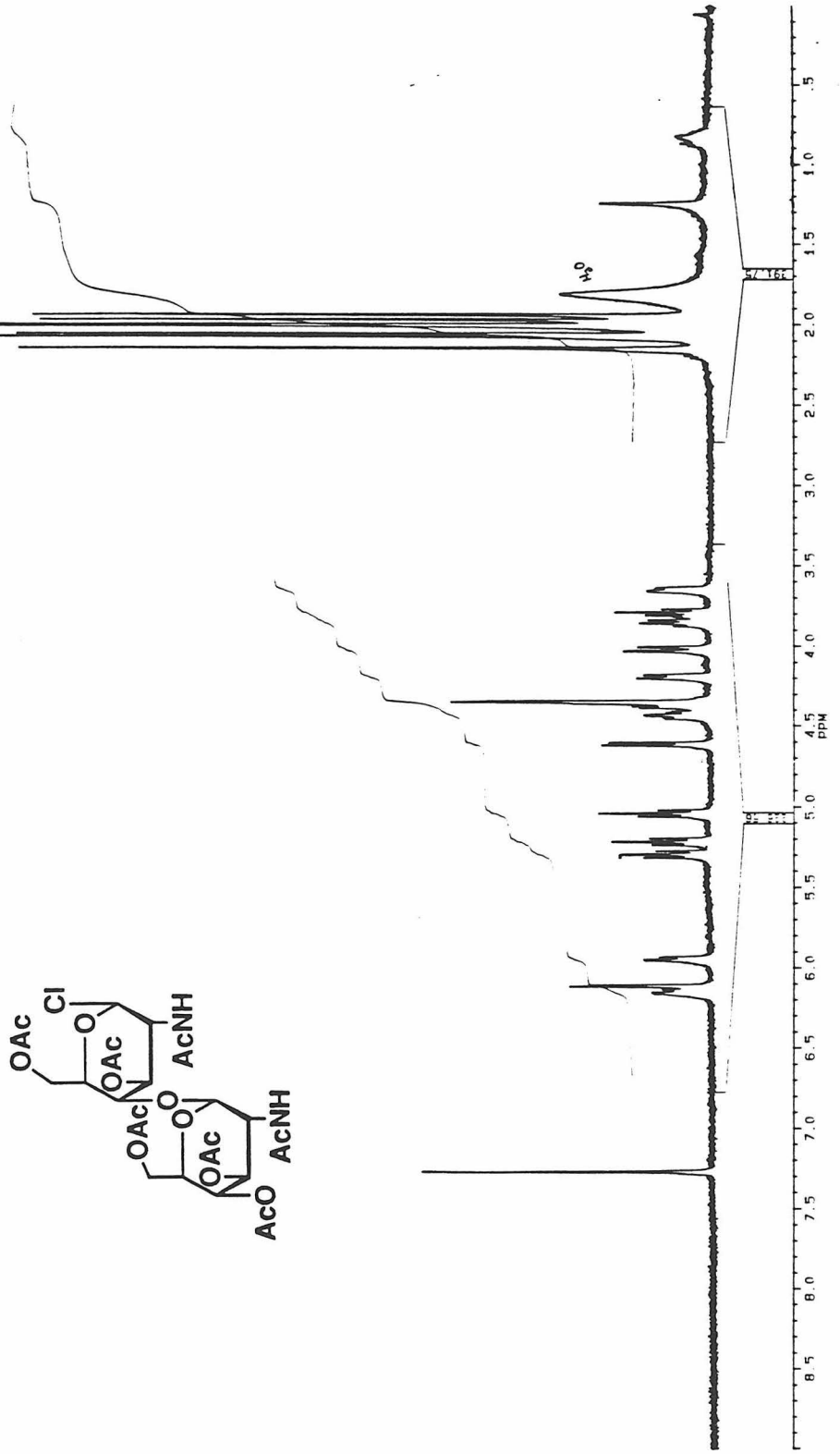

2-Acetamido-3,6-Di-O-acetyl-1,5-anhydro-4-O-(2-acetamido-3,4,6-tri-O-acetyl-2-deoxy-glucopyranosyl)-2-deoxy-D-glucitol

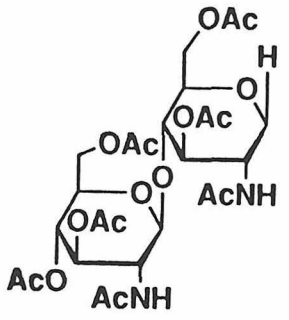

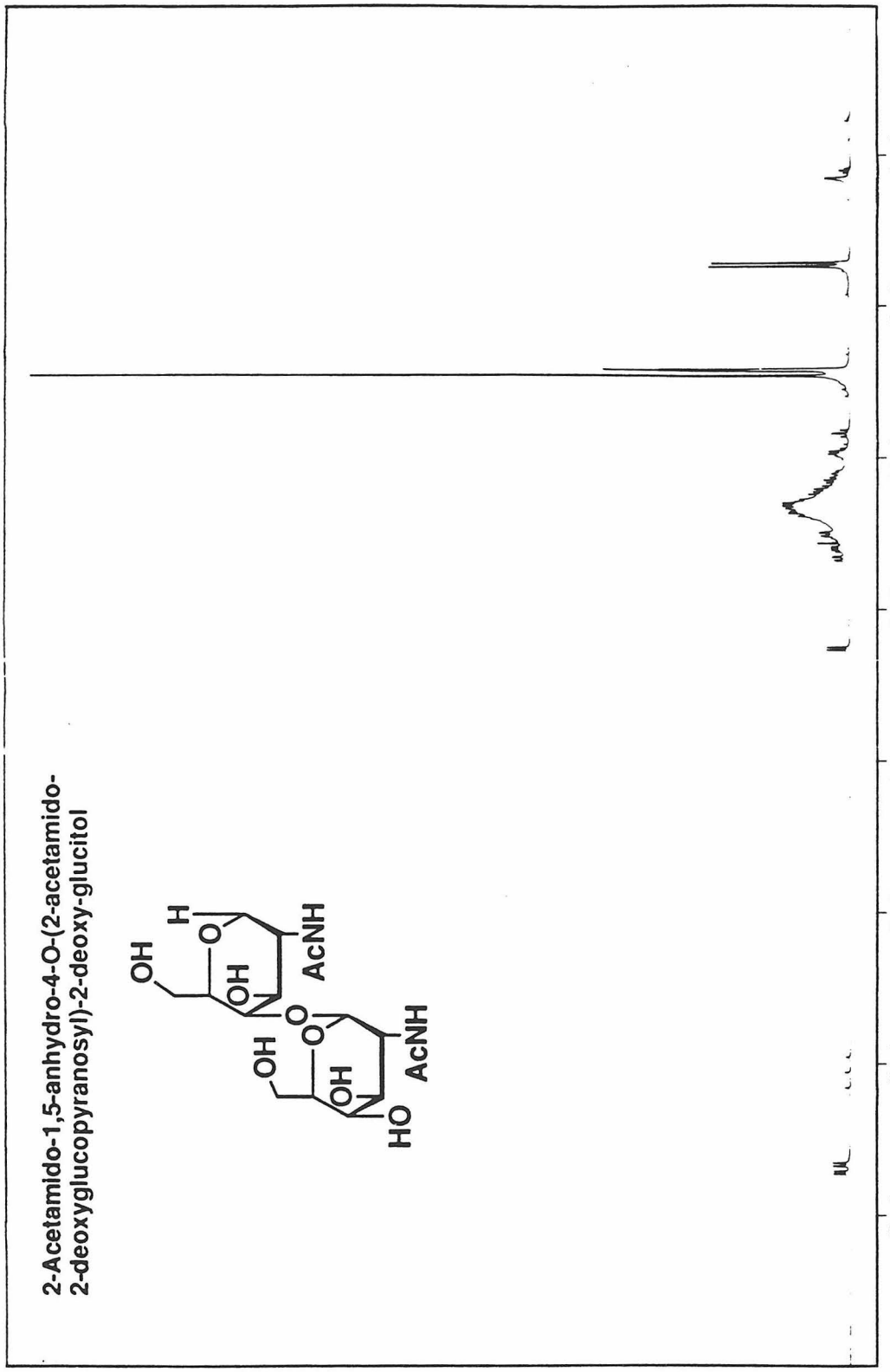
2-Acetamido-1,5-anhydro-4-O-(2-acetamido-2-deoxyglucopyranosyl)-2-deoxy-glucitol
OH
H
O
OH
AcNH
O
O
OH
OH
HO
AcNH
8.0
7.0
6.0
5.0
4.0
3.0
2.0
1.0
ppm

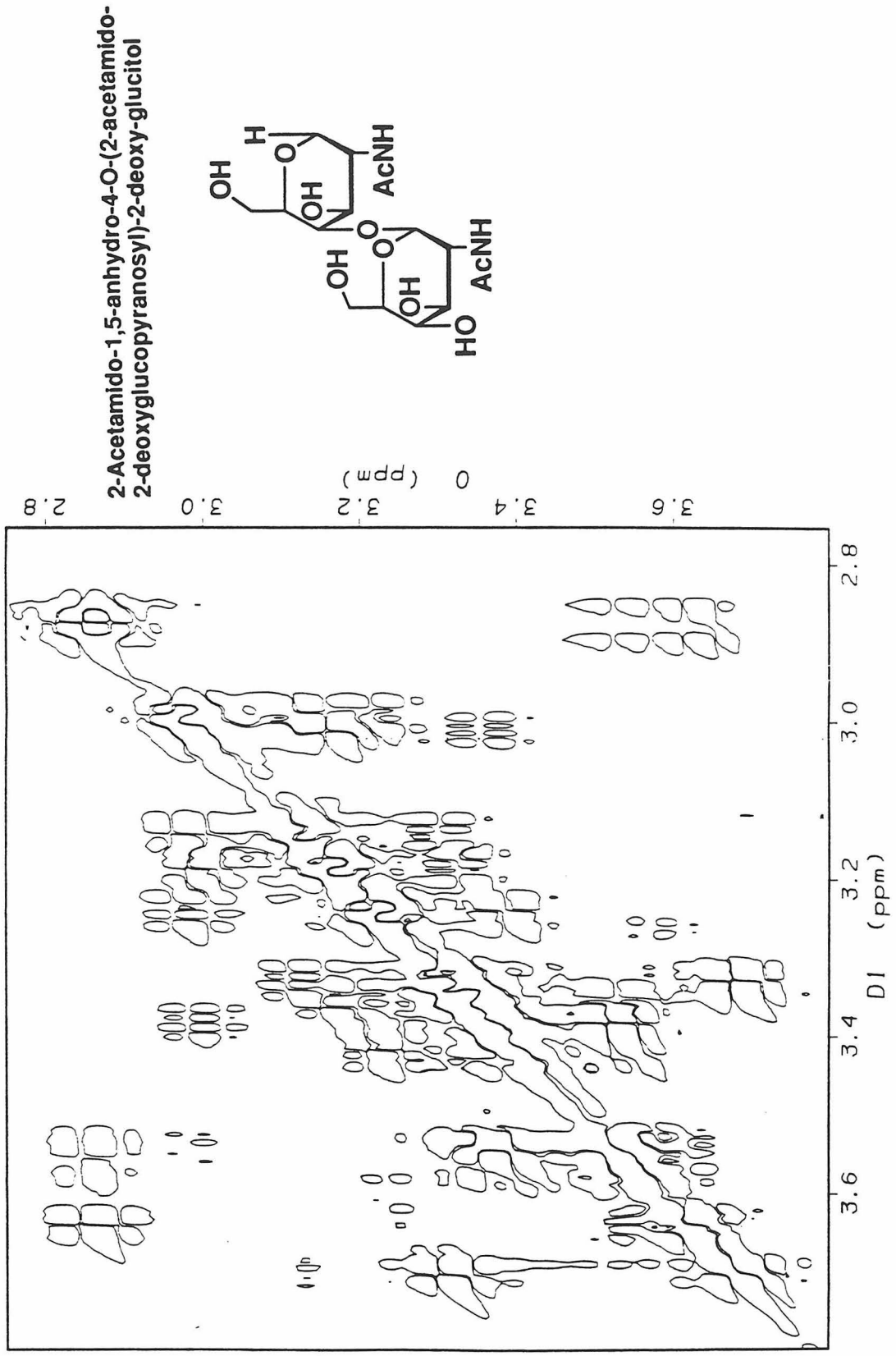
2-Acetamido-1,5-anhydro-4-O-(2-acetamido-2-deoxyglucopyranosyl)-2-deoxy-glucitol
OH
H
O
OH
AcNH
O
OH
O
OH
AcNH
HO
2.8
3.0
3.2
3.4
3.6
(ppm)
0
3.6
3.4
3.2
3.0
2.8
D1 (ppm)

Chapter Four

Cyclo[SHex-Amb-Cys]-Thr-Val-Thr-Nph-NH_2 (5)

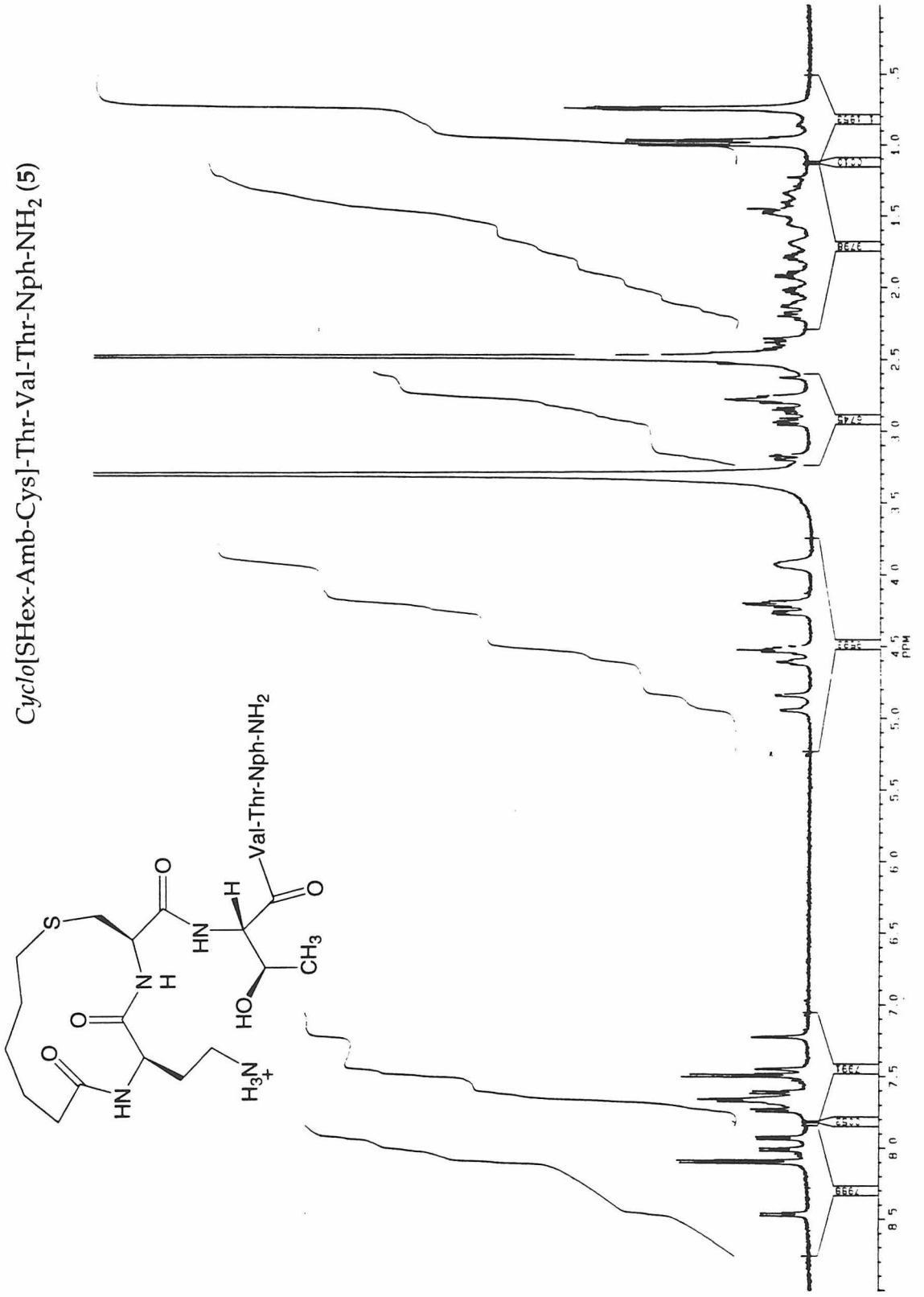

Chapter Five

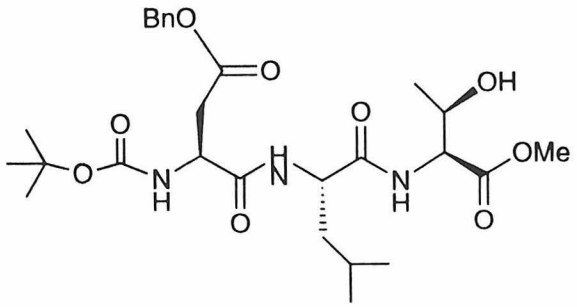

Boc-Asp(OBn)-Leu-Thr-OMe

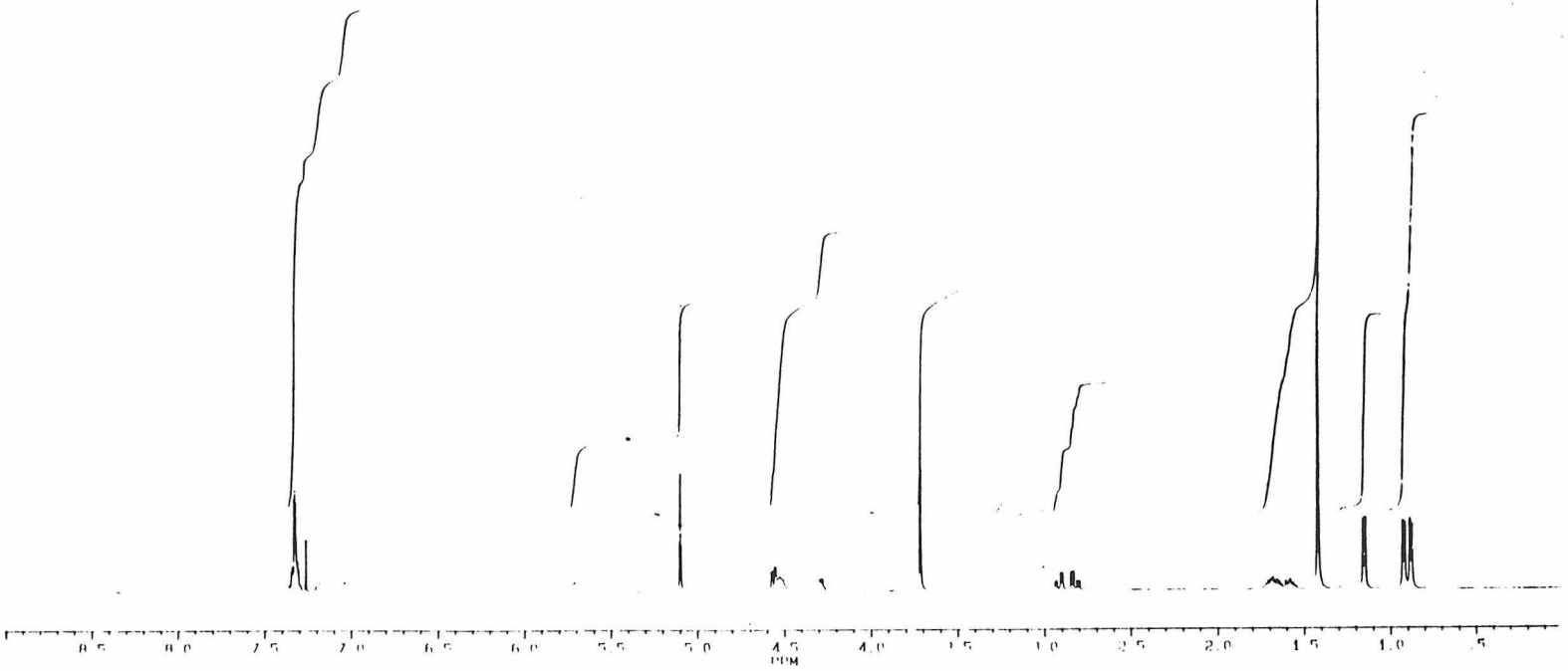

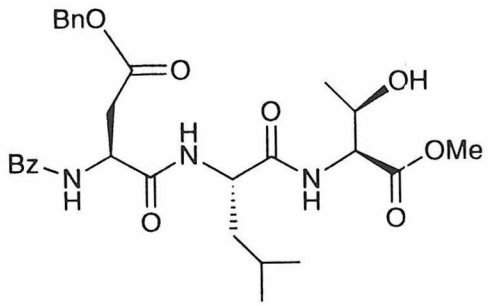

Bz-Asp(OBn)-Leu-Thr-OMe

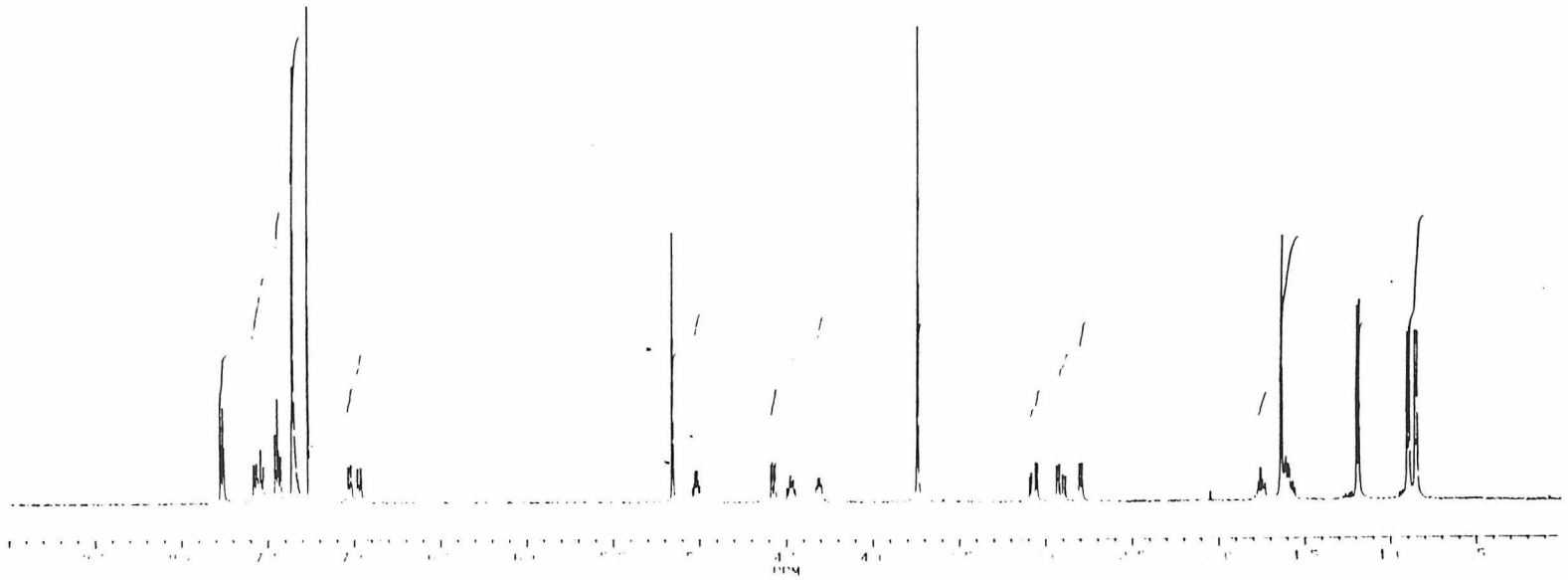

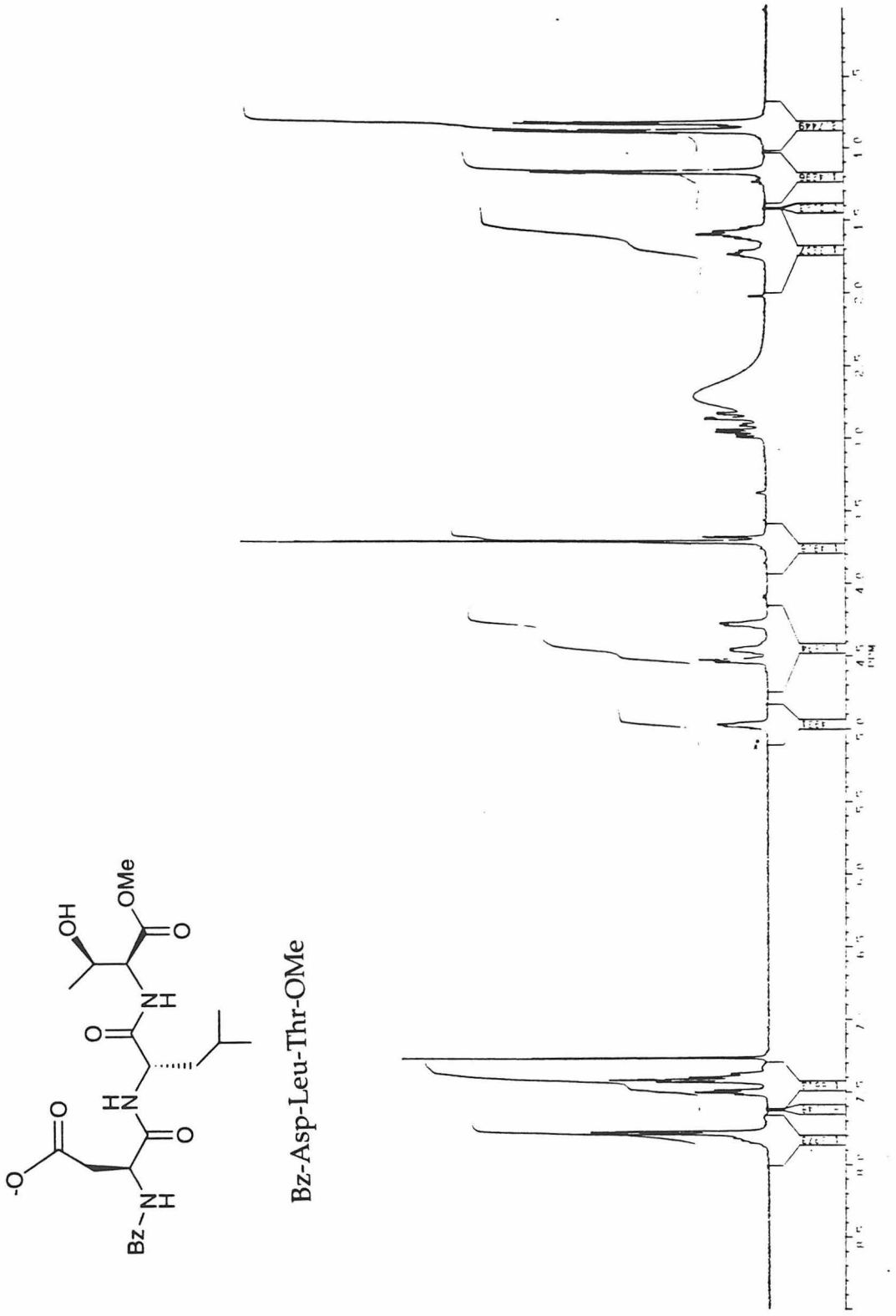

Bz-Asp-Leu-Thr-OMe

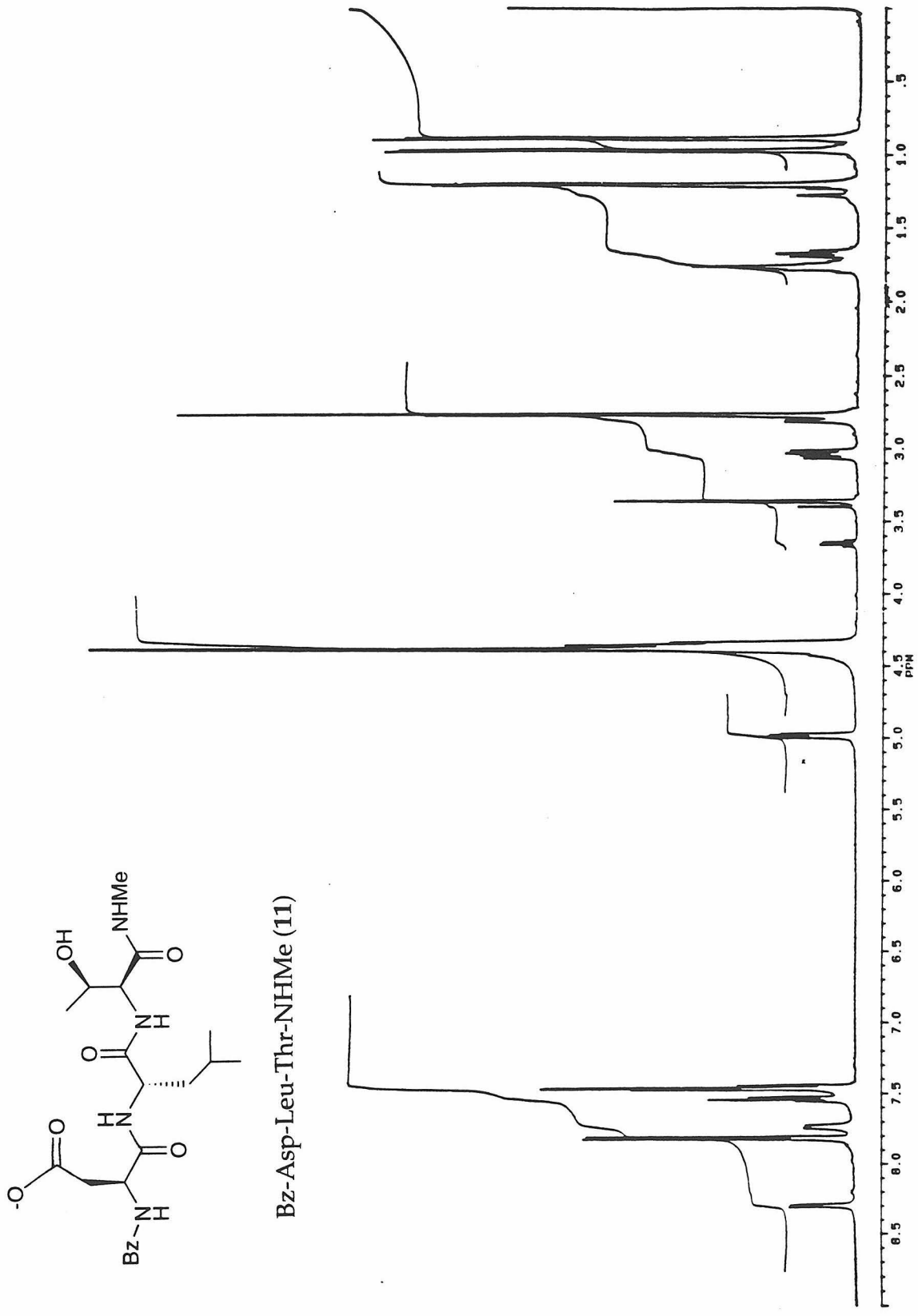
Bz-Asp-Leu-Thr-NHMe (11)
PPM

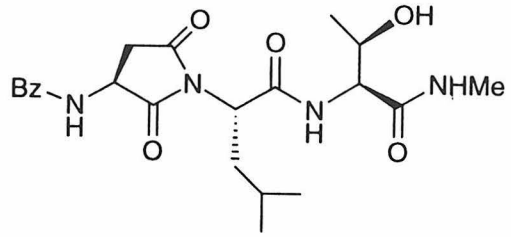

Succinimide of Bz-Asp-Leu-Thr-NHMe (**13**)

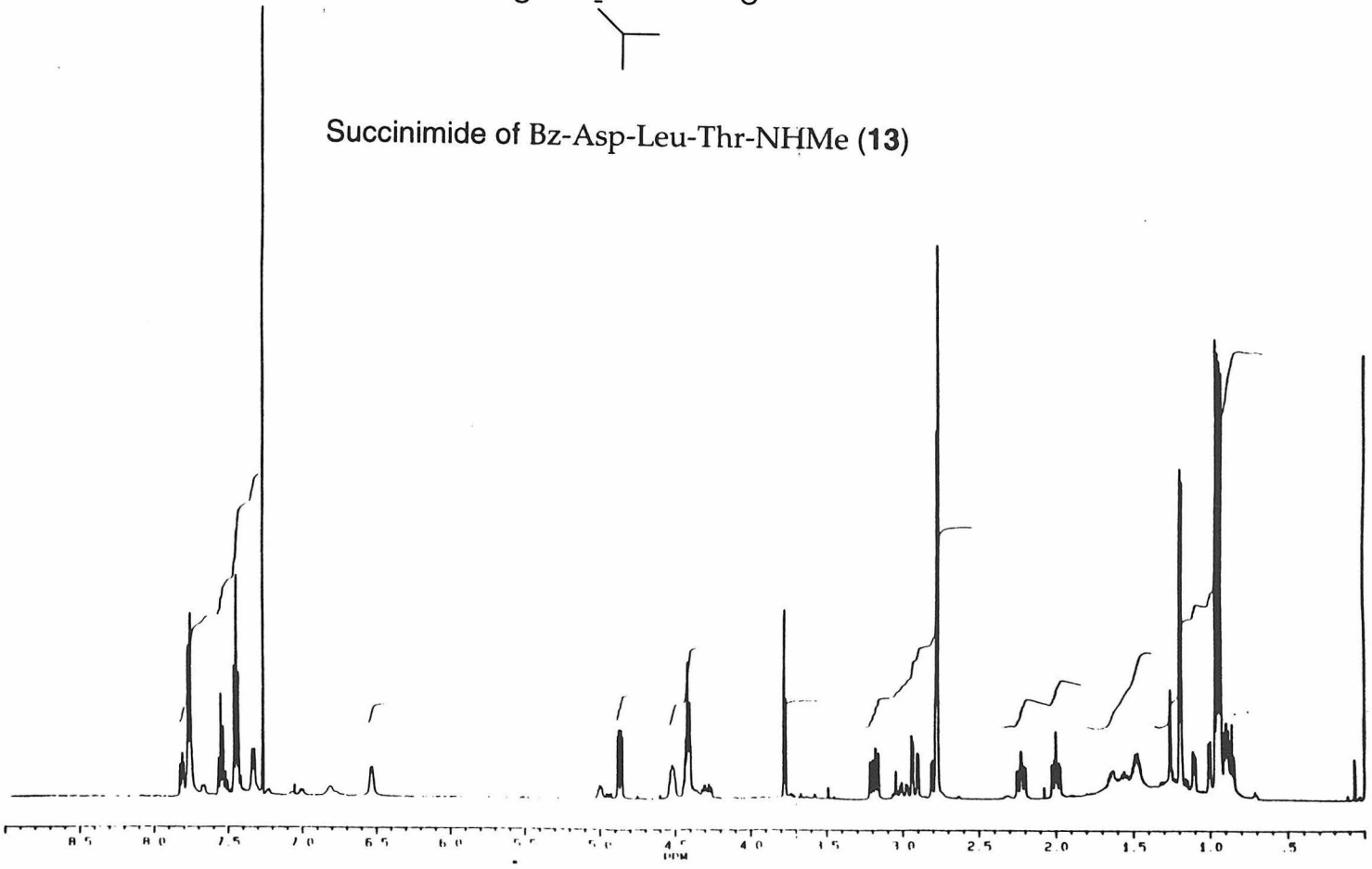

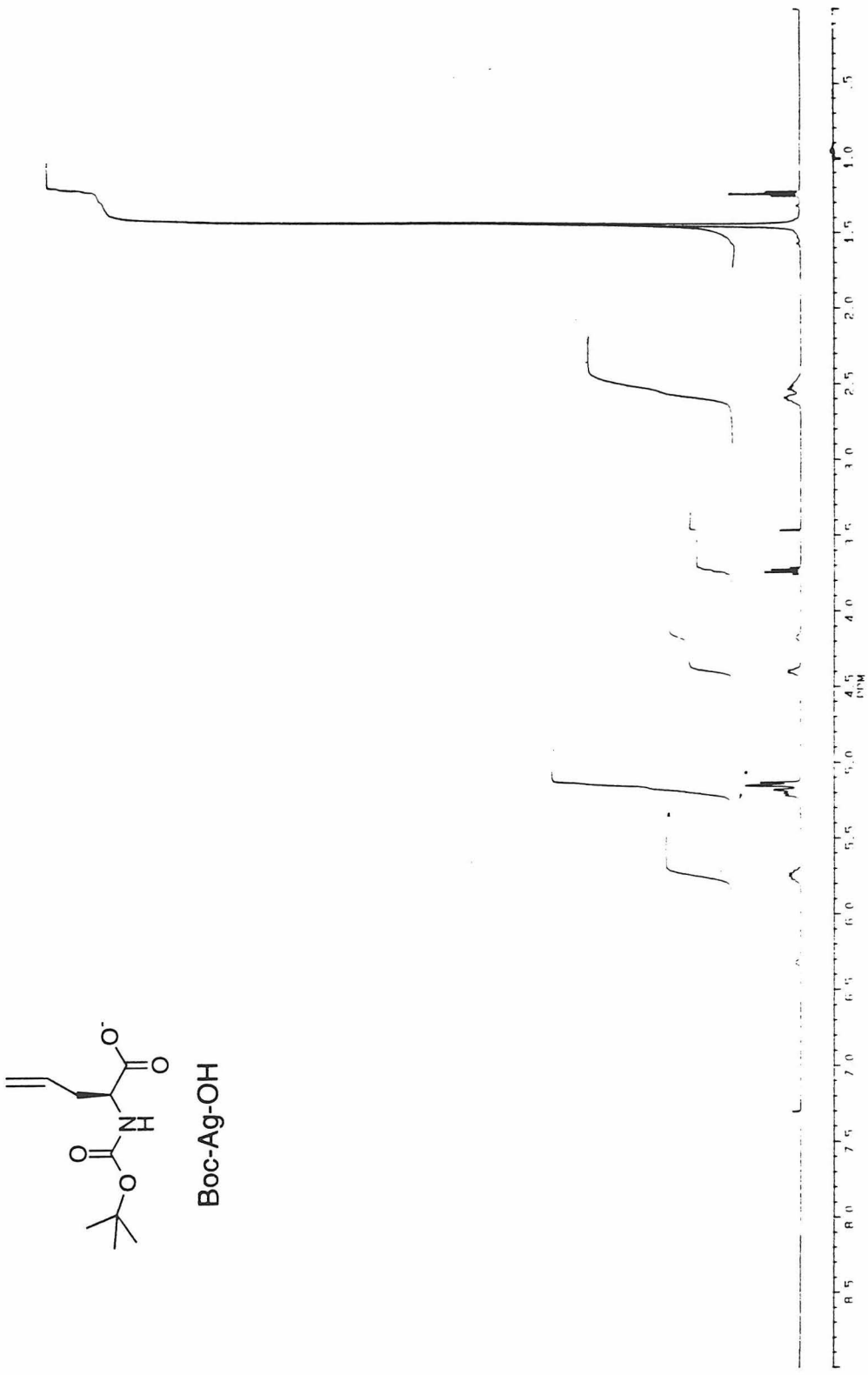

Boc-Ag-OH

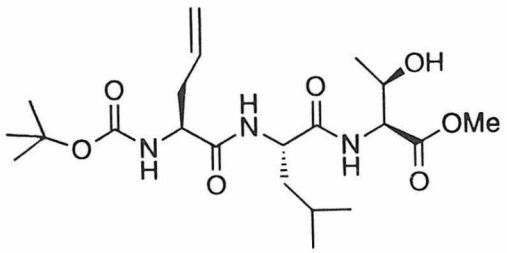

Boc-Ag-Leu-Thr-OMe

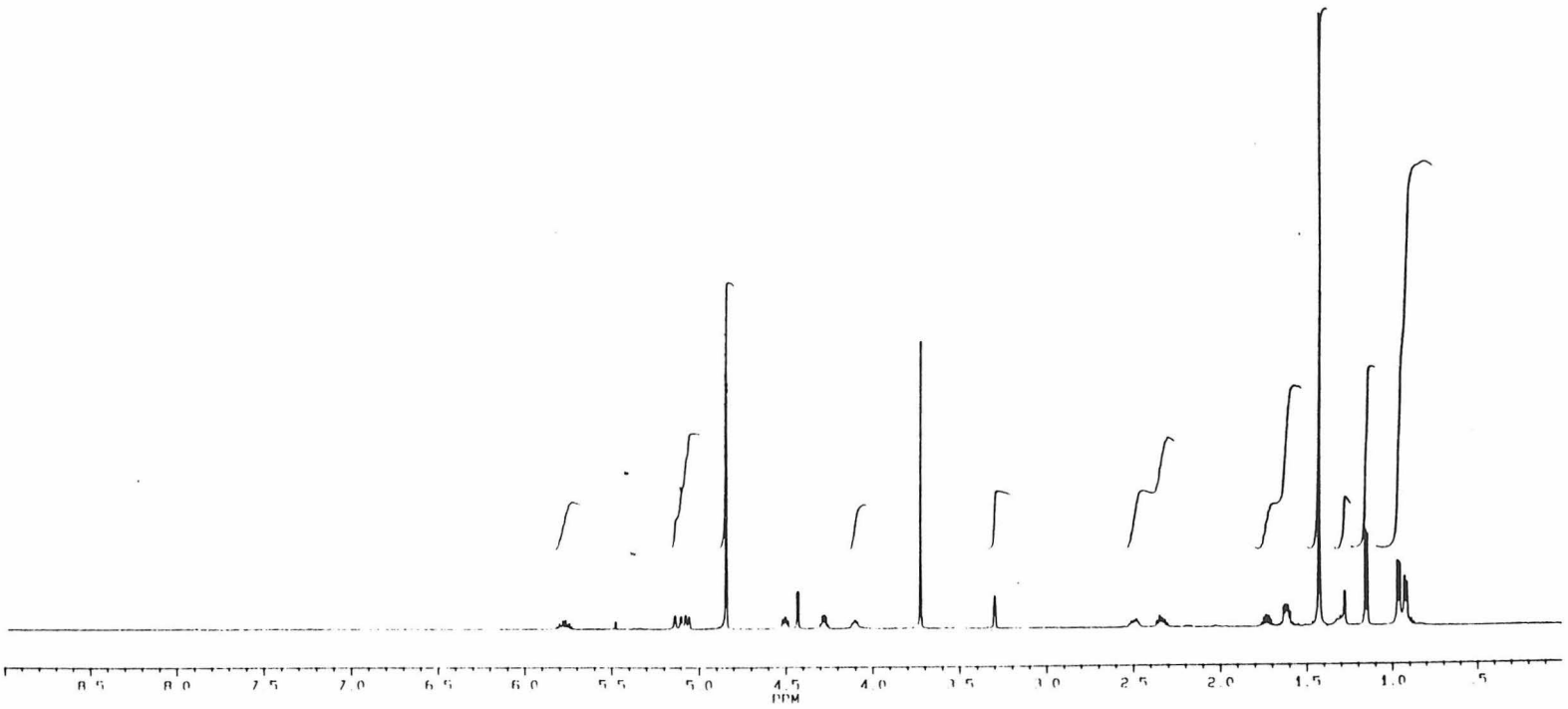

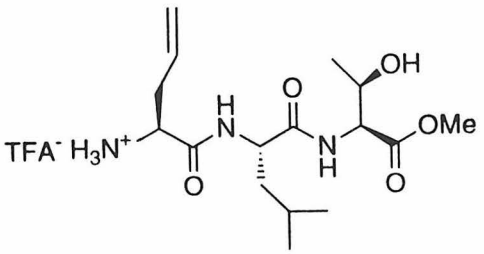

TFA-Ag-Leu-Thr-OMe

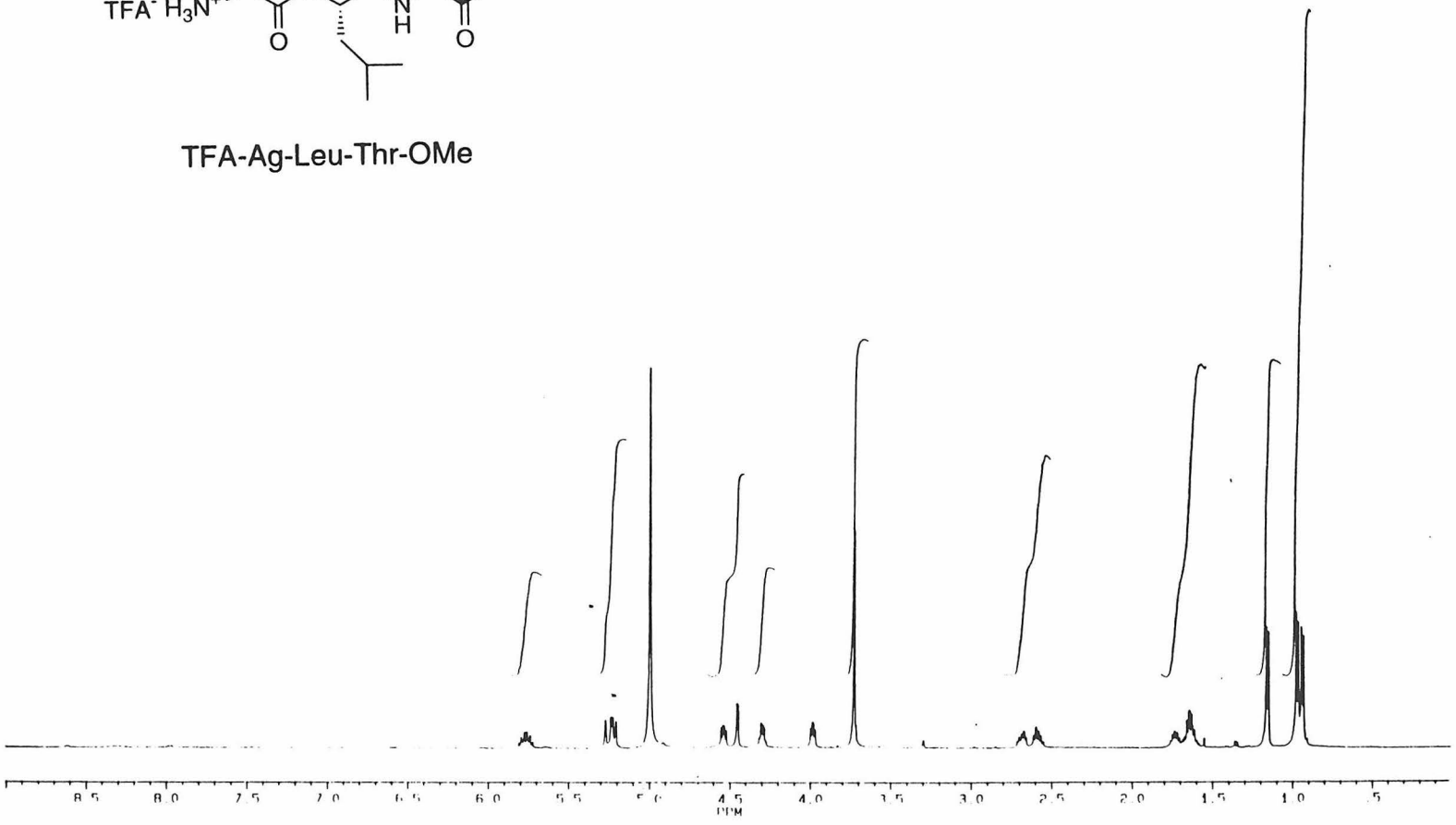

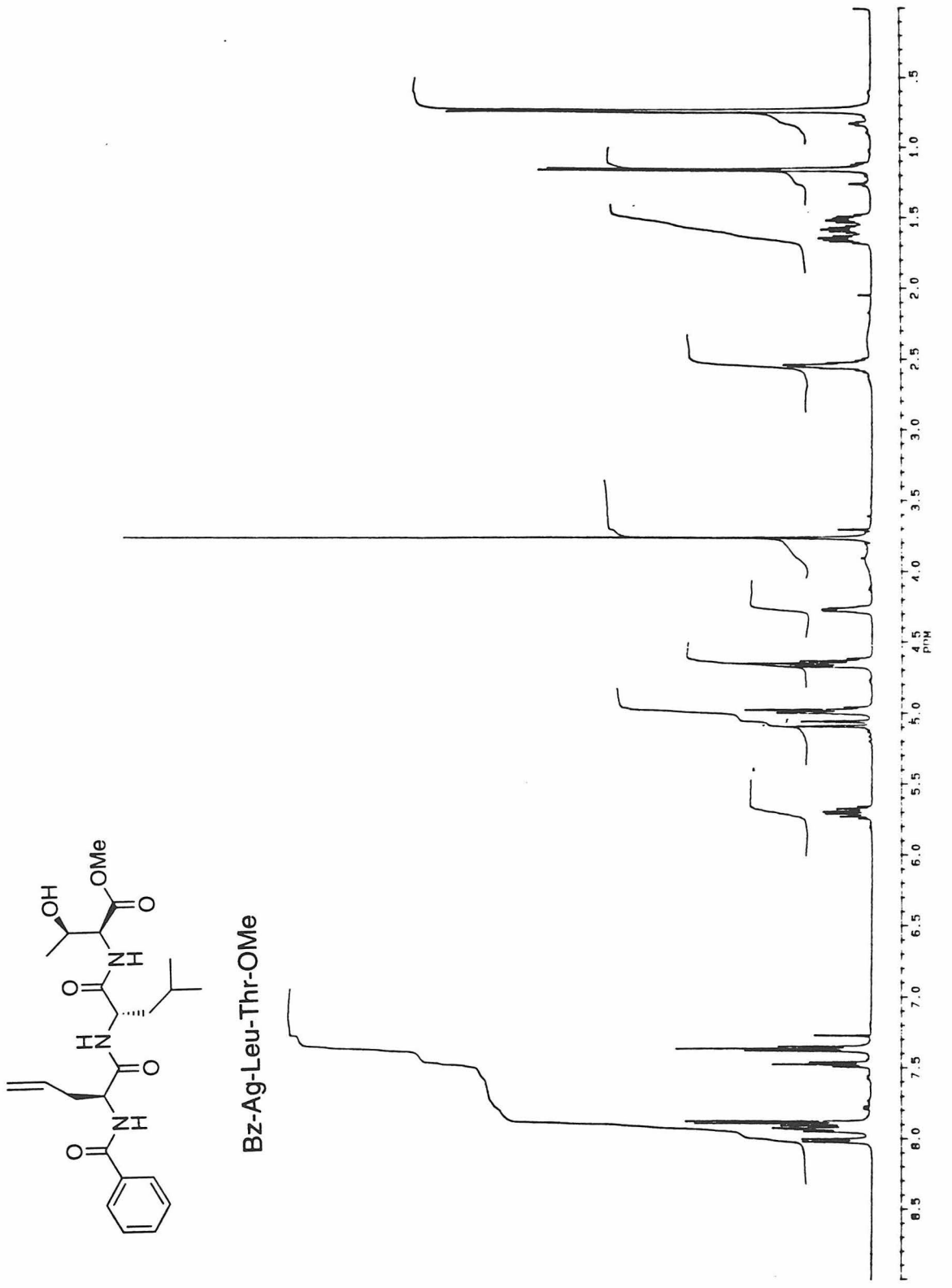
OH
OMe
O
N
H
O
N
H
O
N
H
O
Bz-Ag-Leu-Thr-OMe
8.5
8.0
7.5
7.0
6.5
6.0
5.5
5.0
4.5
PPM
4.0
3.5
3.0
2.5
2.0
1.5
1.0
.5

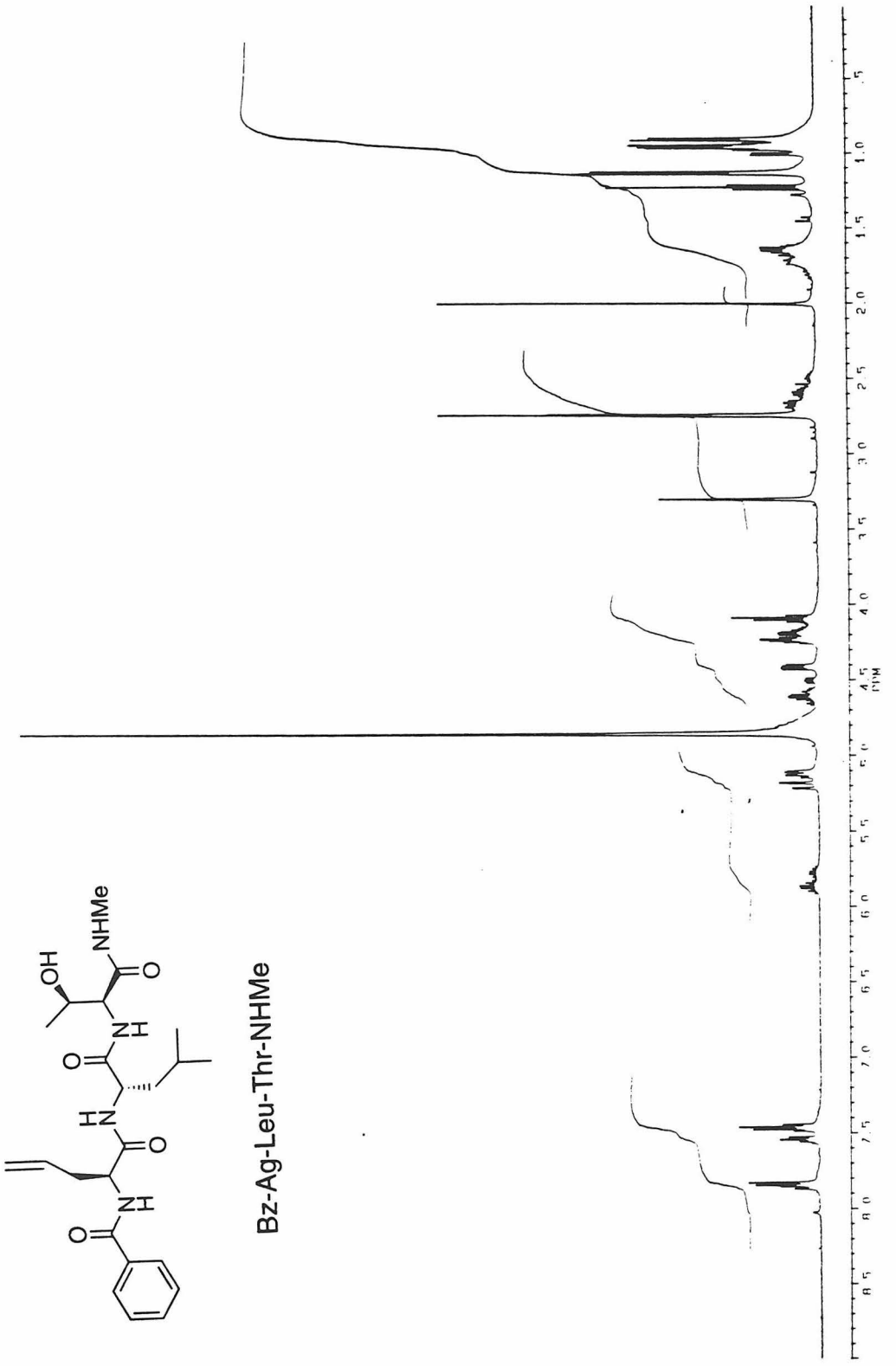
NHMe
OH
O
N
H
O
N
H
O
N
H
O
Bz-Ag-Leu-Thr-NHMe

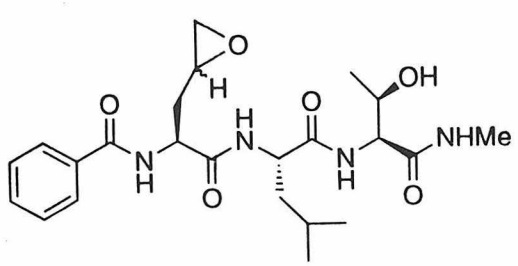

Bz-Epx-Leu-Thr-NHMe (**14**)

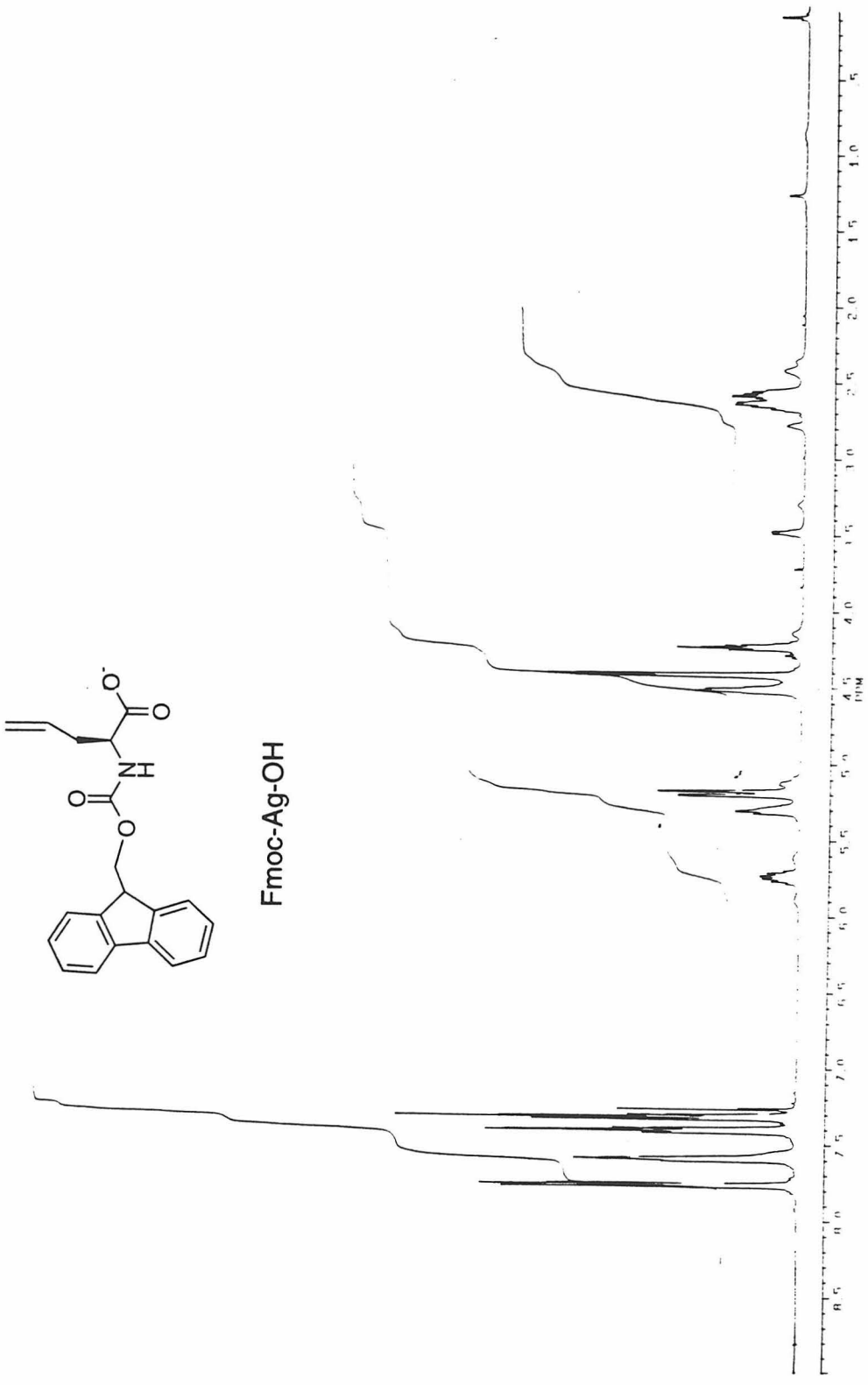
Fmoc-Ag-OH

Appendix B

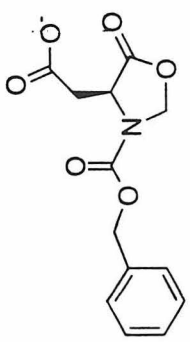

(S)-3-Benzyloxycarbonyl-5-oxo-4-oxazolidinineacetic Acid

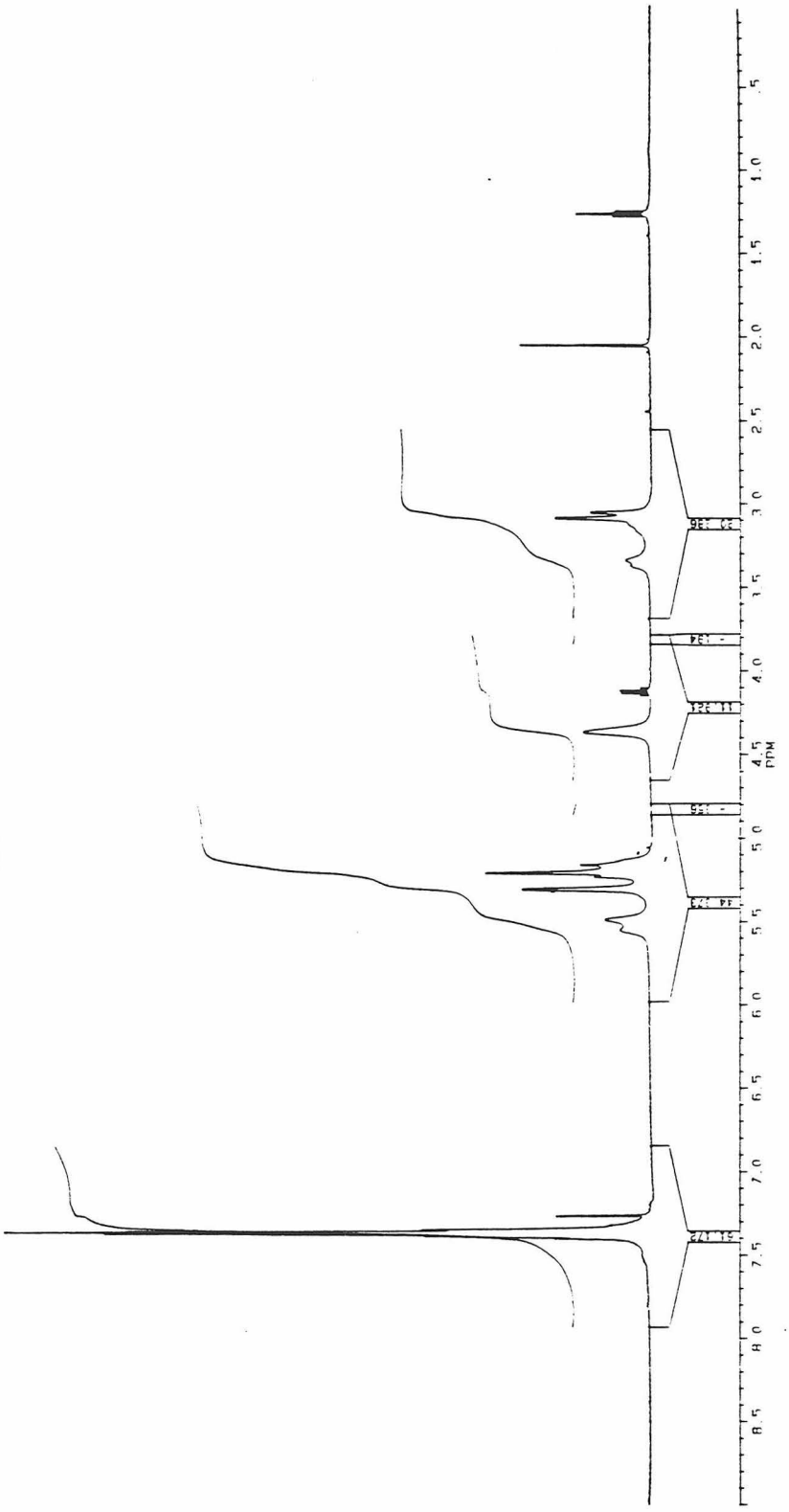

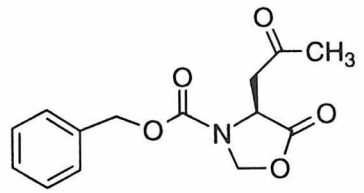

(*S*)-3-Benzyloxycarbonyl-4-
(2-oxopropyl)-5-oxazolidinone

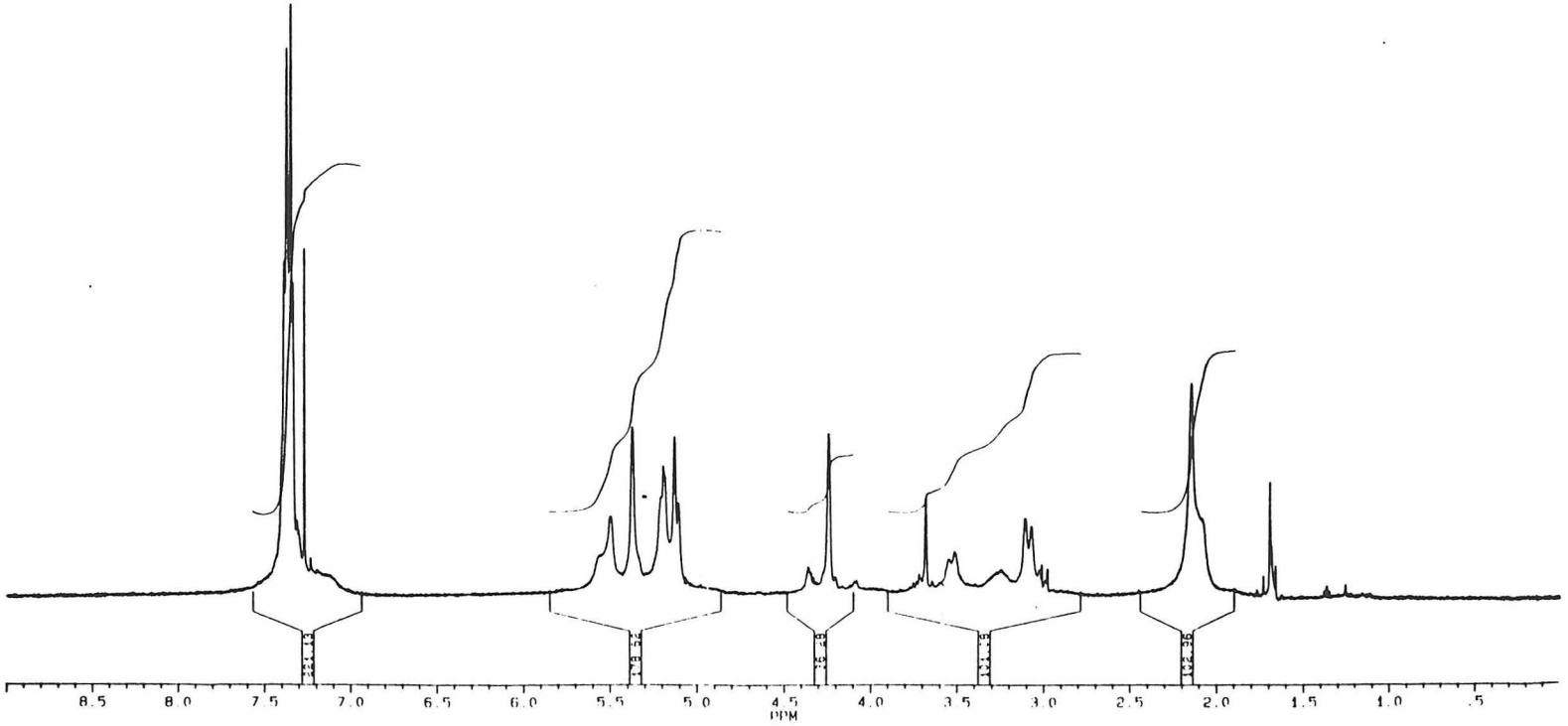

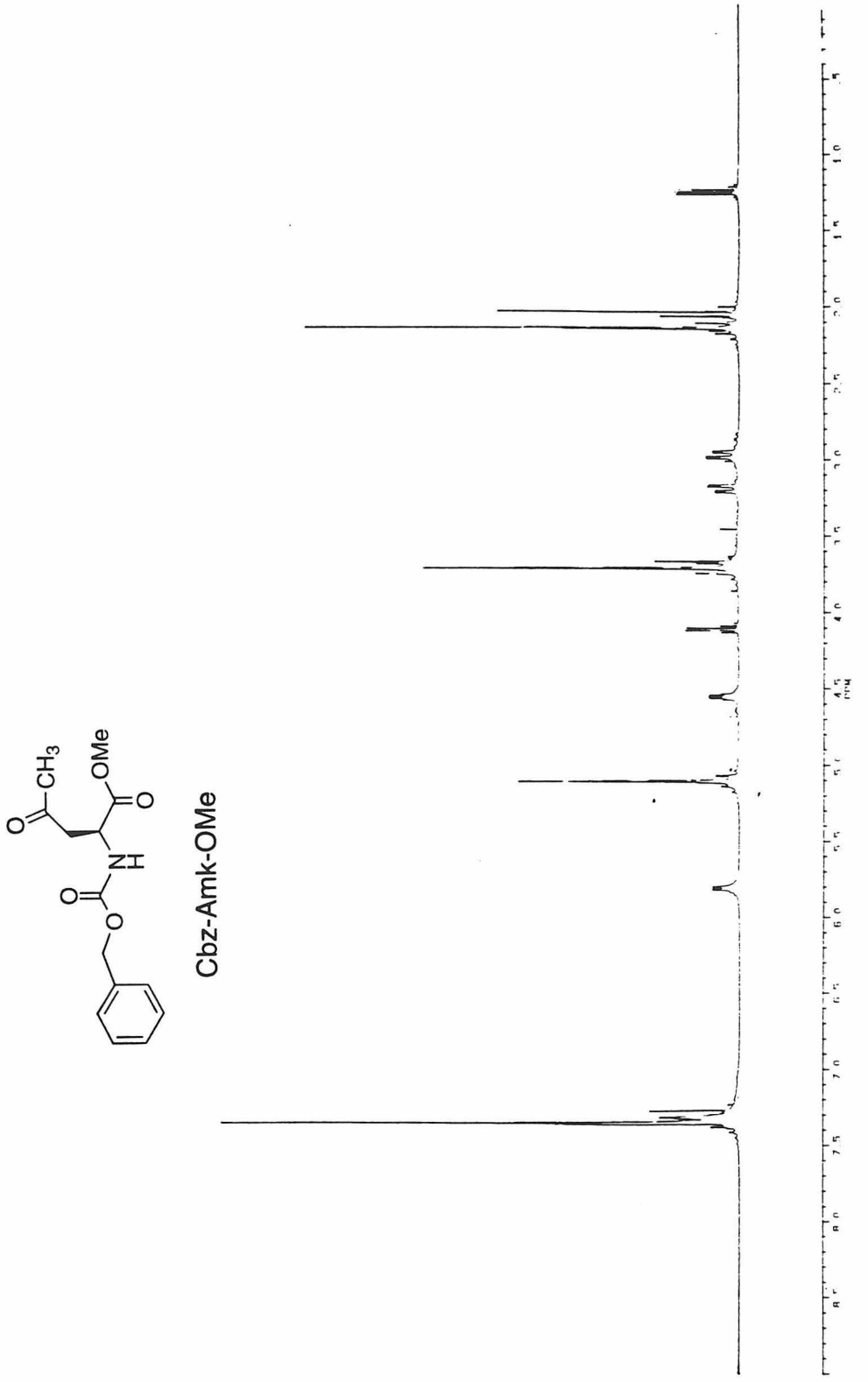
CH3
OMe
O
O
N
H
O
O
Cbz-Amk-OMe

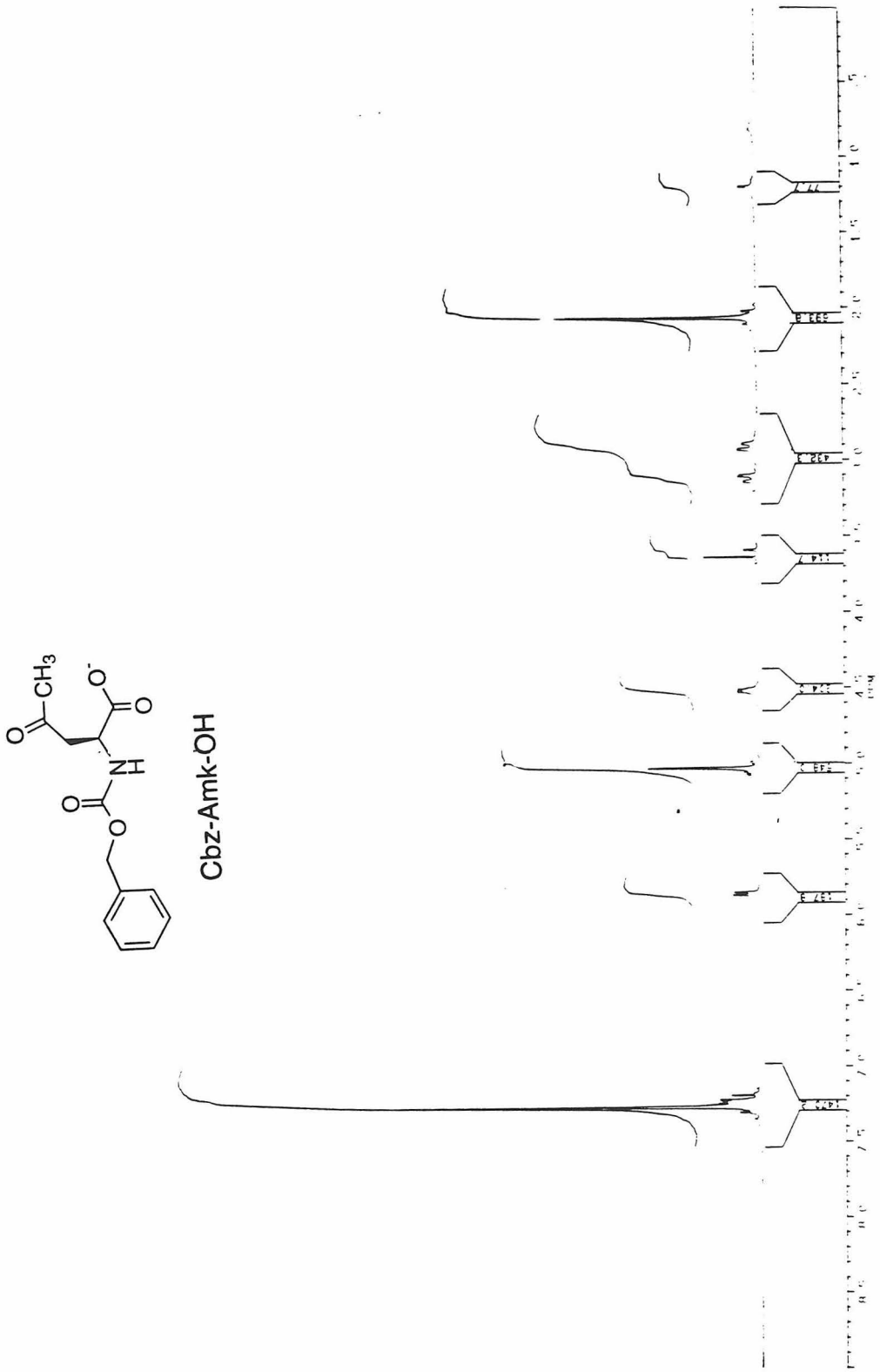
Cbz-Amk-OH

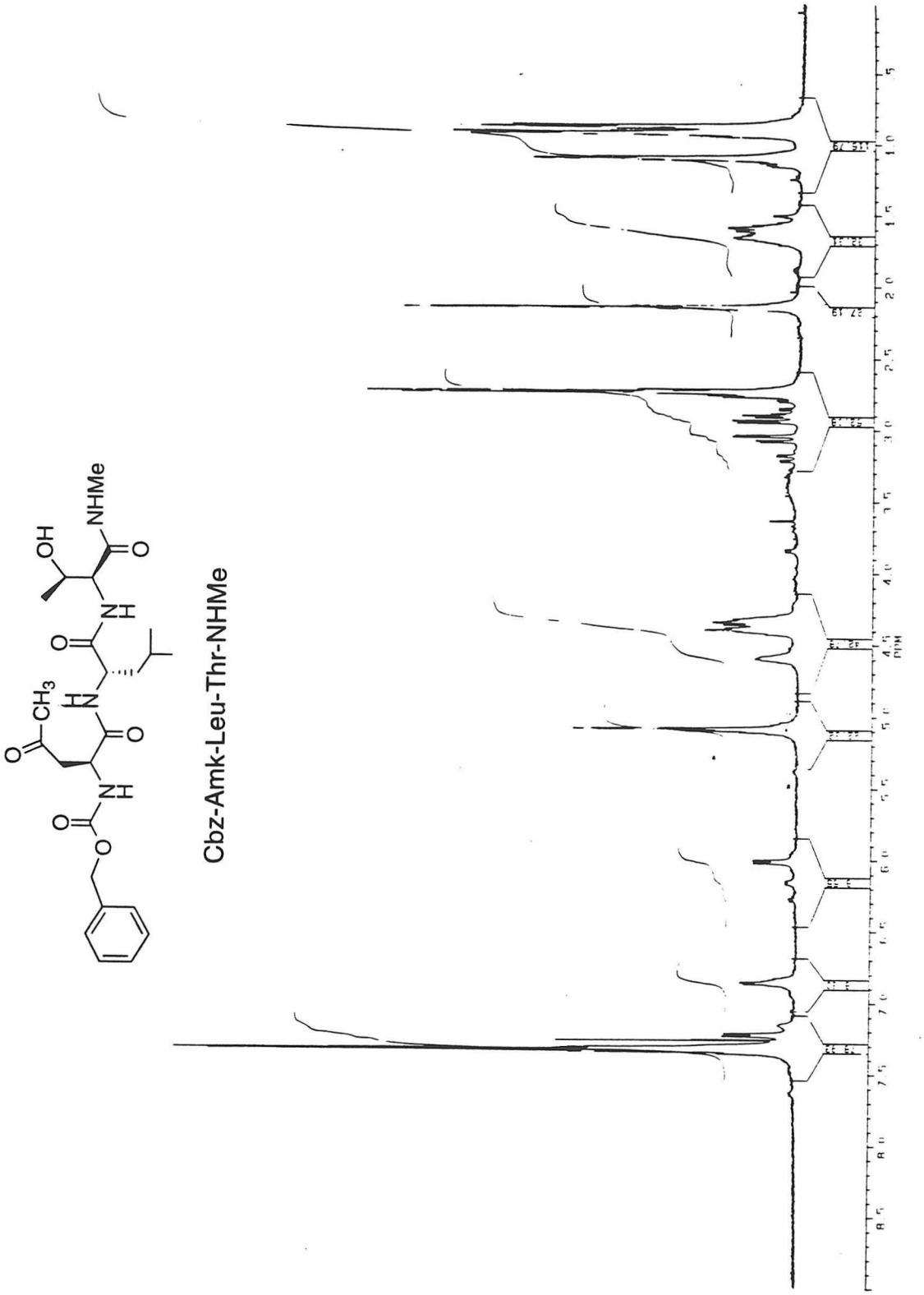
Cbz-Amk-Leu-Thr-NHMe
NHMe
OH
O
N
H
CH3
PPM

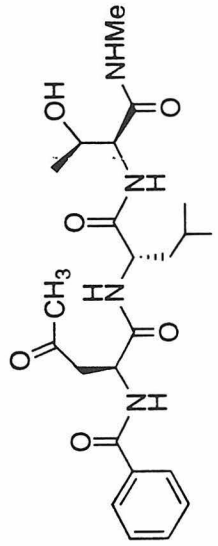

Bz-Amk-Leu-Thr-NHMe (**2**)

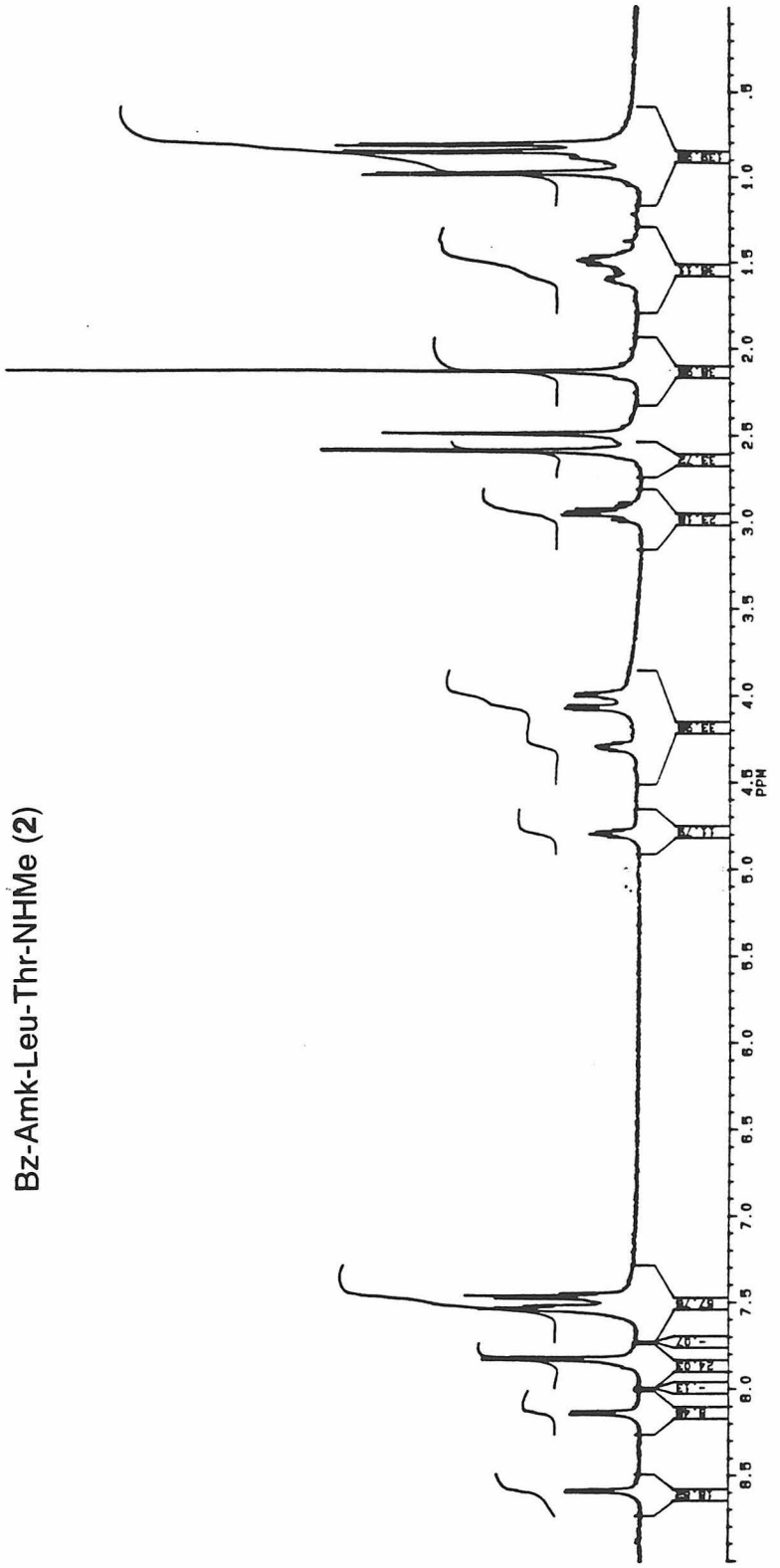

Appendix C

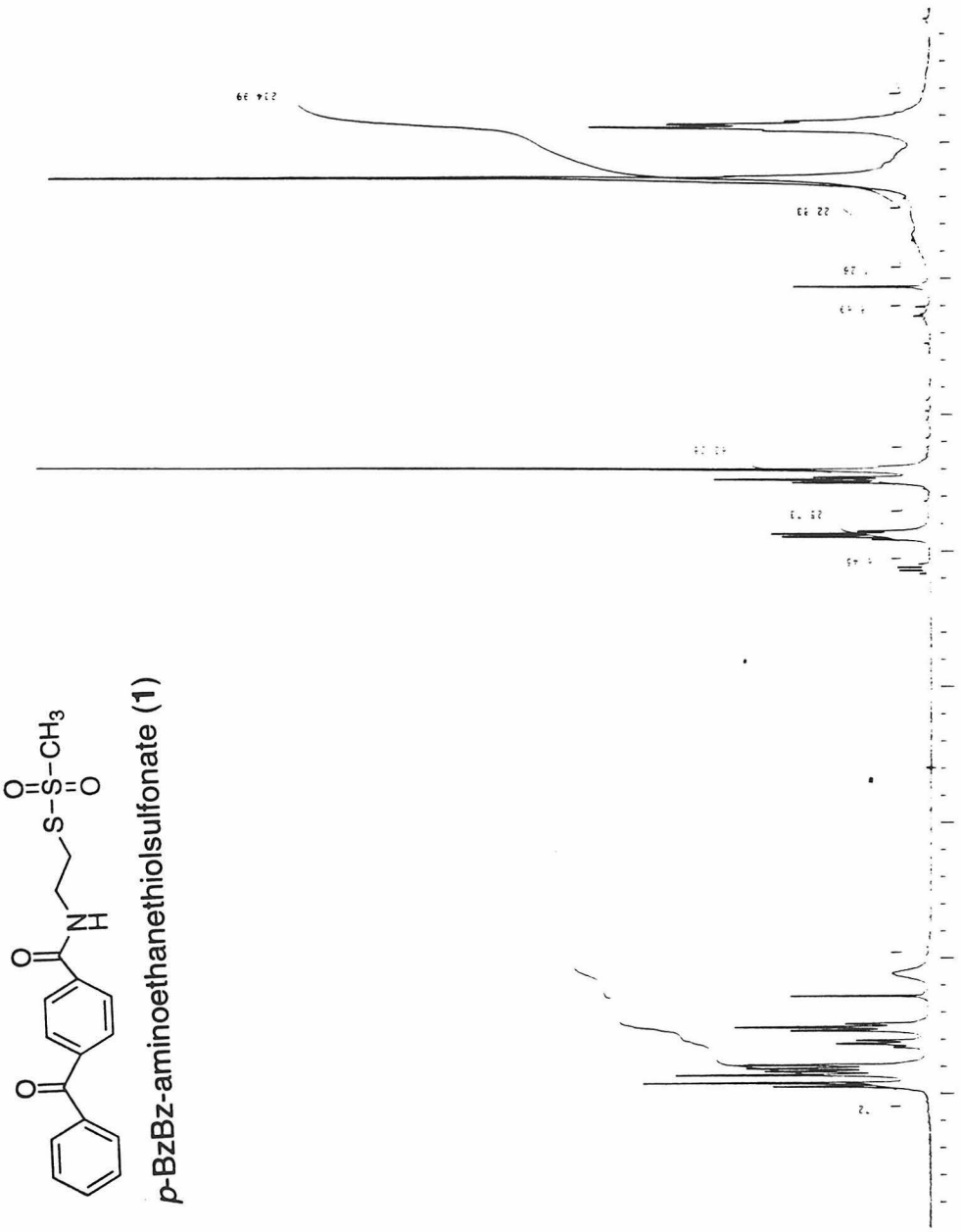

p-BzBz-aminoethanethiolsulfonate (1)

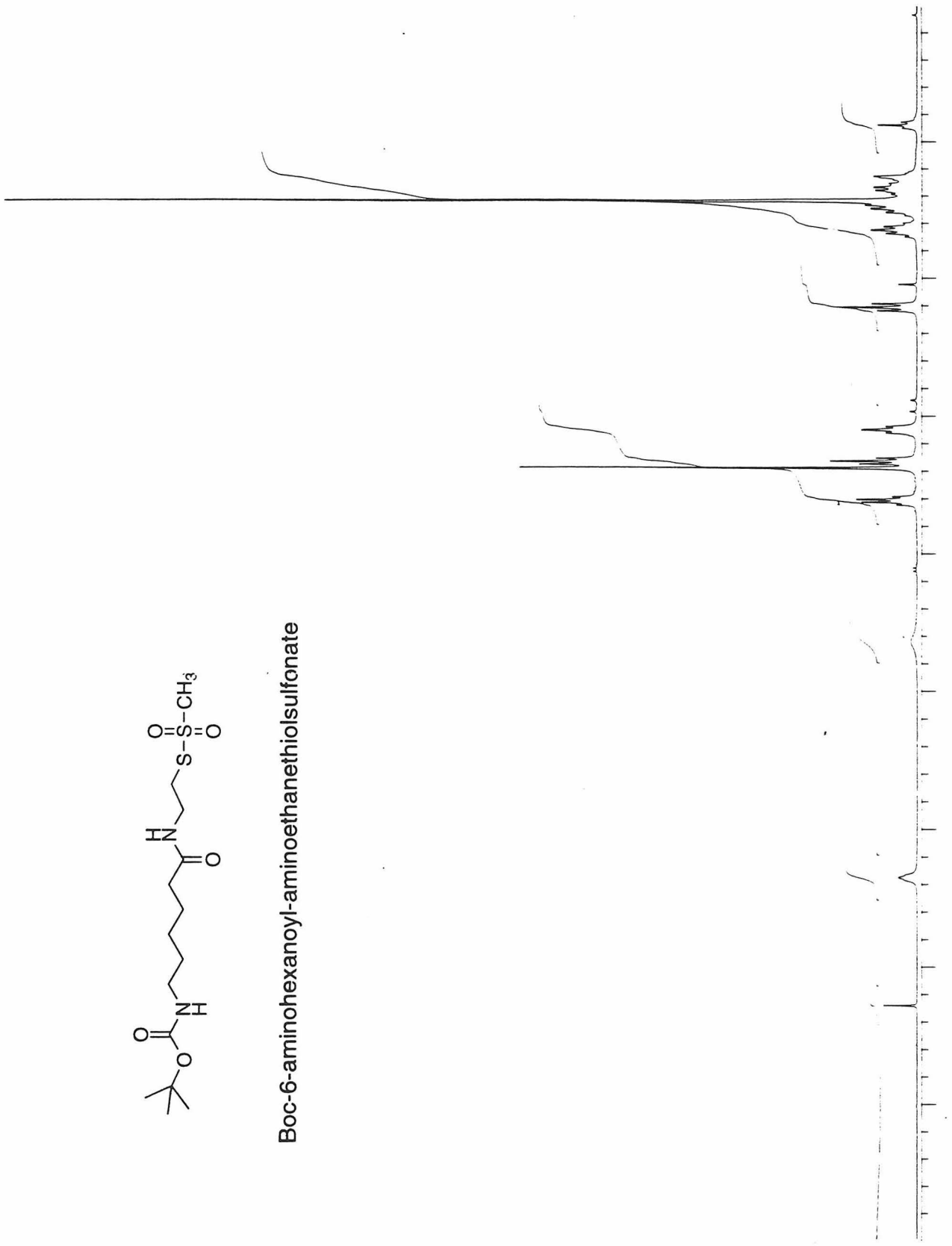

Boc-6-aminohexanoyl-aminoethanethiolsulfonate

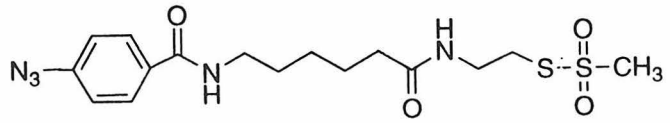

p-azidoBz-6-aminohexanoyl-aminoethanethiolsulfonate (**2**)

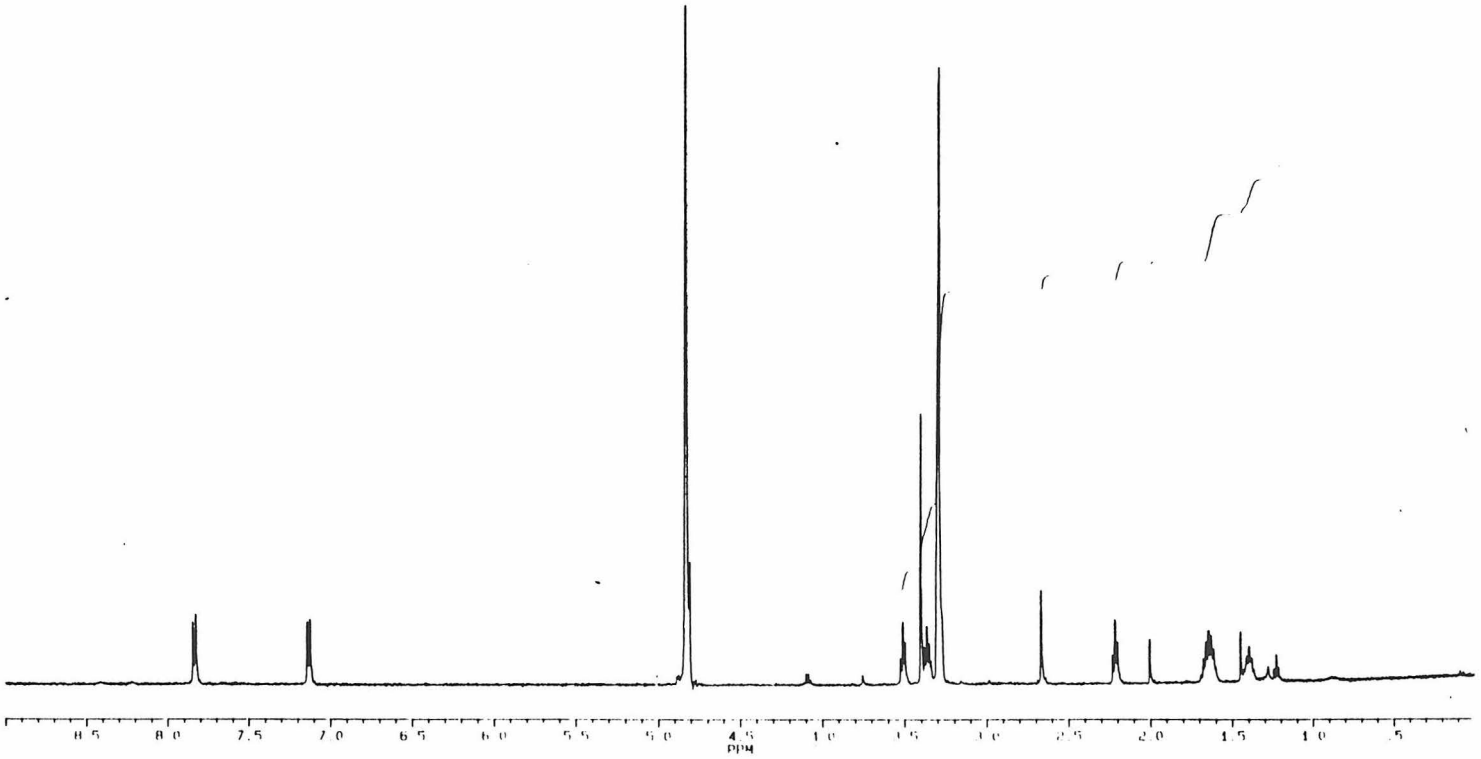

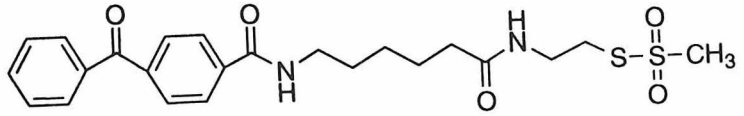

p-BzBz-6-aminohexanoyl-aminoethanethiolsulfonate (**3**)